THE THIRD INTERNATIONAL FORUM

PHYSICS – 2024

Samarkand, Uzbekistan **April 23-25, 2024**

BOOK OF ABSTRACTS

FORUM ORGANIZERS:

Academy of Sciences of the Republic of Uzbekistan
Institute of Nuclear Physics of Uzbekistan Academy of Sciences
Samarkand State University named after Sharof Rashidov
Institute of Engineering Physics of Samarkand State University

Tashkent - 2024

Academy of Sciences of the Republic of Uzbekistan
Institute of Nuclear Physics of Uzbekistan Academy of Sciences
Samarkand State University named after Sharof Rashidov
Institute of Engineering Physics of Samarkand State University

PHYSICS – 2024

THE THIRD INTERNATIONAL FORUM

April 23-25, 2024

Samarkand, Uzbekistan

BOOK OF ABSTRACTS

Samarkand - 2024

THE THIRD INTERNATIONAL FORUM

PHYSICS – 2024

April 23-25, 2024, Samarkand, Uzbekistan

BOOK OF ABSTRACTS

Institute of Nuclear Physics, Academy of Sciences of Uzbekistan, 2024, 174 pages.

THE THIRD INTERNATIONAL FORUM

PHYSICS – 2024

April 23-25, 2024, Samarkand, Uzbekistan

Organized by

Academy of Sciences of the Republic of Uzbekistan
Institute of Nuclear Physics of Uzbekistan Academy of Sciences
Samarkand State University named after Sharof Rashidov
Institute of Engineering Physics of Samarkand State University

UCHINCHI XALQARO FORUM

FIZIKA – 2024

Aprel 23-25, 2024, Samarqand, O‘zbekiston

TASHKILOTCHILAR:

O‘zbekiston Fanlar Akademiyasi
O‘zbekiston Fanlar Akademiyasi Yadro Fizikasi Instituti
Sharof Rasidov nomidagi Samarqand davlat universiteti
Samarqand davlat universiteti Muhandislik fizikasi instituti

INTERNATIONAL ADVISORY COMMITTEE

Belushkin A. (JINR)
Blagov A. (Russia)
Dadhich N. (India)
Hecker S. (USA)
Kadyrov A. (Australia)
Kaprin A. (Russia)
Kardjilov N. (Germany)
Kovalchuk M. (Russia)
Kucuk N. (Türkiye)
Likhachev A. (Rosatom)
Logachev P. (Russia)
Lubatti H. (USA)
Maksimov V. (Russia)
Mamatkarimov O. (Uzbekistan)
Mustafaev I. (Azerbaijan)
Nasirov A. (JINR)
Penyazkov O. (Belarus)
Rusek K. (Poland)
Sakhiev S. (Kazakhstan)
Trubnikov G. (JINR)
Yuldashev B. (Uzbekistan)
Zakhidov A. (USA)
Zyuzin A. (Canada)

ORGANIZING COMMITTEE

Chairman: Bekhzod Yuldashev
Co-Chairman: Rustam Khalmuradov
Vice-Chairmen: Sirojiddin Mirzaev
Sadulla Bakhramov

Absanov A.
Akhatov A.
Akhmedov B.
Ashurov Kh.
Ashurov M.
Bozorov E.
Egamberdiev Sh.
Eshankulov G.
Khushvaktov Kh.
Kurbanova Z.
Mirtoshev Z.
Olimov Kh.
Parpiev O.
Sadikov I.
Safarov A.
Soleev A.
Tashmetov M.
Usmanov P.

PROGRAM COMMITTEE

Chairman: Ilkham Sadikov
Vice-Chairman: Mannab Tashmetov

Artemov S.
Bakhramov S.
Ibragimova E.
Ismatov N.
Khaydarov R.
Khugaev A.
Khujaev S.
Kulabdullaev G.
Kungurov F.
Kurbanov B.
Kurbanov U.
Makhkamov Sh.
Malikov Sh.
Mukhtarov A.
Nuritdinov I.
Olimov Kh.
Polvonov S.
Tojiboev O.
Turakulov S.
Tursunov E.
Usmanov P.
Vasidov A.

FORUM SECRETARIAT

Samarkand State University, University blv. 15, 140104, Samarkand city

Khursanov Dunyobek, dunyobek_kh@mail.ru, tel:+99893 343 2737

Oblokulov Dilshod, irossu1420@gmail.com; tel:+99866 2403853, +998 93 355 0278

Safarov Askar, askarsafarov@gmail.com; tel: +998 937200303

Institute of Nuclear Physics, Ulugbek, 100214, Tashkent

Fazilova Zekie, fazilovaz@mail.ru, tel.: +99871-2893141 (work); +99893-5576904 (mob.)

Valieva Leyla, vleila@mail.ru, tel.: +99871-2893557 (work); +99897-7660747 (mob.)

https://conference.samdu.uz/ru/index.php

THE THIRD INTERNATIONAL FORUM

PHYSICS – 2024

is sponsored by the following organizations:

"RADIOPREPARAT" Enterprise, Tashkent, Uzbekistan

Gamma systematics Ltd., Tashkent, Uzbekistan

The organizers of the forum thank the sponsors of forum and authors of reports and all participants for their contribution to success of the Forum

PHYSICS - 2024

THE THIRD INTERNATIONAL FORUM

Samarkand, 23-25 April, 2024

PHYSICS - 2024

THE THIRD INTERNATIONAL FORUM

Samarkand, 23-25 April, 2024

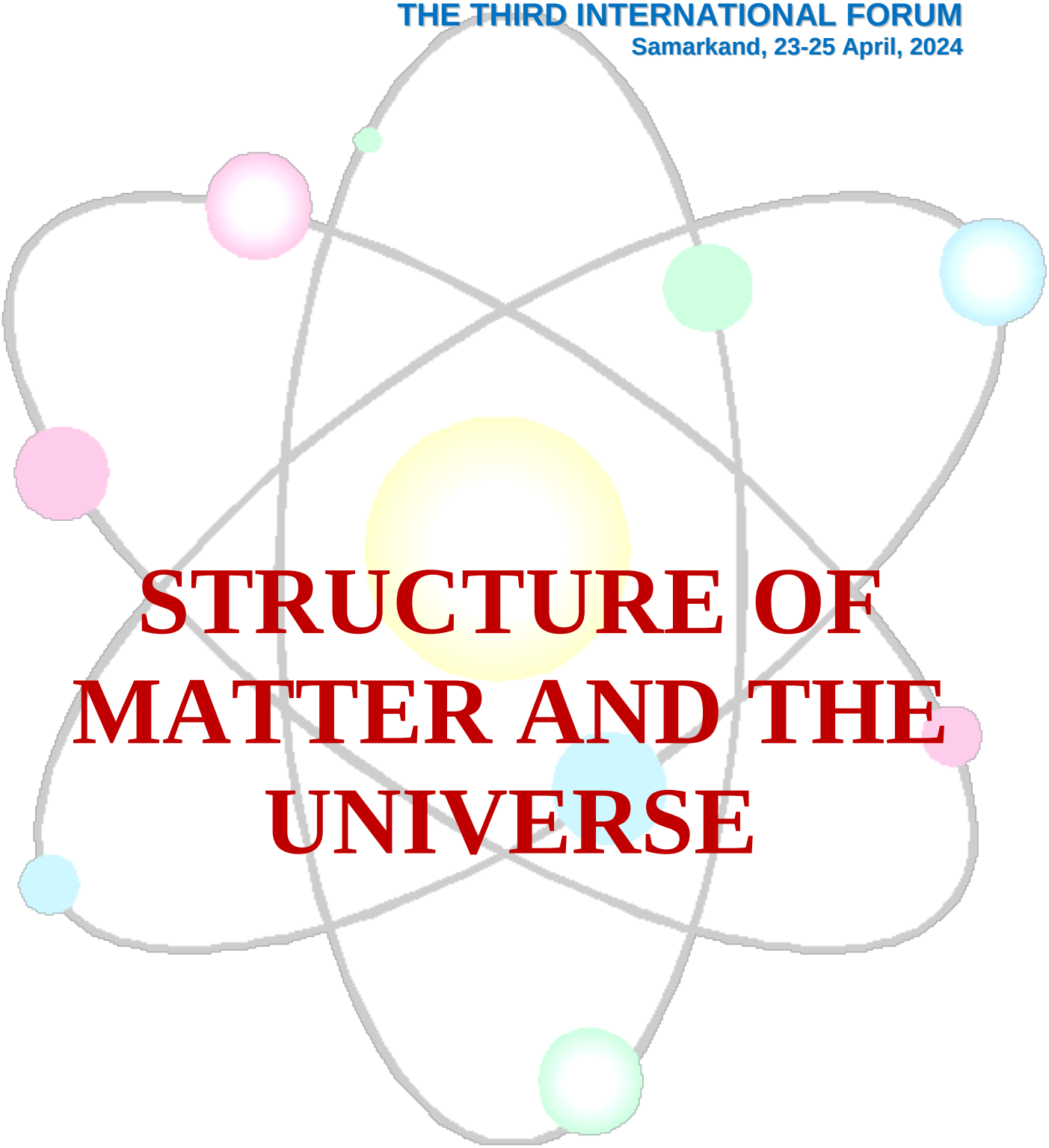

STRUCTURE OF MATTER AND THE UNIVERSE

FIRST EXPERIMENTS AT THE SUPERHEAVY ELEMENTS FACTORY

Voinov A. on behalf of JINR-IMP collaboration
Joint Institute for Nuclear Research, Dubna, Russia

With the recognition of the discovery of the heaviest element Og (Z=118), the filling of the seventh row of the Periodic Table was completed. The synthesis of isotopes of even heavier elements as well as a deeper investigation of the properties of already known nuclei and the production of new isotopes of elements with Z≤118 require a significant increase in the sensitivity of the experiment. For these purposes, a new experimental complex has been developed at FLNR JINR – the Factory of Superheavy Elements (SHE Factory), the basic accelerator of which is the DC280 cyclotron with planned beam intensity ten times higher than that for the existing U400 cyclotron. The first research facility was the Dubna gas-filled recoil separator DGFRS-2, which surpasses the previous separator DGFRS by twice the transmission of synthesized nuclei and by two orders of magnitude greater background particle suppression factors.

To explore the capabilities of the Factory and more detailed study the properties of isotopes of elements Fl, Mc, and their decay products, a series of experiments using a ^{48}Ca beam and targets of enriched isotopes ^{238}U, ^{242}Pu, and ^{243}Am were carried out. The new data on decay properties as of already known heavy isotopes as newly observed in these experiments are presented. The studies demonstrated an enhanced discovery potential of the SHE Factory for further studies of physical and chemical properties of superheavy elements.

Experiments on the synthesis of new elements 119 and 120 are under preparation.

1. Yu.Ts. Oganessian *et al.*, First experiment at the Super Heavy Element Factory: High cross section of ^{288}Mc in the ^{243}Am +^{48}Ca reaction and identification of the new isotope ^{264}Lr, Phys. Rev. C **106**, L031301 (2022).
2. Yu.Ts. Oganessian *et al.*, Investigation of ^{48}Ca-induced reactions with ^{242}Pu and ^{238}U targets at the JINR Superheavy Element Factory, *Phys. Rev. C* **106**, 024612 (2022).

HOW THE UNIVERSE WORKS: NEW COSMOLOGICAL OBSERVATIONAL DATA AND SURPRISES

Ahmedov B.J.
Ulugh Beg Astronomical Institute, Uzbekistan Academy of Sciences, Tashkent, Uzbekistan

The James Webb Space Telescope (JWST) has revolutionized our understanding of the cosmos through its groundbreaking observations, revealing new insights into the fundamental workings of the universe. Recent discoveries with the JWST have provided astronomers with a wealth of cosmological data, uncovering surprises and challenging existing theories.

One of the key findings from JWST observations is the detection of ancient galaxies dating back to the early universe. These observations have shed light on the formation and evolution of galaxies, offering clues about the conditions that prevailed during the universe's infancy. By studying these distant galaxies, astronomers have gained valuable insights into the processes driving cosmic evolution over billions of years.

Additionally, the JWST has played a crucial role in studying the atmospheres of exoplanets,

offering tantalizing glimpses into worlds beyond our solar system. These observations have identified potential signs of habitability and provided vital information about the composition and dynamics of exoplanetary atmospheres. Such discoveries have profound implications for our understanding of the prevalence of life in the universe.

Furthermore, the JWST has contributed to our knowledge of star formation and stellar evolution within our own galaxy and beyond. By peering through cosmic dust clouds and observing stellar nurseries, the telescope has provided unprecedented views of the birth and death of stars, illuminating the processes that shape the cosmic landscape.

In addition to these discoveries, the JWST has unveiled unexpected phenomena and cosmic puzzles, challenging astronomers to rethink existing models of the universe. From mysterious dark matter structures to enigmatic cosmic phenomena, the telescope's observations continue to inspire awe and curiosity, driving forward our quest to unravel the mysteries of the cosmos. The James Webb Space Telescope's recent discoveries have transformed our understanding of the universe, offering new insights into its origins, evolution, and composition. As the telescope continues to probe the depths of space, we can anticipate even more groundbreaking discoveries that will shape our understanding of how the universe works.

Modern astronomical observations on the international level on the ground and space telescopes, and recent discoveries have provided convincing evidence that black holes have a significant impact on nearby objects around, emitting powerful gamma-ray bursts, absorbing the next star, and stimulating the growth of newborn stars in the surrounding areas.

Study the photons motion around rotating black holes, in particular, the discovery and analysis of the form of silhouettes of these objects, setting and effective implementation of relevant radiostronomical observations on the proof of the existence of the black hole horizon and retrieval of information events on the central object in our galaxy within the Black Hole Cam (BHC) and Event Horizon Telesop (EHT) international projects is one of the most important tasks of modern astrophysics. Recently on April 2019 the first image of the 'shadow' of the supermassive black hole candidate in the galaxy M87 has been released by the EHT collaboration. The image shows the distinctive features of a black hole showing an inner edge for the accretion disk and suggesting the existence of an infinitely red-shifted surface.

I will discuss end state of evolution of massive stars, various observational properties of magnetized neutron stars. The energetics of rotating black holes and neutron stars is also in the scope of my talk.

NICA MEGAPROJECT: ACCELERATOR COMPLEX, EXPERIMENTAL FACILITIES, TASKS (BRIEF OVERVIEW)

Merkin M. on behalf of BM@N Collaboration
Moscow State University, D.V. Skobeltsyn Institute of Nuclear Physics, Moscow, Russia

The international mega-science project “NICA complex” is aimed in the study in the даboratory of the properties of nuclear matter in the region of the maximum baryonic density. Such matter existed only at the early stages of the evolution of our Universe and in the interiors of neutron stars. Lattice QCD calculations predict both the deconfinement phase transition and chiral symmetry restoration to be happened at high enough energy densities and there is strong experimental evidence that the deconfined phase of nuclear matter (Quark-Gluon Plasma – QGP) can be created

in ultra-high-energy nuclear collisions. Experimental data on hadron production properties at SPS (CERN) suggest that this transition occurs within the NICA energy range. Moreover, this range is sufficiently large to encompass both, collisions in which the plasma phase is well developed and collisions in which the matter remains purely hadronic throughout. Furthermore, in addition to determining the existence and location of the transition region, it is of fundamental interest to establish the character of the associated phase transformation, namely, whether it remains a smooth cross over, or has become a first-order one, as several models predict. In the latter case, the phase diagram of strongly interacting matter must contain a critical point and its experimental identification forms a focal point for this research field.

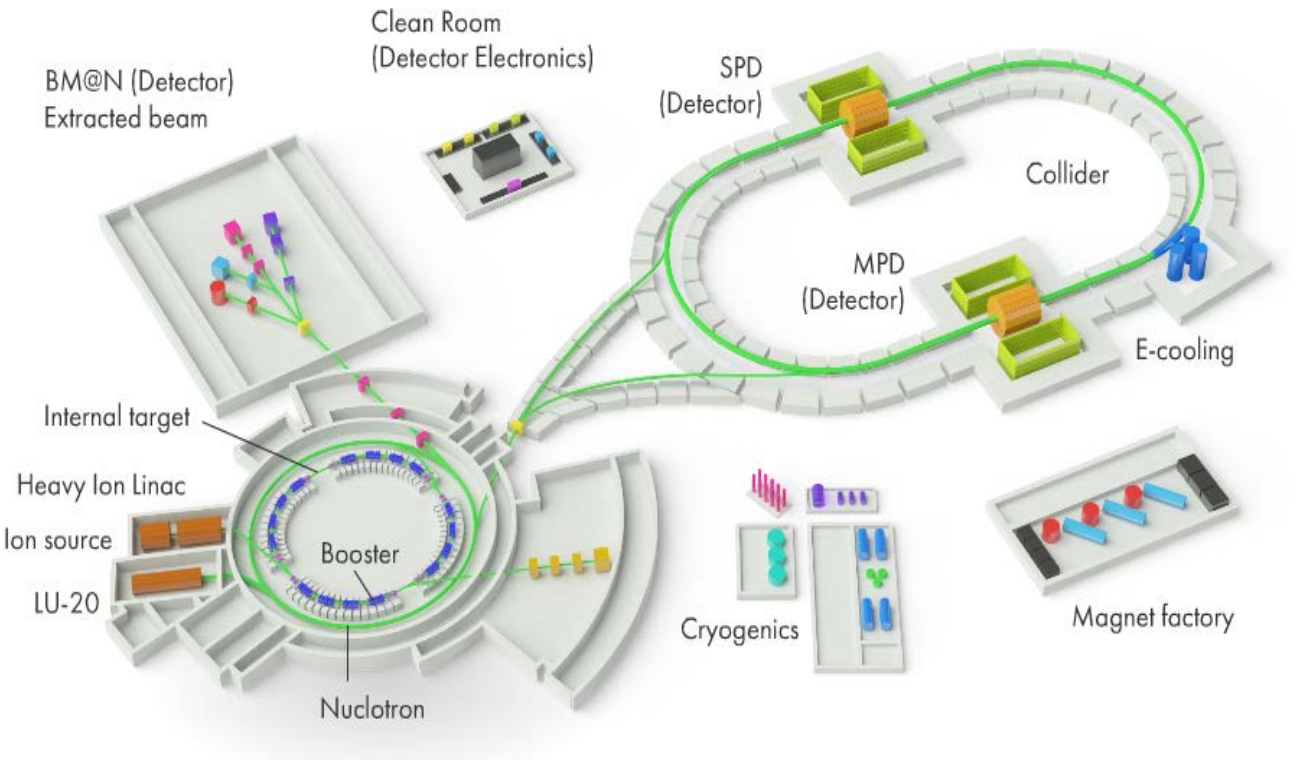

Specific scope elements of the project NICA/MPD facility are expected to include:

- injection complex,
- superconducting Booster synchrotron (that will be located inside the yoke of the decommissioned Synchrophasotron),
- the existing superconducting heavy ion synchrotron Nuclotron (being developed presently to match the project specifications),
- collider having two new superconducting storage rings,
- beam transfer channels.

BM@N EXPERIMENT AT NICA/NUCLOTRON: SCIENTIFIC PROGRAM AND FIRST PHYSICS RESULTS

Kapishin M. on behalf of BM@N Collaboration
Joint Institute for Nuclear Research, Dubna, Russia

The BM@N (Baryonic Matter at Nuclotron) is the first operational experiment at the NICA-Nuclotron accelerator complex. The aim of the experiment is to study interactions of heavy-ion beams with fixed targets. The scientific program of the experiment comprises studies of nuclear matter in the intermediate energy range between experiments at SIS and NICA collider/FAIR facilities. In central heavy nucleus-nucleus collisions at the Nuclotron beam energies, baryon densities of 4-5 of the saturation density are reached. At these densities, the nucleons may already partly overlap, and start to melt into their elementary constituents. The primary goal of the experiment is to constrain the parameters of the equation of state of high-density nuclear matter and to search for the conjectured critical end point and the onset of the deconfinement phase transition. The main aspects of the physics program of the experiment and the relevant observables are discussed.

Earlier, the experiment recorded first data using carbon and argon beams with kinetic beam energies ranging from 2.3 to 4.5 GeV per nucleon. In 2023 the physics run was performed with the 3.8 A GeV and 3.0 AGeV xenon beam. The experiment recorded over 550 million Xe+CsI interactions in a full set of detectors. Now the experiment is on the way to study relativistic interactions of even more heavy nuclei up to Bi+Bi.

First physics results of the experiment are presented on the charged pi+, K+, proton, deuteron and triton yields and their ratios in argon-nucleus interactions at the beam kinetic energy of 3.2 AGeV. Transverse mass distributions, rapidity spectra and multiplicities are measured. The deuteron to proton and triton to proton yield ratios are interpreted within a coalescence approach. The results are compared with theoretical models of relativistic nucleus-nucleus interactions and with the previously published results of other experiments.

HYPERFINE ANOMALIES CALCULATIONS IN SPECTRA OF ATOMS

Demidov Yu.A.[1,2], Konovalova E.A.[1], Holmes S.D.[1,3], Kozlov M.G.[1,2]
[1]Petersburg Nuclear Physics Institute of NRC "Kurchatov Institute", Gatchina, Russia
[2]St. Petersburg Electrotechnical University "LETI", St. Petersburg, Russia
[3]St. Petersburg School of Physics, Mathematics and Computer Science, St. Petersburg, Russia

The study of the properties of short-lived, heavy and superheavy nuclei has enabled atomic physics based tests of nuclear models. To determine the root-mean-square charge radii and magnetic moments of the nuclei, it is necessary to carry out calculations of atoms and ions taking into account relativistic effects, electron correlations and QED corrections. To accurately determine the nuclear magnetic moments, it is necessary to take into account the hyperfine anomaly — the dependence of the hyperfine structure (HFS) constants on the size of the nucleus and on the distribution of the magnetization inside it.

Usually the value of the relative hyperfine structure anomaly $^{A}\Delta^{A'}$ for isotopes A and A' is within the range of $10^{-2} \div 10^{-4}$ and for the short-lived nuclei it is neglected. Correspondingly, uncertainty of the extracted magnetic moments is increased by ~1%. In the most cases it is acceptable in view of the experimental errors. However, there is a marked exception: for gold the anomaly for the isotopes 197 and 198 is known to be huge, $^{197}\Delta^{198}$ = 8.53(8)% [1]. Because of that we need to estimate anomaly for the short-lived isotopes in order to get reliable magnetic moments from the optical experiments. The same situation is realized in neutral potassium [2] and iridium for isotopes with the nuclear spin I = 3/2. These corrections to HFS constants related with changes in charge and magnetization distributions inside the atomic nucleus are extremely large in muonic atoms. In muonic atoms the muon situated in the unscreened field of the nucleus, and muon-electron interactions can be neglected. This makes it possible to calculate the HFS constants with high accuracy and study the magnetic hyperfine anomalies using experimental data.

The report discusses the method of computation of the hyperfine anomaly [2, 3]. We tested this method for the hydrogen-like ions [4]. Calculated hyperfine anomalies in hydrogen-like ions are in good agreement with analytical expressions. After that we calculated hyperfine anomaly for neutral gold, potassium and several muonic atoms.

The work was supported by the Russian Science Foundation grant No. 23-22-00079.

1. C. Ekström et al. Nucl. Phys. A 348, 25 (1980).
2. Yu. A. Demidov et al. Phys. Rev. C, V. 107, P. 024307 (2023).
3. Yu. A. Demidov et al. Pys. Rev. A 103, 032824 (2021).
4. E. A. Konovalova, Yu. A. Demidov, M. G. Kozlov Opt. Spectrosc., V. 128, P. 1530 (2020).

BINDING ENERGY OF ^{14}A NUCLEI BASED ON THE THREE-BODY MODEL

Irgaziev B.F., Yovqochev P.N.
National University of Uzbekistan, Tashkent, Uzbekistan

As is known, light nuclei are well described by the shell model. However, the shell model does not take into account residual interactions between nucleons. It is the residual forces of proton-proton and neutron-neutron pairing that cause the zero spin of a nucleus whose shells are filled. We propose to apply a three-particle model for the ^{14}A nucleus, which we will consider as a system consisting of a ^{12}C core nucleus and two nucleons. The most acceptable approach to solving three-particle problems in nuclear physics is solving the Faddeev equation [1]. However, in the general case, one has to solve a system of two-dimensional differential or integral equations, which become more complicated when taking into account the Coulomb interaction between charged particles. From the point of view of simplicity of solving the problem of bound states of three particles, the method of hyper spherical functions [2,3] is the most convenient.

As an initial stage, we consider the ^{14}C=^{12}C+2n nucleus. We expand the desired three-particle wave function into a system of hyper spherical functions and additionally use the Rayleigh-Ritz variational principle:

$$|\Psi^{JJ_z}> = \sum_\mu c_\mu |\Psi_\mu^{JJ_z}> \quad (1)$$

$$< \delta\Psi^{JJ_z}|H - E|\Psi^{JJ_z}>, \quad (2)$$

where $\delta\Psi^{JJ_z}$ indicates the variation of Ψ^{JJ_z} for arbitrary infinitesimal changes of the linear coefficients c_μ, μ is the index set. The problem of determining c_μ and the energy E is then reduced to a generalized eigenvalue and eigenvector problem of matrix.
The expansion states $|\Psi_\mu^{JJ_z}>$ of Eq. (1) are then given by

$$|\Psi_\mu^{JJ_z}>= \rho^\mu Y_{\{G\}}(\Omega_5), \tag{3}$$

where ρ and $Y_{\{G\}}(\Omega_5)$ are hyper radius and hyper spherical function, respectively. Ω_5 is a five dimensional solid angle. As a result, we obtain a system of linear equations for finding the energy and expansion coefficients:

$$\sum_{K'L'S'l_x'l_y'\nu'} [(< KLSl_xl_y\nu|T-\kappa^2\left|K'L'S'l_x'l_y'\nu'>\right)\delta_{KK'}\delta_{LL'}\delta_{SS'}\delta_{l_xl_x'}\delta_{l_yl_y'} -$$
$$-\frac{2m}{\hbar^2}< KLSl_xl_y\nu\,|V_1+V_2+V_3\,|\,K'L'S'l_x'l_y'\nu'>]c_{\nu'K'L'S'}^{l_x'l_y'}=0, \tag{4}$$

$T=\frac{d^2}{d\rho^2}-\frac{K(K+4)+15/4}{\rho^2}$ is the hyper radial kinetic energy operator, $\kappa=\sqrt{\frac{2m}{\hbar^2}\varepsilon}$ is a wave number for the bound state and V_1, V_2, V_3 are the interaction potentials between particles. .

The calculations use the *n*-*n* potential from article [4] and the ^{12}C-*n* potential from article [5], adjusted to describe low-energy data. We calculate the linear system of Eq. (4) and receive the following results for the ground state energy ($\varepsilon_{12C\text{-}2n}$) of ^{14}C=^{12}C+2*n*.

Set of potentials	Our result for the binding energy (MeV)	Experimental value of the binding energy (MeV)
1	14.32	13.12
2	14.10	

1. L.D. Faddeev, S.P. Merkuriev, Quantum Scattering Theory for Several Particle Systems, Springer, August 31, 1993.
2. Delves, L. M.: Nucl. Phys. **9**, 391 (1959); **20**, 275 (1960).
3. Smith, F. T.: Phys. Rev. **120**, 1058 (1960); J. Math. Phys. **3**, 735 (1962).
4. B. F. Irgaziev, V. B. Belyaev, Jameel-Un Nabi, Phys., Rev.C 87, 035804 (2013).
5. B. F. Irgaziev, Abdul Kabir, Jameel-Un Nabi, Can. J. Phys. **99**, 176-184 (2021).

THE ENERGIES OF THE LOWEST LEVELS OF YRAST BANDS IN EVEN-EVEN TRANSFERMIUM NUCLEI

EfimovA.D.[1,2], Izosimov I.N.[3], Usmanov P.N.[4]
[1]*Admiral Makarov State University of Maritime and Inland Shipping, St.Petersburg, Russia*
[2]*Ioffe Physical-Technical Institute, Russian Academy of Sciences, St.Petersburg, Russia*
[3]*Joint Institute for Nuclear Research, Dubna, Russia*
[4]*Namangan Institute of Engineering and Technology, Namangan, Uzbekistan*

The report discusses some approaches currently being developed to describe the level energies of heavy and superheavy nuclei. Studies of the decay characteristics of transfermium and superheavy nuclei [1], due to the small statistics, make it especially desirable to obtain estimates of the energies of the lowest states of these nuclei. Previously, a correlation was found between the energy of 2^+_1 levels and the deformation energy E_{def}, as well as the systematics of the energy ratios within the rotational bands depending on $E(2^+_1)$ energy. This allowed us to obtain estimates for the energies of the first few excitations, namely, 2^+_1, 4^+_1, 6^+_1 in even-even heavy and superheavy nuclei with Z from 96 to 118 [2]. Similar correlations and corresponding estimates of the level energies were also obtained for the nuclei in the rare earth region [3].

Experiments have shown the importance of high-spin orbitals for the formation and description of decays of high-spin isomers in the transfermium region [4]. In the rotation bands of heavy and superheavy nuclei, there is a special feature - the absence of a reverse bend (backbanding) in the dependence of the moment of inertia from the square of the rotation frequency. The nature of this special feature was considered in the framework of the extended model of interacting bosons in its microscopic version [5]. The expansion of the configuration space due to excitation modes with spins $J^\pi > 10^+$ made it possible to significantly expand the scope of the model both for describing the effects of band crossing and for its absence in this mass region at fairly high spins (up to $I^\pi \leq 34^+$). The fact that some excitation modes not clearly manifested in heavy nuclei up to high spins [5] makes heavy and superheavy nuclei the most suitable for testing of the nuclear models. For example, the two-parameter Harris formula [6,7] describes the rotational energy spectra of these nuclei up to spins $J^\pi < 12^+$ [8,9]. However, the use of the Harris formula does not allow us to describe the high-spin yrast states of the nuclei in the rare earth region.

1. Yu.Ts. Oganessian, Herald of the Russian Academy of Sciences. 90, 207 (2020).
2. A.D. Efimov, I.N. Izosimov, Moscow University Physics Bulletin. 78, 121(2023).
3. A.D. Efimov, I.N. Izosimov, Bull. Russ. Acad. Sci.: Phys. 2024 (in print).
4. K. Rezynkina, et al., Phys.Rev. 97C, 054332(2018).
5. A.D. Efimov, I.N. Izosimov, Phys. At. Nucl. 86, 333(2021).
6. P.N.Usmanov, U.S.Salikhbaev, N.Z. Goibova, Uzbek Journal of Physics. 9(4), 217 (2007).
7. A.A.Okhunov, H.A.Kassim, P.N.Usmanov, Sains Malaysiana. 40 (1), 1 (2011).
8. P.N. Usmanov, I.N. Izosimov, S.B. Bokiev, Proc. of the Intern. Conf. “Fundamental and applied problems of modern physics”, October 19-21, 2023, Tashkent, Uzbekistan, p.69.
9. P.N. Usmanov, I.N. Izosimov, S.B. Bokiev, Proc. of the Intern. Forum “Physics-2022” October 4-5, 2022, Namangan, Uzbekistan, p.135.

IMPACT OF VECTOR MESON POLARIZATION ON ITS INTERACTION WITH MATTER

Gevorkyan S.R., Guskov A.V.
Joint Institute for Nuclear Research, Dubna, Russia

The production of unstable particles off different nuclei provides the possibility to determine the total cross section of the interaction of vector mesons $V = \rho, \omega, \phi, K^*(892), J/\psi$ etc. with nucleons. This interaction is defined by a set of amplitudes that correspond to the transverse (helicity $\lambda = \pm 1$) or longitudinal ($\lambda = 0$) polarization of the vector meson. The total cross section for the interaction of transversely polarized vector mesons with nucleon, $\sigma_T = \sigma(V_T N)$ has been extracted from the coherent photoproduction of vector mesons off nuclei, while the vector meson production in charge exchange reactions as $\pi^{\pm}(K^{\pm}) + A \rightarrow V^0 + A^t$ provides the unique opportunity to obtain the not yet measured total cross section for longitudinally polarized vector meson interacting with nucleon $\sigma_L = \sigma(V_L N)$.

We shortly discuss the importance of the knowledge of σ_L and possibility to extract its value from experiments on nuclear target.

FORMATION OF MULTIPROTON RESONANCE STATES IN NUCLEUS-NUCLEUS INTERACTIONS AT HIGH ENERGIES – HADRONIC MOLECULES

Olimov K.[1], Yuldashev B.S.[2], Olimov Kh.K.[1]
[1]*Physical-Technical Institute, Uzbekistan Academy of Sciences, Tashkent, Uzbekistan*
[2]*Institute of Nuclear Physics, Uzbekistan Academy of Sciences, Tashkent, Uzbekistan*

New experimental data on formation of three- and four-proton resonance states in nucleus-nucleus collisions at high energies are presented. The experimental material was obtained using a 2-meter propane bubble chamber of the High Energy Laboratory of the Joint Institute for Nuclear Research (Dubna, Moscow region, Russia), exposed at the Dubna Synchrophasotron with beams of deuterons, α-particles and carbon nuclei with incident momentum of 4.2 GeV/c per nucleon. The analyzed statistics consists of 7071 d^{12}C-, 11714 α^{12}C- and 20527 ^{12}C^{12}C- collision events.

Formation of three- and four-proton resonance states in the interactions of deuterons, α-particles and carbon nuclei with carbon nuclei at 4.2 A GeV/c was experimentally discovered. The masses, widths (Γ) of mass distributions as well as the inclusive cross section of formation of these resonance states were determined, which turned out to be M(ppp) = 2920 ± 2 MeV, Γ(ppp) = 2.1 ± 0.8 MeV, σ_{incl}(ppp) = 1.8 ± 0.2 mb, M(pppp)=3920 ± 3 MeV, Γ(pppp)=1.8 ± 0.3 MeV, σ_{incl}(pppp)=1.7 ± 0.3 mb.

As can be seen from these results, the inclusive cross sections of formation and the widths (Γ) of these resonances proved to be the same within the limits of statistical errors. It has been shown that a three-proton (four-proton) resonance is observed only in the collision events with four (five) protons in the final state. Based on this fact and taking into account the predominance of the α-cluster structure in the carbon-12 nucleus, it was concluded that the observed resonance states are

likely to be hadronic molecules. The three-proton resonance state is probably formed due to the combination of a two-proton bound state, which is preserved during the destruction of one of the α-clusters, with a proton of another destroyed α-cluster of the carbon-12 nucleus. The four-proton resonance state is possibly formed by combining two pairs of two-proton bound states, which are preserved during the destruction of two α-clusters of the carbon-12 nucleus.

OVERVIEW OF UNSTABLE STATE STUDIES IN FRAGMENTATION OF RELATIVISTIC NUCLEI

Zaitsev A., Zarubin P.
Joint Institute for Nuclear Research, Dubna, Russia
P.N. Lebedev Physical Institute of the Russian Academy of Sciences, Moscow, Russia

Starting with the discovery of the nuclear component of cosmic rays, the nuclear track emulsion method (NTE) makes an opportunity to study the composition of the relativistic fragmentation of nuclei at high-energy accelerators. The promising potential of the relativistic approach to the analysis of ensembles of fragments was manifested in NTE exposed by nuclei at several GeV per nucleon accelerated at the JINR Synchrophasotron and Bevalac (USA) in the 1970s. Since the 2000s of the NTE method is applied in the BECQUEREL experiment at the JINR Nuclotron/NICA in respect to the cluster structure of nuclei, including radioactive ones, as well as the search for unstable nuclear-molecular states. Due to its unique sensitivity and spatial resolution the used NTE method gives an opportunity to study in a unified approach multiple final states arising in the dissociation of relativistic nuclei. The aims to search in the relativistic approach for the α-particle Bose-Einstein condensate (αBEC), an unstable state of *S*-wave α-particles. The extremely short-lived ^{8}Be nucleus is described as 2αBEC, and the ^{12}C(0^{+}_{2}) excitation or Hoyle state (HS) as 3αBEC. The realizability of more complex states is essential in nuclear astrophysics.

Using NTE layers exposed longitudinally to relativistic nuclei the invariant mass of ensembles of He and H fragments can be determined over the emission angles in the approximation of conservation of initial momentum per nucleon. The ^{8}Be and HS decays, as well as ^{9}B → ^{8}Bep decays, are identified in fragmentation of light nuclei by an upper constraint on the invariant mass [1]. This approach has been used to identify ^{8}Be and HS and search for more complex states of αBEC in fragmentation of medium and heavy nuclei. Recently, based on the statistics of dozens of ^{8}Be decays, an increase in the probability of detecting ^{8}Be with an increase in the number of associated α-particles nα was found [2]. The exotically large sizes and lifetimes of ^{8}Be and HS suggest the possibility of synthesizing αBEC by successively connecting the emerging α-particles 2α → ^{8}Be, ^{8}Beα → ^{12}C(0^{+}_{2}), ^{12}C(0^{+}_{2})α → ^{16}O(0^{+}_{6}), 2^{8}Be → ^{16}O(0^{+}_{6}) and further with a decreasing probability at each step, when γ-quanta or recoil particles are emitted. Ongoing investigation aims to measure nα channels of ^{84}Kr fragmentation at energies up to 950 *A* MeV per nucleon to determine the contributions of 2α decays of ^{8}Be, the Hoyle 3α state, and the search for a 4α particle condensate state [3].

1. D.A.Artemenkov et al., Eur. Phys. J. A **56** (2020) 250; arXiv: 2004.10277.
2. A.A.Zaitsev et al., Phys. Lett. B **820** (2021) 136460; arXiv: 2102.09541.
3. D.A.Artemenkov et al., Phys. At. Nucl., **85**, 528 (2022); arXiv: 2206.09690.

BLACK HOLES: HISTORY, CURRENT STUDIES AND FUTURE PROSPECTIVES

Abdujabbarov A.
Ulugh Beg Astronomical Institute, Uzbekistan Academy of Sciences, Tashkent, Uzbekistan

In this talk we offer an in-depth exploration of black holes, tracing their historical discovery, current scientific understanding, and potential future directions. Beginning with the pioneering work of physicists like Albert Einstein and Karl Schwarzschild, it charts the evolution of theories and observations that led to the recognition of these enigmatic cosmic phenomena. Emphasizing key milestones such as the discovery of supermassive black holes at the centers of galaxies and the recent imaging of the shadow of the supermassive black hole in the galaxy M87, the presentation highlights the remarkable progress made in black hole research.

Furthermore, we discuss the current status of black hole science, including ongoing efforts to study their properties, behavior, and interactions with surrounding matter and radiation. It explores cutting-edge observational techniques, such as gravitational wave detection, that have revolutionized our ability to probe black holes and their environments.

Looking ahead, the presentation considers future prospects and avenues of exploration in black hole research. This includes the study of intermediate-mass black holes, the role of black holes in galactic evolution, and the potential implications of black hole mergers for our understanding of fundamental physics and the cosmos at large. Overall, the presentation aims to provide a comprehensive overview of black holes and their significance in astrophysics, cosmology, and beyond.

THE EXPERIMENTAL STUDY OF MULTINUCLEON TRANSFER REACTION

Knyazheva G.N., Kozulin E.M.
Joint Institute for Nuclear Research, Dubna, Russia

During recent years it becomes more evident that multinucleon transfer (MNT) reactions can be considered as the promising way to synthesize and investigate heavy and superheavy elements which cannot be produced in other reaction mechanisms. In the collisions of heavy ions at energies near the Coulomb barrier, the potential energy surface determines strongly the evolution of the nuclear system, driving the interacting system in the direction of decreasing its potential energy in the multidimensional space of collective variables. The appearance of the shell structure in potential energy can lead to an increase in the yield of MNT fragments in the regions of magic nuclei.

In experimental study of mass-energy distributions of the fragments formed in the ^{160}Gd+^{186}W and ^{88}Sr+^{176}Yb reactions near the Coulomb barrier energies [1, 2] with CORSET setup the enhanced yield of products with masses around the closed shells at Z = 82 and N = 82, 126 was found supporting the important role of shell effects in MNT process. It was also shown that the orientation effect caused by the strong deformation of colliding nuclei can result in a gain in the yield of heavy target-like fragments.

The ^{238}U ions are apparently the best bombarding particles in the synthesis of superheavy elements in MNT reactions. However, the production of U beam is available in a few laboratories

now. In this respect, extensive study of the reactions like $^{136}Xe+^{238}U$ and $^{209}Bi+^{238}U$ can be very useful for deeper understanding of the MNT mechanisms and the best planning the future experiments on the production of new heavy isotopes in the reactions with ^{238}U beam.

Primary and secondary mass and energy distributions of projectilelike fragments formed in the $^{136}Xe+^{238}U$ [3], $^{209}Bi+^{238}U$ reactions at the beam energy of 1.11 GeV and 1.85 GeV for ^{136}Xe and ^{209}Bi, respectively, have been experimentally investigated with the multi-arm spectrometer CORSET setup independently and in coincidence with survived heavy targetlike fragments. Since the heavy fragments formed in the MNT reactions are highly excited, the masses, energies and angles of their both sequential fission products have been measured. Our study was organized using two independent experimental techniques, namely, double-arm Time-of-Flight measurements (ToF-ToF method) to investigate the two body coincidences and correlation measurements of three arms combining Time-of-Flight and energy measurements (ToF-E method) to investigate three body coincidences. The obtained experimental results will be presented and discussed.

1. E. M. Kozulin, G. N. Knyazheva, S. N. Dmitriev, I. M. Itkis, M. G. Itkis, T. A. Loktev *et al.*, Phys. Rev. C 89, 014614 (2014).
2. E. M. Kozulin, V. I. Zagrebaev, G. N. Knyazheva, I. M. Itkis, K. V. Novikov, M. G. Itkis *et al.*, Phys. Rev. C 96, 064621 (2017).
3. E.M. Kozulin, G.N. Knyazheva, A.V. Karpov et al, accepted in Phys. Rev. C (2024).

MULTINUCLEON TRANSFER MECHANISM OF COMPLETE FUSION

Nasirov A.K.[1,2], Kayumov B.M.[2,3], Ganiev O.K.[2,3,4], Khusanov E.D.[2,4], Yusupov A.R.[2]
[1]Joint Institute for Nuclear Research, Dubna, Russia
[2]Institute of Nuclear Physics, Uzbekistan Academy of Sciences, Tashkent, Uzbekistan
[3]New Uzbekistan University, Tashkent, Uzbekistan
[4]National University of Uzbekistan, Tashkent, Uzbekistan

The new heaviest chemical elements are synthesized in the collision projectile nucleus with the target nucleus as result of their complete fusion reaction. The nature of the hindrance to complete fusion in the reactions with massive nuclei is of interest of the experimentalists to find favorable pair projectile-target nuclei and beam energy to reach as possible large cross sections in their experiments. A dinuclear system model (DNS) developed by authors has been applied to describe experimental results of the yield of the binary products and evaporation residues [1,2]. The evaporation residue cross sections measured for the $^{48}Ca + ^{243}Am$ reaction leading to superheavy element $^{287\text{-}288}Mc$ (Z=115) described well [1]. The reactions $^{54}Cr + ^{243}Am$ [1] and $^{51}V + ^{248}Cm$ [3] have been theoretically explored to predict the evaporation residue cross sections for the future experiments. The predicted results are 25 fb and 12.5 fb for these reactions, respectively.

But the association of the binary products to the reaction mechanisms of their formation may be ambiguous due to overlapping the mass and charge distributions, i.e. the yield of quasifission products may overlap with the deep-inelastic collision or fusion-fission products registered by the same detectors. The theoretical analysis of the multinucleon transfer between the DNS fragments as function of the kinematics of collision and properties of colliding nuclei leads to interesting and useful conclusions. The hindrance to complete fusion is related with the appearance of the intrinsic fusion barrier, which depends on the orbital angular momentum and mass (charge) asymmetry. As a result the possibility of the yield of the quasifission products increases. The evolution of the charge

and mass distribution between the DNS fragments and yield of the quasifission products have been calculated by the solution of the transport master equations with the nucleon transition coefficients which dependence on single-particle states of nucleons. The experimentally observed yield of the asymmetric fission in the $^{12}C+^{204}Pb$ reaction was 1.5%, whereas it was 30% in the $^{48}Ca+^{168}Er$ case. This difference was interpret as a large contribution of the quasifission products in the $^{48}Ca+^{168}Er$ reaction.

In Ref. [2] we have found a new mechanism of incomplete fusion which is observed at high energies allowing population of the large values (L>30 h) orbital angular momentum L. In collisions with large L, the strong increase of the intrinsic fusion barrier $B^*_{fus}(L)$ occurs and a hindrance to the complete fusion by nucleon transfer appears at the small values of the charge and mass numbers of a cluster (α particle) combined to conjugate nucleus. As a result the α-particle formation probability increases (that has been proved by the solution of the transport master equation) and it removed from the DNS due to centrifugal forces.

Our experience of description of the events of the synthesis of superheavy elements and yields quasifission products convince us that multinucleon transfer is main mechanism of the complete fusion in reactions of the heavy ion collisions.

1. B.M. Kayumov, O.K. Ganiev, A.K. Nasirov, et al., Phys.Rev. C **105**, 014618 (2022).
2. A. K. Nasirov, B. M. Kayumov, O. K. Ganiev, G.A. Yuldasheva, Phys. Lett. **B 842,** 137976 (2023).
3. A. K. Nasirov and B. M. Kayumov, Phys.Rev. C **109**, 024613 (2024).

WHAT IS PRIMARY IN THE UNIVERSE: CENTRAL BLACK HOLES, GLOBULAR CLUSTERS OR GALAXIES?

Nuritdinov S.N., Turaev S.J.
National University of Uzbekistan, Tashkent, Uzbekistan

The term "Central Black Holes" (CBH) refers to two types of black holes (BH):
- Supermassive BH (SBH) with masses $10^6 – 10^{10}M_\odot$ in the nuclei of galaxies;
- Intermediate-mass BH (IMBH) $10^2 – 10^5M_\odot$ in the centers of globular clusters (GC).

Below we have created samples of SBH and IMBH masses and found their correlations with the physical characteristics of the corresponding self-gravitating systems, in the centers of which these CBH are located.

1). SBH masses have been found in a number of works by studying the motion of 'test' bodies around CBH or based on known spectral methods of measuring the width of emission and absorption lines in them. We found that the behavior of the dependence of the SBH mass on the observed physical characteristics of galaxies strongly depends on their morphological type and therefore we further consider only spiral galaxies (SG). We have created a sample of 65 SG with known values of SBH masses and their basic physical characteristics. In this way, we have found empirical dependencies of the SBH mass on the masses of the halo and bulge, on the luminosity of the latter, on the number of GC in SG, on the velocity dispersion in the bulges, etc. Correlation coefficient between the masses of the SBH and the halo is cc = 0.64. It was found that the logarithmic relationship between them has the following form:

$$lg(M_{SBH}/M_{\odot}) = (0.59 \pm 0.15) \cdot lg(M_{HALO}/M_{\odot}) + (6.45 \pm 1.13). \quad (1)$$

In our sample for 54 galaxies, we have been able to determine the GC number N_{GC} in them. In this case, the correlation coefficient is cc=0.86 and the empirical formula has the form:

$$lg(M_{SBH}/M_{\odot}) = (1.15 \pm 0.09) \cdot lg(N_{GC}) + (5.07 \pm 0.20). \quad (2)$$

The strong relationships of the main parameters of the SG subsystems from the mass of the CBH found by us, in our opinion, do not yet fully solve the primacy problem.

2). Peebles and Dicke (1968) first proposed the origin theory of GC, thanks to which they created the hierarchical formation theory of the large-scale structure of the Universe. According to this theory, the GC could be primary. Now when IMBHs have been discovered, this question requires finding exact dependencies of the CBH mass on the physical characteristics of the GC. We have for the first time found a dependence of the IMBH mass on the degree of concentration of stars in the GC to their center. The correlation coefficient between the mass value of the central IMBHs in the GC and concentration parameter (γ) is equal to cc = 0.72 and the empirical formula between them has the following form:

$$lg(M_{IMBH}/M_{\odot}) = -(0.39 \pm 0.08) \cdot \gamma + (0.99 \pm 0.09). \quad (3)$$

There is a correlation between the masses of the GC and the IMBHs (cc =0.69), and the empirical formula:

$$lg(M_{IMBH}/M_{\odot}) = -(1.38 \pm 0.28) \cdot lg(M_{GC}/M_{\odot}) + (1.86 \pm 0.17). \quad (4)$$

We also found dependencies of the IMBH mass on a number of physical characteristics of GC (the absolute magnitude, the Kukarkin index, the radius of their core, the King parameter, etc.). We have shown the absence of a correlation of the IMBH mass from the age of the GC and their metallicity. Despite all this, we believe that it is still too early to answer the question posed by us definitively and it is necessary, first of all, to increase the sample of IMBH masses at least twice.

SPONTANEOUS BREAKING OF VARIOUS SYMMETRIES FOR THE SCALAR THEORY WITH FUNDAMENTAL MASS

Ibadov R.
Samarkand State University, Samarkand, Uzbekistan

V.G.Kadyshevsky [1,2] in the quantum theory of a field on a strict mathematical basis the parameter M - " fundamental mass " which alongside with parameters of the standard quantum theory to play an essential role in physics high energy is entered. We in the given work, we have strived for the connection of the universal constants ($\hbar, c, G$), m_{Planck} - "Plank's mass", m_{maximon}- "maximon" and M -"fundamental mass" on a basis of the spontaneous breaking of symmetry.

The simple examples of spontaneous breaking of various symmetries for the scalar theory with fundamental mass have been considered. Higgs' generalizations on "fundamental mass" that was introduced into the theory on a basis of the five-dimensional de Sitter space. The connection among "fundamental mass", "Planck's mass" and "maximons" has been found. Consequently, the relationship among G- gravitational constant and other universal parameters can be established. The

spontaneous breaking of symmetry is a fundamental concept in theoretical physics, and it occurs in various theories, including the scalar theory with a fundamental mass [1]. Spontaneous symmetry breaking plays a crucial role in understanding the behavior of physical systems and the origin of mass in particle physics. Further exploration and mathematical analysis of specific scalar theories with a fundamental mass can provide deeper insights into the phenomenon of spontaneous symmetry breaking [3]. The mass of elementary particles is the Kasimir's operator of the noncompact Paunkare group, and those representations of the given group, that are being used in Quantum Field Theory (QFT), and it can take any values in the big interval.

Let's consider simple examples of spontaneous breaking of various symmetries for the scalar theory with a fundamental mass [15-18]. The real scalar field, whose Lagrangian can be obtained from the beneath expression:

$$L(x,M) = \frac{1}{2}\left[\frac{\partial\Phi(x)}{\partial x_n}\right]^2 - \frac{1}{2}m^2\varphi^2(x) - \frac{1}{2}M^2[\chi(x) - cos\mu\,\varphi(x)]^2 - \chi(x)U(\varphi(x)),$$

here $cos\mu = \sqrt{1-\frac{m^2}{M^2}}$ where m - mass of particles, described by fields $\varphi, U(\varphi)$- an unknown function characterizing interactions among these particles. Is it possible to select the interaction L_{int} between the fields $\varphi(x)$ and $\chi(x)$ in order that under the exclusion of the field $\chi(x)$, the Higgs potential is appropriate to the field $\varphi(x)$.

The Goldstone scalar mass less particle $\varphi_2(x)$ has appeared as a result of the spontaneous breaking of the symmetry, and a real scalar particle with a mass $m_1 = \frac{\lambda h}{\sqrt{1+\frac{\lambda^2 h^2}{16M^2}}}$. Under $M \to \infty$ from (25) we have $m_1 = \sqrt{2m}$. If we consider the real scalar particle as a maximon, then from (25) we obtain $m_{1\,maximon} = \frac{2M}{\sqrt{\sqrt{2}+125}}$.

1. Kadyshevsky V.G., Nuclear Physics, B141, p.477, 1978,
2. Kadyshevsky V.G. Particles and Nuclei, II, i.1, 1980, p.5. 3.
3. Ibadov R.M., Kadyshevsky V.G, about transformations of supersymmetry in Theories of a Field with Fundamental Mass, Preprint JINR. 2-86-835 Dubna (1986), 4 p.

PHYSICS OF DIMUONS IN THE CMS EXPERIMENT AT THE LHC

Lanyov A.
Joint Institute for Nuclear Research, Dubna, Russia

We present an overview of the recent results by the CMS collaboration on the physics of dimuons in proton–proton collisions at energy of 8 and 13 TeV of the Large Hadron Collider (LHC), starting with the precision measurements of Drell–Yan differential cross sections and rare processes, and extending into the search for narrow heavy resonances and other effects beyond the Standard model of elementary particles in the dimuon channel.

Events in the pair of two-muons $\mu^+\mu^-$ (dimuon) channel are known to be clean from the point of view of searching and identifying particles. This allows them to be effectively used to search for new narrow resonances. In this way, many great discoveries were made in the dimuon channel (J/ψ, ϒ, Z, etc.). Moreover, sometimes these were unexpected findings in search experiments without theoretical predictions. Theoretical calculations of the differential cross section are well-known up to the NNLO order of quantum chromodynamics (QCD).

The CMS collaboration these studied processes in the framework of the Standard model (SM) of elementary particles, as well as searched for processes beyond the SM. The SM measurements were done for the production cross sections of Z and W bosons, differential cross section of the Drell-Yan (DY) process producing dilepton pairs at the hadron collider, DY forward-backward asymmetry, and, in general, angular coefficients in the full angular analysis of polar and azimuthal angles of muons in the $Z \rightarrow \mu^+\mu^-$ decay. In the recent years, an increase in statistics at the LHC made it possible to achieve new results also in the search and analysis of rare decays of heavy states, including study of B^0 meson decays $B^0 \rightarrow \mu^+\mu^-$ which have extremely low branching ratio of the order of 10^{-10}-10^{-9} and are sensitive to physics beyond the SM. Latest CMS results published in 2022 give results of the branching ratio of $B_s{}^0 \rightarrow \mu^+\mu^-$ decay in accordance to the SM prediction. Also, the CMS found a first evidence of rare decay $H \rightarrow \mu^+\mu^-$ with significance 3σ.

We also discuss the development of research of searches for narrow heavy dimuon resonances Z' beyond the SM, their results in the range of invariant masses from several hundred GeV to several TeV, and their interpretation in the framework of new models. Three main models used as theoretical guidelines in this work were the following: Sequential Standard Model (SSM) with the SM-like coupling constants for the new boson; model Z_ψ predicted by the grand unified theories, and Kaluza–Klein graviton excitations arising in the Randall–Sundrum (RS1) model of extra dimensions.

Results and Conclusions

An overview of dimuon physics in the CMS experiment at the LHC is presented. Data with large integrated luminosity were obtained in Run1 and Run2, and physical analysis was carried out in new energy ranges. This allowed to better explore the physics of the Standard Model and set the limits for the New Physics. For the SSM model, the mass limit in the dilepton channel has reached 5.15 TeV and 4.56 TeV for Z_ψ model. Results for other and generalized Z' models have been also published.

New interpretations were proposed for various models and physical variables. While analyzing the Run2 data, the results on the search for new heavy dilepton resonances were also interpreted for the first time in the context of signals from candidate dark matter (DM) particles, using a simplified model with one DM particle and one mediator of interaction between the SM and DM sectors. Also, universality of the lepton flavor was tested for the first time at the TeV energy scale. For the future LHC high luminosity regime, it is expected to reach 7 TeV for the SSM model.

ESTIMATION OF THE WEIGHTS OF THE P AND CP SYMMETRY VIOLATING TERMS IN THE SOLUTIONS OF THE TWO-BODY DIRAC EQUATION FOR THE PARA- AND ORTHO-POSITRONIUM GROUND STATES

Tursunov E.M., Norbutaev Sh.G.

Institute of Nuclear Physics, Uzbekistan Academy of Sciences, Tashkent, Uzbekistan

Positronium is used for the precision tests of the violation of discrete symmetries such as C (charge conjugation), P (spatial parity), T (time reversal) and their combinations. Recent experimental study of the P, T, and CP symmetry violation tests at 10^{-4} precision using linear polarization of photons from positronium annigilations did not indicate a strong evidence of the

violations of above symmetries [1]. These tests confirm the results of previous CP violation search in the ortho-positronium decay with a sensitivity of 2.2×10^{-3} [2].

The para-positronium (*p*-Ps) is the spin singlet, and the ortho-positronium (*o*-Ps) is the spin-triplet bound states of the electron ($\mathbf{e}^-$) and its antiparticle, the positron ($\mathbf{e}^+$). The P-symmetry is defined by the factor $(-1)^{l+1}$, and the C-symmetry is defined by the number $(-1)^{l+S}$, which results in the CP-symmetry eigenvalue of $(-1)^{S+1}$. An important question is, whether it is possible to predict any theoretical limit for the estimates of above discrete symmetry violation tests. A possible limitation of the precision needed for the discrete symmetry violation search would be very useful for planning an experimental setup.

We solve the two-body Dirac equation (TBDE) for the positronium bound states within a new theoretical method. The new method is based on the Dirac Hamiltonian in the form of the 4×4 matrix, each element of which presents a four-component operator. The solution of the two-body Dirac equation for the positronium state with total momentum $\mathbf{J}$ and its projection $\mathbf{M}$ with the couplings $\mathbf{J}=\mathbf{L}+\mathbf{S}$ and $\mathbf{S}=\mathbf{S}_1+\mathbf{S}_2$, can be expressed in the form of a column of four components. Each of the large-large (LL), large-small (LS), small-large (SL) and small-small (SS) components of the eigen function presents a four-component spinor. The radial parts of these components are expressed as linear combination of the harmonic oscillator basic functions. The main advantage of the method is that this form of the Dirac Hamiltonian contains a term responsible for the violation of the P and CP symmetries. Numerical calculations have been performed within the variational method. The energy values of the ground and lowest excited states of the para- and ortho-positronium have been reproduced with a good accuracy. Our estimates for the weights of the P and CP symmetry violating components in the para- and ortho-positronium ground state wave functions are 6.6E-6 and 2.2E-6, respectively. These numbers are less by two-order of magnitude than the precision of current experimental facilities [1].

1. Moskal, P., Czerwiński, E., Raj, J. *et al.* *Nat Commun* **15**, 78 (2024).
2. T. Yamazaki et al. Phys.Rev.Lett. 104 (2010) 083401.

SOME-NUCLEAR REACTIONS OF ASTROPHYSICAL INTEREST

Lukyanov S.M., Penionzhkevich Yu.E.
Joint Institute for Nuclear Research, Dubna, Russia

Nuclear reactions involved in stellar evolution generally occur at energies close to the Coulomb barrier. This property makes their cross sections extremely small. We start with a general discussion of low-energy scattering and transfer reactions, in particular for the nucleosynthesis of the light elements. A specificity of nuclear astrophysics is to require rates of the cross sections of a large number of reactions. These reaction rates are obtained from various sources, experimental as well as theoretical ones.

The formation of ^{12}C is currently well- understood from the triple α process. From the observed abundances of the elements, a gap between masses 5 and 8 is explained by the particle instability of ^{5}He and ^{5}Li. A few nucleons transfer reactions were studied in the reaction with ^{9}Be target. This study shows many interest aspects in which we could not neglect the structure of the nuclei.

Angular distributions for the transfer reactions in collision of ^{2}H, ^{3,4}He and ^{6}Li projectiles on Be target channels were measured. Experimental angular distributions were described within the optical model, the coupled channel approach, and the distorted wave Born approximation. The spectroscopic factors for the systems ^{9}Be =α+ ^{5}He and ^{7}Li = d + ^{5}He are close to unity, which confirms the contribution of the considered cluster configurations to the structure of ground states. The transfer of cluster of 2-neutron system was observed in reactions ^{9}Be(^{3}He,^{6}He)^{6}Be and ^{9}Be(^{6}Li,^{8}Li)^{7}Be.

Neutron dark decays have been suggested as a solution to the discrepancy between bottle an beam experiments, providing a dark matter candidate that can be searched for in halo nuclei. The yield of a free neutron from ^{6}He decay was studied with a goal to find a unique signature for the neutron dark decay. The free neutron in the final state following the decay of ^{6}He into ^{4}He + n + χ provides an exceptionally clean detection signature when combined with a high efficiency neutron detector. Using a high intensity ^{6}He^{+1} beam at the GANIL(France)-JCLab(France)-MSU(USA)-JINR(RF) common experiment to search for a coincident neutron signal resulted in an upper limit on a dark decay branching ratio has been carried out in 2021. We have used our unique neutron detector TETRA and the high intensity and high purity of the SPIRAL1 ^{6}He^{1+} beams to observe this hypothesized decay channel for the first time or set an upper limit to branching ratio and thus help clarify the so-called “ neutron lifetime anomaly”.

The main goal of this presentation is to show the closest relation between nuclear reaction study and astrophysics in field of light elements.

A NEW TYPE OF PARTICLE ACCELERATOR-BASED SIMULATOR OF COSMIC RADIATION FIELDS

Gordeev I.S.
Joint Institute for Nuclear Research, Dubna, Russia

The problem of full-scale ground-based simulation of cosmic radiation fields using heavy ion accelerators for space radiobiology is very relevant. The results of computer Monte Carlo modeling the internal radiation field of the model of habitable module of a spacecraft with a shell of 15 g/cm^{2} Al, generated by particles of galactic cosmic rays during minimum and maximum solar activity are presented. Various accelerator-based approaches of modeling a complex radiation fields are discussed. A new type of cosmic radiation simulator based on a ^{56}Fe ion beam with an energy 1 GeV/n is proposed. The simulator uses rotating converters consisting of segmented targets of various thicknesses, this design ensures the uniformity of the fields of all secondary particles behind the targets using a flat uniform field of primary ^{56}Fe ions. The proposed setup with four replaceable converters makes it possible to simulate not only the distribution of linear energy transfer (LET) of cosmic radiation represented by the galactic cosmic rays (GCR) component, but also to reproduce continuous energy spectra of all charged fragments of a projectile ion from protons up to Co ions.

REACTOR NEUTRINOS FOR APPLIED PROBLEMS AND FUNDAMENTAL PHYSICS

Ponomarev D.
Joint Institute for Nuclear Research, Dubna, Russia

Neutrino physics is one of the most relevant areas of particle physics. The first registration of neutrinos was made in a reactor-based experiment in 1956. Nuclear reactors are the most intense artificial source of neutrinos, making them a valuable tool in the study of this elusive particle. Even at a distance of tens of meters from the reactor, it remains the most powerful source of antineutrinos, two orders of magnitude greater than the neutrino flux from the Sun.

The talk will provide an overview and present recent results of some of the main neutrino experiments on reactors conducted with JINR (Dubna) participation. In particular: an unprecedented accuracy of reactor monitoring at the level of percent was achieved with the use of inverse β-processes induced by reactor antineutrinos in the DANSS experiment at the Kalinin NPP. The fundamental task of detecting neutrinos in reactors now has a new goal: the detection and study of nuclear recoil in the almost zero energy range arising from coherent elastic scattering of neutrino-nucleus (νGeN and Ricochet experiments). The goal is to search for New physics with the highest precision.

PRELIMINARY RESULTS OF OBSERVATIONS OF THE XPM 229-0610636 STAR IN THE STOCK 1 AREA

Parmanova M.[2]., Burkhanov O.[1,2], Karimov R.G.[2]
[1]*Samarkand State University, Samarkand, Uzbekistan*
[2]*Astronomical Institute, Uzbekistan Academy of Sciences, Tashkent, Uzbekistan*

Here we present the results of optical observation of the eclipsing binary star XPM 229-0610636 performed at the Maidanak Observatory in July 2023. The eclipsing binary star XPM 229-0610636 (RA_2000 =19:35:15.769, Dec_2000 = +24:59:41.15), which we chose for research, was discovered in 2024 at the Maidanak Astronomical Observatory [1]. Optical observations were carried out on a 0.5-meter telescope equipped with CCD camera and a Bessell R filter. IRAF (Image Reduction and Analysis Facility) [2] software package designed for astronomical image processing was used for pre-processing of CCD images (removing instrumental artefacts). To carry out photometry of target star, the VaST program [3] was used.

Based on the observational data, it was determined that XPM 229-0610636 has a standard stellar magnitude of 16.23, a variation amplitude of 0.57, and a period of 0.4394 days (10.5456 hours).

Map of an area of the sky with the marked variable star and light curve are shown in Figure 1, the phased light curve is shown in Figure 2.

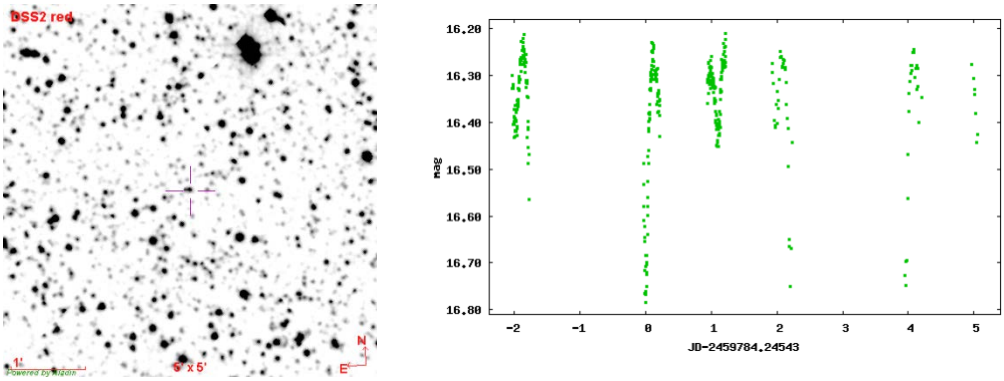

Fig. 1. Map of an area of the sky with the marked variable star XPM 229-0610636 (left) and light curve (right)

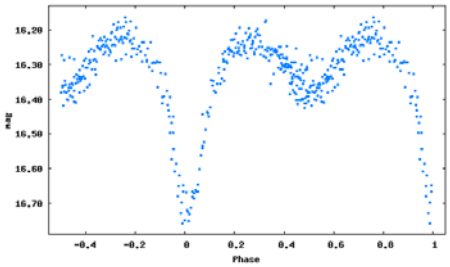

Fig. 2. Phased light curve of XPM 229-0610636

1. Parmanova.M., Gaysin R., Karimov R., Burkhanov O., Satovskiy B., Khafizov B., Ehgamberdiyev S.A. Study of Variable Stars in the Field of Open Cluster Stock 1 // “Peremennye Zvezdy”, Prilozhenie, vol. 24, N 2. 2024
2. IRAF (2022). IRAF Community Distribution https://iraf-community.github.io/
3. https://scan.sai.msu.ru/vast/

STUDYING THE PROPERTIES OF ROTATIONAL LEVELS OCTUPOLE EXCITATIONS ^{236,238}U

Usmanov P.N.[1], Vdovin A.I.[2], Nishonov A.N.[1]
[1]Namangan Institute of Engineering and Technology, Namangan, Uzbekistan
[2]Joint Institute for Nuclear Research, Dubna, Russia

Currently, one of the current areas of research in the field of atomic nucleus structure is the experimental and theoretical study of negative parity states in nuclei of the actinide region. The collective nature of low-lying states of negative parity in actinides was clarified in theoretical studies using the RPA- method. Theoretical predictions are consistent with data obtained using Coulomb excitation.

The most complete results for ^{236,238}U nuclei are presented in [1, 2]. There are four known octupole bands with $K^{\pi} = 0^{-}$, 1^{-}, 2^{-} and 3^{-}. In ^{236}U, data were obtained on the levels of rotational

bands from $K^{\pi}=0^{-}$ to spin $I=21\hbar$, $K^{\pi}=1^{-}$ to $I=5\hbar$, $K^{\pi}=2^{-}$ to $I=3\hbar$ and $K^{\pi}=3^{-}$ to $I=7\hbar$. In the ^{236}U nucleus, experimental data for the ratios $R_{IK}=B(E1;IK\to(I+1)gr)/B(E1;IK\to(I-1)gr)$ are known only for transitions from the octupole states $IK^{\pi}=10^{-}$, 11^{-} and 31^{-}.

In ^{238}U the lowest band with a head energy $E_0=680$ keV with $K^{\pi}=0^{-}$ is traced to spin $I=33\hbar$. In the band with $K^{\pi}=1^{-}$, with a head energy $E_1=931$ keV, levels with even spins known up to $I=28\hbar$ and with odd to $I=3\hbar$. The given probabilities of dipole electrical transitions are known only from the head levels $K^{\pi}=0^{-}$ and 1^{-} bands. The relationships of E1-transitions from $K^{\pi}=0^{-}$ the band are known before spin $I=15\hbar$.

In this work, the energies and electrical characteristics of the octupole states of ^{236,238}U nuclei are studied within the framework of the phenomenological model [3-5], which takes into account the Coriolis mixing of the states of rotational bands. The energies and structure of states of rotational bands with bases $K^{\pi}=0^{-}$, 1^{-}, 2^{-}, 3^{-} and the probabilities of dipole E1- transitions from these states are calculated. Theoretical values of energies, reduced probabilities of E1-transitions and their ratios are compared with experimental data. The agreement between experimental data and theoretical results is good.

1. Sh. Zhu. *Nuclear Data Sheets*, vol.182, pp. 2-129, 2022
2. E. Browne, J. Tuli. *Nuclear Data Sheets*, vol.127, pp. 191-255, 2015.
3. P.N. Usmanov, A.A. Solnyshkin, A.I. Vdovin, U.S. Salikhbaev. *Phys. of Atomic Nuclei*, vol. 77, pp. 1343-1349, 2014.
4. К.Я. Громов, П.Н. Усманов, А.Х. Холматов, Т.А. Исламов, Ю.С. Бутабаев, Р.А. Ниязов. *Изв. РАН. Сер. Физ*, том.56, сс. 36-42, 1992
5. P.N. Usmanov, A.I. Vdovin, A.N. Nishonov. *Bull. Russ. Acad. Sci.: Phys*, vol. 86(8), pp. 1112-1118, 2022.

ANALYSIS OF ENERGY AND ELECTRICAL E2-TRANSITIONS OF POSITIVE PARITY STATES OF ISOTOPES ^{182,184}W

Usmanov P.N.[1], Yusupov E.K.[1], Korjavov M.J.[2]

[1]Namangan Institute of Engineering and Technology, Namangan, Uzbekistan

[2]Karshi Institute of Engineering and Economical, Karshi, Uzbekistan

Complete results on $^{182,184}W$ nuclei are presented in [1,2]. In [3], using the Coulomb excitation method with projectiles ^{58}Ni and ^{136}Xe, the quadrupole collectivity in these nuclei was studied and reduced of electromagnetic matrix elements for low-lying states was experimentally determined. In a separate experiment, the lifetimes were measured for five and eight states ^{182}W and ^{184}W, respectively, using the recoil method after Coulomb excitation by a projectile ^{58}Ni with an energy of 245 MeV. These lifetime measurements are in good agreement with the Coulomb excitation yield measurements. The correlation of the extracted E2 matrix elements is discussed within various collective models.

Experimental values of the energy and probabilities of electrical transitions indicate the presence of deviations from the adiabatic theory.

In [4], a theoretical analysis of the nonlinearity of Mikhailov graphs for interband transitions was carried out. The results obtained on the spectral and electromagnetic properties of tungsten nuclei, the Mikhailov plot for γ→gr transitions in the ^{182}W nucleus has a clearly nonlinear character. Within the framework of perturbation theory, it was shown that the anomaly for interband E2-transitions is due to strong mixing of nearby $\beta-$ and $\gamma-$vibrational states and the difference in the internal quadrupole moments of the bands.

In this work, the energy and electromagnetic properties of the states of positive parity of $^{182,184}W$ nuclei are studied within the framework of a phenomenological model [5-7], which takes into account the Coriolis mixing of states of low-lying rotational bands. The energy, level structure, and reduced probabilities of intraband and interband transitions from $\beta-$ and $\gamma-$vibrational states are calculated. It is shown that the main contribution to the interband probabilities of E2 transitions comes from the m.e. describing transitions between the internal wave functions of the main and other bands included in the basis of the model Hamiltonian. Contribution of part of m.e. associated with internal quadrupole moments is not significant. The calculated values of energies, reduced probabilities E2-transitions and their ratios are compared with existing experimental data, which provide good agreement.

1. Balraj S. // Nuclear Data Sheets, 2015. V. 130, pp. 21-126.
2. Coral M. Baglin// Nuclear Data Sheets, 2010.V. 111, pp. 275-523.
3. Wu C.Y., Cline D., Vogt E.G. and et al. // Nucl. Phys. A, 1991. V. 533. pp. 359.
4. Begjanov R.B., Choriev B.Ch., Korjavov M.J. and Muminov T.M. // Nucl. Phys. A, V. 575, 1994, pp. 237-250.
5. Usmanov P.N., Mikhailov I.N.// Phys. Part. Nucl. 1997, V. 28, pp. 348–373.
6. Usmanov P.N., Vdovin A.I., Yusupov E.K., Salikhbaev U.S.// Phys. Part. Nucl. Lett. 2019, V. 19, pp. 706–712.
7. Usmanov P.N., Okhunov A.A., Salikhbaev U.S., Vdovin A.I.// Phys. Part. Nucl. Lett. 2010, V. 7(3), pp. 185–191.
8. Usmanov P.N., Vdovin A.I., Yusupov E.K. // Bull. Rus. Acad. Scien.: Phys., 2021, V. 85, No 10, pp. 1102-1107.
9. Usmanov P.N., Adam I., Salikhbaev U.S., Solnyshkin A.A. // Phys. Atom. Nucl. 73, 2010, pp.1990-1996.

COMPARISION OF QUASIFISSION FRAGMENTS IN THE $^{12}C+^{204}Pb$ AND $^{48}Ca+^{168}Er$ REACTIONS

Nasirov A.K.[1,2], Khusanov E.D.[2,3]
[1]Joint Institute for Nuclear Research, Dubna, Russia
[2]Institute of Nuclear Physics, Uzbekistan Academy of Sciences, Tashkent, Uzbekistan
[3]National University of Uzbekistan, Tashkent, Uzbekistan

One of the problems of modern physics is for the synthesis of the extremely heavy chemical elements, therefore, the investigation of the target and projectile pair and corresponding range of the beam energy leading to as possible large cross sections of the evaporation residues is an important aim of researchers of nuclear physics.

The experimental and theoretical studies of the peculiarities of the processes occurring in heavy ion collisions are important to establish complete fusion mechanism. It can be done by the

analysis of the observed reaction products. The absence of the full understanding the reaction mechanisms is related with difficulties of the unambiguous identifications of the mechanisms which are responsible for the yield of the corresponding observed reaction products. There is a probability of the overlap of the mass distributions of the contributions from the two mechanisms: for example, the quasifission and fusion-fission mass distributions may overlap in the mass asymmetric part of the yields [1,2].

We have theoretically studied charge and mass distributions of the quasifission fragments for two – ^{12}C+^{204}Pb and ^{48}Ca+^{168}Er reactions – that lead to the same compound nucleus ^{216}Ra* as a function of the orbital momentum of collisions at the beam energies corresponding to the CN excitation energy of around 40 MeV. The experimentally observed yield of the asymmetric fission in the former reaction was 1.5%, whereas it was 30% in the latter case. This difference was interpret as a large contribution of the quasifission products in the ^{48}Ca+^{168}Er reaction. Application of the DNS model has allowed us to establish a nature of hindrance to complete fusion by comparison results of the partial capture cross sections, charge (D_Z) and mass distributions of the DNS fragments before its breakup and quasifission (Y_Z) products obtained for the ^{12}C+^{204}Pb and ^{48}Ca+^{168}Er reactions. The theoretical study of the evolution of the charge (D_Z) distributions of DNS fragments and quasifission (Y_Z) products shows strong influence of the orbital angular momentum of collision (L) on the hindrance of the complete fusion process. The difference in the hindrance observed in these reactions is related by the intrinsic fusion barrier B^{*}_{fus} determined by the driving potential calculated for the reactions leading to formation of the compound nucleus ^{216}Ra*.

The comparisons of the partial capture cross sections and charge (mass) distributions of the quasifission fragments calculated in this work for these two ^{12}C+^{204}Pb and ^{48}Ca+^{168}Er reactions show that the role of the entrance channel characteristics is very strong. This result confirms the conclusion of the authors of Ref. [3].

1. M.Thakur *et al.*, The European Physical Journal A **53**, 133(2017).
2. K. Atreya *et al.*, Phys.Rev. C **108**, 034615 (2023).
3. Y. Chizhov *et al.*, Phys.Rev. C **67**, 011603 (2003).

SYNTHESIS AND STUDY OF THE RADIOACTIVE PROPERTIES OF THE LIGHTEST ISOTOPES OF PLUTONIUM

Kuznetsova A.A.[1], Svirikhin A.I.[1,2], Yeremin A.V.[1,2], Popeko A.G.[1,2], Malyshev O.N.[1,2], Chepigin V.I.[1], Isaev A.V.[1], Popov Yu.A.[1,2], Chelnokov M.L.[1], Tezekbayeva M.S.[1,3], Sailaubekov B.[4], Sokol E.A.[1], Izosimov I.N.[1], Devaraja H. M.[1], Bychkov M.A.[1], Zamyatin N.I.[1], Mukhin R.S.[1,2], Rachkov V.A.[1,2]

[1]Joint Institute for Nuclear Research, Dubna, Russia
[2]State University «Dubna», Dubna, Russia
[3] Institute of Nuclear Physics, Almaty, Kazakhstan
[4]L.N.Gumilyov Eurasian National University, Astana, Kazakhstan

Two new isotopes ^{226}Pu and ^{227}Pu were produced as evaporation residues in the fusion reactions ^{26}Mg+^{204,206}Pb at the gas-filled recoil separator GRAND [1]. An α decay with an energy of E_α = 8156±26 keV and half-life $T_{1/2}$ = 4.1±1.4 s was attributed to ^{227}Pu (see Fig 1). The isotope

^{226}Pu was identified in α decay chain starting with E_α = 8754±24 keV and $T_{1/2}$ = 5.1 ms leading to pile-up of known daughters.

In frameworks experiments at the GRAND and the velocity filter SHELS [2-3] were received new data for isotopes $^{228-230}$Pu and its daughters. Evaporation residues formation cross-section xn, αxn, 2αxn, 3αxn and pxn-channels were measured in reactions ^{26}Mg+^{204,206,208}Pb.

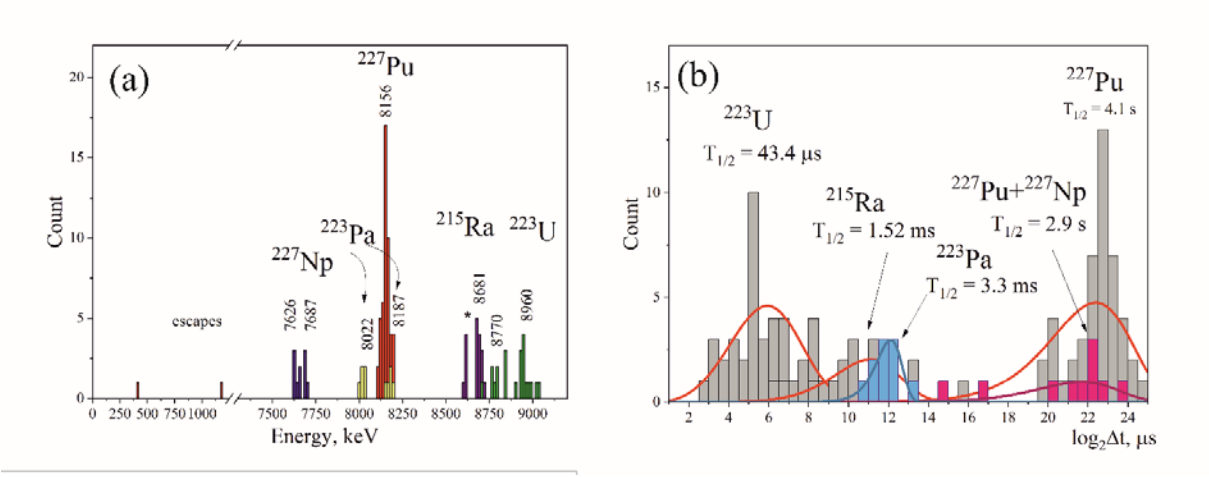

Fig. 1. a) α-spectrum of ^{227}Pu, which was observed in reaction of ^{26}Mg+^{206}Pb by E_b = 140-150 MeV; **b)** Lifetime distributions of ^{227}Pu, ^{223}U and ^{215}Ra.

1. Kuznetsova A.A., Bulletin of the Russian Academy of Sciences: Physics, 2023, Vol.87, No.8, pp.1105–1111.
2. Yeremin, A.V., Popeko, A.G., Malyshev, O.N., et al., Phys. Part. Nucl. Lett., 2015, vol. 12, no. 1, p. 35.
3. Yeremin, A.V., Popeko, A.G., Malyshev, O.N., et al., *Phys. Part. Nucl. Lett., 2015, vol. 12, no. 1, p. 43.*

RESEARCH OF ACCELERATOR DRIVEN SYSTEMS AT JINR

Khushvaktov J.H.[1,2], Adam J.[3,5], Baldin A.A.[1], Baznat M.[1,6], Berlev A.I.[1], Chilap V.V.[4], Furman W.I.[1], Gustov S.A.[1], Katovsky K.[5], Kral D.[5], Paraipan M.[1,7], Solnyshkin A.A.[1], Stegailov V.I.[1], Svoboda J.[5], Tichy P.[3], Tyutyunnikov S.I.[1], Vespalec R.[3], Vrzalova J.[5], Wagner V.[3], Yuldashev B.S.[2], Yudin I.P.[1], Zavorka L.[3], Zeman M.[5]

[1]Joint Institute for Nuclear Research, Dubna, Russia
[2]Institute of Nuclear Physics, Uzbekistan Academy of Sciences, Tashkent, Uzbekistan
[3]Nuclear Physics Institute CAS, Czech Republic
[4]Center of Physical and Technical Projects “Atomenergomash”, Moscow, Russia
[5]Brno University of Technology, Brno, Czech Republic
[6]Institute of Applied Physics ASM, Moldova
[7]Institute of Space Science, Bucharest-Magurele, Romania

In the last two decades, a number of experiments have been carried out at Joint Institute for Nuclear Research by members of the international collaboration “Energy and Transmutation of Radioactive Waste” to test relativistic nuclear technologies in subcritical nuclear systems. These experiments assessed the possibility of energy production and radioactive waste transmutation in subcritical nuclear systems. The “Energy+Transmutation”, “QUINTA” and “BURAN” setups were chosen as subcritical nuclear systems.

The "Energy+Transmutation" setup is composed of four identical hexagonal sections. The central part of each section is formed by a 114 mm long cylindrical lead target of 84 mm in diameter. Each target section is surrounded by the uranium blanket that consists of 30 natural uranium cylinders of 104 mm in length and 36 mm in diameter.

The "QUINTA" setup is composed of 512 kg of natural uranium surrounded by the 10 cm thick lead shielding. The setup is composed of five hexagonal sections (114 mm in length, 350 mm in height) with a 17 mm air gap between each other. The sections are filled with metallic uranium cylinders. Whereas the first section facing the proton (or deuteron) beam contains 54 uranium cylinders (central uranium-free region serves as a beam window), the other sections are composed of 61 cylinders. Each cylinder is 104 mm long and 36 mm in diameter. A total length of the target excluding the lead shielding is 638 mm. For safety reasons, each cylinder is encased in a 1 mm thick aluminium casing. Each section is encapsulated in aluminium as well.

The "BURAN" setup consists of 19.6 tons of depleted uranium, has a diameter of 120 cm and is 100 cm long. The setup has 72 void narrow channels for irradiation of the experimental samples and there is a channel with a diameter of 20 cm in the center of the setup to accommodate a heavy-metal spallation target, which is made either of depleted uranium or lead.

The "Energy+Transmutation", "QUINTA" and "BURAN" (only the central lead part) setups were irradiated with a beam of relativistic particles (protons and deuterons). In these experiments, spallation and fission reactions in heavy nuclei were studied, neutron fluence was measured, the possibility of transmutation of long-lived radionuclides was assessed, heat release inside the targets was measured using thermocouples, calculations were performed and the Monte Carlo simulation codes were tested.

THEORETICAL STUDY OF THE $^{11}B(p,\gamma)^{12}C$ DIRECT CAPTURE REACTION AT LOW ENERGIES WITHIN THE POTENTIAL MODEL

Rakhimov B.A.[1], Tursunov E.M.[1], Baye D.[2]
[1]*Institute of Nuclear Physics, Uzbekistan Academy of Sciences, Tashkent, Uzbekistan*
[2]*Physique Quantique and Physique Nuclaire Thorique et Physique Mathmatique, Universit Libre de Bruxelles, Belgium*

Interest in proton-boron reaction has been increasing for last years although the $p+^{11}B$ fusion is very difficult technically in the thermonuclear plasma environment [1].

The spin-orbit interaction potential is used for the ground $^3P_0(0^+;0)$ and first excited bound states $^3P_2(2^+;0)$ f the ^{12}C nucleus [2]. The initial scattering channels are isotriplets and There are three mixed channels $^3P_0(0^+;1)$, $^3P_1(1^+;1)$ and $^3P_2(2^+;1)$ which are described with the help of tensor term in addition to the central Gaussian potential. The potential parameters in the $^3S_1(1^-;1)$, $^3D_2(2^-;1)$ scattering states have been adjusted with the help of central potentials of the Gaussian form.

The cross section is evaluated within the shell-model coupling scheme. It is used for calculating the astrophysical S factor.

The main contribution to the $^{11}B(p,\gamma)^{12}C$ process is due to the E1 transition from the initial $^3S_1$ scattering state.

1. R.M. Magee, K. Ogawa, T. Tajima *et al.*, First measurements of $p^{11}B$ fusion in a magnetically confined plasma. Nature Commun. 14, 955 (2023).
2. J.H.Kelley *et al.*, Energy levels of light nuclei $A = 12$, Nucl. Phys. A 968, 71 (2017).

SPECTROSCOPIC SIGNATURE OF NONCOVALENT BONDS

Amonov A.[1], Scheiner S.[2], Murodov G.[1], Khushvaktov Kh.[1]
[1]Institute of Engineering Physics of Samarkand State University, Samarkand, Uzbekistan
[2]Department of Chemistry and Biochemistry, Utah State University Logan, USA

A great deal of research over the last few years has turned to a family of noncovalent bonds that are close cousins of the venerable hydrogen bond (HB). These interactions simply replace the bridging proton of an HB by any of a large assortment of atoms, usually but not always, more electro-negative than H. The HB is the prototype for a collection of similar bonds in which the bridging proton is replaced by other atoms, most of which are more electronegative than H. The thiazole molecule presents a fascinating assortment of possibilities. Its five-membered heterocyclic ring contains both a N and S atom. Electron localization function (ELF) of thiazole and molecular electrostatic potential (MEP) diagrams showing in Fig 1.

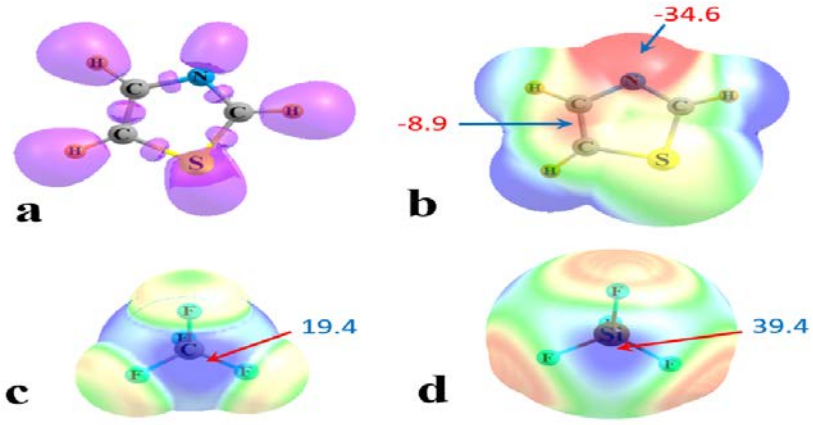

Fig 1. a) ELF diagram showing lone pairs on N and S of thiazole, contour shown is 0.8. Molecular electrostatic potential (MEP) surrounding b) thiazole, c) CF_4, d) SiF_4 on surface corresponding to 1.5 x vdW radii. Blue and red colors respectively indicate positive and negative regions, with extrema of a) +20, -10, b) +10, 0, and c) +13, -6 kcal/mol. Maximum (in blue) and minimum (in red) values displayed in kcal/mol

The work described to explore the entire range of possibilities of bonding arrangements between thiazole and both CF_4 and SiF_4. We have examined these systems in detail and made following conclusions. Firstly, they demonstrate how a molecule like thiazole, with a few electrophilic sites, is able to bind to a simple molecule like CF_4 in a number of entirely different ways. A second important conclusion is connected with the modification that arises when the C of CF_4 is replaced by its Si congener. All of the structures are weakly bound with interaction energies less than 2 kcal/mol. The most stable interaction energy belongs to Si··N tetrel-bond and it is equal to 30.6 kcal/mol.

APPLICATION OF THE TSALLIS DISTRIBUTION FUNCTION IN THE DESCRIPTION OF HEAVY-ION COLLISIONS AT HIGH ENERGIES

Olimov Kh.K.[1], Kakhorova A.N.[2]
[1]*Physical-Technical Institute, Uzbekistan Academy of Science, Tashkent, Uzbekistan*
[2]*Samarkand State University, Samarkand, Uzbekistan*

It is known that in the first fractions of seconds after the Big Bang our universe existed in the form of quark-gluon plasma (KGP) – highly heated, dense and expanding matter. The only way to reproduce such state in laboratory conditions is the collision of heavy ions at high energies in colliders such as the LHC (Large Hadron Collider, CERN, Switzerland) and RHIC (Relativistic Heavy Ion Collider, Brookhaven, USA). As a result of collisions, the temperature, density and other parameters of our universe during the first moments of its existence can be determined. However, it is difficult to directly obtain information about KGP due to the short lifetime of this condition. The characteristics of secondary particles: pions, kaons, protons and antiprotons, such as rapidity and transverse momentum distributions, are sensitive to the nature of the phase transition in nuclear matter and their correct interpretation allows us to obtain information about the KGP.

Phenomenological distribution functions such as the Boltzmann-Gibbs, Tsallis, Hagedorn, Pearson distribution function are using in the describing the transverse momentum distributions of particles produced in the collisions. In this paper, the successes of the thermodynamically consistent Tsallis distribution function with embedded transverse flow, first applied in [1], will be discussed:

$$\frac{d^2N}{2\pi N_{ev} p_T dp_T dy} = C_q \langle\gamma_T\rangle \left(m_T - p_T \langle\beta_T\rangle\right)\left(1+\langle\gamma_T\rangle \frac{(q-1)(m_T - p_T\langle\beta_T\rangle)}{T_0}\right)^{-q/(q-1)} \quad (1)$$

Table 1. Parameters obtained from the combined minimum $\chi 2$ fits of a thermodynamically consistent Tsallis function with an included transverse flow (Eq.(1)) of p_t spectra of particles in Pb+Pb collisions at $(s_{nn})^{1/2}$=2.76 TeV. The combined fitting ranges in p_t are [0.5-3.0] GeV/c for $\pi^+ + \pi^-$, [0.2-3.0] GeV/c for $K^+ + K^-$, and [0.3-4.6] GeV/c for $p+\bar{p}$

Centrality	q ($\pi^+ + \pi^-$)	q ($K^+ + K^-$)	q ($p+\bar{p}$)	T_0 (MeV)	$\langle\beta_T\rangle$	χ^2/ n.d.f
0-	1.084	1.083±	1.082±	7	0.60±0.	1.
5-	1.087	1.086±	1.085±	7	0.58±0.	1.
10-	1.091	1.089±	1.086±	7	0.58±0.	1.
20-	1.097	1.094±	1.089±	7	0.55±0.	0.
30-	1.103	1.099±	1.092±	7	0.52±0.	0.
40-	1.111	1.108±	1.098±	7	0.47±0.	0.
50-	1.118	1.115±	1.103±	8	0.40±0.	0.
60-	1.126	1.124±	1.108±	8	0.33±0.	0.
70-	1.133	1.133±	1.112±	8	0.24±0.	0.
80-	1.139	1.143±	1.114±	8	0.12±0.	0.

1. Olimov Kh. K. et al., Mod. Phys. Lett. A 37, 2250095 (2022).

SCATTERING AND TRANSFER REACTIONS WITH HEAVY IONS AND THEIR ASTROPHYSICAL APPLICATION

Ergashev F.Kh.[1], Artemov S.V.[1], Tojiboev O.R.[1], Karakhodjaev A.A.[1], Igamov S.B.[2], Sakuta S.B.[3], Burtebayev N.[4], Nassurlla Maulen [4], Mauyey B.[5], Amangeldi N.[5], Rusek K.[6], Trzcinska A.[6], Wolinska-Cichocka M.[6], Piasecki E.[6], La Cognata M.[7]

[1]Institute of Nuclear Physics, Uzbekistan Academy of Science, Tashkent, Uzbekistan
[2]Branch of National Research Nuclear University MEPhI, Tashkent, Uzbekistan
[3]National Research Center "Kurchatov Institute", Moscow, Russia
[4]Institute of Nuclear Physics, Almaty, Kazakhstan
[5]L.N.Gumilyov Eurasian National University, Nur-Sultan, Kazakhstan
[6]Heavy Ion Laboratory, University of Warsaw, Poland
[7]Istituto Nazionale di Fisica Nucleare- Laboratori Nazionali del Sud, Catania, Italy

Currently, the most suitable way to obtain information about the structure of light nuclei is direct nuclear reactions with nucleon transfer. Among a number of existing approaches to the analysis of such processes, in recent decades the modified DWBA method has been created and significantly developed, which makes it possible to obtain practically model-free structural quantities important for nuclear theory - asymptotic normalization coefficients (ANC). It allows, in combination with the expansion of the experimental capabilities of accelerator and measuring equipment, to obtain the necessary data on the structure of both ordinary stable and exotic nuclei. A powerful impetus for the development of this method was the possibility of using ANC in calculating cross sections for nuclear astrophysical reactions that are inaccessible for direct measurements at temperatures of the stellar environment (so-called “ANC method”). To obtain data suitable for analysis, precision measurements of experimental differential cross sections for nucleon transfer reactions are necessary at energies close to the Coulomb barrier, where the reactions are peripheral.

This report presents the results of an experimental study of scattering and nucleon transfer reactions on several light nuclei using beams of heavy ions ^{10}B, ^{13}C, ^{15}N and ^{20}Ne. The experimental data obtaining and the following theoretic analysis of the reaction mechanisms, as well as the ANC extracting by the MDWBA method were carried out in collaboration between scientists from Uzbekistan, Kazakhstan, Russia, Poland and Italy at the U-200P cyclotron at the University of Warsaw.

As a result, new experimental data were obtained on the differential cross sections of these processes: the role of channel coupling and transfer of (heavy) clusters was determined, and the dominance of a peripheral nature and a one-step nucleon transfer mechanism in such reactions was revealed. ANCs were obtained for single-particle bound states of ^{12}C, ^{13}N, ^{15}N, ^{17}F and ^{28}Si nuclei. Also, the S-factors and reaction rates of astrophysically important reactions of radiative proton capture at low energies were calculated by the found ANC values.

It has been established that the reactions on heavy ion beams are good tools for accurately ANC obtaining.

PRELIMINARY RESULTS OF ANALYSIS OF ECCENTRIC BINARY SYSTEMS ZTF J200519.89+321314.3

Khamrakulov F.B.[1,2], Burkhonov O.A.[2,1], Satovsky B.L.[3], Lapukhin E.G.[4]
[1]*Samarkand State University, Samarkand, Uzbekistan*
[2]*Astronomical Institute, Uzbekistan Academy of Sciences, Tashkent, Uzbekistan*
[3]*State Space Corporation "Roscosmos", Moscow, Russia*
[4]*Reshetnev Siberian State University of Science and Technology, Krasnoyarsk, Russia*

The selected object is a binary system with an eccentric orbit. Object ZTFJ200519.89+321314.3 discovered by ZTF (Zwicky Transient Facility) [1], type EA, coordinates RA=20:05:19.9 and Dec= +32:13:14.3. The ZTF observations results were downloaded from the link [2] below. Observation results of Maidanak and ZTF were light-curve analyzed using JKTEBOP code [3], orbital and apsidal parameters were calculated. The theoretically calculated model and observational results for each are shown in Figure 1, respectively. The calculated physical parameters of the object are presented in Table 1. The calculated results confirmed the presence of a third body at a long distance of the binary system.

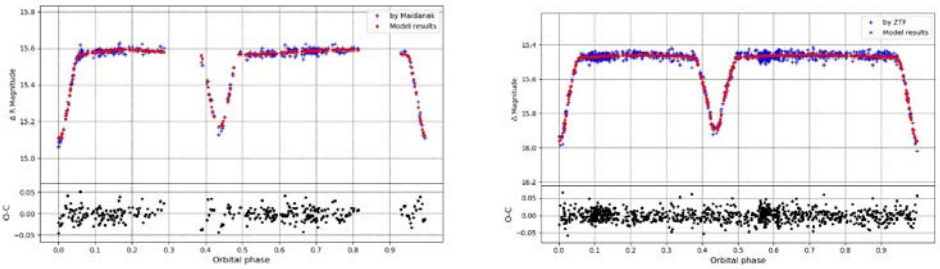

Fig. 1. Maidanak on the right, ZTF on the left, (blue) phase light curve based on the observed result, (red) the theoretically calculated model

Table 1. Parameters measured from the eclipses using the JKTEBOP code

	Final values of the parameters: ZTF J200519.89+321314.3	
Parameter	Maidanak observation results	ZTF observation results
Time of primary eclipse (HJD)	2459780.3323870781±0.00011725	2458366.7001052774 ± 0.000534467
Orbital period (d)	2.1169904710 ± 0.0004759050	2.1193969399 ± 0.0000013279
Orbital inclination (°)	70.876386732 ± 2.8405842369	82.4958545037 ± 0.7384021473
Sum of the fractional radii	0.4638353554 ± 0.0439597057	0.3843795104 ± 0.0162118596
Ratio of the radii	0.512009986 ± 0.000021	0.5110007264 ± 0.000013
e cos ω	-0.0934251606 ± 0.0020609812	-0.0985061063 ± 0.0006977268
e sin ω	0.1699092361 ± 0.0340519640	-0.0714993122 ± 0.1118050306
Central surface brightness ratio	3.4912167970 ± 1.0412540771	0.0736622289 ± 0.0480258518
Third light (L)	1.2309279357 ± 2.288209112	1.5850900739± 0.0593828320
LD (A_1) coefficient c	0.8689162734 ± 0.4968091510	1.0507588561± 0.3557908881
LD (B_1) coefficient α	0.9615311436 ± 0.3791326334	-22.8275639571± 20.7197384832
Derived parameters:		
Fractional radius of star A	0.3092235703 ± 0.0000731	0.2562530070 ± 0.00005003
Fractional radius of star B	0.1546117851 ± 0.0000366	0.1281265035 ± 0.0000501
Eccentricity	0.1939005135 ± 0.00013	0.1217193684 ± 0.00025
Argument of periastron longitude (°)	118.8043418170 ± 0.021	215.9735088444 ± 0.047
Stellar light ratio ℓ_B/ℓ_A	(phase 0.219) 0.8099724996 ±0.0038	(phase 0.2186) 0.2675064417 ± 0.0043

1.Chen, Xiaodian et al. "The Zwicky Transient Facility Catalog of Periodic Variable Stars"// The Astrophysical Journal Supplement Series, Volume 249, Issue 1, id.18
2.http://www.astro.keele.ac.uk/jkt/codes/jktebop.html
3.https://irsa.ipac.caltech.edu/cgi-bin/Gator/nph-scan?mission=irsa&submit=Select&projshort=ZTF

INVESTIGATION OF THE ECCENTRIC BINARY SYSTEM ZTFJ200519.89+321314.3

Khamrakulov F.B.[1,2], Burkhonov O.A.[2,1], Karimov R.G.[2], Lapukhin E.G.[4]
[1]Samarkand State University, Samarkand, Uzbekistan
[2]Astronomical Institute, Uzbekistan Academy of Sciences, Tashkent, Uzbekistan
[3]Reshetnev Siberian State University of Science and Technology, Krasnoyarsk, Russia;

Object ZTF J200601.96+315223.3 discovered by ZTF (Zwicky Transient Facility) [1], type EA, coordinates RA=20:06:01.96 and Dec=+31:52:23.3. The ZTF observations results were downloaded from the link [2] below. Observation results of Maidanak and ZTF were light-curve analyzed using JKTEBOP code [3], orbital and apsidal parameters were calculated. The theoretically calculated model and observational results for each are shown in Figure 1, respectively. The calculated physical parameters of the object are presented in Table 1. Orbital, apsidal and some physical parameters of the object were calculated for the first time. The results of observation between short periods of time confirm small changes in the physical parameters of the object. This is due to the impact of the third body and tidal effect.

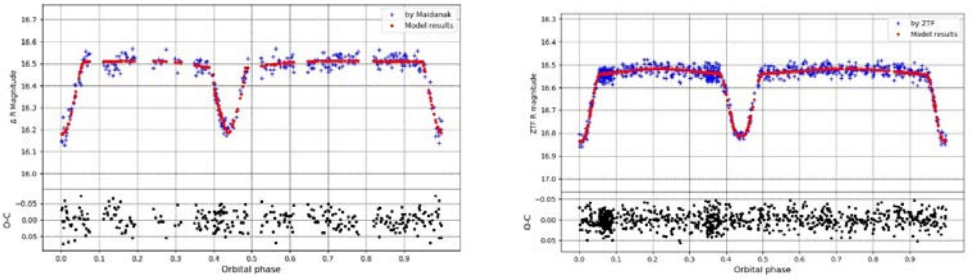

Fig. 1. Maidanak on the right, ZTF on the left, (blue) phase light curve based on the observed result, (red) the theoretically calculated model

Table 1. Parameters measured from the eclipses using the JKTEBOP code

	Final values of the parameters: ZTFJ200519.89+321314.3	
Parameter	Maidanak observation results	ZTF observation results
Time of primary eclipse (HJD)	2459780.2207403630±0.0046464915	2458355.7563223052 ± 0.0013962184
Orbital period (d)	3.4152398148 ± 0.0019879506	3.4159861654 ± 0.0000055710
Orbital inclination (°)	76.6775724563± 2.3612014552	80.5474542955 ± 0.6305881433
Sum of the fractional radii	0.3879628629± 0.0304532247	0.3732430305 ± 0.0072742912
Ratio of the radii	0.584002183 ± 0.000028	0.5910004364 ± 0.000015
e cos ω	-0.0937878341 ± 0.0038754746	-0.0942969289 ± 0.0007796988
e sin ω	-0.2401066432 ± 0.0912890440	0.0266296786 ± 0.0232482388
Central surface brightness ratio	-0.0452377161 ± 0.1214534772	1.0156533609 ± 0.3190378780
Third light (L)	6.0585598608 ± 3.1755051175	-0.8855453505 ± 0.0325634810
LD (A_1) coefficient *c*	0.1187264756 ± 0.7111029305	-0.0343007860 ± 0.1964298312
LD (B_1) coefficient *α*	28.0821850839 ± 64.4728228091	-0.4821498534 ± 0.9080069859
Derived parameters:		
Fractional radius of star A	0.2586419086 ± 0.0000642	0.2724401683 ± 0.00001018
Fractional radius of star B	0.1293209543 ± 0.0000261	0.1008028623± 0.0000341
Eccentricity	0.2577738504 ± 0.00014	0.0979849508 ± 0.00041
Argument of periastron longitude (°)	248.6639322977± 0.0721	164.2301931735± 0.037
Stellar light ratio ℓ_B/ℓ_A	(phase 0.219) 0.105100429 ±0.0012	(phase 0.220) 0.157016809 ± 0.0013

1. Chen, Xiaodian et al. The Zwicky Transient Facility Catalog of Periodic Variable Stars // The Astrophysical Journal Supplement Series, Volume 249, Issue 1, id.18
2. http://www.astro.keele.ac.uk/jkt/codes/jktebop.html
3. https://irsa.ipac.caltech.edu/cgi-bin/Gator/nph-scan?mission=irsa&submit=Select&projshort=ZTF

INVESTIGATION OF Δ^0-ISOBAR FORMATION IN CENTRAL $p^{12}C$- AND $d^{12}C$-COLLISIONS AT 4.2 *A* GeV/c

Sultanov M.[1], Olimov K.[2], Bekmirzaev R.[3], Yuldashev S.[4]
[1]*Samarkand State University of Architecture and Construction, Samarkand, Uzbekistan*
[2]*Physics - Technical Institute, Uzbekistan Academy of Sciences, Tashkent, Uzbekistan*
[3]*Jizzak State Pedagogical University, Jizzak, Uzbekistan*
[4]*Samarkand State University, Samarkand, Uzbekistan*

The study of baryon resonance formation in central hadron and nuclear collisions at intermediate and high energies is also lacking. Previous results on baryon resonances indicate that the mass width of Δ^0-isobars is 20-25% smaller (Γ = 85-95 MeV) than that (Γ = 120 MeV) for isobars produced in nucleon-nucleon or pion-nucleon collisions. The study in [7] investigated the formation of the Δ^0-resonance in the target fragmentation region and the projectile fragmentation region separately, for the first time in $n^{12}C$ collisions at 4.2 *A*GeV/c. The width of the Δ^0-isobar in the fragmentation region of the target was found to be 47 ± 2 MeV, which is 2.5 times smaller than the width of the delta resonance formed in collisions of free nucleons. The hypothesis was put forward that the nuclear potential inside the target nucleus prevents the isobar from decaying before it leaves the nuclear potential. This result suggests that the nuclear potential has a significant effect on the decay of the isobar. The author demonstrated that the lifetime Δ^0 of the isobar formed within the target nucleus is composed of two distinct parts: the time it takes to pass through the nucleus and the time it takes for the free Δ^0-isobar to decay. This study examines the formation of Δ^0 resonances in central $p^{12}C$- and $d^{12}C$- collisions at 4.2 *A* GeV/c.

Experimental material and results. Questions regarding the experiment's methodology are addressed in [1-4]. In this work, we consider the contributions of secondary π^--mesons with a track projection length of less than 4 cm to the momentum characteristics. For π-mesons, only their departure angles were measured, making it impossible to calculate their momenta due to the short track projection length in the chamber's working volume. The momenta of these π^--mesons were reconstructed as follows.The momentum spectra of π^--mesons with track projection lengths greater than 4 cm were divided into 18 histograms based on their departure angle θ ($0 \le \theta \le 180°$) in the laboratory system, with an angular interval width of $\Delta\theta$=10°. As the average number of protons in both collisions was close to 1 (refer to Table), only $p^{12}C$- and $d^{12}C$- collisions with at least ≥3 participating protons were considered central collisions.

Table. Value of mass M_Δ and mass spectrum width Γ Δ^0-isobar

Type of collisions	Mean number of participating protons	M_Δ, MeV	Γ, MeV	χ^2/number degreeoffreedom
$p^{12}C$	0.91±0.01	1235±3	51±6	0.69
$d^{12}C$	1.12±0.01	1234 ±2	44.9±3.8	0.54

1. D. Higgins, *Phys. Rev. D***19**, 731 (1979).
2. K. Olimov et al., Int. J. Mod. Phys. E 29 (2020) 2050058.
3. K. Olimov et al., Int. J. Mod. Phys. E 29 (2020) 2050042.
4. K. Olimov et al., Int. J. Mod. Phys. E Vol. 30, No. 10 (2021) 2150086

CHARACTERISTICS OF $\pi^{\pm}$ MESONS AND PROTONS FROM pC-, dC-, αC-, and CC-COLLISIONS IN RELATION TO THE CENTRALITY DEFINITION AT 4.2 AGeV/c AND THEIR COMPARATIVE ANALYSIS

Sultanov M.[1], Bekmirzaev B.[2], Yuldashev S.[3]
[1]*Samarkand State University of Architecture and Construction, Samarkand, Uzbekistan*
[2]*Jizzax State Pedagogical University, Jizzax, Uzbekistan*
[3]*Samarkand State University, Samarkand, Uzbekistan*

In our work, to determine the degree of centrality of collisions, we take the "net" charge Q: for pC interactions Q = n+- n-- npevp, where n+ and n-are the number of single-charged positive and negative particles in the event, npevp – is the number of evaporating protons; for other collisions Q = n+- n-- nps-nts,where nps and npt are the number of stripping protons from the projectile nucleus and from the target nucleus, respectively. For nps we assume spectator particles with P>3 GeV/c and departure angle Θ<4°. Protons with momentum P<0.3 GeV/c were considered to be spectator protons from the target nucleus. The experimental data are compared with the predictions of the FRITIOF model [1,2], adapted to energies below 10 GeV. As the impact parameter decreases, the number of secondary particles and the number of cascade interactions in the remnant nuclei increase. Therefore, one can expect preferential nucleon births in the fragmentation regions of the nuclei. In central collisions, due to the large number of primary interactions, the nucleon yield in the fragmentation regions should be minimal.

The material obtained on a two-metre propane bubble chamber of the JINR LHE placed in a magnetic field with a strength of 1.5 T and irradiated in a beam of deuteron, helium, and carbon nuclei with a momentum of 4.2 AGeV/c at the JINR synchrophasatron was used for processing. The separation of inelastic interaction events between the colliding nuclei and the carbon nucleus and the introduction of corrections for the number of secondary particles and their momentum and angular characteristics are described in detail in [3-4].

Kinemstical characteristics of charged hadrons. The correlation between the mean momenta of π-mesons and their mean departure angle leads to a weak dependence on Q of the mean transverse momenta of π-mesons for all AC interactions studied by us. For $<p_t>$ π^+ -mesons, a weak (~10%) increase with increasing Q is observed. The vast majority of π -mesons have transverse momentum up to 0.5 GeV/s, nevertheless hard collisions leading to the formation of π -mesons with large pt (0.5-1 GeV/c) take place in the considered interactions. The dependence of the average π-meson velocities on the collision parameter of the studied AC collisions. It can be seen that in peripheral pC-, dC-, and αC collisions (Q<2) π-mesons are formed predominantly in the central fastness region (y=1-1.1). As the collision parameter increases, there is a shift of <y> to the region of smaller values, apparently due to π-mesons formed in secondary nucleon-nucleon collisions (this is clearly seen in pC collisions). In CC collisions, both $<y_{\pi^-}>$ and $<y_{\pi^+}>$ are practically independent of Q.

1. Uzhinskii V.V. Preprint IINR E2-96-192. Dubna. 1996
2. R.T.Glauber, in Lectures in Theoretical Physics. Ed.W.E.Brittin et al, v.1 (Interscience Publishes, N.Y.,1959)
3. BondarenkoA.I.et al., Features of CC interactins at a momentum of 4.2 GeV/c per nucleon fo various degrees of nuclear collision centrality. Phys. Atom. Nucl. 65, 90, (2002).
4. R. N. Bekmirzaev1), M. U. Sultanov, and S. K. Yuldashev. Quark–Gluon String Model and Its Applicationto Inelastic ***d***C Interactions at a Momentum of 4.2 GeV/***c*** per Nucleon.Physics of Atomic Nuclei, 2022, Vol. 85, No. 6, pp. 1011–1016.

SOLITONS IN BOSE-EINSTEIN CONDENSATES: RECENT ADVANCES

Abdullaev F.Kh.
Physical-Technical Institute, Uzbekistan Academy of Sciences, Tashkent, Uzbekistan

In the talk few recent advances in the dynamics of matter wave solitons in BEC are reviewed.

1. Confinement of bright matter-wave solitons on top of a pedestal- shaped potential

Reflection of wave packets from downward potential steps and attractive potentials, known as a quantum reflection, has been explored for bright matter-wave soli- tons and breathers with the main emphasis on the possibility to trap them on top of a pedestal-shaped potential. In numerical simulations with particular parameter settings, we observed that moving solitons return from the borders of the potential and remain trapped for a sufficiently long time.

2. Modulational instability and quantum droplets in a two-dimensional Bose-Einstein condensate

Modulational instability of a uniform two-dimensional binary Bose-Einstein condensate (BEC) in the presence of quantum fluctuations is studied. The analysis is based on the coupled Gross-Pitaevskii equations. It is shown that quantum fluc- tuations can induce instability when the BEC density is below a threshold. The dependence of the growth rate of modulations on the BEC parameters is found.

3. Dynamics of imbalanced quasi-one-dimensional binary Bose-Einstein condensate in external potentials

In the framework of coupled 1D Gross-Pitaevskii equations, we explore the dynamics of a binary Bose-Einstein condensate where the intra-component interaction is repulsive, while the intercomponent one is attractive. The existence regimes of stable self-trapped localized states in the form of symbiotic solitons have been ana- lyzed. Imbalanced mixtures, where the number of atoms in one component exceeds the number of atoms in the other component, are considered in parabolic potential and box-like trap.

PHOTONUCLEAR REACTIONS ON STABLE ISOTOPES OF SELENIUM AT BREMSSTRAHLUNG END-POINT ENERGIES OF 10-23 MEV

Rasulova F.A.[1,2], Aksenov N.V.[1], Alekseev S.I.[1], Aliev R.A.[3,4], Belyshev S.S.[5,6], Chuprakov I.[1,7], Fursova N.Yu.[5,6], Madumarov A.S.[1], Khushvaktov J.H.[1,2], Kuznetsov A.A.[5,6], Yuldashev B.S.[1,2]
[1]Joint Institute for Nuclear Research, Dubna, Russia
[2]Institute of Nuclear Physics, Uzbekistan Academy of Sciences, Tashkent, Uzbekistan
[3]Faculty of Chemistry of M.V.Lomonosov Moscow State University, Moscow, Russia
[4]National Research Center "Kurchatov Institute", Moscow, Russia
[5]Skobeltsyn Institute of Nuclear Physics of Lomonosov Moscow State University, Moscow, Russia
[6]Faculty of Physics of M.V.Lomonosov Moscow State University, Moscow, Russia
[7]Institute of Nuclear Physics, Almaty, Republic of Kazakhstan

In this study, experiments were performed at the beam from the MT-25 microtron using the γ-activation technique. The electron energies were in range of 10-23 MeV with an energy step of 1 MeV. To produce gamma radiation a radiator target made of tungsten, which is a common convertor

material, was used. We used High Purity Germanium γ-detector with resolution of 16 keV at 1332 keV for measuring of induced activity in the irradiated target. Experimental yield data were calculated from the areas of photopeaks in the spectra of residual activity, taking into account the time of death of the detector and the accelerator current during irradiation. The use of the relative yields will make it possible to obtain the dependence of the probability of photonuclear reactions on the maximum energy of bremsstrahlung under different experimental conditions. In our case, the dominant reaction is ^{82}Se(γ,1n)$^{81m+g}$Se. The experimental values of relative yields were compared with theoretical results obtained on the basis of TALYS with the standard parameters and the combined model of photonucleon reactions (CMPR).

Fig. 1 shows the experimental values of the relative yields for the photoproton reactions on natural mixture of selenium, and also, the data computed with the use of the codes TALYS and CMPR. In the case of relative yields for photoproton reactions on the heavy selenium isotopes the theoretical values calculated using CMPR are much larger than the TALYS results. For photoproton reactions on the isotopes of ^{78}Se and ^{80}Se the ratios of theoretical relative yields Y_{relCMPR} / Y_{relTALYS} with increasing energy increase in the range of 3-11 and 11-23, respectively. Experimentally obtained results lie closer to the theoretical curve according to CMPR. Including isospin splitting in the CMPR allows to describe experimental data on reactions with proton escape in energies range from 10 to 23 MeV.

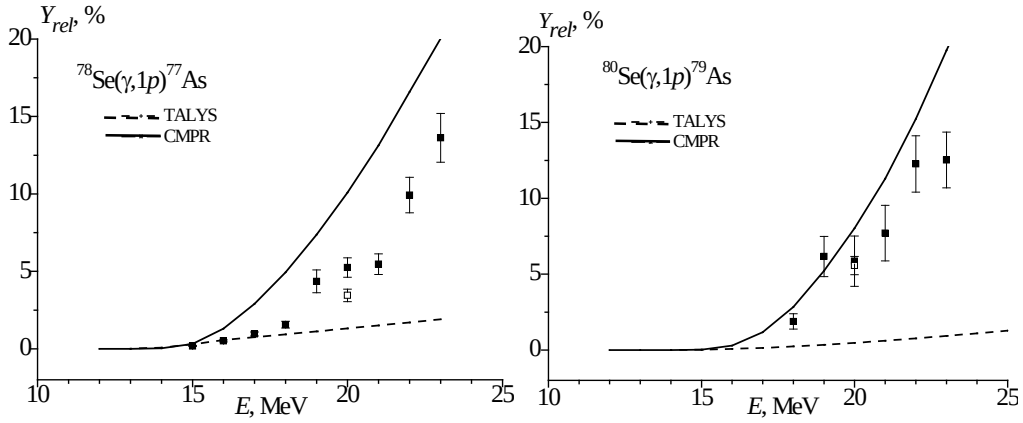

Fig.1. The relative yields of ^{nat}Se(γ,1p) reactions as a function of bremsstrahlung end-point energy from the present work (solid rectangles), literature data (open rectangle) and the simulated values using CMPR (solid line) and TALYS code (dashed line) based on monoenergetic photons

SPECTRA OF THE ENERGY OPERATOR OF FOUR-ELECTRON SYSTEMS IN THE IMPURITY HUBBARD MODEL IN THE THREE-DIMENSIONAL LATTICE. THIRD TRIPLET STATE

Tashpulatov S.M, Parmanova R.T.
Institute of Nuclear Physics, Uzbekistan Academy of Sciences, Tashkent, Uzbekistan

We consider of the energy operator of four-electron systems in the impurity Hubbard model and investigated the structure of essential spectra and discrete spectrum of the system in the three-dimensional lattice for third triplet state of the system. Hamiltonian of the considering system has

the form $H = A\sum_{m,\gamma} a^+_{m,\gamma} a_{m,\gamma} + B\sum_{m,\tau,\gamma} a^+_{m,\gamma} a_{m+\tau,\gamma} + U\sum_m a^+_{m,\uparrow} a_{m,\uparrow} a^+_{m,\downarrow} a_{m,\downarrow}$ $+(A_0 - A)\sum_\gamma a^+_{0,\gamma} a_{0,\gamma} + (B_0 - B)\sum_{\tau,\gamma}(a^+_{0,\gamma} a_{\tau,\gamma} + a^+_{\tau,\gamma} a_{0,\gamma}) + (U_0 - U)a^+_{0,\uparrow} a_{0,\uparrow} a^+_{0,\downarrow} a_{0,\downarrow}$. Here A (A_0) is the electron energy at a regular (impurity) lattice site; $B > 0$ $(B_0 > 0)$ is the transfer integral between electrons (between electron and impurity) in a neighboring sites, $\tau = \pm e_j, j = 1,2,\dots,v$, where e_j are unit mutually orthogonal vectors, which means that summation is taken over the nearest neighbors, U (U_0) is the parameter of the on-site Coulomb interaction of two electrons, correspondingly in the regular (impurity) lattice site; γ is the spin index, $\gamma = \uparrow$ or $\gamma = \downarrow$, and $a^+_{m,\gamma}$ and $a_{m,\gamma}$ are the respective electron creation and annihilation operators at a site $m \in Z^v$. The third triplet state corresponds four-electron states (or anti bound states) to the basis functions: ${}^3t^1_{p,q,r,k\in Z^v} = a^+_{p,\uparrow} a^+_{q,\downarrow} a^+_{r,\uparrow} a^+_{k,\uparrow}$. The subspace ${}^3\mathcal{H}^1_t$, corresponding to the third triplet state is the set of all vectors of the form ${}^3\psi^1_t = \sum_{p,q,r,k\le\in Z^v} f(p,q,r,k)\ {}^3t^1_{p,q,r,k\in Z^v}, f \in l^{as}_2$, where l^{as}_2 is the subspace of antisymmetric functions in $l_2(\left(Z^v\right)^4)$. In this case, the Hamiltonian H acts in the antisymmetric Fock space ${}^3\mathcal{H}^1_t$. Let ${}^3\tilde{H}^1_t$ be the restriction H to the subspace ${}^3\mathcal{H}^1_t$. The third triplet state corresponds the free motions of four-electrons in the lattice and their interactions. Let $\varepsilon_1 = A_0 - A$, $\varepsilon_2 = B_0 - B$, and $\varepsilon_2 = U_0 - U$. The energy of the system depends on its total spin S. The Hamiltonian H acts in the antisymmetric Fock space $\mathcal{H}_{as}$. Let φ_0 be the vacuum vector in the space $\mathcal{H}_{as}$.

Theorem. 1. Let $v = 3$ and $\varepsilon_2 = -B$ and $\varepsilon_1 < -6B$ (respectively, $\varepsilon_2 = -B$ and $\varepsilon_1 > 6B$), then the essential spectrum of the operator ${}^3\tilde{H}^1_t$ is consists of the union of eight segments: $\sigma_{ess}\left({}^3\tilde{H}^1_t\right) = [4A - 24B, 4A + 24B] \cup [3A - 18B + z, 3A + 18B + z] \cup [2A - 12B + 2z, 2A + 12B + 2z] \cup [A - 6B + 3z, A + 6B + 3z] \cup [2A - 12B + z_3, 2A + 12B + z_3] \cup [2A - 12B + z_4, 2A + 12B + z_4] \cup [A - 6B + z + z_3, A + 6B + z + z_3] \cup [A - 6B + z + z_4, A + 6B + z + z_4]$, and the discrete spectrum of the operator ${}^3\tilde{H}^1_t$ is consists of three eigenvalues: $\sigma_{disc}\left({}^3\tilde{H}^1_t\right) = \{4z, 2z + z_3, 2z + z_4\}$, where $z = A + \varepsilon_1$, and z_3 and z_4 same concrete numbers.

2. Let $v = 3$ and $\varepsilon_2 = -B$ and $-6B \le \varepsilon_1 < 0$ (respectively, $\varepsilon_2 = -B$ and $0 < \varepsilon_1 \le 6B$), then the essential spectrum of the operator ${}^3\tilde{H}^1_t$ is consists of the union of three segments: $\sigma_{ess}\left({}^3\tilde{H}^1_t\right) = [4A - 24B, 4A + 24B] \cup [2A - 12B + z_3, 2A + 12B + z_3] \cup [2A - 12B + z_4, 2A + 12B + z_4]$,

and the discrete spectrum of the operator ${}^3\tilde{H}^1_t$ is consists of empty set: $\sigma_{disc}\left({}^3\tilde{H}^1_t\right) = \emptyset$.

LASER SPECTROSCOPIC METHOD FOR OBTAINING HIGHLY PURE SUBSTANCES AT THE ATOMIC-MOLECULAR LEVEL

Eshkabilov N.B., Khaydarov Sh.R., Kurbaniyazov A.S.
Samarkand State University, Samarkand, Uzbekistan

The method of selective stepwise photoionization of atoms (SSPA) with laser radiation, developed for the separation of isotopes [1], makes it possible to develop a new approach to the technology of matter at the atomic-molecular level, when with the help of laser radiation it is

possible to manipulate directly atoms or molecules of a certain type, i.e. that is, to collect macroscopic quantities of a substance one atom at a time or one molecule at a time. The most important process of laser atomic-molecular technology of matter is, undoubtedly, the production of especially pure substances in the atomic state, alloys and films [2]. Estimates show that the optimally chosen SSPA scheme under the influence of two or three laser beams with specifically tuned frequencies and selected intensities makes it possible to ionize each atom in a time of 10^{-5}-10^{-7} s. At 20% of the use of radiation energy with an average power of 10^3 W for photoionization of atoms it is possible to ionize selectively about one mole of a substance per hour. Laser technology for substance purification has a number of significant advantages compared to existing methods of substance purification, based on the difference in any chemical or physical properties of the substance being purified and impurities. Firstly, the degree of purification in the process of isolating a given element from any impurities can reach values of more than 10^3, i.e. if for purification we take mass-produced material with a purity of 10^{-7} %, then the SSPA method can purify it up to 10^{-10} %. Secondly, the method is universal, i.e. practically applicable to any element, regardless of its physicochemical characteristics.

The entire process of SSPA, extraction of ions from the beam and their deposition onto the substrate is carried out in high vacuum. The process does not require contact of the substance to be purified with any reagents or materials, except for the substrate, which can always be used as a material without undesirable impurities. One of the possible applications of highly pure photoionic beams obtained by the SSPA method is the production of complex superlattice-type heterostructures. Currently, the most advanced method is the vacuum epitaxy from molecular beams. However, this method can only create one-dimensional superlattices. For example, alternating layers of $Ga_{1-x}Al_xAs$ with a thickness of 10 $\mathring{A}$ and GaAs with a thickness of 60 $\mathring{A}$ with a total number of layers of about 100. When using photoionic beams of Ga^+, Al^+, As^+ it is fundamentally possible to create three-dimensional heterostructural structures using an electromagnetic focusing and deflection system superlattices. This ability to spatially control deposited ions appears to be fundamentally important for semiconductor nuclear materials technology in the future.

To implement this method, we created a high-temperature atomizer - a source of neutral atoms, based on a tantalum tube with a graphite crucible. The spatial distribution of indium and gallium atoms in an atomic beam has been studied in [3]. The detection of low concentrations of atoms (10^1 -10^2 atom/cm^{-3}) [4] was carried out and the deposition of selected photoionic beams of atoms onto the substrate was realized [5].

1. Letokhov V.S., Moore S.B. Quantum Electronics, 1976, issue 3, pp. 243, 285.
2. Muchnik M.L., et al. Quantum Electronics 1983. v. 10, p. 2331-2335.
3. Eshkabilov N.B., Khaidarov Sh.R. Modern science and nd research.2022 Vol 1. ISSN 2181-3906 p 173-177
4. Eshkabilov N.B., Khaidarov Sh.R. Kurbaniyazov A.S. News of higher educational institutions. Tomsk – 2021. – T. 64. – No. 10. – P 79-85
5. N.B. Eshkabilov, Sh.R. Khaidarov, A.S. Kurbaniyazov A new approach to technologies for obtaining pure substances from rocks using laser radiation . (in print)

INVESTIGATION OF THE TEMPERATURE DEPENDENCE OF THE CENTRALITY OF HeC, CC AND CTA COLLISIONS AT 4.2 GeV/c PER NUCLEON

Sultanov M.U., Usarov U.T.
Samarkand State Architecture and Construction University, Samarkand, Uzbekistan

In this study, the rapidity spectra of secondary hadrons (protons and π^- mesons) were analyzed, focusing on the interpretation of the spectra of protons and π^- mesons. The rapidity spectra of negative pions in dC, CC, and CTa collisions were approximated using a Gaussian function. Experimental data were compared with theoretical predictions made by the Quark-Gluon String Model (QGSM) [1]. The QGSM was found to satisfactorily describe both the width and the central positioning of y_0 rapidity distributions of negative pions in dC, CC, and CTa collisions at 4.2 GeV/c per nucleon. It was observed that the rapidity distributions of protons involved in these collisions underwent significant changes as the centrality of the collisions increased. The QGSM model was able to adequately predict the variation in the shape of the rapidity spectra of the involved protons as the centrality increased in the mentioned collisions.

Key words: Hadron, Spectrum, Participant Protons, Approximation, Rapidity, Momentum

Introduction and Purpouse

Studies of events involving the greatest number of nucleons—participants in the interaction or events related to center collisions of nuclei—are ideal for examining such states. These events are chosen based on several factors. A thorough understanding of the interaction processes of relativistic nuclei requires a thorough investigation of central collisions, as demonstrated by the results presented in these works which include events with a maximum multiplicity of secondary particles or events with a minimum energy flux of secondary particles emitted at zero angle. Both of these situations should, in theory, match the impact parameter $b \to 0$ value.

Materials and Methods

Using the bubble chamber approach in a magnetic field, experimental data on HeC, CC, and CTa interactions at 4.2 GeV/c per nucleon (A GeV/c) were acquired. The JINR High Energy Laboratory provided experimental material on the interactions of ^{4}He and ^{12}C nuclei with carbon and tantalum nuclei (^{181}Ta). The material was obtained using a 2-meter propane bubble chamber, and it was irradiated at 4.2 AGeV/c at the Dubna Synchrophasotron (RF) with ^{4}He and ^{12}C nuclei. Inelastic HeC, CC, and CTA collision statistics make up 11974, 20528, and 2420 of the experimental data examined in this paper. Nearly all secondary charged particles were detected and recorded under 4π geometry circumstances. **Results:** the averaged features of negative pions in the experiment are qualitatively described by the KGSM, with the exception of the average multiplicity of π^--mesons in CTa collisions and their $\langle p_t \rangle$ in all three collision systems.

Discussion and Conclusion

In peripheral, semi-central, and central HeC-, CC-, and CTa-collisions at 4.2 GeV/c per nucleon, the temperatures of the soft and hard components pt of the distributions of π^--mesons depend on the geometry (size) and degree of overlap of colliding nuclei. The degree of overlap of colliding nuclei (i.e., growing collision centrality) and the concomitant rise in the number of involved nucleons and binary collisions cause the differences in temperatures in the collision systems under study to increase.

1. R.N.Bekmirzaev, M.U.Sultanov, and S.K.Yuldashev. Quark-Gluon String model and its application to Inelastic dC Interactions at a Momentum of 4.2 GeV/c per Nucleon. Physics of Atomic nuclei, 2022, vol.85, № 6, pp.1011-1016.

TRES-5B EXOPLANET OBSERVED BY MAIDANAK OBSERVATORY

Ergashev S.Sh.[1], Burxonov O.A.[1,2], Karimov R.G.[2]
[1]Samarkand State University, Samarkand, Uzbekistan;
[2]Astronomical Institute, Uzbekistan Academy of Sciences, Tashkent, Uzbekistan

In this article, the observational data of the exoplanets TrES 5b obtained during the months of May, June, July, August, September, October 2019 were photometrically analyzed and their orbital parameters were found using the observed transits[1]. All observations were made using the 0.6 m Zeiss-600 telescope at the Maidanak Observatory (MO) in Uzbekistan. TrES-5 b is an exoplanet orbiting the TrES-5 system, located approximately 1174.2 light-years (360.0 pc) from the Solar System. His discovery was announced to the public in 2011. The main star TrES-5 has an apparent magnitude of 13.7m, and a full magnitude of 5.9m. It is 0.9 times heavier and 0.9 times larger than our Sun. With spectral types of K1, the surface temperature is 51710 ^{0}C [2]. Table 1 below shows some orbital parameters of TrES 5b determined using AstroImageJ software [3]

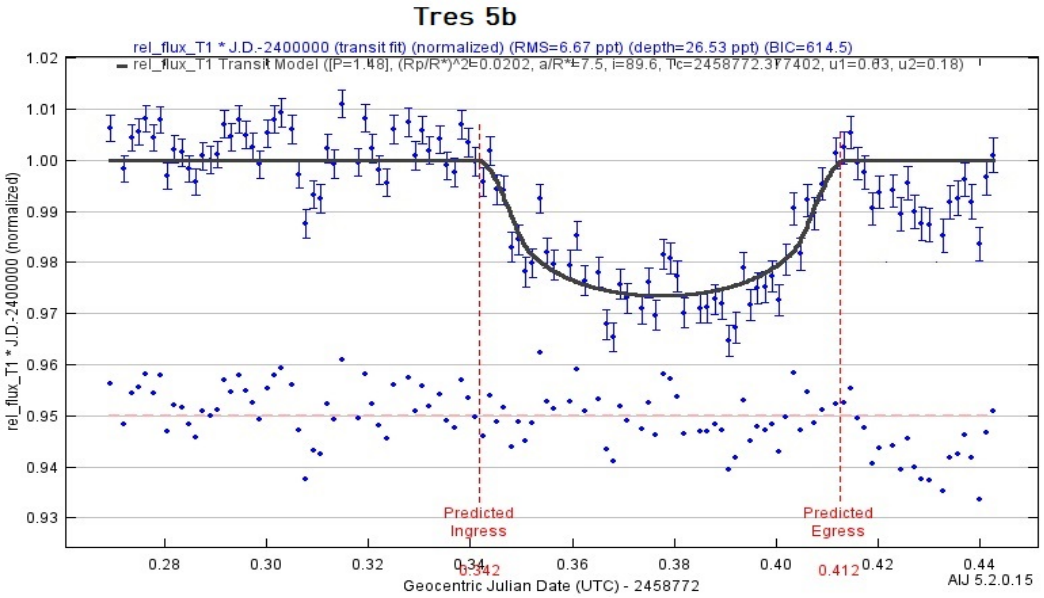

Fig.1. Light curve of TrES 5b

Table 1. Orbital parameters of TrES 5b

Name	Orbital inclination(in degrees)	Radius (in Jupiter radius)	Orbita koeffitsienti a/R*	Transit depth
TrES 5b	84,5085	1,27	6,41579	0,023613

1. Ergashev S.Sh and others "Analysis and results of the light curve of TrES-1b and Qatar-1b" SamSU scientific bulletin № 3/1(139) 2023 118-122p;
2. http://www.exoplanetkyoto.org/exohtml/TrES-5_b.html;
3. https://www.astro.louisville.edu/software/astroimagej;

INTERACTING SPINOR AND ELECTROMAGNETIC FIELDS IN BIANCHI TYPE-I SPACETIME

Saha Bijan
Joint Institute for Nuclear Research, Dubna, Russia
RUDN University, Moscow, Russia

Within the scope of an anisotropic Bianchi type-I (BI) cosmological model an interacting system of spinor and electromagnetic fields is studied. The corresponding field equations are obtained. In some earlier studies it was found that the energy-momentum tensor (EMT) of the nonlinear spinor field possesses nontrivial non-diagonal components in a BI Universe. As a result we come to any of the three possible results: (i) spinor field becomes massless and linear; (ii) the BI space-time transforms into a locally rotationally symmetric (LRS - BI) or (iii) it evolves into a FLRW space-time from the very beginning [1]. On the other hand, if the spacetime in filled with electromagnetic field with induced nonlinearity, it results in the immidiate isotropization [2]. The motivation to consider an interacting system of spinor and electromagnetic fields is to clarify, whether this move can remove the severe restrictions mentioned above.

The interacting system is given in the form

$$L = \frac{i}{2}\left[\bar{\Psi}\,\gamma^{\mu}\nabla_{\mu}\Psi - \nabla_{\mu}\bar{\Psi}\gamma^{\mu}\Psi\right] - m\bar{\Psi}\Psi - \lambda_1 Y(K) - \frac{1}{16\pi}F_{\tau\eta}F^{\tau\eta}X(K), \quad (1)$$

where m is the spinor mass, Y (K) and X (K) ≡ 1 + λ_2Z(K) are the functions of K ={I, J, I + J, I − J}, I = S^2 = $(\bar{\psi}\ \psi)^2$, J = P^2 = $(i\bar{\psi}\ \bar{\gamma}^5\psi)^2$, describe the self-coupling and interaction with the electromagnetic field, respectively. Proper choice of Y (K) can describe different types of matter such as perfect fluid, dark energy etc. The gravitational field we choose in the form

$$ds^2 = dt^2 - a_1^2(t)dx_1^2 - a_2^2(t)dx_2^2 - a_3^2(t)dx_3^2. \quad (2)$$

The electromagnetic 4-potential is taken as Aμ = (0, A1, A2, A3). We assume the spinor and electromagnetics fields be the functions of time only. The nontrivial non-diagonal components of the EMT leads to the following interesting relation between electromagnetic, spinor and gravitational fields:

$$c_1c_2q_1q_2a_1a_2 + c_2c_3q_2q_3a_2a_3 + c_3c_1q_3q_1a_3a_1 = 0. \quad (3)$$

where qi, ci and Ai are the constants related to the electromagnetic and spinor fields, respectively. The corresponding equations are solved numerically.

PACS numbers: 98.80.Cq
Keywords: spinor field; electromagnetic field; energy-momentum tensor

1. Bijan Saha, Astrophys. Space Sci. **357**, 28 (2015);
2. Bijan saha, Phys. Part. Nuclei **49**(2), 146 (2018)
3. Rybakov Yu.P., Shikin G.N., Popov Yu.A. and Bijan Saha, Central European J. Phys. **9**(5), 1165 (2011)

RESEARCH OF GRAVITATIONALLY LENSED QUASARS IN THE FRAMEWORK OF INTERNATIONAL COOPERATION

Asfandiyarov I.M.
Astronomical Institute, Uzbekistan Academy of Sciences, Tashkent, Uzbekistan

One of the current modern areas of astrophysics is the observation and research of gravitational lensed quasars (GLQs). These unique objects, observed exclusively on a cosmic scale, make it possible to directly estimate the Hubble constant H0, calculate the time delay in the GLC, study the effects of microlensing, modeling the distribution of baryonic and dark matter in lensing galaxies, and estimate the size of a quasar black hole.

However, such studies require the best possible angular resolution and long-term monitoring observations with a seeing quality of ~1”, as an example, observations at the Maidanak Observatory of the Academy of Sciences of the Republic of Uzbekistan, which makes it possible to measure the time delay in the GLQs. Also, high-quality images from the Hubble Space Telescope (HST) and spectroscopy from the James Webb Space Telescope (JWST) are needed to model the GLQ. Such comprehensive studies of GLQs are possible only within the framework of international scientific cooperation. Such cooperation is an agreement between the Ulugh Beg Astronomical Institute (UBAI) Laboratory of Astrophysics Ecole Polytechnique Federale of Lausanne (EPFL).

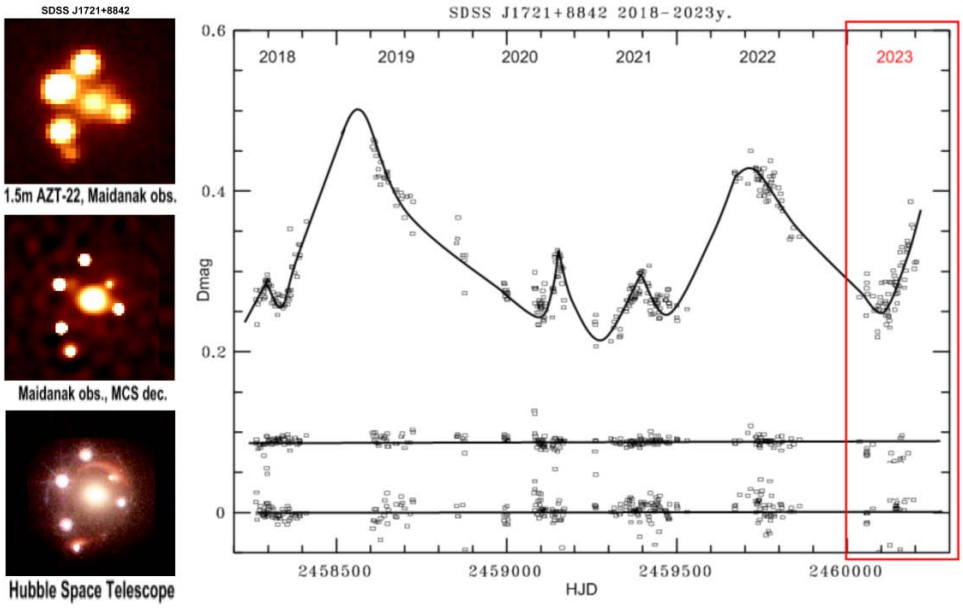

Fig.1. Images of the GLQ SDSS J1721+8842 from the Maidnak observatory with the results of reductions in comparison with the HST and the light curve for 2018-2023

As part of this collaboration between UBAI and EPFL at the Maidanak Observatory on the 1.5m AZT-22 telescope since 2018 monitoring observations of GLQ SDSS J1721+8842, SDSS J1433+6007 and SDSS J2145+6345 are being carried out. A specialized numerical MCS deconvolution method is used to reductions of GLQ images. This method makes it possible to significantly increase the angular resolution, as well as to separate the lensed components of the GLQ for photometry and time delay calculations.

APPLICATION OF INNOVATIVE DIGITAL OBSERVATION METHODS ON MAYDANAK OBSERVATORY TELESCOPES

Asfandiyarov I.M., Baltamuratov J.
Astronomical Institute, Uzbekistan Academy of Sciences, Tashkent, Uzbekistan

The application of modern digital control methods and the digital CCD imaging from telescopes, as well as the ability to analyze images in real time, can significantly improve the quality and quantity of astronomical observations within the framework of international agreements. One of such agreements is BVRI monitoring observations of special double interacting stars at the Maidanak Observatory as part of an international project with the Yunnan Observatory (China). The cooperation is carried out within the framework of the allocated grant from the Ministry of Innovation of the Republic of Uzbekistan AL-5921122128 “Research and observations of special eclipsing binary systems according to LAMOST data on telescopes of Uzbekistan and China”.

At the Astronomical Institute for the ZEISS-600-East telescope at the Maidanak Observatory, a digital fine correction system CS-ET-60 was developed and implemented. This made it possible to improve the quality of observations of double stars within the framework of an international project, as well as to resolve the task of remote control of the telescope’s precise correction from a computer.

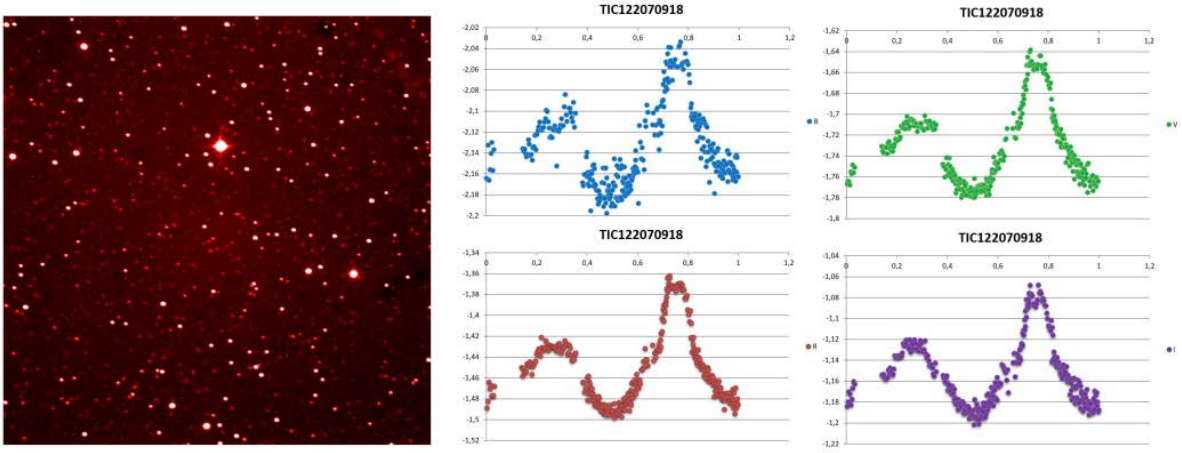

Fig.1. Field of stars long 300 sec. exposures from the Zeiss-600-East telescope and phase light curves of 2023 year monitoring observations of the eclipsing binary star system TIC122070918

Increasing the efficiency and speed of observations under the international project requires further modernization of the telescope through the development of computer-aided design (CAD) methods and 3-D modeling of innovative mechanical and electronic components and using modern technologies. This will make possible the subsequent introduction of modern IT technologies for complete remote control of telescopes. The application of such innovative digital systems will also significantly increase the speed of pointing telescopes to astronomical objects and analyze CCD image data in real time.

INVESTIGATION OF THE EXCITATION OF ISOMERIC STATES IN THE REACTIONS (γ,n), (γ,2n), (γ,p) AND (n,2n) IN THE ENERGY RANGE l0-35 MeV

Polvonov S., Eshonkulov G., Tuymuradov A., Ramazonov A., Tuymurodov D., Ashurov S., Akhmedov S.

National University of Uzbekistan, Tashkent, Uzbekistan

The study of isomeric ratios of yields and cross sections of photonuclear reactions and reactions under the influence of fast neutrons makes it possible to obtain information about the reaction mechanism, in particular, about the moment of inertia of the nucleus, about the spin dependence of the level density and about the nature of transitions between highly excited nuclear states [1,2]. Data on the isomeric ratios of the yields of photonuclear reactions are necessary to replenish nuclear data in this area and to optimize experiments when conducting analytical studies using gamma and neutron activation analysis methods. Long-lived isomers also play a special role in astrophysics, where their existence can influence nucleosynthesis channels.

This work presents the results of studies of the excitation of isomeric states in reactions (γ,n) and (n,2n) on nuclei with $45 \leq A \leq 87$ in the energy range 10-35 MeV, the relative probability of excitation (isomeric ratios of yields and reaction cross sections) of isomeric states. In this mass number region, a change in the shape of the nucleus is observed. These changes affect the probability of excitation of isomeric states of the final nuclei.The experiments were carried out on the NG-150 neutron generator at the Institute of Nuclear Physics of the Academy of Sciences of the Republic of Uzbekistan [3]. The isomeric yield ratios were measured by the induced radioactivity method.

The isomeric cross-section ratios was determined in the case of the reaction (n, 2n). In order to obtain the absolute values of the cross sections for the ground state and for the isomeric state, use was made of methods based comparing the yields of the reaction under study and the monitoring reaction. The reaction $^{27}Al(n,\alpha)^{24}Na$ ($T_{1/2}$ = 15 h, E_γ = 1368 keV)[4].

Cross-sections of reactions $(\gamma,n)^{m,g}$ in the energy range 10-25 MeV with a step of 1 MeV are determined. The experimental received sections of reactions are compared to results of other works and the calculated data which were carried out with use of a software package of TALYS-1.6 [5]. The isomeric ratios of cross-sections of reactions at $E_\gamma=E_m$ are also estimated. The experimental results have been discussed, compared with those of other authors as well as considered by the statistical model [2]. Theoretical values of the isomeric yield ratios have been calculated by using code TALYS-1.6.

1. Palvanov S.R. Physics of Atomic Nuclei, 2014. - Vol. 77, No. 1. - pp. 35.
2. Мазур В.М. ЭЧАЯ. 2000. - Vol. 31, No. 2. - С. 1043.
3. http://www.inp.uz
4. Filatenkov A.A., IAEA Report INDC(CCP)-402. – Vienna: IAEA, 2000. - pp. 1-40.
5. A.J. Koning, J.P. Delaroche. Nucl. Phys. A 713 (2003) 231.

IMPACT OF NOVEL CLADDING MATERIALS ON SMR NEUTRONICS

Tuymuradov A.A., Tuymurodov D.I., Ashurov S.A., Polvonov S.R.
National University of Uzbekistan, Tashkent, Uzbekistan

The advent of novel cladding materials has opened new avenues for improving the neutronic performance of Small Modular Reactors (SMRs). This study presents a comprehensive analysis of the impact of Silicon Carbide (SiC) cladding on the neutronics of an SMR core, using the NuScale Multi-Application Small Light Water Reactor (MASLWR) [1] design as a reference model. Utilizing OpenMC [2], a sophisticated Monte Carlo simulation tool, we assessed the neutron flux distribution and neutron spectrum, comparing the results with those obtained from traditional Zircaloy cladding.

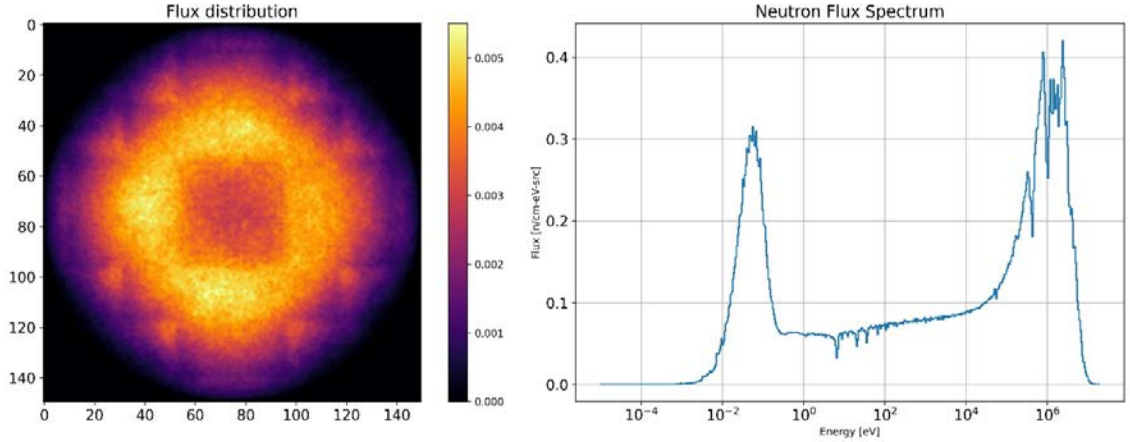

Fig.1. Flux distribution (left), neutron flux spectrum (right)

The flux distribution with SiC cladding shows a high concentration of neutron flux in the core's center with a smooth gradient towards the edges, indicating an efficient moderation and reflection scenario within the SMR core. The neutron flux spectrum reveals a favorable shift with pronounced thermal peaks and moderated fast flux, corroborating SiC's capacity to sustain a desirable neutron economy. These results imply that SiC cladding substantially improves the neutronic performance of SMRs, enhancing the reactor's efficiency and potentially reducing operational costs through prolonged fuel cycles. The findings also suggest an improved safety profile due to the lower hydrogen generation and superior high-temperature resilience of SiC under irradiation conditions.

1. Modro S.M., Fisher J.E. Multi-Application Small Light Water Reactor Final Report (NuScale). December 2003.
2. Romano P., Forget B., Siegel A., and Smith K. (2013). OpenMC: A State-of-the-Art Monte Carlo Code for Research and Development. Annals of Nuclear Energy, 82, 90-97.

SPECTRAL PROPERTIES OF TWO-PARTICLE HAMILTONIANS WITH INTERACTIONS UP TO NEXT-NEIGHBORING SITES

Lakaev S.N.[1], Motovilov A.K.[2,3], Akhmadova M.O.[1]
[1]Samarkand State University, Samarkand, Uzbekistan
[2]Joint Institute for Nuclear Research, Dubna, Russia
[3]Dubna State University, Dubna, Russia

A system of two identical spinless bosons on the one and two-dimensional latticeis considered under the assumption that on-site and first and second nearest-neighboring site interactions between the bosons are only nontrivial and that these interactions are of magnitudes γ, λ, and μ, respectively. A partition of the (γ,λ,μ)-space into connected components is established such that, in each connected component, the two-boson Schrodinger operator corresponding to the zero quasi-momentum of the center of mass has a definite (fixed) number of eigenvalues, which are situated below the bottom of the essential (continuous) spectrum and above its top. Moreover, for each connected component, a sharp lower bound is established on the number of isolated eigenvalues for the two-boson Schrodinger operator corresponding to any admissible nonzero value of the center-of-mass quasimomentum.

PHYSICS - 2024
THE THIRD INTERNATIONAL FORUM
Samarkand, 23-25 April, 2024

PHYSICS OF CONDENSED MATTER

QUANTUM TECHNOLOGIES IN UZBEKISTAN: CURRENT DIRECTIONS AND FUTURE PERSPECTIVES

Zakhidov A.
NanoTech Institute, University of Texas at Dallas, Richardson, USA
Samarkand Quantum Center, Samarkand State University, Samarkand, Uzbekistan
Quantum Technology Center, NRU TIIAME, Tashkent, Uzbekistan

Modern world entered the age of Quantum technologies. And last year Uzbekistan joined the world quantum tech race by creating two quantum centers: first SQC has been founded in Samarkand State University in August of 2023 and little later QTC in Tashkent in NRU TIIAME. Surprisingly it was initiated not by physicists but by technologists: rector of SamSU and supported by Ministry of Science. Why everyone is so anxious, about Quantum Physics again, despite the fact that quantum physics is already 100 years old. It is all due to Second Quantum Revolution (SQR), which is one of most important challenges in modern physics, as was atomic project in mid-40-s .

If First quantum revolution (FQR) of 1925-s was about manipulation of **many degrees** of freedom, which led to development of Transistors, Lasers, Quantum electronics, computer chips, and most of modern technology, now we are in era of Second Quantum Revolution, that started with invention of ideas of Quantum Algorithms and Quantum computations around 1991, SQR is about manipulation of **individual quantum states** in order to run Quantum computers, Quantum sensors Two new physical concepts are key here: (as compared to earlier FQR): Quantum **superposition** (**basis of Qubit**) and Quantum **entanglement** (basis of Quantum cybersecurity and quantum telecommunications). I will briefly describe the goals of SQC, which are mostly related to search and study of quantum materials, that have long coherence time for operation of Qubits. Our major goal here is to develop Qubits, that can operate at high enough temperatures, as opposed to superconducting qubits (developed by Google and IBM for their QC) that operate in millikelvin cryogenic temperatures. One challenge here is Polaritonic Qubit, based on 2-dimensional perovskites. Another targets are Quantum Dots, that can be used for single photon emitters for photonic Qubits and also for energy devices. On the other hand major challenges of QTC in TIIAME are related with quantum telecommunications, Quantum algorithms for massive optimization tasks in Energy grids and Water networks, that are both critically important for Uzbekistan. I will then describe in more detail the near goals of SQC in creating energy conversion devices, based on perovskite Quantum Dots (QDs). One such device is envisioned as Transparent Solar window with QD-luminescent concentrators sketched at Fig. below (with permission of our partners in UbiQD). Another concept is based on QDs embedded into polymeric films for transformation of solar spectrum into light favorable for control of temperature in houses and can find practical application in smart green houses.

ROLE OF MODERN ELECTROPHYSICS IN PROMISING AVIATION TECHNOLOGIES

Khomich V.Yu.
Institute for Electrophysics and Electric Power of Russian Academy of Sciences, St. Peterburg, Russia

With the growth of cities and the increase in air travel, the problem of reducing harmful emissions into the atmosphere, reducing noise and vibration becomes more urgent every year. Given the continued growth trends in air transport, the aviation sector will increasingly become a significant source of greenhouse gases, and their impact on local air quality and global climate change is expected to increase in the future.

To solve the described problems, the principles of “green aviation” have been developed, based on optimizing flight schedules, changing the design of aircraft, using lightweight composite materials, changing the operating principle and design of aircraft and the fuel used, etc. Most of the promising aviation technologies are inextricably linked with the achievements of modern electrophysics. The future aircraft is a fully electric one, or at list hybrid or more electric one. The main advantages of such aircrafts are the absence of harmful emissions and the ability to recharge batteries during flight. But today there are only low-power electric aircraft due to the high cost of the battery, its short service life, long charging time, which leads to short flight range. By using a hybrid powertrain in aircraft, it is possible to increase the range and significantly reduce emissions from fuel combustion and noise from aircraft. This can be done if the aircraft uses energy from electrical sources during takeoff and landing, and the remaining energy during cruising mode from turbojet engines.

Electrophysicists in all major companies are working to create optimal propulsion systems for new electric and more electric aircraft. An integral part of any propulsion system are the DC/DC and AC/DC power converters, which serve to properly transfer and distribute power on board both electric and hybrid aircraft. Future converters must meet high requirements: have a high power density, a high power-to-weight ratio (tens of kW/kg), operate stably in the event of a failure, and have high reliability. The IEE RAS is also working on creating scalable, powerful DC/DC converters for charging batteries on board aircraft. A number of such fully controlled devices have been developed with a power density of about 10 kW/kg for various input and output voltages and currents with an efficiency of 98-99%.

Plasma aerodynamics is another interesting and promising area of electrophysics. The general applied goal of this direction is to reduce the aerodynamic drag of aircraft by using cold (weakly ionized) plasma for active control of aerodynamic flows. The use of plasma actuators of a certain geometry at a certain pulse power makes it possible to increase the lifting force of the aircraft, control the instability preceding the laminar-turbulent transition in the boundary layer and thereby slow down and suppress its development, or create volumetric flows with high gas consumption.

Thus, we can conclude that the future of aviation is inextricably linked with electrophysics, since modern electrophysical technologies will make it possible to create a silent aircraft with low emissions, where most systems will operate using electricity.

THE IBR-2 PULSED RESEARCH REACTOR FOR CONDENSED MATTER INVESTIGATIONS

Kulikov S.
Joint Institute for Nuclear Research, Dubna, Russia

The IBR-2 pulsed research reactor of the Joint Institute for Nuclear Research is one of the leading neutron sources in the world with one of the highest neutron fluxes per pulse. The main purpose of the IBR-2 reactor is to produce neutrons using a complex of instruments on extracted beams, which are used in neutron research and applications in the field of condensed matter studies (materials and life sciences, geology, archeology, chemistry, etc.). The reactor operates in a pulsed mode due to mechanical modulation of its reactivity. The average power of the reactor is 2 MW, but it generates a neutron flux on the surface of the moderator up to ~10^16 n/cm^2/s in burst at a power of 1850 MW. The report will present the current status of the reactor, neutron spectrometers (diffractometers, reflectometers, small-angle and inelastic scattering instruments, etc.), as well as the development of equipment and experimental infrastructure. The capabilities of the international scientific community to access neutron instruments through the implemented user program will be described in detail.

OPTIMIZED PERTURBATION THEORY IN QUANTUM MECHANICS AND STATISTICAL PHYSICS

Rakhimov A.M.
Institute of Nuclear Physics, Uzbekistan Academy of Sciences, Tashkent, Uzbekistan

There are many problems in quantum mechanics and field theories that can not be solved exactly. In some cases, for example, in Quantum Electrodynamics, one may use standard perturbation theory, making power expansion in orders of the coupling constant $\alpha \sim 1/137$. However, in most of cases, the perturbation theory fails, since the expansion becomes divergent. Examples are anharmonic oscillator in quantum mechanics, $\lambda\varphi^4$ scalar field theory, finite temperature field theory of thermodynamics...

Nearly 15 years ago an alternative version of the standard perturbation theory was developed, and referred in literature as Optimized Perturbation Theory (OPT). It has been successfully applied in relativistic field theories, thermodynamics and even in quantum chemistry.

We shall make a brief review on OPT, concentrating on its application in finite temperature field theories of condensed matter physics.

INNOVATIVE BIONANOMATERIALS FOR TISSUE ENGINEERING AND TRANSPLANTOLOGY

Gorshkova Yu.
Joint Institute for Nuclear Research, Dubna, Russia

The creation of innovative bionanomaterials based on organic and organic-inorganic components for tissue engineering and transplantology has increased sufficiently in recent decades. Identification of high-potential materials with the required physicochemical or mechanical properties is possible already at the stage of structural studies using small-angle neutron and X-ray scattering (SANS/SAXS) and complementary methods, which significantly reduces the time and costs of *in vitro* and *in vivo* tests.

The changes of the structure of the bacterial cellulose developed for skin tissue engineeringunder the action of enzymes or incorporation of biocide components into BC matrix will be discussed.

The optimal conditions (temperature and humidity) for the preservation of corneal stromal grafts for keratoplasty obtained by dehydrothermal cross-linking will be identified.

The structure of the ultra-high molecular weight polyethylene (UHMWPE) using for creation of the novel hip joint endoprosthesis under stretching will be examined.

The cellulose produced by bacteria (BC) in the form of a gelled film with a fine-fiber net structure were tested. For example, under the action of enzymes, as shown by SANS, the size and shape of the components of BC polymer matrix begin to approach those in natural collagen: after 24 hof the enzymatic hydrolysis the thickness of the nanoribbons increased from 8.4 to 13.8 nm and the width exceeded the maximum size > 330 nm.Besides, the BC can plays the role of scaffoldin forming organic-inorganic matrix based on Gluconacetobacterxylinus cellulose (GxC) and poly-1-vinyl-1,2,4-triazole (PVT) with Cu nanoparticles. The composite hydrogels’ mesostructure has been studied from 1.6 nm to 2.5 μm by (U)SANS. The polymer complexes have three types of inhomogeneities: GxC, PVT, and PVT complex with Cu^{2+}. Three hierarchy levels of GxC remained in the supramolecular structure ofcomposite hydrogels. BC-PVT matrix plays the role of reducing agent of copper (II).

The possibility of controlling the structural properties in the process of dehydrothermal crosslinking of stromal corneal grafts was studied by SAXS. The shortening of fibrils along the axis by 3 nm in the intersection zone, which occurs at 140°C, should be recognized as already critical, leading to a loss of strength, a decrease in the average distance between triple helices in the quaternary structure may be due to the thermal degradation of polysaccharides. The structure of grafts is more sensitive to changes in temperature than humidity.

Structural parameters of semicrystalline polymers UHMWPE was extracted from in situ SAXS-tension experiment. For the three elongationstates it was obtained values of long period of lamellar phase as 11.5 nm, 13.6 nm and 15.9 nm respectively, reflecting the stretching effect of the imposed deformation.

SANS is an effective method for investigating the nanostructure and morphology of bacterial cellulose (BC).The obtained results will contribute to the creation of biotechnologies for the development of wound dressings with desired properties for the treatment of various skin lesions.The introduction of biocides (copper ions) into the BC matrix makes it possible to obtain biomaterials with antimicrobial properties.

In addition, SAXScan be successfully used as a certification method in transplantology, as shown by the example of a study of keratoprostheses from corneas of various animal origins developed at the Russian Ophthalmological Center “Vostok-Prozrenie”.

The unique possibilities of studying the structure of polymers, in particular UHMWPE, under tension in situ SAXS experiment are demonstrated. Such tests are extremely important for studying the wear resistance of materials used in endoprosthetics.

MODERN PROBLEMS OF QUANTUM THEORY OF MATERIALS CONTAINING TRANSITION METALS, LANTHANIDES AND ACTINIDES

Titov A.V.

Peterburg Nuclear Physics Institute of NRC "Kurchatov Institute", Gatchna, Russia

The creation of new materials based on heavy transition metals (d-elements), lanthanides and actinides (f-elements) is one of the key tasks of the rapid development of the scientific and technical base of in the world in the coming decades. Digital materials science, including computer modeling of such materials, is one of the most important components of such development. Theoretical study of materials containing d- and f-elements with high accuracy is necessary for a correct understanding of the processes occurring in them at the atomic level, predicting the properties of materials and developing innovative technological processes. Computer modeling can play an important role in the creation of new magnetic, optical, radiopharmaceuticals, diagnostic, and other materials with unique properties. Theoretical simulation of such materials and the availability of effective methods for non-destructive testing of the chemical (electronic) state of d- and f-elements together with their experimental studies, it is most reasonable way to carry out a reliable long-term forecast of the properties of materials and processes occurring in innovative matrices for the disposal of high-level waste, including transuranium elements, in deep underground storage facilities.

The problems of modeling such materials are discussed in the report, as well as ways to overcome these problems using the generalized (Gatchina) relativistic pseudopotential (GRPP) method [1]. It is shown in the report that the principles of constructing GRPP [2] can be applied in constructing embedding potentials for studying crystal fragments [3]. They can be used for precise studies of various properties of materials (both periodic structures with d- and f-elements, and structures with impurity centers containing d,f-elements) in the framework of cluster modeling of materials. First of all, this concerns calculations of the properties of “atoms in a compound” [4], such as chemical shifts of the X-ray emission (fluorescent) spectra of heavy atoms in a crystalline environment, fine and hyperfine splitting, and other properties, which are, in particular, required for the search for “new physics" [5]. It is shown for ionic-covalent crystals that the embedding potential can be represented as a linear combination of semilocal “compound-tunable” PPs and a set of Coulomb partial charges on the environmental atoms without explicit including the electrons of the environmental atoms in the calculation.

The research is supported by the RFBR grant No. 20–13–00225.

1. A. Oleynichenko et al., Symmetry, 15, 1 (2023).
2. A.Titov & N.Mosyagin IJQC **71**, 359 (1999) [https://doi.org/10.1002/(SICI)1097-461X(1999)71:5<359::AID-QUA1>3.0.CO;2-U]

3. Y. Lomachuk et al., PCCP **22**, 17922 (2020) [https://doi.org/10.1039/D0CP02277B];
4. D. Maltsev et al., PRB **103**, 205105 (2021) [https://doi.org/10.1103/PhysRevB.103.205105];
5. V. Shakhova et al., PCCP **104**, 19333 (2022) [https://doi.org/10.1039/D2CP01738E];
6. A.Oleynichenko et al. PRB **109**, 125106 (2024) [https://doi.org/10.1103/PhysRevB.109.125106]
7. A. Titov et al., PRA **90**, 052522 (2014) [https://doi.org/10.1103/PhysRevA.90.052522]
8. A. Petrov et al., PRA 107, 062814 (2023) [https://doi.org/10.1103/PhysRevA.107.062814];
9. L. Skripnikov et al. , PCCP 22, 18374 (2020) [https://doi.org/10.1039/D0CP01989E]

ESTABLISHMENT OF NEW POLYTYPES IN Cd(Mn,Mg)-In-Ga-S SYSTEM BY NEW ELECTRON- DIFFRACTION METHODS

Kyazumov M.G.[1], Rzayeva S.M.[1], Rustamova L.V.[1], Avilov A.S.[2]
[1]Institute of Physics, Ministry of Science and Education, Baku, Azerbaijan
[2]Shubnikov Institute of Crystallography, Federal Scientific Research Centre "Crystallography and Photonics", Russian Academy of Sciences, Moscow, Russian

By tilting and rotating a thin single-crystal film (**TSCF**) in various ways (TSCF lies exactly on the plane of the crystal holder) we have obtained an electron diffraction pattern of the type of lamellar oblique textures and acicular textures (Fig. 1*a*). From the reflections (h00) we have determined the value of the parameter *a* ofthe crystal lattice, and from the reflections (10*l*) the value of the parameter *c*. By the distribution of reflections (11*l*), we have determined the thickness of the package (layer, structural unit), and by the value of the second strong reflection in this case, (116) we have established the structural type in this series.

For some reason, the TSCF does not lie in the plane of the crystal holder (**CH**), and we are unable to correct it. In such cases, after tilting the CH and rotating around an axis perpendicular to the CH plane, on the obtained electron diffraction pattern, some reflections shift from the line of ellipses. We give diagrams explaining such rotation and helping to easy processing of the obtained electron diffraction patterns (Fig.1*b*,*c*).

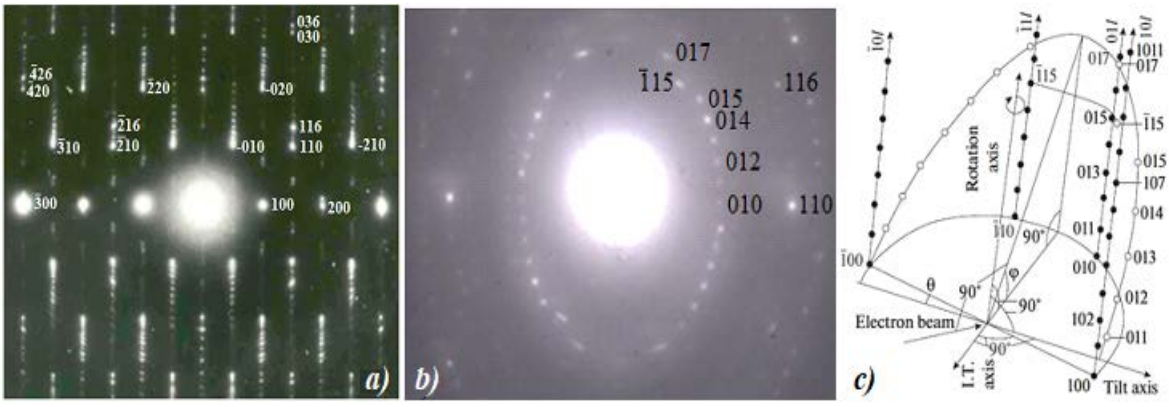

Fig.1. a) rotation electron diffraction patterns of the $CdInGaS_4$ single-crystal thin films, imitating electron diffraction patterns of acicular texture, *b*, *c*) 2H-polytype $Mg_{0.7}Ga_{1.4}In_{0.8}S_4$single crystal: *b*) rotation electron diffraction pattern($\varphi = 35^{\circ}$, $\omega = 60^{\circ}$), imitating electron diffraction patterns of lamellartexture and *c*) scheme of rotation and detection of sites of the reciprocal lattice in the Ewald plane. Closed circles show reciprocal lattice sites located parallel to the 00*l* axis, open circles correspond to the 01*l* and $\bar{1}1l$ sites detected in the Ewald sphere cross section, I.T. is the axis of the initial tilt of the film relative to the plane of the crystal holder, and θ is the angle between the film and crystal holder planes.

A NEW METHOD FOR OBTAINING ONE-DIMENSIONAL FULLERENE STRUCTURES

Bakhramov S.A., Makhmanov U.K.
Institute of Ion-Plasma and Laser Technologies, Uzbekistan Academy of Sciences, Tashkent, Uzbekistan

Currently, carbon nanoparticles, in particular fullerenes, are becoming key components of nanotechnology for creating complex functional nanostructures of various dimensions [1]. One dimensional fullerene nanostructures are widely used today to create miniature elements of devices in optoelectronics, nanoengineering, microelectronics, solar energy, biomedicine, gas sensing and nanoelectromechanics [2]. Today, various methods are known for obtaining one dimensional nanostructures of a wide range of semiconductor materials, such as growth by molecular beam epitaxy, vapor deposition, growth catalysts, magnetron deposition, laser ablation, chemical epitaxy in high vacuum and others. In all cases, the regulation and control of the size and structure of the one dimensional nanostructures is of great importance. All methods for producing one-dimensional semiconductor nanostructures have their own characteristics and disadvantages, for example, many of them are energy-consuming and expensive. For the development of nanotechnology, it is important to develop cheap technologies for producing one-dimensional nanostructures, including fullerene ones. One of these methods is the use of the evaporation method of solution droplets, which is directly related to the processes of self-organization of nanoparticles, is difficult to predict and has not been sufficiently studied to date. The purpose of this work is to obtain one-dimensional nanostructures (nanowhiskers, nanotubes) based on fullerene molecules (C_{60}, C_{70}), as well as to study their optical and morphological features. In our experiments, ethylbenzene, xylene and isopropyl alcohol were used as organic solvents for crystalline fullerenes C_{60} and C_{70} (purity >99.7%). All reagents were purchased from the supplier Sigma Aldrich (USA).

Figure 1 shows an SEM image of C_{60} fullerene nanotubes synthesized during the thermal evaporation of organic solvents from the volume of an isolated drop of a C_{60} solution located on the smooth surface of a horizontally located silicon substrate.

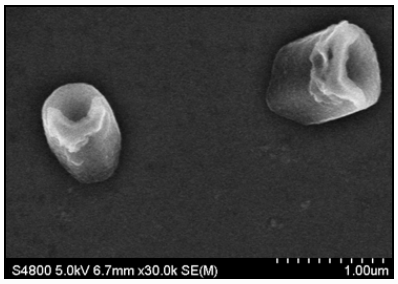

Fig.1. SEM image of C_{60} fullerene nanotubes synthesized on the surface of a silicon substrate

It can be seen that the outer and inner diameters of the nanotubes are ~580 nm and ~400 nm, respectively. The average length of the resulting nanotubes is ~800 nm. A major role in the formation of nanotubes based on C_{60} fullerene is played by the temperature gradient. It should be noted that the closedness of one end of the nanotubes synthesized by us allows them to be used in practice as nanocapillaries, nanosorbents and nanocontainers. Note that the method used to synthesize fullerene nanotubes is efficient, economical and much easier to implement.

1. Speranza G. // Nanomaterials (Basel). 2021, 11(4), 967.
2. Bakhramov S.A., Makhmanov U.K., Aslonov B.A. // Condensed Matter 2023, 8, 62-71.

THE NATURE OF INTERMOLECULAR INTERACTIONS IN SOLUTIONS OF FULLERENE C_{70}

Bakhramov S.A., Kokhkharov A.M., Makhmanov U.K., Aslonov B.A., Chuliyev T.A.
Institute of Ion-Plasma and Laser Technologies, Uzbekistan Academy of Sciences, Tashkent, Uzbekistan

Currently, the attention of scientists around the world is focused on studying the characteristics of nanoparticles of various natures, the synthesis of nanostructured functional materials based on them, as well as the possibility of using them as promising materials for various applications [1]. Among the currently most studied families of fullerene molecules is the C_{70} molecule, the structure of which corresponds to a cellular ring structure reminiscent of a rugby ball. Due to its unique physical and chemical properties, C_{70} fullerene has a wide range of applications as basic building nanoblocks in nanotechnology, electromagnetic devices, solar panels, sensors, pharmaceuticals, tribological materials, etc. [2-3]. Understanding the self-organization of C_{70} molecules in solutions is necessary for the synthesis of nanostructured materials with new properties based on them. At the same time, many questions about intermolecular interactions leading to clustering of C_{70} fullerene molecules in binary solutions remain controversial.

The purpose of this work is to experimentally study the optical properties (UV-visible absorption spectra and refractive index) of C_{70} fullerene solutions in binary xylene/tetrahydrofuran solvent mixtures and the dimensional characteristics (dynamic light scattering data) of C_{70} nanoclusters in solutions at room temperature. In the experiments, crystalline powders of C_{70} fullerene with a purity of >99.5%, as well as organic solvents - xylene and tetrahydrofuran with a purity of ≥99%, were used.

It was established that with increasing concentration of C_{70} in a solution, leads to an increase in the number of bonds between the “C_{70}-C_{70}” and “C_{70}-solvent” molecules and an increase in the refractive index of solutions. When storing a C_{70}/xylene/tetrahydrofuran solution of a fixed concentration at room temperature, an increase in the refractive index of the solution is initially observed, but with further storage of the solution (in the period of 3-9 days), its decrease begins. The latter is associated with an increase in the size of the synthesized C_{70} nanoclusters over time and, as a consequence, a decrease in their amount in the solution.

It was shown that the features of the optical absorption spectrum of the C_{70}/xylene/tetrahydrofuran mixture at a fixed low concentration of fullerene are sensitive to its storage time. The apparent increase in the intensity of the absorption spectrum and the red shift of the characteristic maxima are due to a decrease in the energy gap between the excited S_1 and ground S_0 states of fullerene; ultimately, the competition between intermolecular interactions “C_{70}-C_{70}” and “C_{70}-solvent” is dominated by the binding of C_{70} molecules over time, forming nanoclusters. Using the dynamic light scattering method, it was established that the time of onset of the formation of C_{70} nanoclusters and their final size depend on the concentration of fullerene and the exposure time of the solution. The scientific results obtained can be used to assess the formation of various nanostructures in binary solutions of fullerenes and similar nanoparticles.

1. Fabbiani M., Cesano F., Pellegrino F., Negri Ch. // Molecules, 2021, 26, 7097A.
2. Sachdeva Sh., Singh D., Tripathi S.K. // Opt. Mater. 2020, 101, 109717.
3. Makhmanov U.K., Esanov S.A., Sidigaliyev D.T., Musurmonov K.N., Aslonov B.A., Chuliev T.A. // Liquids, 2023, 3, 385-392.

NANOSCALE STRUCTURAL PROCESSES IN AQUEOUS SOLUTIONS OF ORGANIC MOLECULES

Bunkin N.[1], Sabirov L.[2], Semenov D.[2]
[1]*Bauman Moscow State Technical University, Moscow, Russia*
[2]*Institute of Engineering Physics of Samarkand State University, Samarkand, Uzbekistan*

The reported results of investigating the adiabatic compressibility of aqueous 4MP solutions at the hypersonic frequency allowed existence boundaries to be experimentally established (in temperature–concentration coordinates) for different phases characterized by different structural organization of solution components. The transition between different structures can be either through changing the solution temperature (at fixed concentration) or through changing the solution concentration (at fixed temperature).

The data on adiabatic compressibility of solutions measured at the hypersonic frequency in these investigations serve as experimental evidence, confirming existence of a continuous hydrogen bond network in pure water and aqueous solutions in a certain interval of temperatures and concentrations and its transformation from the undeformed state (at low nonelectrolyte concentrations) to the deformed state followed by destruction (fragmentation) with increasing concentration of nonelectrolyte molecules in the solution.

The presence of an additional adiabatic compressibility minimum at the singular-point concentration (0.06 MF) at the hypersonic frequency and its absence for compressibility measured at the ultrasonic frequency indicate that at the singular point there is an additional mechanism for “strengthening” of the solution structure due to the phase transition of the structural type on the scales of about 10–12 nm.

In acetone-water and 3MP-water solutions the excessive spectral broadening of the spectral fine-structure components in the vicinity of the singular point is due to the interaction of adiabatic density fluctuations with order-parameter fluctuations, which leads to an increase in the attenuation coefficient of hypersound due to its incoherent scattering from order-parameter fluctuations.

The fluctuation dynamics near the singular point temperature in the investigated aqueous solution of acetone is described by the Landau theory of second-order phase transitions with a critical index of generalized susceptibility $\gamma = 1$.

The presence of two maxima in the temperature dependence of the hypersound absorption coefficient, the singularity of the behavior of the displacement of the spectral finestructure components, and adiabatic compressibility, as well as the consistent description of the observed phenomena within the framework of the Landau and Chaban theories are due to the existence of two different states with a minimum of thermodynamic stability in the solution.

ASSEMBLING OF ORDERED NANO-MICRO-STRUCTURES AT INTENSIVE IRRADIATION OF CRYSTALS AND ALLOYS

Ibragimova E.M., Mussaeva M.A., Buzrikov Sh.N., Iskandarov N.E.
Institute of Nuclear Physics, Uzbekistan Academy of Sciences, Tashkent, Uzbekistan

There are experimental evidencesand theoretical models of self-assemble of nano- and micro-structures into 2D- and 3D-periodic arrangements under irradiation by energetic particles, when the exposed material is far from the thermodynamic equilibrium [1]. The modeling, based on stability theory and concepts of non-linear dynamics, determines criteria for the evolutionand spatial symmetry of self-organized microstructures. Experimental observations during and after irradiations (SEM, TEM, AFM, SPM, XRD) on the formation of self-organized defect clusters, dislocation loops, voids and bubbles, and also nanophasesare presented for metals and alloys, dielectrics, semi- and super-conductors.Neutron irradiation produces various self-assembled 3D-defect walls and void lattices with wavelengths in the range of 10-100’s nm.Due to high energy deposition, the problem is to find a composite material stable in the high temperature and dose rate regime, which it would experience as fuel cladding and structural materialfor fission or fusion reactors. It is likely a dynamic stability or equilibrium, when solute atoms are continually ejected from nanoclusters by collision cascades and these re-solved atoms are diffusing to rejoin and re-form nanoclusters, rather than radiation resistance [2]. Large amounts of H and He are generated in irradiated structural metals (Ni and stainless steels) in accelerator-driven systems [3], in LiF and NaCl crystals in fission reactor and ^{60}Co gamma-source [4,5]and in YBCO superconducting tapes [6] due to the availability of radiolytic (radioactive) transmutant isotopes and the formation of radiation-induced cavities (highly pressurized bubbles or under-pressurized voids withboth H and He). Metal cations (especially chemically aggressive Li and Na) react with available H to form hydrides identified by XRD [4,5]. Under intensive 18 MeV proton or 5 MeV electron irradiations the welding PbSn alloy coating the tapes is separated into Pb nanocrystalline dendrite super-structure and Sn nanofilm, Cu microfilm is patterned by shock-waves and micro-tracks. Radiation damage production mechanisms in semiconductors differ clearly from those in metals. For the primary damage production, this has been attributed to the open crystal structure and the much slower recrystallization. The current international standard for quantifying such energetic particle damages is the Norgett-Robinson-Torrens displacements per atom (NRT-dpa) model for metals, although new complementary displacement production estimators such as “athermal recombination corrected dpa” and atomic mixing (“replacements per atom”, rpa) functions are developed [7], but they do not consider nuclear reactions.

1. N.M. Ghoniem, et al. J.of Comput.-Aided Mater. Design. **8** (2002) 1-38.
2. A. Certain, et al. J. of Nucl. Mater. **434** (2013) 311–321.
3. F.A. Garner, et al. J. of Nucl.Mater. **356** (2006) 122–135.
4. E.M. Ibragimova, et al. Intern. Sci. J. "Materials science non–equilibrium phase transformations", **VII** (2021) Iss. 2, 60–63.
5. E.M. Ibragimova, et al. J.of Phys.: Conf. Ser. **2036** (2021) 012016.
6. E.M. Ibragimova, et al.J.of Phys.: Conf. Ser. AAPM-2023. **2573** (2023) 012013
7. K.Nordlund, et al. J.of Nucl. Mater. **512** (2018) 450-479.

TOWARDS UNDERSTANDING SELECTIVE GROWTH OF CARBON NANOSTRUCTURES USING COMPUTATIONAL MATERIALS SCIENCE

Khalilov U.[1,2], Mirzaev S.Z.[1]
[1]*Institute of Ion-Plasma and Laser Technologies, Uzbekistan Academy of Sciences, Tashkent, Uzbekistan*
[2]*University of Antwerp, Belgium*

As Moore's Law confronts limitations, the emergence of carbon nanotechnology presents a promising alternative to silicon, focusing on materials like fullerene, carbon nanotubes (CNTs), and graphene. This presentation highlights the pivotal role of Computational Materials Science (CMS) in advancing the exploration of selectively synthesizing carbon nanostructures (CNS) in contemporary experiments. Specifically, in catalyzed chemical vapor deposition (CVD) for CNT growth, our simulations investigate parameters such as feedstock composition, temperature, and the k-coefficient. These simulations elucidate the potential for tailoring CNT diameters and achieving chirality control. Moreover, our examination extends to plasma-enhanced CVD for selective CNT etching, emphasizing curvature, metallicity, and the γ angle between ortho-hydrogen pairs and the chirality vector. Endohedral synthesis, encompassing carbon peapods and graphene nanoribbon synthesis, sheds light on the interplay between catalyst and feedstock in determining nanostructure outcomes. Consequently, our research outcomes yield insights into carbyne stability, controllable electronic properties, and the potential for current amplification in functionalized samples.

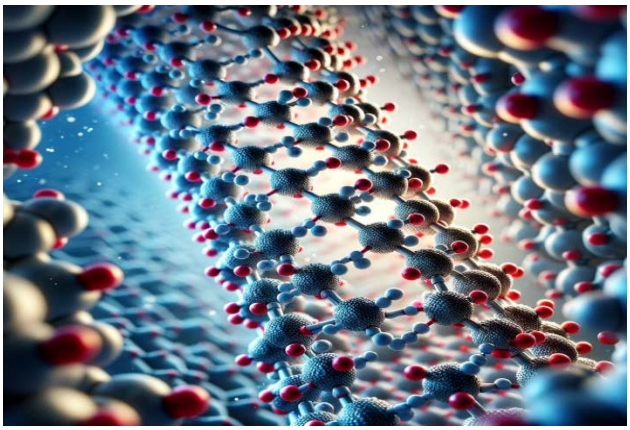

In summary, CMS serves as a crucial bridge between theory and experiment, facilitating the interpretation of key observations in CNS synthesis. The collaborative synergy between CMS and experimentation enriches our understanding of fundamental principles and boosts the development of new carbon materials and technologies that hold transformative potential across various industries.

1. Khalilov U., Bogaerts A., & Neyts E.C. *Nature Communications* 6(2015) 10306.
2. Khalilov U., et al. *Nanoscale* 9(2017) 1653.
3. Khalilov U., et al. *Journal of Physics D: Applied Physics* 50(2017) 184001.
4. Khalilov U., Vets C., & Neyts E.C. *Nanoscale Horizons* 4(2019) 674.
5. Khalilov U., Vets C., & Neyts E.C. *Carbon*153(2019) 1.
6. Khalilov U. & Neyts E. C. *Carbon* 171(2021) 72.
7. Khalilov U. & Mirzaev S. *Dokladi Akademii nauk* 3 (2020) 17.

PEROVSKITE OPTOELECTRONICS, PHOTOVOLTAICS AND LIGHT EMITTING DEVICES: BRIGHT, STABLE, TUNABLE BY IONS

Zakhidov A.
University of Texas at Dallas, Richardson, USA
Samarkand Quantum Center, Samarkand State University, Samarkand, Uzbekistan
Quantum Technology Center, Tashkent, Uzbekistan

Hybrid halide perovskites attracted enormous attention as a new magic class of quantum materials and a playground for optoelectronics and photonics. Particularly PV and light emitting devices, LEDs have been broadly developed. Conventional organic LEDs and perovskite LEDs need multilayered structures: as well-known transport layers (ETL and HTL), surround the emissive layer, EML, providing effective injection of electrons and holes. The presence of intrinsically mobile ions in metal halide perovskites, such as CsPbBr3 allows the formation of dynamic p-i-n structures by self-doping and formation of electric double layers (EDL) at interfaces even in single layer devices. However, the intrinsic ions (e.g. Cs+, Pb+, I- or Br-) migration in electric field destroys the very perovskite ionic lattice and also causes instabilities at interfaces. We have demonstrated in series of recent papers [that small amounts of external ions (e.g. Li+ ions added as Li-salt) in nanocomposites of CsPbBr3 with PEO type solid electrolytes allow to create bright and effective single layer light emitting electrochemical cells (SL-LEC) without need for transport and/or injection layers. Moreover, the lifetime of such SL-LEDs is increased significantly, since external Li ions protect ionic lattice by differentiated ionic migration. Importantly additional interesting properties can be achieved, such as reconfigurability of LEC turning dynamically into PV solar cells. Indeed SL-LEC behaves as light emitting memristor, showing memory effects and in my talk I will describe the various aspects of ionotronic behavior, when drift of external and internal ions creates hysteretic memory behavior similar to that of memristive resistors and diodes.

We have studied the dynamics of ionic migration using various techniques and I will discuss the prospects of ionotronics for perovskite PV solar cells. This concept for Solar cells with gating control of ionic motion is based on the dynamic formation of favorable internal p-i-n structure by external ionic migration in electrical field of applied operation voltage of the gate, composed by porous carbon nanotubes (CNT) or self-gating by photovoltage. These mobile ions of ionic liquid, penetrate into CNT, causing its n-doping by gate voltage, and this leads to significant enhancement of efficiency of solar cells by various ionic liquids, such as DEMO-TFSE.

Blue electroluminescence is highly desired for emerging light-emitting devices for display applications and optoelectronics in general. However, saturated, efficient, and stable blue emission has been challenging to achieve. Here, we leverage $CsPbBr_{3-x}Cl_x$ mixed-halide perovskites, polyelectrolytes, and a salt additive to demonstrate pure blue emission from single-layer light-emitting electrochemical cells (PeLECs). Substituting Cl into $CsPbBr_3$ produced luminescence from green through blue. Polymer and $LiPF_6$ inclusion were found to increase photoluminescence quantum yield, suppress halide segregation, induce thin-film smoothness and uniformity, and reduce crystallite size. Overall, we demonstrate that low-dimensional perovskite LEC devices show superior performance among blue perovskite LEDs and general LECs. We also demonstrate guest-host single PeLEC with widely tunable emitted color.

THE CURRENT STATE AND FUTURE PROSPECTS OF PHYSICS RESEARCH IN THE FERGANA VALLEY

Zainabidinov S.Z.[1], Mamatkarimov O.O.[2]
[1]*Andijan State University, Andijan, Uzbekistan*
[2]*Namangan Institue of Engineering and Technology, Namangan, Uzbekistan*

Currently, the scientific potential of the Fergana Valley consists of scientists and specialists from more than 20 universities and a number of knowledge-intensive manufacturing enterprises, which employ about 30 doctors and 50 candidates of science and doctors of philosophy in physical fields. Scientific schools of such famous scientists as academician S.Zainabidinov, professors O.O.Mamatkarimov, G.Gulyamov, R.Aliyev, N.Yuldashev, U.R.Salomov, A.Kasimokhunova, K.Anarkulov, R.Ya.Rasuvlov, A.Rasulov and others have been formed, which successfully implement the tasks of state programs for the development of physics and technology of the Republic of Uzbekistan. The strategic plan for the innovative development of the region and the sustainability of scientific research in physics is ensured by the following areas of ongoing scientific work:

- study of defect-impurity interactions and mechanisms of formation of micro-and nanoaccumulations on the surface and in the bulk of single-crystalline silicon;
- study of technological regimes for growing structurally perfect multicomponent epitaxial films on silicon and gallium arsenide and study of their structural, electrical and photoelectric properties;
- Grown of metal oxide materials by sol-gel technology for electronic devices for various purposes;
- physics of excitons, photo-tensoelectric, thermo-photovoltaic phenomena in semiconductor micro- and nanostructures;
- study of the linear and circular photogalvonic effect in bulk and low-dimensional semiconductor crystals;
- research and development of scientifically based recommendations for the creation of dye-sensitized solar cells;
- studies of phenomena in semiconductors in strong electromagnetic fields, mathematical modeling of the influence of temperature, pressure and microwave fields on quantum oscillatory phenomena in micro- and nano-sized semiconductor structures;
- the possibility of controlling external influences on the charge states of nano-sized objects, clusters in a crystal lattice, establishing the mechanisms of such anomalous effects as Giant Negative Resistance, deep-IR magnetoresistance and temperature quenching of photoconductivity and others, the role of photosensitive nanolayers and increasing the efficiency of photoconverters are being explored.

Scientists in the region annually carry out about 10 scientific and technical projects commissioned by the Ministry of Higher Education, Science and Innovation, and carry out joint research with foreign partners in current areas of physics. They are published in periodical scientific physics and mathematics journals, and there are basic doctoral, master and bachelor's programs for several physics specialists.

At the same time, it should be noted that currently a number of experimental and theoretical studies remain relevant in the world, such as condensed matter physics, the development of new materials for solar energy, photonics, nanoelectronics and others, which scientists of the republic and the region plan to deal with.

ADVANCED NUCLEAR PHYSICS AND NANOTECHNOLOGICAL RESEARCH ON THE BASE OF THE EG-5 ACCELERATOR AT JINR

Doroshkevich A.[1], Mezentseva Zh.[1], Oksengendler B.[2], Suleymanov S.[2], Didenko E.[1], Parpiev O.[2]

[1]*Joint Institute for Nuclear Research, Dubna, Russia*

[2] *Institute of Material Sciences SPA "Physics-Sun", Tashkent, Uzbekistan*

The electrostatic accelerator EG-5 at JINR is an effective and convenient nuclear physics tool for solving a wide range of urgent problems in nuclear physics, condensed matter physics, biology, electronics, and medicine.

After the completion of the EG-5 modernization (2026), the possibility to generate intense quasi-monoenergetic beams of light charged particles (p+, d+, α+) (continuous energy range: 1 - 4.1 MeV with energy dispersion 15 keV), at a current of up to 200 μA) and neutron fluxes about 10^9 n/c cm^2 in the range (20 keV – 800 keV, 3 MeV-5.5 MeV and 15 MeV) by reactions d(d,n)^{3}He, d(t,n)^{4}He, ^{7}Li(p,n)^{7}Be .

The prospects will opens up for conducting unique experiments to measure the energy spectra and angular distributions of charged particles from reactions (n, α) and (n, p) / (α, n) and (p, n), integral and differential cross sections of the latter in the range of neutron energies up to ~15 MeV, fission processes atomic nuclei with fast neutrons, activation analysis [Nuclear Data High Priority Request List], etc.

Beside nuclear physics research, the work in the field of powder nanotechnology, focused on advanced electronics and energy is being carried out on the basis of the accelerator complex. A rectifying contact operating on new physical principles [1] was practically implemented for the first time [2]. For the barrier potential obtaining, the dimensional effects of distortion of the structure of the energy zones of nanoscale ion crystals by the surface (varizonicity) were used (Fig. 1) [3]. Nanoparticles of identical chemical composition (ZrO_2-x%molY_2O_3 system, x = 0, 3, 4, 8 (YSZ)), but of different sizes in the form of compacts (Fig. 2), were used as contacting objects (7.5nm – 14nm). The hydrate shell of nanoparticles was used to ensure the electrical continuity of the medium in the space between the particles.

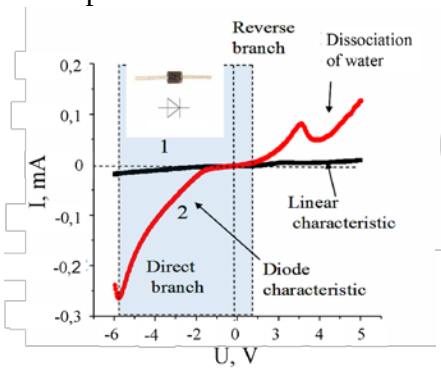

a

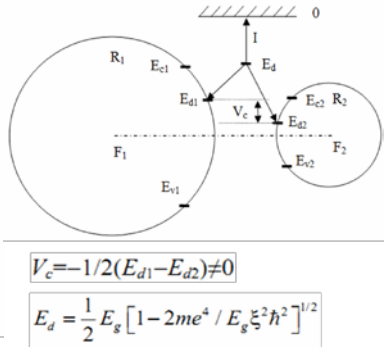

b

Fig. 1a. The contact characteristics of nanoparticles with identical (7.5 nm, curve 1) and different (7.5 and 9nm, curve 2) nanoparticle diameters.

Fig. 1b. The schematic interpretation of the effect of the rectifying contact,where, *m* and *e* are the mass and charge of the electron, ξ is the dielectric constant .

It is shown that an increase in the dispersion of particle sizesover than1.5nm leads to a proportional increase in the value of the limiting reverse voltage (V_{rev}), but a decrease in the value of the limiting forward current (I_{for}). The achieved values of the limit parameters are 2.99V for V_{rev} (at I_{for} = 0.83 mkA) and 276 Mka (at Vrev= 2.62V).

The effect opens up prospects for solving the key problem of semiconductor electronics - the problem of diffusion instability of chemically inhomogeneous heterostructures, which significantly limits the reliability and applicability of classical semiconductor devices under conditions of elevated temperatures and ionizing radiation. The prospects of creating homogeneous electronics devices that allow operation in harsh physical conditions for critical technologies are shown.

Acknowledgments. Serbia—JINR cooperation Projects No. 50 2024 items 7 and 8, Serbia—JINR cooperation Projects No. 51 2024 items 4 and 5, Belarus—JINR cooperation Projects No. 130 2024 items 7 and 8.

1. Karimov Z.I., et al., / Research Highlights in Science and Technology V1. 130-150
doi: 10.9734/bpi/rhst/v1/5397E
2. Doroshkevich A., et al.,Nanomaterials 2022, 12, 4493. doi.org/10.3390/nano12244493
3. Kutlimurotov B.R. et al., Uzbek Journal of Physics, 2022, 24, 4, 254-262.
doi.org/10.52304/.v24i4.378.

SENSORS WITH SUPER-PARA– & FERRO-MAGNETS

Kondratyev V.N.
Joint Institute for Nuclear Research, Dubna, Russia

Advances in micro- and nano-technologies have led to the widespread applications of spintronic magnetoresistive (MR) sensors for both recording and non-recording applications, see e.g. [1]. Such ultramodern magnetoresistive sensors have high sensitivity of the detected ultra-weak fields, which meet the requirements of intelligent sensor applications in the fields of the Internet, mobile devices, space technology, aeronautics, magnetic flux leakage, domotics, environment, healthcare and medicine. Moreover, their adaptability and miniaturization, simple integration and cost-effectiveness make these sensors uniquely competitive in terms of spread applications and production.

In this work, ensembles of superparamagnetic particles (SPM, see [1]) imbedded in an insulator, semiconductor or conductor are considered. At sufficiently high concentration of SPMs these metamaterials show superferromagnetic properties and can be used as MR sensors. We consider the electric current between the SPM particles and show that the resulting tunneling MR increases as the size of the SPM decreases.

1. Kondratyev V.N. and Osipov V.A. Superferromagnetic sensors. Nanomanufacturing **2023**, 3(3), 263-280; **https://doi.org/10.3390/nanomanufacturing3030017**

HIGH-PRESSURE X-RAY DIFFRACTION TECHNIQUES USING LABORATORY MICROFOCUS X-RAY SOURCE XEUSS 3.0

Lukin E.V., Gorshkova Y.E., Kichanov S.E., Kozlenko D.P., Lis O.N., Rutkauskas A.V.
Joint Institute for Nuclear Research, Dubna, Russia

The XEUSS 3.0 X-ray diffractometer at the Laboratory of Neutron Physics of the JINR has been used for the small-angle X-ray scattering (SAXS) studies during last two years. In addition to SAXS, which is the main area of research at this instrument, a technique for X-ray powder diffraction experiments using high-pressure diamond anvil cells technique has been developed. The brightness of the source and the hardness of the X-ray beam of a microfocus tube with a molybdenum anode make it possible to conduct experiments at high pressures and obtain powder diffraction patterns at pressures up to 70 GPa. A review of experimental techniques for high-pressure X-ray diffraction is presented. The results of studies of the crystal structure at high pressures obtained at the laboratory source are shown.

THE ELECTRICAL PROPERTIES OF A CONTACT OF HYDRATED NANO-POWDERS OF DIFFERENT SIZES YSZ FOR HOMOGENIC ELECTRONICS

Mezentseva Zh.V.[1], Doroshkevich A.S.[1], Oksengendler B.L.[2], Kirillov A.K.[1], Didenko E.A.[1], Nikiforova N.N.[2], Carmen Mita[3], Diana Mardare[3], Nicoleta Cornei[3], Suleimanov S.H.[2], Parpiev O.R.[2]
[1]Joint Institute for Nuclear Research, Dubna, Russia
[2] Institute of Material Sciences SPA "Physics-Sun", Tashkent, Uzbekistan
[3]Alexandru Ioan Cuza, University, Iasi, Romania

The diffusion instability of classical semiconductor structures, leading to catastrophic failures of electronic equipment, is a serious scientific and technical problem of modern critical technologies. This problem can be solved by using new physical principles in the creation of functional semiconductor structures, in particular, the effects of the low-dimensional state of matter. The dimensional effects, arising from the contact of hydrated nano-powder systems ZrO_2–Y_2O_3 (YSZ), are extremely interesting in connection with their possible application.

The object of research was the elliptical contact of two planar films based on a PVA binder with additions of chemically homogeneous nanoparticles ZrO2 – 3 mol% Y2O3 of different sizes 7.5 - 7.5, 7.5 - 10, 7.5 - 11 and 7.5 - 14 nm, respectively, deposited on a copper gilded foil. The voltammetry and impedance-metry methods have been used at different relative humidity (85 %, 75% and 65 %) under conditions of hydration.

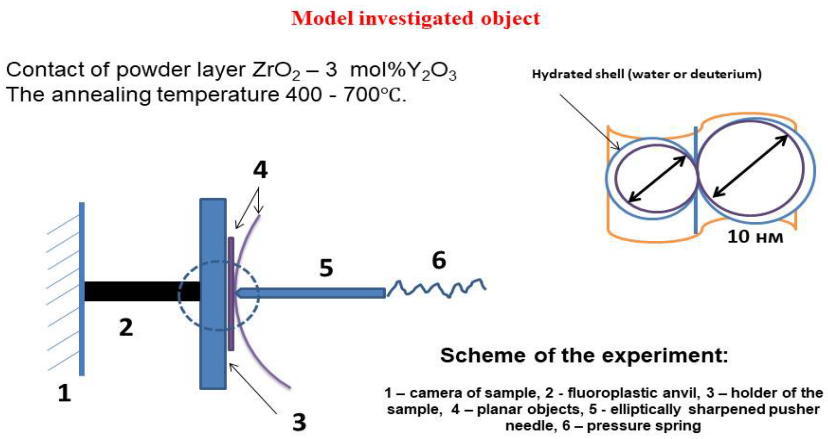

Firstly semiconductor structure as the contact of chemically homogeneous nanoparticles has been realized practically and investigated. It was shown this structure is based on the dimensional effects of distortions of the zone structure. The presence of a contact potential difference due to the difference in the configuration of SCR of nanoparticles has been found. Also the qualitative and quantitative dependence of the effect of overcharging of the contact on atmospheric humidity changing has been investigated.

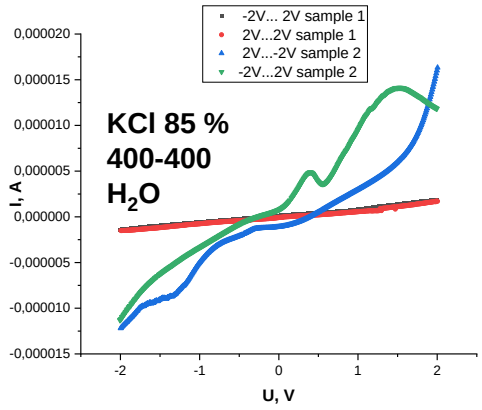

SELF-ORGANIZATION OF CHARGED PARTICLES IN LATERAL POTENTAILS WITH HIGH SYMMETRY

Nazmitdinov R.
Joint Institute for Nuclear Research, Dubna, Russia

A question of the optimal configuration of a finite number of particles in a plane has been a difficult problem of both physics and mathematics formany centuries. Back in 1611, Kepler already posed the question - why a snowflake has perfect hexagonal symmetry [1]. At present, increased interest in the problem of the optimal configuration in a plane is also due to the development of nanotechnologies which make it possible to form systems of similarly charged particles confined by external potentials with a high symmetry. In particular, one of the important achievements of

modern technology consists in the creation of «artificial atoms» or quantum dots, where a finite number of electrons is confined electrostatically in a nanometer-sized region [2].

Here we discuss the basic principles of self-organization of one-component charged particles, confined in disk and circular parabolic potentials. A system of equations is derived, that allows to determine equilibrium configurations for arbitrary, but finite, number of charged particles that are distributed over several rings [3,4]. The results of our approach demonstrate a remarkable agreement with the values provided by molecular dynamics calculations. With the increase of particle number n>180, we find a steady formation of a centered hexagonal lattice. At the same time, the energetic preferences for non-uniform local density, then favor ground states, where this locally hexagonal structure is isotropic dilated and contracted throughout the structure. In fact, the equilibrium configuration is determined by the need to achieve equilibrium through the formation of a hexagonal lattice on one side and a ring-like structure on the other. This competition leads to the formation of internal defects in such systems, in contrast to the case of unlimited regions, where the ground state of the system has no defects. Finally, this structure smoothly transforms to valence circular rings in the ground state configurations for the both potentials. We briefly discuss the precursor of the phase transition of the type "hexagonal lattice - hexatic phase" with the increase of the particle number in the system at zero temperature [5].

1. J. Kepler, “*The Six-Cornered Snowflake*” (Clarendon, Oxford, 1966).
2. J. L. Birman, R. G. Nazmitdinov, V. I. Yukalov, Phys. Rep. **526**, 1 (2013).
3. M. Cerkaski, R. G. Nazmitdinov, A. Puente, Phys.Rev. E **91**, 032312 (2015).
4. R. G. Nazmitdinov, A. Puente, M. Cerkaski, M. Pons, Phys. Rev. E **95**, 042603 (2017).
5. E. G. Nikonov, R. G. Nazmitdinov, P. I. Glukhovtsev, J. Surf. Investigation: X-ray, Synchrotron and Neutron Techniques **17**, 235 (2023).

STUDY OF THE LUMINESCENCE AND THE LIFETIME OF CURRENT CARRIERS IN $Ag_{1-x}Cu_xGaSe_2$ SOLID SOLUTIONS

RakitinV.V.[1], Gapanovich M.V.[1,2], Rabenok E.V.[1], Stanchik A.V.[3], Gremenok V.F.[3], Kabyliatski A.V.[3]

[1]Federal Research Center of Problems of Chemical Physics and Medicinal Chemistry, Chernogolovka, Russia

[2]Moscow State University, Moscow, Russia

[3]Scientific-Practical Materials Research Centre, National Academy of Sciences of Belarus, Minsk, Belarus

In this work the defect structure in the $Ag_{1-x}Cu_xGaSe_2$ solid solutions with a wide range of x was studied by the low-temperature luminescence method at 77 K. Fig. 1 shows the luminescence spectra of the solid solutions. The curve 1 corresponds to the $CuGaSe_2$ sample and contains one significant maximum at 1.63 eV. When silver is added to the powders, an additional peak appears on the spectra, which is apparently due to the luminescence centers associated with silver. In general, as silver content in the samples increases the tendency of peak shift towards the high energies appears.

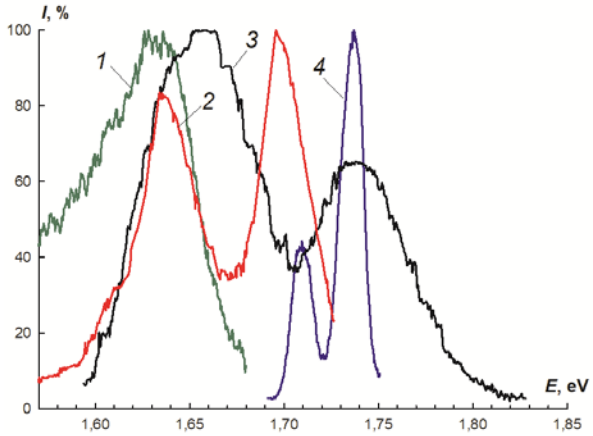

Fig. 1. Luminescence spectra of the $Ag_{1-x}Cu_xGaSe_2$ ($0 \le x \le 1$) solid solutions at 77 K: *1* - $CuGaSe_2$, *2* - $Ag_{0.3}Cu_{0.7}GaSe_2$, *3* - $Ag_{0.46}Cu_{0.54}GaSe_2$, *4* - $Ag_{0.63}Cu_{0.37}GaSe_2$

The lifetime of current carriers have measured by time-resolved microwave photoconductivity (universal research facility «Unit for determining the lifetime of photogenerated current carriers by measuring microwave photoconductivity in the frequency range of 36 GHz»). The time resolution of the electric circuit was ~5 ns. Photoconductivity was excited with an LG-I505 nitrogen laser (wavelength λ= 337 nm, pulse duration 8 ns, I_{max} = 10^{16} photons/cm^2 per pulse). This study has shown that the lifetimes of current carriers vary depending on the composition.

The work was supported by the Russian Science Foundation (RSF) (project number24-43-10003) and the Belarusian Republican Foundation for Fundamental Research (project numberT23PHΦM-029).

INVESTIGATION OF THE PHOTOSENSITIVITY OF $CdTe/Al_2O_3/Al$ NANOCOMPOSITE SYSTEM

Baklanova U.R.[1], Rakitin V.V.[2], Gapanovich M.V.[1, 2]
[1]Moscow State University, Moscow, Russia
[2]Federal Research Center of Problems of Chemical Physics and Medicinal Chemistry, Chernogolovka, Russia

It is known that the use of nanostructures makes it possible to increase the theoretical efficiency of CdTe-based solar cells [1, 2]. The examples of quantum dot-based solar cells are known, but the use of nanotubes or nanowires is practically not found. In this work, the photosensitivity and the possibility of sensitization of $CdTe/Al_2O_3/Al$ nanocomposite systems were investigated. The synthesis of nanoscale cadmium telluride was carried out in a three-electrode electrochemical cell from the solution of 96%H_2SO_4, $CdSO_4 \cdot (8/3)\ H_2O$ and TeO_2. The working electrode was an Al_2O_3/Al plate. The synthesis was carried out at E = -450, -500, -550, -600, -650 mV at 70 °C for one hour with continuous stirring. The XRD and Raman spectroscopy methods were used to study the composition of obtained samples. The method of photoelectrochemical cells was used to study the photosensitivity. Fig. 1 shows the current density/potential dependences for the synthesized samples under the intermittent illumination condition.

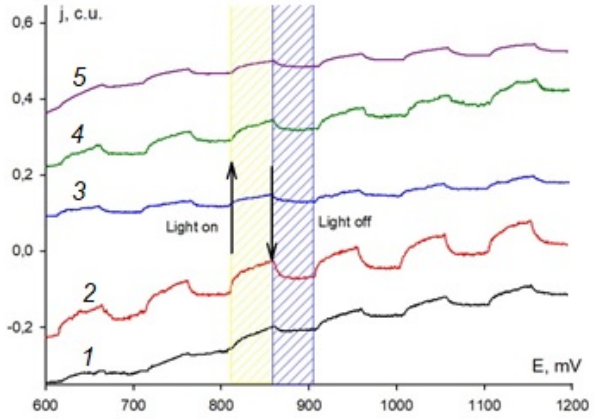

Fig. 1. The current density/potential dependences under the intermittent illumination condition for the samples synthesized at: *1)* -450mV, *2)* -500mV, *3)*-550mV, *4)*-600mV, *5)*-650 mV

It was found that all samples have photosensitivity and *n*-type conductivity, which is due to sensitization of the $CdTe/Al_2O_3/Al$ system. Thus such a system can later be used as a solar sell.

The work was carried out within the framework of state task No. 124013000686-3.

1. KapoorS. etal. //Journal of Alloys and Compounds. – 2019. – V. 809. – P. 151765.
2. Hochbaum A. I. et al. //Nature. – 2008. – V. 451. – №. 7175. – P. 163-167.

ANALYSIS OF DISTRIBUTIONS IN CONDENSED MATTER PHYSICS

Isayeva E.A.
Institute of Physics, Ministry of Science and Education, Baku, Azerbaijan

It is known in the quantum physics there are bosons and fermions which aren't described by classical statistics but quantum one. What is difference between these? It begins from Planck's view on invisible microobjects as identical. Do the such combinatory measures as permutations and arrangements exist for them? Of course, they don't. Only combinations matter for the statistics of the microworld. Therefore, combinations answer on only question how many atoms from all atoms.

The combinations without repetition $C_P^N = \frac{P!}{N!(P-N)!}$ are for fermions. Due to without repetition of energy states each fermion is one own state.

The combinations with repetitions $A_N^P = \frac{(N+P-1)!}{(P-1)!\,N!}$ are for bosons. Due to repetition of energy states the all bosons can occupy one state. For example, atoms are in the lowest energy state in Boze-Einstein condensate.

These formulae tell us that it is important to know how many states a system can have. The meaning of P is that even before combinations without repetitions, we announce the qualities of an atom, that is, energies $E_1, E_2, ..E_P$. The number P is the number of "qualities" of a micro-object to be in one state or another, and the number N is the "quantity" of the objects themselves. In combinatorics, the categories "quantity" and "quality" in terms of permutation, combination and placement are necessarily with the meaning that the same "quality" can simultaneously have the entire number of objects. But not vice versa, that one and the same object has simultaneously all the "qualities" of the set. As we can see, the two-valued logic of Aristotle is necessarily present in

combinatorics. It is also present in Planck's vision of the identity of particles of the microworld. So, his combinations with repetitions were useful to Bose-Einstein, and combinations without repetitions were useful to Fermi-Dirac in their derivation of the distribution of ideal quantum gas molecules.

Today we distinguish between classical particles, fermions and bosons. The logic of all these statistics remains classical, Aristotelian, two-valued. But did such logic remain for Planck in study of the radiation of absolutely black body. No, it doesn't. Planck sees many resonators N in the atom; but because time of measurement of macroscopic observer is so little, the average energy of resonator is absent. Therefore, the energy N resonators contain of P sets quantum energy U_N=NU= Pε, where ε is 1 quanta of energy. As above the combinations with repetitions $A_P^N = \frac{(N+P-1)!}{(N-1)!\,P!}$ but the categories "quantity" and "quality" are replace each other. This mean one atom may be in many states in same time. It is fuzzy logic, which may be described by Zadeh's Fuzzy Sets Theory.

Fuzzy logic helps us to understand that there are energy states as set of quants or monads of Leibnitz. 1 quanta is the object. It looks like count of objects in macroworld. Object is the same and 1 quanta is the same. Plank wanted explain it but he couldn't because he stayed in classical view. There is a quantity of quants. Their quality is the atom resonator having them.

SPECTROSCOPIC STUDY OF BINARY NANOOXIDE SYSTEMS IN CONTACT WITH WATER

Melikova S.Z., Agayev T.N.
Institute of Radiation Problems, Ministry of Science and Education, Baku, Azerbaijan

Recently, nanooxide powders have been widely used in various fields of science and technology, including radiation-catalytic processes for producing molecular hydrogen from water and hydrocarbons [1,2]. The paper presents the results of Fourier-IR spectroscopic studies of the radiation-catalytic decomposition of water in the systems nano-ZrO_2+nano-Al_2O_3+H_2O, nano-ZrO_2+nano-SiO_2+H_2O, nano-SiO_2+nano-Al_2O_3+H_2O under the influence of gamma radiation. The influence of the second component on the radiation-catalytic properties of the binary systems nano-ZrO_2+nano-Al_2O_3, nano-ZrO_2+nano-SiO_2, nano-SiO_2+nano-Al_2O_3 has been studied.

For this purpose, nanopowders nano-ZrO_2, nano-Al_2O_3 and nano-SiO_2 (Sky Spring Nanomaterials) with particle sizes d=20-60 nm were used. Before adsorption, all nanopowders were subjected to thermal vacuum treatment. Fourier transform IR spectra were recorded on a Varian 640 FT-IR spectrometer in the frequency range 4000 – 400 cm^{-1}. Pellets of ~50 μm thick were pressed from samples of the nanopowder mixture, then were irradiated using ^{60}Co source at the dose rate of 0.11 Gy/s.

It has been shown that the adsorption of water molecules in a mixture of zirconium and aluminum oxides occurs through molecular and dissociative mechanisms. Intermediate products of the radiation-heterogeneous decomposition of water are radical ions of molecular oxygen, surface hydrides of zirconium, silicon and aluminum, as well as hydroxyl groups. The dependences of the intensities of absorption bands of molecular water and surface hydrogen bonds and isolated hydroxyl groups characterizing nano-ZrO_2, nano-SiO_2 and nano-Al_2O_3 on temperature were studied. Based on a comparative analysis of these relationships, the radiation-catalytic activity of nano-ZrO_2 was revealed in the radiation-thermal process of water molecule splitting.

1. Agayev, T.N., Gadzhieva, N.N. &Melikova, S.Z. Fourier Transform IR Spectroscopic Study of Nano-ZrO_2+ Nano-SiO_2+ Nano-H_2O Systems Upon the Action of Gamma Radiation. *J Appl. Spectrosc.* **85**, 365–368 (2018). https://doi.org/10.1007/s10812-018-0658-9.
2. Agayev, T.N., Melikova, S.Z., Gadzhieva, N.N. *et al.* Fourier-IR Spectroscopic Study of Radiation–Thermal Water Decomposition in the Nano-ZrO_2+ Nano-SiO_2+ H_2O System. *Nanotechnol Russia* **15**, 158–162 (2020). https://doi.org/10.1134/S1995078020020032.

OPTICAL PROPERTIES OF $TlInSe_2$<Au> SİNGLE CRYSTALS

Mammadova G.N.
Nakhchivan State University, Nakhchivan, Azerbaijan

This paper presents the results of studying the surface microrelief in 2D and 3D models and analyzing the spectroscopy of a three-junction TlInSe2<Au> crystal. Analysis of the results obtained showed that with a change in the composition of the TlInSe2<Au> crystal, sharp changes occur in the microrelief of its surface. An X-ray optical diffraction analysis of the TlInSe2<Au> crystal was experimentally carried out [1-3]. Based on ellipsometric data, optical functions were determined - the real and imaginary parts of the dielectric permittivity of crystals, the coefficients of optical absorption and reflection, the dependence of energy losses and electric field power on the effective density, the spectral dependences of the real (σ_r) and imaginary (σ_i) parts, optical electrical conductivity were experimentally studied. The fluorescence spectra of the ternary compound TlInSe2<Au> were isolated and analyzed, when excited by light with a wavelength of 532 nm. X-ray studies of TlInSe2<Au> showed that this phase crystallizes into tetragonal systems [4,5]. Ellipsometric measurements showed that the real (ε_1) and imaginary (ε_2) parts of the dielectric constant are components of the dielectric constant tensor of the uniaxial joints under consideration and do not depend on the angle. Analysis of the dependence of the real and imaginary parts of the refractive index of the TlInSe2<Au> crystal on photon energy showed that the nature of the change in the real and imaginary parts of the dielectric constant does not differ significantly. When analyzing the spectral dependences of the real (σ_r) and imaginary (σ_i) parts of the optical electrical conductivity, it was noticed that the real part of the optical electrical conductivity increases exponentially in the energy range 0.894 - 3.505 eV. In the energy range of 0.654 - 2.91 eV, the imaginary part of the optical electrical conductivity increases linearly, reaches the maximum value, and decreases at an energy of 2.91 eV. At 3.6 eV, an inversion of the imaginary part of the optical electrical conductivity of the TlInSe2<Au> compound is observed. From the graphs of the effective power density versus electric field energy losses, it is known that the effective power density increases significantly in the energy range of 0.805 – 3.52 eV [6]. The fluorescence spectrum of the ternary compound TlInSe2<Au> upon excitation at the wavelength of 532 nm has been studied and it has been found that this phase has luminescent properties.

1. E.M.Gojayev, G.N. Mammadova, S.S. Osmanova et al. Int. J. Mod. Phys. B 35 (2021) 2150011.
2. E.M.Gojaev, G.N.Mammadova, R.S.Rehimov, P.F. Aliyeva Int. J. Mod. Phys. B 36 (2022) 2250083.
3. E.M.Gojayev, G.N. Mammadova Int. J. Mod. Phys. B 35 (2021) 2150201.
4. E.M.Gojayev, G.N. Mammadova, F. Mammadov, et al., Int. J. Mod. Phys. B 36 (2022) 2250102.
5. E.M.Gojayev, G.N.Mammadova, B.V.Aliyeva. Global Journal of Engineering Science and Research, 5(2018) 177.
6. E.M. Gojaev, S.O. Kulieva, G.N. Mamedova. Am. Sci. Journal. 1 (2017) 45.

THERMAL CONDUCTIVITY OF A SOLID SOLUTION CRYSTAL $TlInSe_2$ -$TlIn_{1-x}Dy_xSe_2$

Jafarov M.B.[1], Verdiyeva N.A.[2]
[1]*Azerbaijan Technology University, Baku, Azerbaijan*
[2]*Ganja State University, Ganja, Azerbaijan*

Recently, along with simple substances various structures of compounds such as $A^{III}B^{V}$ and $A^{III}B^{VI}$, which have a wide band gap, have been of great interest. At present, the object of such studies is the semiconductor chain and layered compounds of the $A^{III}B^{III}C_2{}^{VI}$ type (A-Tl; B-Ga, In; C-Se, Te). In these compounds, the chemical bonds and electronic properties are due to unpaired valence electrons. These semiconductor compounds have a number of interesting physical properties: ferroelectric semiconductor, memory and transformation, and other effects. Having a defective crystal structure, these materials are highly sensitive to ultraviolet, visible light, infrared, X-ray, and gamma radiation. It was determined that the thermal conductivity of the crystal depends on the number of impurity atoms added to the structure.

One of the brightest representatives of $A^{III}B^{III}C_2{}^{VI}$ type solid solutions, which has fundamental properties and practical value, is the $TlInSe_2$ solid solution crystal. It was determined that the $TlInSe_2$ solid solution crystal has high anisotropy. The study of the thermal properties of compounds of solid solutions of the $A^{III}B^{III}C_2{}^{VI}$ type provides information about the chemical and structural structure of crystals, the nature of lattice defects, and the thermoelectric properties of binary systems [1]. The change in the conductivity coefficient of a $TlInSe_2$ solid solution crystal over a wide temperature range obeys the law $\chi \approx T^{-1}$. This dependence confirms the predominance of the three-phonon scattering mechanism in the process of thermal energy transfer in the crystal.

As a result of the studies, it was revealed that the addition of a certain percentage of the rare earth metal Dy (dysprosium) to the composition of the $TlInSe_2$ solid solution crystal affects the value of thermal conductivity and the nature of the dependence of the thermal conductivity coefficient on temperature. It was determined that in the solid solution crystal under study the thermal conductivity of electrons is negligibly small. And the process of heat transfer involves mainly phonons [2]. In the temperature range of 100-600 K, a decrease in the thermal conductivity coefficient is observed with increasing temperature. This decrease at 80-300 K obeys the law $\chi \approx T^{-1}$; in the future, this decrease weakens. This dependence of thermal conductivity on temperature corresponds to the process of three-phonon scattering in the crystal.

1. Kerimova E.M. Kristallofizika nizkorazmernix xal'kogenidov BAKU: «Elm», 2012. S.708
2. Zarbaliev M.M. Elektricheskie i teplovie svoystva tverdix rastvorov sistemi TlİnSe2 – TlYbSe2. Fizika. 1998. T.4. №1. C.19-21

PHOTOLUMINESCENCE IN LAYERED GaS CRYSTALS IRRADIATED BY γ-QUANTA

Madatov R.S.[1], Alekperov A.S.[3], Jabarov S. H.[2], Tagiev T.B.[1]
[1]*Institute of Radiation Problems, Ministry of Science and Education, Baku, Azerbaijan*
[2]*Institute of Physics, Ministry of Science and Education, Baku, Azerbaijan*
[3]*Azerbaijan State Pedagogical University, Baku, Azerbaijan*

The studied p-GaS single crystals were grown by the Bridgman method. Er doping was carried out during the growth process. The resistivity of the obtained samples along and perpendicular to the c axis at room temperature was $2 \cdot 10^9$ and $3 \cdot 10^7$ Ohm·cm, respectively. Irradiation of the samples with γ-quanta was carried out on a ^{60}Co installation at 300 K. A helium-cadmium laser (λ=0.3716 μm) was used for excitation.

The PL spectra of GaS and GaS:Er samples at 77 K before and after irradiation were studied. Intense exciton emission bands with λ_1 = 0.48 μm were observed in unirradiated GaS crystals. After irradiation of samples with a dose of 30 krad, a wide structureless band of much higher intensity appears with maxima at λ_1 = 0.48 μm, λ_2 = 0.52 μm and λ_3= 0.66 μm. At high irradiation doses (100 krad), the observed maximum λ_3= 0.66 μm disappears and the dependence takes on the same form as before irradiation.

It has been shown that in doped crystals the exciton radiation band slightly shifts to the long-wave region (495 nm) and at the same time its intensity increases. In addition, three clear emission lines with high intensity in the region λ_1 =550-552 nm are observed in the PL spectrum. After irradiation with gamma rays with a dose of 30 krad, new high-intensity emission peaks appeared in the GaS:Er crystals in the region of 552-570 nm. In this case, the peak in the region of 495 μm is not observed, and the intensity of the peak at 550 μm increases. Irradiation with a dose of 100 krad leads to an increase in line intensity in the spectral region of 550-570 μm and the appearance of new peaks at 521, 526 and 585 μm. Further irradiation gradually reduces the intensity of the peaks, and the spectrum looks like that of unirradiated samples.

It has been established that when doping GaS single crystals, Er enters the lattice as an impurity, which replace Ga atoms in the cationic sublattice of the crystal, forming small Er acceptor centers. The peaks observed for pure crystals at 77 K are defective in nature and disappear at high erbium concentrations...The addition of erbium to GaS quenches the PL in the region of 0.48 eV, caused by the recombination of the free exciton n=1, and promotes the excitation of the PL in the region of 0.510-0.580 μm. The redistribution of PL intensity in the region of 0.510-0.580 μm is due to the transfer of energy to the rare-earth centers in the activated crystals. The observed number of bands in the spectrum and their narrowness give grounds to believe that Er+3 ions occupy predominantly one position in the studied samples, forming the main erbium center. Along with the main Er+3 center, complexes consisting of Er+3 ions, intrinsic crystal defects, or uncontrolled impurities can form in GaS. This is evidenced by the results of a photoluminescence study, which made it possible to identify 3 different erbium centers. With increasing irradiation dose in crystals, both the intensities of interlayer bonds and the degree of spatial heterogeneity in the distribution of defects in the samples change. It is assumed that complexes containing gallium vacancies and erbium atoms, their concentration depending on the irradiation dose, are responsible for the new recombination centers. The experimental results obtained in irradiated GaS crystals are satisfactorily explained within the framework of the model.

CERTAIN ASPECTS OF ELECTRICAL CURRENT RELAXATION IN $TlInSe_2$ COMPOUND

Madatov R.S.[1], Najafov A.İ.[2], Mammadov M.A.[1], Mamishova R.M.[1], Asadov F.Q.[1], Asadova Z.İ.[1]

[1]*Institute of Radiation Problems, Ministry of Science and Education, Baku, Azerbaijan*
[2]*Institute of Physics, Ministry of Science and Education, Baku, Azerbaijan*

In this work, the relaxation of the electric current at different voltages (at different values of the electric field intensity) in the TlInSe2 compound at a temperature of 300 K was studied. It was determined that at constant low voltages, relaxation processes occur in the $TlInSe_2$ compound resulting in a decrease in current as a result of accumulation of electric charge. At relatively large voltages, relaxation processes accompanied by an increase in current occur due to charge carriers injected from the contacts.

$TlInSe_2$ semiconductor compound belongs to the group of $A^{III}B^{III}C_2{}^{VI}$ ternary compounds and has a chain structure. The interest to these compounds is due to the small size of their crystal structure, unique electrical and photoelectric properties, as well as sharp anisotropy of physical properties in different crystallographic directions.

In many cases, the relaxation of the current at a constant value of the voltage is observed in the samples of these compounds, which results in the accumulation of a certain amount of electric charge in the internal region of the studied systems. Current relaxation and accumulation of electric charge in these compounds are associated with the presence of local levels in the forbidden zone due to inhomogeneities, impurities, etc. in them.

In the presented work, the relaxation of electric current at constant voltage was studied in TlInSe2 compound, which is a representative of $A^{III}B^{III}C_2{}^{VI}$ compounds. Unlike other analogues, in samples of this connection, at constant small values of voltage (at values of electric field intensity of 3-25 V/m), the intensity of the current decreases within 0-120 seconds, and then increases again. After the values of the intensity of the field E>25 V/m, and at constant values of the voltage, the intensity of the current constantly increases over time.

The analysis of the obtained results shows that at constant and small values of the electric field, the flight time of the charge carriers between the electrodes is greater than the time of their capture by the traps, and within 1-2 minutes a part of the free charge carriers is captured by the local levels existing in the forbidden zone. The value of the electric charge accumulated as a result of the capture of charge carriers by the traps during the first 2 minutes at the value of the electric field intensity of 19.2 V/m was calculated. Over time, after the filling of the traps holding the charge carriers, the current intensity at a constant value of the voltage begins to increase. At small values of the field intensity, the rate of increase of the current is relatively slow at large values, and the rate of change gradually decreases.

It was determined by the conducted studies that at constant low voltages, relaxation processes occur in the $TlInSe_2$ compound resulting in a decrease in current as a result of the accumulation of electric charge. At relatively high voltages, relaxation processes accompanied by an increase in current occur due to charge carriers injected from the contacts.

EFFECT OF GAMMA RADIATION ON SURFACE MORPHOLOGY OF GaSe LAYERED MONOCRYSTAL

Madatov R.S., Hajiyeva S.A.
Institute of Radiation Problems, Ministry of Science and Education, Baku, Azerbaijan

Increasing the possibilities of controlling the physical properties of materials with the application of radiation technology as a convenient method for the modification of semiconductor materials allows predicting the characteristics of diodes in advance [1]. By controlling the distribution of surface defects under the influence of radiation, it allows to increase photosensitivity in the ultraviolet and visible zones of the spectrum. The GaSe layered single crystal from the $A^{III}B^{VI}$ group compounds was obtained under laboratory conditions by the Bridgman-Stockbarger method and its band gap energy is 2 eV [2]. The dimensions of GaSe single crystal studied by AFM method were 0.21x5.212x9.625mm. The degree of anisotropy with respect to the crystal axis was ~10^2. The γ rays from $C_0$60 isotope were used as the radiation source and the samples were irradiated with a dose of Dγ=50-100 Krad.

The aim of the work is the analysis of the three-dimensional surface images of GaSe layered single crystal exposed to initial, γ-irradiation and irradiated after 60 minutes at 100^0 C thermal annealing samples.

Surface images were acquired through AFM. As it is shown from the figures, the dark colors represent gallium (Ga) atoms, and the light colors represent selenium (Se) atoms. It can be seen from Figure 1a that there is roughness on the surface of the crystal, and the size of this rough part is 13nm, which is determined from the histogram curve. The convex and concave parts are obtained as a result of the distribution of Ga and Se atoms.

a) 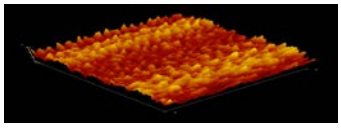 **b)** 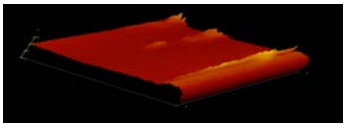 **c)** 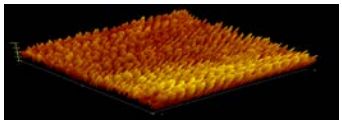

Fig. 1. Three-dimensional 3D images of GaSe single crystal before irradiation (initial)(a), after 100 Krad irradiation (b), and after 100 Krad irradiation of GaSe single crystal thermally brewed at 100° for 60 minutes (c)

This is due to the migration of radiation defects. Thus, defects are observed to accumulate around the corresponding centers. The histograms of these layers are characterized by the presence of nanoparticles in the range from 80 nm to 120 nm. After irradiating the thermally brewed crystal with gamma quanta at a dose of 100 krad, the distribution of different types of nanoparticles covers a wider range - from 120 nm to 250 nm. The number of nanoparticles decreased by 8.2 times and reached to 85 compared to 50 Krad radiation. Based on the obtained results, it can be said that it is possible to purposefully control the distribution and size of defects in layered crystals by the influence of gamma irradiation.

1. A.Z.Abasova, R.S.Madatov, V.I.Stafeev, Radiation-stimulated processes in chalcogenide structures, ELM (Science), 352 (2010)
2. Singh N.B., Suhre D.R., Balakrishna V., Marable M., Meyer R., Fernelius N., Hopkins F.K., Zelmon D. Far-infrared conversion materials: gallium selenide for far-infrared conversion applications // Prog. Cryst. Growth Character. Mater. 1998. V.37. P. 47-102.

ELASTIC PROPERTIES OF GALLIUM ARSENIDE CRYSTALS

Akhmedzhanov F.R., Toshpulatov I.Sh.
Institute of Ion-Plasma and Laser Technologies, Uzbekistan Academy of Sciences, Tashkent, Uzbekistan

Cubic crystals of gallium arsenide have a high acousto-optical quality factor and are widely used as working media in acousto-optical devices in the infrared range [1]. To improve the characteristics of these devices, it is necessary to know the anisotropy of their elastic properties. We have studied the elastic properties of GaAs, including the anisotropy of the velocity of acoustic waves and the deviation of the energy flow from the direction of the wave vector in the (001) and (110) planes. Acoustic wave velocity measurements were carried out in the frequency range 30 – 450 MHz. The GaAs samples had the shape of a parallelepiped, ~1 cm long, oriented along the [100], [110] directions with an accuracy of 1^0. Piezoelectric transducers made of X- or Y-cut quartz were used to excite acoustic waves. The velocity of acoustic waves V was determined either by the pulse interference method with an accuracy of 0.01%, or using a delay generator, which makes it possible to measure the time intervals between elastic pulses with an accuracy of 0.01 μs [1]:

$$V = \frac{2L}{t}, \tag{1}$$

where L is the length of the sample under study. The accuracy of determining the velocity was approximately 0.2%.

From the measured values of the velocity of acoustic waves *V* along the [100] and [110] directions and reference data from [1], all independent components of the tensor of elastic constants of gallium arsenide were determined: c'_{11}, c'_{44} and c'_{12} [1]. These constants were used to calculate the anisotropy of the velocity of acoustic waves, as well as the elastic anisotropy parameter of GaAs [2]:

$$\Delta c' = c'_{12} + 2c'_{44} - c'_{11}, \tag{2}$$

which turned out to be equal to $\Delta c' = 5.4 \cdot 10^{10}$ N/m^2. The results of calculating the deviation of the polarization of longitudinal waves from the direction of their propagation in the (001) plane are shown in Fig. 1.

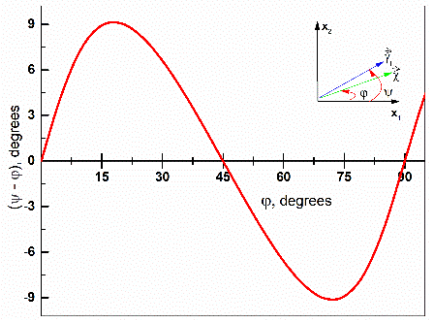

Fig. 1. Deviation of the direction of polarization of longitudinal waves from their direction of propagation in the plane (001). The angles are counted down relative to the [010] direction

The results obtained can be useful for predicting the general nature of the anisotropy of the elastic properties of cubic crystals.

1. Dieulesain E., Royer D, Elastic waves in solids I Free and guided propagation. pp. 177-199, 1996.
2. Jan W.Jaekena., Stefaan Cottenier, Solving the Christoffel equation: phase and group velocities. 2016.

MANIFESTATION OF THE EFFECT OF SUPERFLUIDITY IN QUANTUM GASES

Baizakov B.B.
Physical-Technical Institute, Uzbekistan Academy of Sciences, Tashkent, Uzbekistan

We have studied the manifestation of the effect of superfluidity in binary quantum gases with an unequal number of atoms in two components in a trap of toroidal shape. For the case of a weak imbalance in the number of atoms, a variational approximation has been developed that makes it possible to determine the critical value of the difference between atom numbers in the components, below which a localized state exists in the form of a vector soliton or quantum droplet. At a supercritical value of the imbalance, the unbound part of the atoms of the large component is pushed to the periphery and forms a gas with a constant density in a toroidal trap.

The small component is then set in motion through the larger component using an external potential.It was found that the slow motion of the smaller component does not excite density waves in the larger component, indicating a complete absence of friction/viscosity.Upon reaching a certain critical speed, the system goes into dissipative mode, and the property of superfluidity disappears. A new method for determining the critical speed of a probe object, at which the superfluidity disrupts, is proposed.

STUDY OF PLASMON OSCILLATION DISPERSION IN Si AND Ge CRYSTALS

Isakhanov Z.A., Umirzakov B.E., Khalmatov A.S.
Institute of Ion-Plasma and Laser Technologies, Uzbekistan Academy of Sciences, Tashkent, Uzbekistan

It is known that the structure of the characteristic electron energy loss (CEEL) spectra provides rich information not only about the electronic structure of crystals of various classes, but also about the change in this structure as a result of external factors. In this work, the dispersion effects in the CEEL spectra, which manifest themselves in bulk samples of Si and Ge, have been studied. The electron energy loss was studied by the CEEL method upon their reflection from Si(111) and Ge(111) at different angles of incidence of the electron beam on the surface. The sample surface was cleaned by prolonged heating (4-5 h) up to a temperature of 900-1100°C for silicon and 800-850°C for germanium under vacuum (2-3)×10^{-8} Torr and by short-term heating (5-10 min) immediately before taking spectra at temperature closer to the melting point. The control of the surface state during the cleaning process was carried out by the electron oje-spectroscopy (EOS) method.

The energy of primary electrons varied within E_p=500-1600 eV. Angular divergence of the primary electron beam was ~2°. The target current was ~10^{-7} A. The incidence angle of the electron beam on the sample surface (relative to the normal to the surface) changed from φ_2=35° to φ_1=45°, and the reflection angle from θ_2=55° to θ_1=45°, respectively. We have improved the program for calculating the absolute dispersion of plasmons in germanium and silicon since the structure factor and atomic form-factor differs significantly from noble metals [1]. The results of calculations made

for several values of the wave vector (100), (110), and (111) of the Si and Ge crystal planes are given in Table.

Figure show the energy losses of primary electrons for plasmon excitation in silicon. It can be seen from Fig. 1 that the absolute plasmon dispersions for silicon calculated from different crystallographic directions [100], [110], [111] differ significantly from each other. The [111] direction has 8 equivalent directions, and so on.

The absolute dispersion for Si and Ge calculated for different directions in the crystal will be as follows

Energy loss for excitation $\hbar\omega_v$ in Si and Ge

(hkl)	*Si (ΔE, эВ)*		*Ge (ΔE, эВ)*	
	calcul.	exper.	calcul.	exper.
(100)	14.89	16.20	13.63	14.2
(110)	15.20		14.20	
(111)	18.23	17.30	17.30	17.5

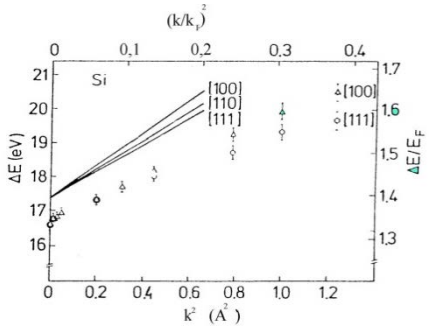

Fig.1. Dispersion of electron energy loss in silicon (symbols - experimental values; solid lines - calculated ones)

Si[100] 19.8–17.6=2.2 eV;Ge[100] 18.7–16.6=2.1 eV;
Si[110] 20.2–17.6=2.6 eV;Ge[110] 19,6–16.6=3.0 eV;
Si[111] 20.6–17.6=3.0 eV;Ge[111] 20.3–16.6=3.7 eV.

The absolute dispersion averages 2.6 eV for silicon and 2.73 eV for germanium; experimentally obtained data is 2.3 eV for silicon and 2.64 eV for germanium [2].

Thus, the theoretical and experimental results show that in the case of single-crystalline Si and Ge, with increasing k, the values of the bulk plasma oscillation increase by 2-3 eV.

1. A.A. Aliev, M.K. Ruzibaeva, Z.A. Isakhanov. Uzbek Physical Journal, 2005, Volume 7, No. 3, P.213–217.
2. A.S. Parshin, G.A. Alexandrova, A.V. Zyuganova. Surface, x-ray, synchrotron. and neutron. Research, 2007, No. 6, p. 32-38.

NEW DEVELOPMENTS IN THE THEORY OF RELATIVISTIC IDEAL GAZES - FROM CLASSICAL TO QUANTUM

Jumaev M.R.
Bukhara Engineering Technological Institute, Bukhara, Uzbekistan

The work presents an invariant relativistic theory of classical and quantum ideal gases subject to the relativistic distributions of Maxwell-Boltzmann, Fermi-Dirac and Bose-Einstein. Without applying the Gibbs canonical distribution method and the principle of maximum entropy, an alternative theory of ideal gases has been developed based on finding the macroscopic

characteristics of classical and quantum ideal gases (particle number density, pressure and average energy) by statistical averaging over relativistic - invariant velocity distributions (for Maxwell-Boltzmann gas) and moments (for the Fermi-Dirac and Bose-Einstein gas).

For the first time, expressions have been found for the average and root-mean-square particle velocities, which are valid for any ratio of thermal energy and rest energy of particles. For the first time, the limiting velocity of particle flows of quantum relativistic ideal gases has been determined. It has also been established that all real-life relativistic quantum ideal gases have adiabatic exponents that satisfy a certain fundamental inequality.

Content

INFLUENCE OF ELECTRON IRRADIATION ON THE CRYSTAL STRUCTURE OF $TlIn_{0,98}Fe_{0,02}Se_2$ SINGLE CRYSTALS

Khodzhaev U.O., Umarov S.H., Khallokov F.K.
Bukhara State Medical Institute, Bukhara, Uzbekistan,

The work investigated the effect of electron irradiation on the structure of $TlIn_{0.98}Fe_{0.02}Se_2$ single - and polycrystals. Irradiation of single crystals with electrons with an energy of 2 MeV and a fluence of up to 5×10^{16} el./cm^2 leads to a change in the parameters of the crystal lattice. Helps increase the size of nanocrystallites from 32.50 - 43.33 nm.

Introduction. $TlInSe^2$ crystals belong to the group of thallium chalcogenide compounds of type $A^{III}B^{III}C_2{}^{VI}$ with a pronounced layered structure.

There is very little information about radiation effects in doped $TlInSe_2$ crystals. Taking into account the above, the purpose of this work is to study the effect of electron irradiation on the crystal structure of p-$TlIn_{0.98}Fe_{0.02}Se_2$ doped with iron impurities, since there are no experimental data on the effect of irradiation on the physicochemical characteristics of these crystals in the literature.

Experimental methods. Irradiation of samples of the crystals under study with electrons with energy of 2 MeV and a beam current density of 0.085 μA/cm^2 was carried out at the “Electronics U-003” accelerator of the Institute of Nuclear Physics of the Academy of Sciences of the Republic of Uzbekistan. X-ray diffraction studies of the structure of $TlIn_{0.98}Fe_{0.02}Se_2$ were carried out on a Malvern Panalytical Empyrean diffractometer.

Experimental results and discussion. Results of measurement and processing of X-ray diffraction data of $TlIn_{0.98}Fe_{0.02}Se_2$ single crystals measured under the same conditions. Inter planar distances calculated from X-ray diffraction patterns can be unambiguously identified based on the tetragonal system that the lattice parameters have Inter planar distances calculated from X-ray patterns can be unambiguously identified on the basis of the tetragonal system, such that the lattice parameters have the following values: $a\sim b$ = 8.067746 Å, c = 6.815503Å, (sp. gr. I4/mcm) α=β=γ = 90^o. To obtain relatively complete information about the structure and compare the structural data of a single crystal and a powdered sample of $TlIn_{0.98}Fe_{0.02}Se_2$, an X-ray diffraction study of a powdered sample of $TlIn_{0.98}Fe_{0.02}Se_2$ was carried out, the results were compared with the X-ray diffraction characteristics of the single crystal. Based on calculations of X-ray diffraction data, the crystal structure was constructed (Fig. 1), the sizes of $TlIn_{0.98}Fe_{0.02}Se_2$ crystallites and some other characteristics were determined, from which it can be seen that the crystallite size increases with increasing electron irradiation fluence.

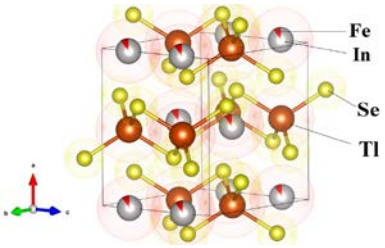

Fig.1. Crystal structure of $TlIn_{0,98}Fe_{0,02}Se_2$

Conclusion. When studying the X-ray diffraction method, it was found that doping $TlInSe_2$ crystals with 2 mol. % $TlFeSe_2$, as well as their irradiation with accelerated electrons with an energy of 2 MeV and a beam current density of 0.085 μA/cm2 to a fluence of 10^{17} el./cm^2, the single-phase nature of the samples is maintained.

DIELECTRIC LOSSES InCdO-pCdTe STRUCTURE

Utamuradova Sh.B., Muzafarova S.A., Mavlyanov A.Sh., Achilov A.S.
Research Institute of Semiconductor Physics and Microelectronics at the National University of Uzbekistan, Tashkent, Uzbekistan

MOS structures occupy a special place in modern microelectronics, especially when processing information in large arrays and large integrated circuits. The electrical and structural properties of the dielectric (high-resistivity oxide layer) and the surface layer of the semiconductor determine the quality of the oxide-semiconductor interface, on which the kinetic and degradation processes in MOS structures strongly depend. In addition, local centers in MOS structures ~~per~~form the acception, recording and storage of inputsignals. Therefore, control and management of the properties of local centers in the high-resistivity oxide layer and at the oxide-semiconductor interface becomes of paramount importance. The dissipated power in dielectrics is related to the presence of inhomogeneities - local defects. Local centers, molecules in the dielectric (oxide) and in the near-surface layer of the semiconductor cause polarization phenomena, effect mainly on the dynamic characteristics of MOS structures at a small alternating signal (V = 10 mV).

The dynamic characteristics of CdO-pCdTeMOS structures were studied on low alternating signal in a wide frequency range of 2 kHz-10 mHz when applying a bias voltage V = 0-7 V of positive and negative polarity on the external metal electrode. The study of admittance on a small alternating signal was carried out using bridges R-571 and L 2-7, which have a parallel equivalent circuit with ideal capacitance (C) and active resistance (R).

The frequency dependences of the capacitance (C), dielectric loss tangent (tan) and conductivity (G) of the In-CdO-p CdTe structure at different values of the applied constant voltage (V) have been studied.The studies showedthat the dependences tgδ(w), G(w) and C(w) are quite complex. For example, the dependence G(w) at V=0 at least at two points passes through maxima and minima. The first maximum in it is observed at a test signal frequency of $6\cdot10^3$Hz, and the second at $2.8\cdot10^4$Hz. The minimum values of G are realized at frequencies $w_1=10^4$Hz and $w_2=2.5\cdot10^5$Hz. It should be noted that the slopes of the G(w) dependence after the first and second extrema are different, which depends on the change in surface states in the high-resistivity layer of wide-gap CdO oxide.

After the first maximum and minimum, the slope of the G(w) dependence is much greater than that of the second extreme points. The conductivity value at low frequencies is much greater than at high frequencies. The capacitance at W = 10^3 Hz is equal to 950-960 pF, which, with increasing frequency, slowly drops to a value of 930 pF, then, passing through a minimum, it begins to increase to a value of C = 1500 pF, after which, with a further increase in frequency, it again begins to rapidly decrease and reaches a value of ~100 pF at w=10^7 Hz. With an increase in the applied constant voltage, the capacitance value at the maximum in the dependence C(W) falls, as a result of which the extremum completely disappears at a negative voltage equal to V = -2V. The experimental results obtained indicate that the high-resistivity oxide layer in the MOS structure under study is inhomogeneous due to the formation of a transition layer between the CdO and CdTe layers.

The conductivity and dielectric loss tangent in the structure under study are much greater than in silicon-based MOS structures. However, their optical and photoelectric properties are practically the same as silicon MOS structures.

SOLAR CELL WITH A MOS STRUCTURE BASED ON LARGE BLOCK pCdTe FILMS

Muzafarova S.A., Mavlyanov A.Sh., Achilov A.S., Faizullaev Q.M.
Research Institute of Semiconductor Physics and Microelectronics at the National University of Uzbekistan, Tashkent, Uzbekistan

To obtain pCdTe/CdO-film MOS structures, the authors deposed pCdTe at temperature of substrate T_s=700-720^{0}C by applying gas-transport method. After completing the process of synthesis, a substrate was cooled at a speed 6 - 8 C/ minute.

At a substrate temperature of 700-7200C, a polycrystalline CdTe film with a thickness of 30 microns and a resistivity of ρ=102-103 Ohm.cm with high values of microparameters and an excess amount of free Te tellurium atoms on the surface is synthesized. The CdTe film consists of blocks of microcrystals with a columnar grain structure, oriented along the growth direction and azimuth counting time, while the effective diffusion length of minority carrier electrons is Leff d=30 microns, and the lifetime t=1 μs.CdO layers were deposited onto such CdTe films using the magnetron method by ion dispersion in an atmosphere of 80-85% Ar, 12-15% O2. The resistivity of CdO films is 5 Ohm.cm.

Further increase in the concentration of oxygen in theoperating volume leads toa factor reduction of mobility, while specific resistance of films increases. Thus in a uniform work cycle structure CdO - TeO_2 is formed MOS - pCdTe in which dielectric layer TeO_2 has a thickness d=50 A^0, transparent conductor layer CdO in structure has following electro physical parameters: transparency T≥85 %, specific resistance R_s=5.10^{-3}Ω·cm of cm, concentration and mobility N = 3.10^{19} cm^{-3}.In the course of ionic dispersionthe temperature of a substrate is no more 500^{0}C. After that thermal evaporation in vacuum had been received top current demountable contact in the form ofΠ it temperature of a substrate 700^{0}C and values of pressure of residual gas 10^{-5} Torr. The area of such photo detectors made 1 cm^2.

The mode of obtaining the desired thickness of the TeO2 and CdO oxide layer with the necessary electrophysical and optical parameters is regulated by controlling the distance between the cadmium electrode and the CdTe film, the pressure applied between them, as well as the oxygen pressure in the system.

The thickness of the p-CdTe film is 0.8-1.0 μm, the concentration of equilibrium electron carriers is n0~10^{12} cm^{-3}. The CdO layer in this structure is an antireflection coating and serves as a passivator of surface states on the front region of n-CdTe.

The solar cell, made in the form of a rectangle with current-collecting electrodes with an area of 1 cm^2, had an efficiency of 16%. Solar energy parameters were measured under natural conditions at a solar luminous flux power of P = 55 mWt/cm^2.

The parameters of the solar cells under study had the following values: fill factor ξ = 0.51-0.55, I_{sc} = (20-22)·10-3 mA/cm^2 A, V_{oc} = 0.71-0.74 V at luminous flux power 220 mW incident on the sample, efficiency ξ = 12-15%. With the introduction of additional current, the connector contacts Rn did not change. Thus, it has been established that the leakage resistance does not make a noticeable contribution to Rn, which is obviously determined by the thickness of the CdTe layer and the transition resistance at the interface with the Mo substrate.

THE EFFECT OF LASER NANOSTRUCTURING OF SURFACES ON IMPROVING THE DIFFUSION WELDING PROCESS

Khomich Yu.V.
Institute for Electrophysics and Electric Power, Russian Academy of Sciences, St. Petersburg, Russia

Preparation of micro and nanostructures on the surface of solids is of great scientific interest and has an important application value associated with the possibility of modifying the surface properties of various materials. In this field of research lasers generating nanosecond, picosecond and femtosecond pulses are widely used. For the development of laser technologies, we have developed an approach based on the method of direct laser micro and nano-surface structuring using nanosecond sources of UV and VUV radiation. At a relatively low cost, such lasers are simpler and more reliable to operate, they have higher output energy and stability of radiation pulses. In addition, the depth of the surface layer modified by nanosecond laser radiation, determined by long thermal diffusion, is much greater than when irradiated with femtosecond pulses and for metals it can reach several microns**.**

This paper presents the results of a study of the formation of micro and nanostructures on the surfaces of metals, ceramics and dielectrics under nanosecond laser irradiation with wavelengths of 355 nm, 193 nm and 157 nm. The emphasis will be placed on multiple irradiation (100 pulses per spot) both in the stationary radiation spot and when it is scanned over the surface. Experimental results on the influence of the energy density and the wavelength of the radiation on the shape and geometric dimensions of the obtained structures will be presented. To explain the results obtained, the mechanisms of formation of micro and nanostructures will be briefly considered, taking into account such processes as laser ablation with the presence of local inhomogeneities of the material; melting of the material and the formation of crystalline phase nuclei from the melt; nonlinear relaxation of temperature stresses created by laser heating; ejection of liquid jets of the melt in the direction across the surface. The effectiveness of this approach is confirmed by the results of experiments that demonstrate improving of the quality of metal alloy joints in diffusion welding by pre-laser treatment of workpiece surfaces.

INFLUENCE OF DISPERSION ON THE LIGHT PROPAGATION IN CONDENSED MATTER

Tsoy E.N.[1], Suyunov L.A.[2]
[1]Physical-Technical Institute, Uzbekistan Academy of Sciences, Tashkent, Uzbekistan
[2]Karshi State University, Karshi, Uzbekistan

In general, the refractive index condensed media depends on the frequency of light. Due to this dependence, waves with different frequencies travel with different group velocities. The dispersion of the group velocity results, for example, in the pulse broadening during the propagation. For large intensities, nonlinear variation of the refractive index (the Kerr effect) become important. A balance between dispersive broadening of pulses and nonlinear effects can give rise to a formation of stable localized waves – solitons. Usually, optical solitons are formed due to a balance of

quadratic dispersion and cubic nonlinearity [1]. In present work, we considera media with dispersion of the fourth order (FOD) in a general form. The dynamics of light in nonlinear dispersive media is described by the following equation:

$$i\,u_z - \frac{\beta_2}{2}u_{\tau\tau} - i\frac{\beta_3}{2}u_{\tau\tau\tau} + \frac{\beta_4}{24}u_{\tau\tau\tau\tau} + \gamma|u|^2u = 0,$$

where $u(\tau, z)$ is the field envelope of the electric τ isthe time in the retarded frame, z is the propagation distance,β_j is the parameter of dispersion of the j-th order, j = 2, 3, and 4, and γ is the Kerr nonlinearity parameter. Usually, β_3 and β_4 are considered as small parameters, compared with β_2 [1-3]. For frequencies, close to zero dispersion points [1], quadratic dispersion is negligible [4,5]. We consider a general case when all dispersion parameters are of the same order.

The existence of stable electromagnetic pulses in media with FOD is shown. The parameters of these pulses (the amplitude, the width, the velocity and the phase increment) are obtained by using the variational approach. It is obtained that stable pulses exist for such values of the system parameters when there is no resonance interaction between linear waves and solitons. The dependence of the velocity of solitons in the retarded frame on parameters of dispersion and nonlinearity is found. In particular, it is demonstrated that a soliton moves when β_3 is present. Numerical simulations of the main equation confirm the results of the theoretical analysis. A generalization of results, related to an existence and stability of localized waves in condensed media with higher order dispersion, is also presented.

1. G.P. Agrawal, Nonlinear Fiber Optics, 4th ed. (Academic Press, 2007).
2. N. Akhmediev and M. Karlsson, Phys. Rev. A 51, 2602 (1995).
3. E.N. Tsoy and C. M. de Sterke, Phys. Rev. A 76, 043804(2007).
4. A. Blanco-Redondo, et al. Nature Commun. 7, 10427 (2016).
5. A.F.J. Runge, et al. Nat. Photonics 14, 492 (2020).

PICOSECOND LASER-INDUCED SURFACE STRUCTURE OF TITANIUM

Tojinazarov F.M.[1,3], Sobirov B.R.[2], Ibragimova E.M.[1,4], Iskandarov N.[1], Nazarov Kh.T.[1]
[1]Center for Advanced Technologies, Tashkent, Uzbekistan
[2]Institute of Ion-Plasma and Laser Technologies, Uzbekistan Academy of Sciences, Tashkent, Uzbekistan
[3]Ajou University in Tashkent, Tashkent, Uzbekistan
[4]Institute of Nuclear Physics, Uzbekistan Academy of Sciences, Tashkent, Uzbekistan

Several techniques are available for generating surface structures, including chemical etching, ion or electron beam lithography, mechanical probing using an atomic force microscope, and various laser methods [1,2]. The use of lasers is advantageous because it eliminates the need for dangerous chemicals or a vacuum, is more cost-effective than electron and ion beams, and offers high efficiency. The most effective and simple method for creating nano- and micro-surface structures with lasers is using weakly focused laser pulses that generate structures simultaneously across the entire laser beam exposure area [3-4].

A picosecond laser system is employed to create Laser-Induced Periodic Surface Structures (LIPSS) on Titanium surfaces utilizing dynamic laser scanning techniques. Operating at a

fundamental wavelength of 1064 nm, the system generates pulses with a duration of 28 picoseconds at a repetition rate of 50 Hz and pulse energy is set at 1 mJ. 15×15 cm^2 Titanium sample is positioned on a translational stage, with the scanning speed set at 50 mm/min. After processing, the surface morphology was studied by scanning electron microscopy (SEM).

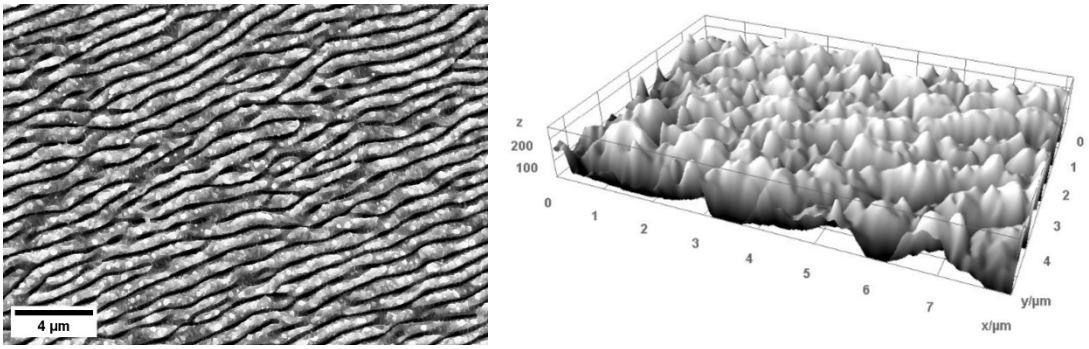

Fig.1. SEM micrograph of the LIPSS formed on a Ti and its 3 dimentional view

The laser-irradiated area exhibited a rainbow-like luster appearance. Figure 1 illustrates SEM images of the periodic structures and 3D view obtained via ImageJ software. The SEM image reveals the formation of LIPSS with an approaching regular pattern, oriented perpendicular to the laser polarization.The average spatial period, estimated using 2D-FFT analysis, measures approximately 910 nm. Topographic images indicate an increase in surface roughness. These treatments facilitate modifications in surface wetting, tribology, and optical properties.

1. BonseJ. et. al., Laser Micro- Nano-Engineering, Springer Int. Pub.(2021).
2. Gnilitskyi I. et al. Sci Rep 7, 8485 (2017).
3. Fraggelakis F. et al. Opt. Express. 25, 18131 (2017).
4. M.H. Dar, R. Kuladeep, V. Saikiran, N.D. Rao, Appl. Surf. Sci. 371 (2016).

CHARACTERIZATION OF THIN GRAPHENE FILMS SYNTHESIZED BY CHEMICAL VAPOR DEPOSITION

Tursunkulov O.M.[1], Xojiyev Sh.G.[1], Kim Sungjin [2]
[1]Center for Advanced Technologies, Tashkent, Uzbekistan
[2]Kumoh National Institute of Technology, Gumi, South Korea

The recent market of graphene applications is essentially driven by progress in the production of graphene with properties appropriate for the specific application, and this situation is likely to continue until each of graphene's many potential applications meets its own requirements. The great interest has developed in using graphene as nanoelectronic application due to its excellent physical and electrical properties such as tunable band gap, high thermal conductivity, and mechanical strength. It has exceptional carrier transport properties which makes it a promising material for future nanoelectronics. Besides graphene's high optical transmittance and conductivity it is also being considered as transparent electrode for flexible transparent displays and printable electronics. In order to realize these potential applications, it is essential to synthesize high-quality graphene films. The experimental results of the synthesis of graphene on a copper substrate by chemical vapor

deposition were present in this work.The growth of large graphene layers by chemical vapor deposition on copper substrates was demonstrated. In experiments polycrystalline Cu foil (Alpha Aesar, 99,9999% metal basis) is used as a substrate. The high pure methane gas precursor gas is carried with controlled pressure and the graphene formation time is 20-40 min at 800-1000 °C. After graphene formation, samples are cooled down by mechanically opening CVD box to decrease temperature in argon gas flow. The film was directly transferred to silicon substrate. The optimal growth of graphene films were found by varying the different CVD conditions such as annealing temperature and gas flow rate. The process of transferring graphene onto a silicon substrate was carried out by covering of polymethyl methacrylate organic films, followed by copper etching. Then, the process of transferring the organic film – graphene structure to an insulated silicon substrate was carried out. The surface morphology of a copper substrate with graphene domains which is grown on this surface are investigated by optical and scanning electron microscopies. Also this method allows to study of the microstructure of the surface of a polymethyl methacrylate-graphene films on the surface of an isolated silicon substrate before and after dissolution of the polymer coating. According above-mentioned experiments the growing processes of graphene on copper surface using chemical vapor deposition was carried out. It was observed appearance of graphene domains on copper surface which has quasi-tetragolnal shapes. Probably these domains are caused by methane decomposition on the grains of copper surface and probably, sizes depend from on grain boundaries and surface states of copper surface.The optimal CVD condition for 8 inch quartz tube (in dependence of temperature, pressure and gas conditions) for fabrication large area multilayer graphene was developed. At the same time, the properties of the grown graphene were determined by Raman spectroscopy, and the kinetics of the formation of discrete graphene domains both on the copper surface and on the surface of the silicon substrate were studied. According to the ratio of the intensities of the bands of the Raman spectrum, the formation of multilayer graphene is shown.

MICROPATTERN FORMATION ON TITANIUM SURFACE STIMULATED BY PULSED LASER IRRADIATION

Sultanov D.Sh., Tursunkulov O.M., Tojinazarov F.M., Nazarov Kh.T., Xojiyeva G.B.
Center for Advanced Technologies Tashkent, Uzbekistan

Metal based materials with highly ordered pattern have been widely investigated for various applications due to the high surface area, such as catalysis, microfiltration membranes, sensors, porous electrode and templates for preparation complex nanostructures.The treatment of a thick metallic samples by UV output from a diode-pumped Nd:YAG laser with specific frequency and tripling, gives a significant advantage due to controlled average speed and accuracy, and minimal recast layer. Therefore the effect of laser pulse interaction on the repeatability of micro-texturing pattern formation was studied for pulsed Nd:YAG laser irradiation of titanium surface. It was shown that picosecond diode pumped Nd:YAG laser (PL2231-50, Ekspla, Litvania) operating at the fundamental (UV line at λ =1064 nm) within the pulse energy range 0,7 mJ at the repetition rate 50 Hz are satisfactory for surface treatment. In this case, the titanium surface was irradiated with a pulsed laser in the form of a pattern of horizontal, vertical and diagonal stripes. Before exposure to pulsed laser irradiation, the metallic surface of titanium was fixed and mechanical polished on a

TM-1F Power Tool polishing machine, until obtaining mirrored surface. Then a sequential cleaning of the metal surface was carried out in ultrasonic bath, first in acetone, then in ethanol and deionized water, respectively, for 15 minutes at room temperature. Next, the sample was dried in a drying chamber for 3 hours at a temperature of 50 C. At low intensity of pulsed laser radiation, the metal surface start intensively heated, and at higher intensity, melting of the material will occur on subsurface area. If the power density becomes even higher, evaporation of the material will begin (removal of material from the surface). Surface topology, microstructure and elemental composition were characterized using the optical microscopy and scanning electron microscope. According to images of optical microscope, the surface of the initial sample original is homogenous. As can be seen from this image on the surface of the titanium presents very small surface inclusions formed as a result of the heating and cooling process. Besides, there are notobserved any longitudinal micro strips or specific surface defects (after mechanical polishing). In general, the morphology of the initial sample is identical over the entire surface. X-ray diffractometry was used to investigate the crystallinity and state of phase induced by the laser treatment. It has been shown that after exposing by pulsed picosecond laser radiation, uniformly distributed and ordered microcrystals are formed on the surface of titanium surface in the form of uniformly directed linear strips, i.e. ordered lattices of microcrystallites. Elemental analysis data show a significant concentration of titanium and the remaining oxygen content. The same data are confirmed by the X-ray diffraction pattern of the phase analysis of the sample. According to diffraction data, the main phase consists of titanium. At the same time, pulsed laser irradiation will be one of the advantageous tools for obtaining a rough surface with a uniformly distributed layer of microcrystallites, onto the metallic of which can be used for heterocatalysts and photocatalysts on a titanium substrate. Thus, the studies performed made it possible to determine the optimal parameters leading to the formation of a regular pattern structure and ordered lattices of microcrystals that can be used as carriers for metal catalysts. The research is supported by The World Bank projects REP-03032022/186.

NEW PHOTOENERGY MATERIALS BASED ON GaP BINARY COMPOUNDS IN SILICON

Zikrillaev N.F.[1], Ismaylov B.K.[1], Urakova F.E.[1], Turekeev H.S.[1], Kurbonaliev K.K.[2]
[1]Tashkent State Technical University, Tashkent, Uzbekistan
[2]Kokand State Pedagogical Institute, Kokand,Uzbekistan

Obtaining binary compounds of gallium and phosphorus elements in the crystal lattice of silicon leads to changes in the fundamental parameters of the initial material. The developed diffusion production technology allowing to create the necessary thermodynamic conditions for the formation of binary compounds in silicon made it possible to obtain a structure with heterovarizon transitions on the surface and near-surface region of silicon.

Samples of silicon doped with phosphorus and gallium atoms were obtained by the diffusion method in evacuated quartz ampoules. It is known that the maximum concentration of impurity in semiconductors is limited by the solubility limit of impurity atoms, which depends on the temperature of the diffusion process and the nature of impurity atoms.

The formation of binary elementary compounds with the maximum concentration of impurity atoms of gallium and phosphorus ($\sim 10^{22} cm^{-3}$) and their distribution on the surface and near-surface

layer of silicon was investigated using a scanning electron microscope Jeol super probe JXA-8800 R/RL. From the analysis of the study results, it was found that GaP binary compounds with maximum concentrations are formed on the surface and near-surface layer of silicon up to 0.3 μm.

The atom concentration distribution of GaP binary compound GaP to silicon can be divided into four sites:

1. At the surface where the GaP binary compound concentration is equal to or greater than the concentration of individual silicon atoms in the starting material;

2. The concentration of binary compounds decreases and neutral-molecular compounds like Si_2GaP appear;

3. The number of neutral-molecular compounds increases and GaP binary compounds actually disappear;

4. A site that is mainly composed of silicon atoms. Binary GaP compounds and neutral-molecular compounds Si_2GaP can be found in this section, but their concentration is much less than the concentration of the original silicon atoms.

The obtained research results allow to create efficient solar cells based on silicon with GaP binary compounds, which in the future will provide a complete replacement of multi-cascade, expensive photovoltaic cells based on binary semiconductors $A^{III}B^{V}$ or $A^{II}B^{VI}$.

Development and creation of heterovarison structures based on binary Ge_xSi_{1-x} compounds in silicon is not only of scientific, but also of great practical interest. Obtaining such structures with certain electrophysical parameters significantly extends the spectral range of sensitivity, which makes it possible to create on their basis photodetectors and sensors with a wide spectral operating range, and efficient photocells in photoenergetics.

EFFECT OF TELLURIUM IMPURITY ON THE STRUCTURAL PARAMETERS OF A SILICON NANOCLUSTER IN Si CRYSTAL

Sulaymanov N.T., Tashmetov M.Y., Makhkamov Sh.M., Rafikov A.K., Egamov S.R., Nazarmamatov Sh.M.

Institute of Nuclear Physics, Uzbekistan Academy of Sciences, Tashkent, Uzbekistan

Some of the low-dimensional structural formations in silicon are clusters, which can significantly affect the properties and characteristics of monocrystalline silicon and an impurity changes the structural parameters of the silicon hydride clusters.

This raises a number of fundamental issues related to the choice of impurity, allowing for control of material properties. To obtain nanostructures with specified parameters and energy characteristics, technological chains of synthesis methods or doping of the original material with the desired impurities are often used in practice. However, the structural parameters and properties of nanoclusters can be predicted if computational methods of modeling the structure are applied at certain stages of the researchinstead of instrumental ones. In this work, the method of computer modeling was usedwithin the ORCA software package to determine the structural parameters and main energy characteristics of the nanoclusters $Si_{29}H_{36}$ and $Si_{87}H_{70}$ containing a dopant tellurium atom in the cluster center or nearby.

According to the calculations and optimization of the structure, it is shown that Te, occupying the central node in the crystal lattice of the cluster $Si_{28}H_{36}$:Te, and not forming equilibrium covalent

bonds with neighboring silicon atoms, reduces the symmetry in the local defect area from T_d to C_{2v}. In the optimized structure of the cluster $Si_{86}H_{70}$:Te, tellurium occupies an interstitial position near the geometric center of the cluster and forms equilibrium polarized bonds with neighboring silicon atoms, reducing the symmetry in the local defect area from T_d to C_∞.

Since the tellurium atom becomes positively charged, the surface of the cluster gains a negativecharge. Also, the energy band structure changes: the forbidden gap of the original clusters $Si_{29}H_{36}$ with E_g=-5.138 eV and $Si_{87}H_{70}$ with E_g= -2.686 eV widens to E_g= -5.546 eV and E_g= -3.092 eV, respectively, when tellurium atom is placed into the clusters $Si_{28}H_{36}$:Te and $Si_{86}H_{70}$:Te, and a deep level is formed.

It was established that if the impurity atom Te is introduced near an existing Si vacancy, the width of the forbidden gap for $Si_{28}H_{36}$:[V+Te] and $Si_{85}H_{70}$:[V+Te] will be closer to the gap width of the original cluster.

Thus, the results of computer modeling showed that the introduction of tellurium into silicon nanoclusters leads to structure changes in the area of defect formation and the formation of electronic traps in the forbidden gap. The Te^{2-} impurity deep level persists when interacting with a vacancy, which indicates the electrical activity of tellurium in the matrix of silicon atoms. The computer modeling of silicon cluster structures $Si_{28}H_{36}$:Te, $Si_{28}H_{36}$:[V+Te], $Si_{86}H_{70}$:Te, and $Si_{85}H_{70}$:[V+Te] conducted within the ORCA software package confirms the dependence of the position of the Te atom in the Si atom matrix on the size of the nanocluster and the manifestation of the *Jahn-Teller effect* when interacting with a vacancy.

VIBRATION SPECTRA AND VARIOUS TOPOLOGICAL ANALYZES FOR ACETOPHENONE AND ITS SOLUTIONS. EXPERIMENTAL AND DFT CALCULATIONS

Khudaykulov B., Jumabaev A., Absanov A., Holikulov U., Norkulov A.
Samarkand State University, Samarkand, Uzbekistan

Intermolecular interactions, particularly hydrogen bonding (HB) and Van der Waals forces, are closely related to many physical and chemical phenomena [1]. In particular, hydrogen bonding plays an important role in the structure of proteins and DNA, which are important in the functioning of living organisms.

In this work, biologically active acetophenone and its interactions with ethanol and chloroform were investigated using vibrational spectroscopy (Raman) via C=O, C-H stretching and C-H breathing vibrational bands which involved in intermolecular interactions. The obtained experimental results show that in both solutions of acetopenone, a red shift was observed in the C=O stretching vibration band, and a blue shift was observed in the C-H stretching and ring breathing vibration bands. It was predicted that the reason for such shifts is H-bond formed by C=O and weak (non-classical) H-bond formed by C-H in acetophenone and solvents. Quantum chemical calculations, i.e. AIM, NCI and RDG, were performed to determine noncovalent interactions. It was confirmed that in the acetophenon-ethanol and acetopheon-chloroform complexes there are weak H-bonds through the C=O group and mainly Van der Waals bonds are formed through the C-H group. By comparing the Raman frequencies and the calculated frequencies by PED analysis, agreement was observed. Using the molecular electrostatic potential surface map, the charge distribution in

acetophenone molecules was visualized and the charge-dependent parameters were determined. It was found that the parts of the negative electron potential for ethanol moved from the carbonyl group of acetophenone to the carboxyl group of ethanol, and for chloroform, the potential around the carbonyl group of acetophenone decreased.Through FMO analysis, electronic properties, thermodynamic and chemical parameters of acetophenone monomer, dimer and solvents, as well as parameters determined by HOMO and LUMO energy difference, were determined. When looking at the charge distribution in the formation of the complex through the Mulliken charge distribution analysis, it was observed that the atoms participating in the interaction changed more. Through electron localization function (ELF) and localized orbital locator (LOL) analyses, the chemical bonds and electron regions in the atomic and molecular systems of the titlle complexes were studied using colors differences.

1. Y.-Y. Shan, X.-H. Ren, H.-J. Wang, W.B. Dong, Struct. Chem. 18 (2007) 709–716.

RADIATION CHANGES IN THE STRUCTURE OF CRYSTALS OF SOLID SOLUTIONS BASED ON BARIUM HEXAFERRITE

Salakhitdinova M.K.[1], Ibragimova E.M.[2], Kuvandikov O.K.[1], Kulmatova G.[1]
[1]Samarkand State University, Samarkand, Uzbekistan
[2]Institute of Nuclear Physics, Uzbekistan Academy of Sciences, Tashkent, Uzbekistan

Increased interest in barium hexaferrites ($BaFe_{12}O_{19}$) is due to its unique properties, characterized by high anisotropy, corrosion and chemical resistance, high Curie temperatures and saturated magnetization, whichmake them usefulfor the manufacture of magnetic and magneto-optical devices, as well as elements in ultra-high frequency electronics devices (ferrite absorbers of electromagnetic waves, antennas, cores, memory elements) [1].

The purpose of this work is to study the effect of gamma irradiation and electron irradiation on the crystal structure and magnetic properties of barium hexaferrite.The research objects were prepared according to the methodology described in [2, 3]. Samples with an area of 1 cm^2 had thickness of 1±0.05 and 8±0.1 mmwere irradiated in the ^{60}Coγ-field with the isotropic4π-geometry at the dose rate of 84 R/s in air at thetemperature of 323 K (Institute of Nuclear Physics Acad.Sci.Rep.Uzb., INP).Irradiation with the gamma–quantawith energies of 1.17 and 1.33 MeV is sufficient to excite the nuclei of Ba, Fe, Oand thereby displace atoms from their lattice sites. The measurements were carried out after long-term crystal lattice relaxation of the samples after the formation ofinitially unstable defects.The structure and phase composition of barium hexaferrite samples were determined using XRD diffractometer (PANalytic, Netherland) installed in the INP. Since the samples can be modeled as highly compacted powder, they were measured on the stage rotating at 30 rpm.The diffractometer uses CuK_α radiation (β-filter, Ni, tube current and voltage 30 mA and 30 kV), the detector moves along the goniometerark at the constant speed of 4 deg/min, and the reflected photons are registered with step of 0.02 deg. The spectra were scanned in the 2Θ angle range 5-140 deg.

When excited with energies above the threshold 1.02 MeV, electron-positron pairs are formed, which affect the electronic structure. At the irradiation in γ-beam converging on sample, the highest density of γ-exposure is achievedthere, and the crystal lattice is heated by deposited radiation, sufficient for structural-phase transitions. Analysis of X-ray diffraction measurements of barium

hexaferrite shows that γ-irradiation to dose of 2×10^7 R caused an increase in the main structural phase $BaFe_{12}O_{19}$ due to decrease in the amount of the $Ba_2Fe_{30}O_{46}$ phase. At the same time, the amounts ofminor Fe_2O_3 and $Fe_{2.957}O_4$ phases practically did not change.Studies of the magnetic properties of Ba-hexaferriteat 300 Kshowed that before irradiation their magnetization was 1.2 emu/g, and after γ-irradiation of the sample to dose of 10^7 R, the saturated magnetization reached its maximum value (~34 emu/g). This makes it possible to use Ba-hexaferrite in spin-wave and microwave devices.

The authors express their gratitude to Prof. Vinnik D.A. for providing barium hexaferritesamples and Prof. Granovsky A.B. for useful discussions.

1. Jalli J. *et all. J.of Magnetism and Magnetic Materials,* **32** (2011), 2627-2631
2. Meng Y.Y. *et all. J.of Alloys and Compounds,* **583** (2014), 220-225.
3. VinnikD.A.*et all. J. of Structural Chemistry,* **64** (2023), iss.6, p.1-9.

FEATURES OF FORMATION OF OXYGEN-CONTAINING PRECIPITATES IN SINGLE-CRYSTAL SILICON

Makhmudov Sh.A., Rafikov A.K., Erdonov M.N., Tashmetov M.Yu., Makhkamov Sh.
Institute of Nuclear Physics, Uzbekistan Academy of Sciences, Tashkent, Uzbekistan

It is known that the Czochralski method is mainly used to obtain monocrystalline silicon.These crystals are widely used for the production of resistors, diodes, transistors and the manufacture of solar cells, which do not require a high degree of purification from oxygen impurities. However, such crystals cannot be used for making large integrated circuits, since silicon monoxide and other uncontrolled impurities enter the bulk of the silicon crystal from the crucible material, and it causes the formation of defects and changes in the properties of the final product.

Oxygen in silicon existis in two states: in the composition of a solid solution up to a concentration of $2\cdot10^{18}$ cm^{-3} and in the oxide SiO_x in the form of phase inclusions with a size of 1÷50 μm, distributed uniformly in the volume of Si up to concentrations of $\sim 10^7$ cm^{-3}. Heat treatment of silicon crystals containing the mentioned inhomogeneities causes the decomposition of a supersaturated solid solution of oxygen and the SiO_4 complex with the release of oxygen and the formation of oxygen-containing structural defects of various sizes.

The purpose of this work was to study the formation of low-dimensional inhomogeneities including oxygen on the surface of heat-treated silicon.

The experiments were carried out with single-crystal *n*-type silicon grown by the Czochralski method, having a resistivity of $\rho\approx 3$ Ω·cm, phosphorus and oxygen concentrations up to 10^{15} cm^{-3} and $2\cdot10^{17}$ cm^3, respectively.The samples had a working surface (111) with an area of 4×22 mm and a thickness of 1.4 mm. Before measurements, the samples were subjected to isothermal annealing at a temperature of 900°C (which corresponds to the optimal decomposition temperature of a supersaturated solid solution of oxygen in Si), and then polished. The crystal structure and phase composition were studied by X-ray diffractometry.The Bragg symmetric reflection of $Cu_{K\alpha}$ radiation from the sample surface was measured in the range of 2θ angles from 15° to 140° with a scanning rate of 0.33 deg/min and an angular step of 0.0200 degrees.A number of reflections were found in the X-ray diffraction patterns of the samples before and after heat treatment, which are

associated with diffuse reflections at angles of 17.4°, 28.7°, 41.5°, 91.7°, 94.9° and 104.6°. It has been shown that heat treatment results in changes in the X-ray diffraction patterns of single-crystal silicon due to the decomposition of the SiO_n solid solution with the formation of amorphous SiO_2 and critical oxygen precipitation nuclei with different contents of oxygen atoms, both on the surface and at the boundaries of impurity-defect accumulations in precipitates. Based on the analysis of X-ray diffraction patterns of single-crystalline silicon grown by the Czochralski method, it was revealed that isochronous heat treatment at 900℃ for 6-10 hours causes the formation of precipitate nuclei of various types within the stoichiometric amorphous SiO_2. It has been established that, depending on the concentration of the SiO_n solid solution in the original silicon, upon annealing, oxygen-containing precipitates in the nanocluster form are assembled on the *n*-Si surface and at the Si-SiO_2 boundary, silicon oxide nanocrystalline phase has sizes of 65÷80 nm.

NEGATIVELY CHARGED METAL OXIDES NANOPARTICLES AS DISPERSE PHASE FOR THE FUNCTIONAL HYDROSOL

Mirzaev S.Z., Allaev B.A., Egamberdiev K.B., Trunilina O.V., Avvalboev A.A.
Institute of Ion-Plazma and Lazer Technologies, Uzbekistan Academy of Sciences, Tashkent, Uzbekistan

One of the essential factors of the metal oxide nanoparticles functional hydrosols sedimentation stability is the charge of nanoparticles. The system is stable, if Zeta potential more than 20 mV, at lower charge values coagulation occurs in the system, or the system is stabilized by organic molecules with long polymer chains. Nanoparticles with a negative surface charge, such as TiO_2 and SiO_2, effectively adsorb positively charged ions from the carrier medium, which can be both metal cations and organic cations. This fact must be taken into account for the choice of a stabilizing agent for a hydrosol.

The hydrosol preparing process included the following stages: nanoparticle initial suspension preparation, ultrasonic dispersion and addition of the anionic surfactants (sodium dodecyl sulfate) as stabilizing additives in concentration region above and below the MFCC —micelle formation critical concentration. Depending on the concentration of surfactants, they provide the effect of either an adsorption-solvate or a structural-mechanical factor to increase aggregate stability [1]. Nanoparticles obtained by the method [2] were used as research samples and the control of the size distribution was carried out by the NTA (nanoparticle tracking analysis) using NanoSight LM10 device from Malvern Panalytical operated at the wavelength 405 nm.

Tabl.1. Surfactant concentration influence to metal oxides hydrosol stability

Metal oxide	*Nanoparticle size, nm*	*Nanoparticle concentration, %*	*Surfactant concentration, mmol/l*	*Hydrosol stability*
TiO_2	100	3.5±0,1	4.0±0.1	Stable hydrosol
			8.0±0.1	Disperse phase sedimentation
			16.0±0.1	Phase transition to gel
SiO_2	125	3.0±0,1	4.0±0.1	Stable hydrosol
			8.0±0.1	Disperse phase sedimentation
			16.0±0.1	Phase transition to gel

The stability of the functional hydrosol depends on the concentration of anionic surfactant, as shown in table 1. If the concentration of surfactants corresponds to MFCC, the suspension is unstable. When the MFCC is achieved in the solution, a large number of aggregates of surfactant diphil molecules arise spontaneously. At surfactant concentrations above the MFCC the suspension also loses stability and transforms from a free-dispersed into a cohesive gel system. At the concentration of surfactants below the MFCC, it was possible to increase hydrosol stability up to 3 months and more.

1. T.A. Savitzkaya, I.M. Klimlenko, E.A. Shakhno et.al. *Sviridovskie chteniya*, 11, 121 (2015)
2. M.Sh. Kurbanov, L.S. Andriyko, J.A. Panjiev, S.A. Tulaganov, V.M. Gun'ko, A.I. Marynin, S. Pikus. *Journal of Nanoparticle Research*. 25, 202 (2023) doi.org/10.1007/s11051-023-05852-w.

MAGNETIC CHARACTERISTICS OF ARRAYS OF IRON-BASED NANOWIRES INVESTIGATED BY FORC ANALYSIS

Elmekawy A.[1,5], Sotnichuk S.[2], Nopolskii K.[2], Menzel D.[3], Mistonov A.[4]
[1]*Joint Institute for Nuclear Research, Dubna, Russia*
[2]*M.V.Lomonosov Moscow State University, Moscow, Russia*
[3]*Institute for Condensed Matter Physics, Braunschweig, Germany*
[4]*Institute for Solid state and material physics, Dresden, Germany*
[5]*Nuclear Research Center, Egyptian Atomic Energy Authority, Egypt*

The importance of magnetic nanowires (MNWs) relies on their possible uses in many applications [1]. Among them storage information units based on magnetic nanowires in a three-dimensional form represent the most popular of them. Since the process of recording and reading information takes place through the movement of domain walls, it is supposed to be affected by pinning at crystalline defects influencing the remagnetization processes [2]. In addition, magnetostatic interactions between the nanowires has influence on the remagnetization and will complicate the modelling [3].

For the aforementioned reasons, it is important to study such internal effects and possible reversal magnetization processes inside the material using the first order reversal curve method known by FORC, that plays an important role in explaining internal magnetic interactions in a unique way different from other conventional methods.

In the current work, we apply the FORC analysis for studying the magnetic properties in terms of internal magnetic interactions in arrays of iron nanowires. Iron is a preferable material for information storage application due to its high magnetic moment together with cubic crystal symmetry that should be reliable for magnetization reversal problems.

Studied samples of Iron-based MNWs produced using the template electrodeposition method at room temperature in a three-electrode cell. Porous anodic aluminum oxide (AAO) films with the thickness of 35 μm were used as templates. The samples under investigation have three different aspect ratios with diameters 33, 50, 70 nm and lengths 30, 19, 27 μm respectively. The geometrical parameters for each sample correspond to specific synthesis conditions.

By applying external magnetic field of 1.2 T parallel to the long axis of nanowires the interaction and switching field distributions for the given samples were obtained, indicating change

in the magnetic characteristics dependent on the geometrical parameters (length) reflecting different demagnetization behavior of the internal moments.

1. E. Ortega, S.M. Reddy, et al., J. Mater. Chem. C 5 (30) 7546–7552(2017).
2. Vázquez, M., Vivas, L. G., Physica status solidi (b), 248(10), 2368-2381 (2011).
3. Zighem, F. et al., Journal of Applied Physics, 109(1), 013910 (2011).

MONTE CARLO SIMULATION OF DIRECTIONAL EXTRACTION SYSTEM FOR LOW ENERGY NEUTRONS USING A DIAMOND NANOPARTICLE POWDER REFLECTOR

Teymurov E.[1,2], Nezvanov A.Yu.[1]
[1]*Joint Institute for Nuclear Research, Dubna, Russia*
[2]*Nuclear Research Department, Innovation and Digital Development Agency, Baku, Azerbaijan*

Neutron reflectors play a significant role in neutron physics and the nuclear industry as they reduce neutron losses and redirect fluxes of neutrons with different energies. The active cores of nuclear reactors are usually surrounded by reflectors of fast or thermal neutrons. Many neutron research facilities around the world are interested in increasing the intensity of low-energy neutron source, the applications of which can be found in both fundamental research and neutron scattering techniques [1].

Until recently, efficient reflectors for neutrons with velocities of 40–500 m/s had not been known. A promising solution to this issue is Detonation Nanodiamonds (DND). In a series of previous works, it was experimentally demonstrated that DND powders can be used as an effective diffuse reflector of very cold neutrons (VCNs), providing even the possibility to store the VCNs in a closed trap [2]. This property of DND has been utilized in experimental studies of enhanced directional extraction of VCNs using a DND reflector [3]. The use of such reflectors for enhanced directional extraction of VCNs from neutron sources will make it possible to significantly increase the neutron fluxes delivered to experiments and expand the scope of VCNs applications.

The simulation model of single neutron elastic coherent scattering in the fluorinated DND (F-DND) powder is based on the small-angle neutron scattering (SANS) data. The SANS intensity was described by the calculated intensity for the model-free size distribution of spheres with a diamond bulk density. The obtained size distribution of scatterers was then used for calculating the single scattering cross-section for the studied VCNs velocities within the first Born approximation. A multiple scattering process was simulated using the obtained single scattering cross-sections and the Monte Carlo method using Geant4 and Wolfram Mathematica.

This report presents the results of a Monte Carlo simulation of the probabilities of a directional extraction system for VCNs using a DND reflector. The proposed model also enables the calculation of the reflection coefficient (albedo) of VCNs, which is a critical characteristic of neutron reflectors and is not directly available from the described experiment.

1. Luca. Z., Rizzi, N., Folsom. B. et al. An intense source of very cold neutrons using solid deuterium and nanodiamonds for the European Spallation Source // Nucl. Instrum. Methods Phys. Res. Sect. A 1062 (2024) 169215.

2. Lychagin E.V., Muzychka A.Y., Nesvizhevsky V.V., Pignol G., Protasov K.V., Strelkov A.V. Storage of very cold neutrons in atrap with nano-structured walls // Phys. Lett. B 2009, 679, 186–190.
3. Chernyavsky S.M., Dubois M., Korobkina E., Lychagin E.V., Muzychka A.Yu., Nekhaev, G.V., Nesvizhevsky V.V., Nezvanov A.Yu., Strelkov A.V., Zhernenkov K.N. Enhanced directional extraction of very cold neutrons using a diamond nanoparticle powder reflector // Rev. Sci. Instrum. 93, 123302 (2022). DOI: 10.1063/5.0124833.

EFFECT OF NEUTRON RADIATION ON THE THERMAL CONDUCTIVITY OF “HANFORD” GRADE GRAPHITE

Tojiboev D.D., Kungurov F.R., Baytelesov S.A., Alikulov Sh.A., Tadjibaev D.P., Kudiratov S.N.
Institute of Nuclear Physics, Uzbekistan Academy of Sciences, Tashkent, Uzbekistan

Graphite serves as a key material for heat dissipation in electronic devices and nuclear engineering due to its remarkable thermal properties [1, 2]. Thermal expansion and conductivity of graphite have always been the main scientific parameters in the field of carbon materials. Therefore, great attention is paid to theoretical and experimental research in this area.

Figure 1 shows the results of the thermal conductivity measurements of “Hanford” grade graphite irradiated with a fluence of 3.17×10^{19} n/cm^2, depending on the sample temperature.

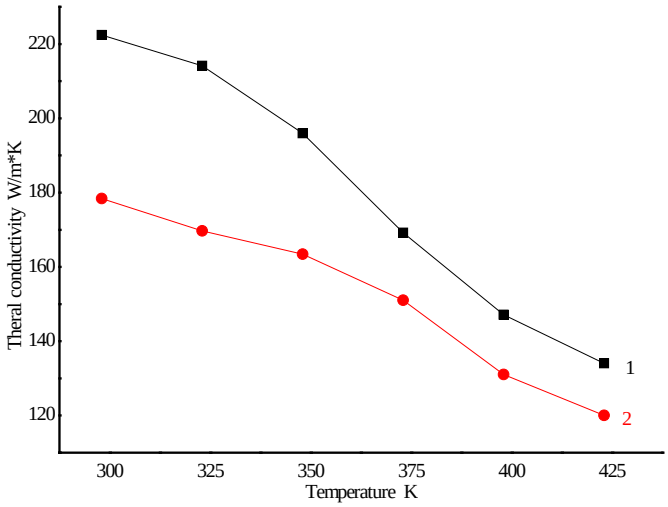

Fig. 1. Thermal conductivity λ(T) of “Hanford” grade graphite samples before and after irradiation with neutrons to the fluency of 3.17×10^{19} n/cm^2. 1 – non-irradiated sample; 2 - irradiated sample

Figure 1 shows that the thermal conductivity of “Hanford” grade graphite at a temperature of 298 K irradiated to the neutron fluency of 3.17×10^{19} n/cm^2 decreases by about 20%, relative to the non-irradiated sample. In this case, a decrease in thermal conductivity was observed depending on the temperature of the sample in the range from 298 K to 423 K.

1. Zhao Lu, Tang Jiang, Zhou Min, Shen Ke. A review of the coefficient of thermal expansion and thermal conductivity of graphite. New Carbon Mater. 2022, 37(3): 544-555. doi: 10.1016/S1872-5805(22)60603-6.
2. Zhmurikov E.I., Romanenko A.I., Bulusheva L.G. and others. Studies of the electronic structure and properties of composites based on the ^{13}C carbon isotope. // Surface. X-ray, synchrotron and neutron studies. 2007. No. 11. pp. 29-35.

THE INFLUENCE OF NEUTRON RADIATION ON THE ELECTRICAL RESISTIVITY OF GMZ GRADE GRAPHITE

Tojiboev D.D., Kungurov F.R., Baytelesov S.A., Alikulov Sh.A., Tadjibaev D.P., Kudiratov S.N.
Institute of Nuclear Physics, Uzbekistan Academy of Sciences, Tashkent, Uzbekistan

Reactor graphite is widely used as a core masonry material in uranium-graphite reactors, in particular, in RBMK-type power reactors. It is known that neutron irradiation leads to a strong degradation of graphite's electrical conductivity, and a particularly rapid decrease in electrical conductivity is observed when neutrons are irradiated with small fluences [1, 2].

The experimental dependencies of the electrical conductivity of GMZ grade graphite on the neutron fluence of 1.59×10^{19} cm^{-2} are presented in this paper.Table 1 shows the results of the electrical resistivity measurements of GMZ grade graphite, non-irradiated and irradiated with a neutron fluence of 1.59×10^{19} cm^{-2}, depending on temperature. The specific resistance measurements were done with micro ohmmeter type 3207 within the measurement error no more than ± 0.01% [3].

Table 1. Electrical resistivity of GMZ grade graphite, non-irradiated and irradiated with a neutron fluence of 1.59×10^{19} cm^{-2}, depending on temperature

T, K	Non-irradiated ρ, Ω×m 10^{-5}	Irradiated ρ, Ω×m 10^{-5}
298	1.14	3.17
323	1.12	3.15
348	1.1	3.13
373	1.08	3.1
398	1.07	3.06
423	1.05	3.01
448	1.03	2.97

As can be seen from table 1, the resistivity value of GMZ grade graphite at room temperature before irradiation was 1.14×10^{-5} Ω×m. The resistivity value of GMZ grade graphite as a result of irradiation increased by 2.78 times and amounted to 3.17×10^{-5} Ω×m. The increase in resistivity is due to the formation of defects as a result of irradiation of samples with fast neutrons in the core of the WWR-SM reactor. In this case, a decrease in resistivity was observed depending on the increase in sample temperature in the range from 298 K to 448 K. A slight decrease in resistivity depending on the increase in sample temperature is associated with an increase in the mobility of charge carriers with increasing temperature.

1. Zhao Lu, Tang Jiang, Zhou Min, Shen Ke. A review of the coefficient of thermal expansion and thermal conductivity of graphite. New Carbon Mater. 2022, 37(3): 544-555.
2. Matthew S.L., Paul Ramsay, Tjark O. at all. Journal of Nuclear Materials, Determining the electrical and thermal resistivities of radiolytically-oxidised nuclear graphite by small sample characterization, Vol. 507, 15 August 2018, pp. 68-77.
3. Instruction manual model 3207 digital micro-ohm meter, USA.-2011.-p. 35.

MAGNETIC AND OPTIC PROPERTIES OF MAGNETIC NANOFLUIDS

Kuvandikov O.K., Kirgizov S.E.
Institute of Engineering Physics of Samarkand State University, Samarkand, Uzbekistan

Magnetic fluids represent a unique and versatile class of fluids with remarkable properties that have caused the interest of researchers and engineers across diverse disciplines. These materials are special intelligent materials with many applications in biosensors, magneto – optical devices, medicine and photonics [1]. In turn, these applications depend on the magnetic and magneto-optical properties of magnetic fluids. High and quick magneto-optic response or light transmission to external magnetic field is fundamental requirement for magneto-optic sensing. With the advent of nanotechnology, developing reliable production techniques for stable nanoparticles in the fluid as well as characterization tools for exact measurement of their size, shape, distribution, and physical properties has become increasingly vital [2].

Magneto-optical light transmission of ferrofluids and their potential applications have been investigated lately [3]. Since then, magnetic and light transmission in ferrofluids has been a hot topic, and in the last few years more and more gained attention. However, according to our knowledge, it is very important to study in depth the role of magneto-optical transmission and the magnetic nanomaterials used.

The magnetization and light transmission of $CoFe_2O_4$ magnetic nanofluids in the external magnetic field range are shown in Fig. 1 and Fig. 2.

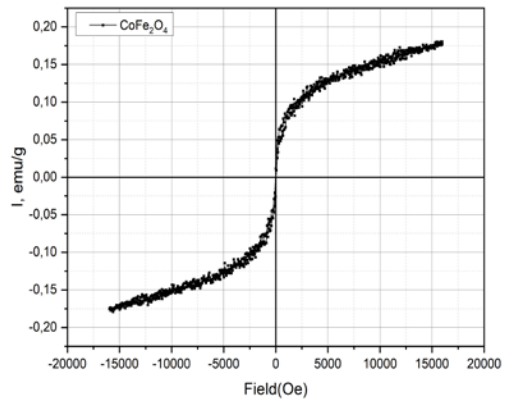

Fig.1. Magnetization curve of $CoFe_2O_4$ magnetic fluids

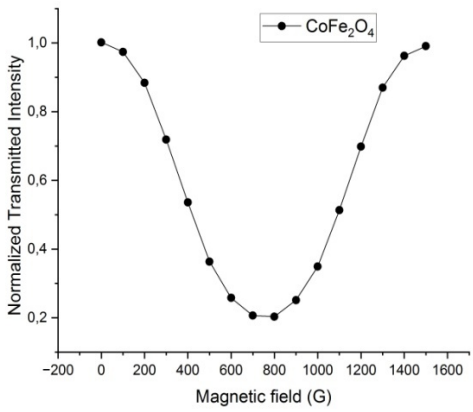

Fig.2. Normalized transmitted intensity as a function of external magnetic field

The experiments show that, the magnetic fluids have a superparamagnetic characteristics and the light transmission in magnetic fluids first decreases with the increase of the external magnetic field, then, above a certain value of the magnetic field (600-800 G), the light transmission increases.

1. Peng Z., Chi Ch.Ch., Wen S.L. et al. Optics Letters. 37. 398-400 (2012).
3. Prakash T, Williams G.V, Kennedy J, Rubanov S. J. Appl. Phys. 120(12), 123905 (2016).
4. Philip J, Laskar J.M. J. Nanofluids. 1(1). 3–20 (2013).

PROPERTIES OF THE BI/PB CUPRATE SYNTHESIZED BY SOLAR TECHNOLOGY

Gulamova D.D., Gulamov T.I.
Institute of Materials Science, Uzbekistan Academy of Sciences, Tashkent, Uzbekistan

The problem of shortage of energy sources and, accordingly, the vital need to preserve natural energy sources force humanity to seek means of saving energy resources. One of the ways is to combine two main factors aimed at energy saving: 1-creation of superconducting materials; 2 – use of solar technology. Show in Fig.1:

Fig.1. Sheme of the technological process in the Large Solar Furnace (Parkent) and the precursors

In the Large Solar Furnace (Parkent) is synthesized Bi/Pb cuprates Bi1.7Pb0.3Sr2Ca(n-1)Cu(n), (n=3 – 30). Precursors n>7 crystalline, homo – phases, nano-structured of the hightexturation is showed in Fig.2.

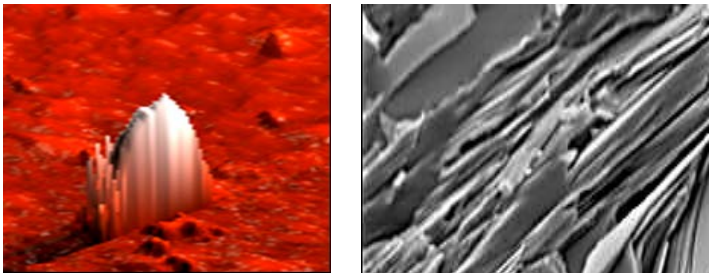

The resistance and magnetic susceptibility of precursors have characteristic anomalies in the temperature range of 280-340K, shown in the Figure. Precursors exhibit the Meissner effect at room temperatures, normal atmospheric pressure, daylight and artificial light.

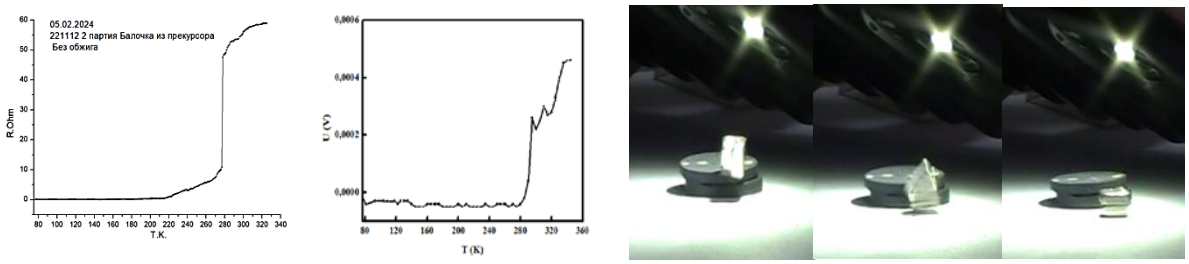

Experimental results allow us to make an assumption about the synthesis of room-temperature Bi/Pb superconducting materials by solar energy.

HIGH-TEMPERATURE SUPERCONDUCTING CUPRATES SYNTHESIZED BY SOLAR ENERGY

Gulamova D.D., Eshonkulov E.B., Bobokulov S.Kh., Lu V.R., Erkinov D., Gulamova K.T.

Institute of Materials Science, Uzbekistan Academy of Sciences, Tashkent, Uzbekistan

Increasing the quality factor of microwave devices, reducing losses and energy consumption, increasing controllability and mobility can be achieved in controllable periodic structures consisting of superconducting (HTSC) and ferroelectric (FE) layers due to the high value and nonlinearity of the dielectric constant in a wide temperature range, the low tangent of the dielectric angle losses. The characteristics of a mixed system can be significantly improved by using nanostructured materials that make up the system, thanks to the analogy of the crystal structure of perovskite-like cuprate superconductors (HTSCs) and ferroelectrics. Superconducting bismuth cuprates and ferroelectrics $SrTiO_3$, $BaTiO_3$ have been synthesized using gradient solar technology is showed in Fig.1. Layered and high textured microstructure is showed in Fig.2. A film of mixed composition is shown in Fig.3.

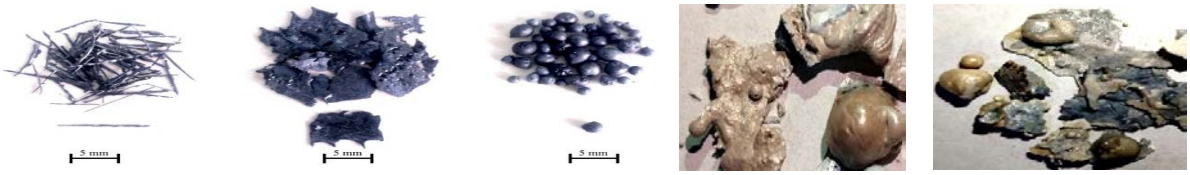

Vc

Fig.1. Bi/Pbcuprate and $SrTiO_3$, BaTiOsynthesizedin Larg Solar Furnace (Parkent) for mixed system preparation.

Fig.2. Layered, textured microstructure of theBi/Pb cuprate and ferroelectric has used for mix systems preparation

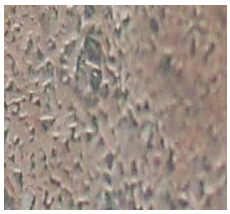

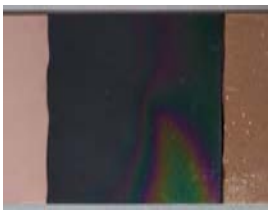

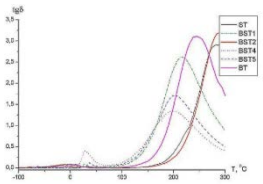

Fig. 3 a,b. Film of the mix system $BaTiO_3$-Bi/Pb - $BaTiO_3$. Contact-Cu. ρ=0.309Om*cm$R_{cont.}$=0.223 kOm*cm^2

Films of the mix composition have higher values of dielectric constant than the SrTiO sample without Bi/Pb cuprate (Fig. 3 a,b).

Low-resistivity films of mixed composition based on perovskite-like high-temperature Bi/Pb superconducting cuprates and ferroelectrics with high dielectric constant show promise for their practical application in solar cells and microwave microelectronics.

PRECIESE ELECTRONIC-STRUCTURE STUDY OF LANTHANIDE-CONTAINING CRYSTALS

Shakhova V.M., Maltsev D.A., Lomachuk Yu.V., Mosyagin N.S., Titov A.V.
Petersburg Nuclear Physics Institute, NRC «Kurchatov Institute», St.Petersburg, Russia

Theoretical studies of crystals containing lanthanides are limited by the current capabilities of modern quantum chemical methods for describing periodic structures: density functional theory, scalar-relativistic versions of "soft" semi-local pseudopotentials and atomic basis sets of moderate size. Precise theoretical research of such structures could become a powerful tool that allows one to solve many fundamental and applied problems.

In this research, the electronic structure of ytterbium halide crystals YbF_2, YbF_3, $YbCl_2$, $YbCl_3$, are studied. For investigating such structures, the combined method is applied. It contains "compound-tunable pseudopotentials" (CTPP) and "compound-tunable embedding potentials" (CTEP) [1-4].

The investigation of a crystal by the CTEP method is carried out in three stages. First, a perfect crystal with periodic boundary conditions is calculated by the CRYSTAL code. Second, short-range large-core CTPP is built for the chosen crystal by using the CRYSTAL code as well. Third, cluster calculations of the crystal fragment are performed, and the long-range Coulomb potential of the environment is constructed as a part of CTEP. A crystal fragment of a "required minimal size” (minimal cluster include a heavy atom and its immediate environment) is cut out, within which the electron density must be reproduced with high accuracy. The atoms of the near environment of the crystal fragment are described by point charges and CTPPs ("pseudoatoms" below) to take into account the influence on a chosen fragment of the "whole crystal" excluding the atoms of the fragment. It is important to note that the relaxation of the crystal fragment environment is considered as negligible by appropriate choosing the fragment, and the whole system is generally electroneutral taking into account the pseudoatoms of the near environment.

The crystal fragment built by the CTEP method using CTPP reproduces the electron density from periodic calculations in the vicinity of the Yb atom with the error less than 0.25%.

In the framework of periodic calculations, the use of precise small-core PP and saturated basis sets is practically impossible. Consequently, the accuracy of such calculations is at the level of 0.1 eV for the energetic characteristics, which is insufficient for precise study of materials with lanthanide atoms. In turn, such a problem does not arise in cluster CTEP calculations, since both good basis sets and PPs are used, and the calculation errors associated with them are drastically reduced. This was shown in the framework of the analysis of the structural parameters of crystals and corresponding clusters.

1. Lomachuk Yu.V., et al. PCCP. 2020. 22. 17922-17931.
2. Maltsev D.A., et al. PRB. 2021. 103. 205105.
3. Shakhova V.M., et al. PCCP. 2022. 24. 19333-19345.
4. Oleynichenko A.V., et al. PRB 109, 125106 (2024).

INFLUENCE OF GAMMA RADIATION ON RAMAN SPECTRA OF ETHYLENE-TETRAFLUOROETHYLENE POWDER

Tashmetov M.Yu.[1], Ismatov N.B.[1], Allayarov S.R.[2], Saidov R.P.[1]
[1]Institute of Nuclear Physics, Academy of Science, Tashkent, Uzbekistan
[2]Federal Research Center of Problems of Chemical Physics and Medicinal Chemistry, Russian Academy of Sciences, Chernogolovka, Russia

Currently, many areas of industry require materials with dielectric properties that have corrosion, radiation, thermal and chemical resistance. One of the most promising polymers are alternating copolymers of $(CF_2\text{-}CF_2\text{-}CH_2\text{-}CH_2)_n$ ethylene-tetrafluoroethylene (ETFE). ETFE copolymers are widely used in a variety of applications: automotive wire and cable coatings, robotics and electronic equipment, chemical equipment coatings such as pipe parts, films, sheets, tapes, and semiconductor industry parts. Analysis of literature data has shown that radiation has a different effect on the Raman spectrum of ETFE, and additional research is required to determine its capabilities and limitations, including under radiation conditions.

This work is devoted to the study of the effect of gamma radiation of various doses on the vibration of ETFE molecules. Figure 1 shows the initial spectrum, as well as the dependence of the Raman spectra of ETFE on the absorbed doses of 300 kGy, 1000 kGy and 2000 kGy in the frequency range 200–3300 cm^{-1}. The intensity of the Raman spectra in this range is due to vibrations of CF_2, CH_2, CC and various deformation movements.

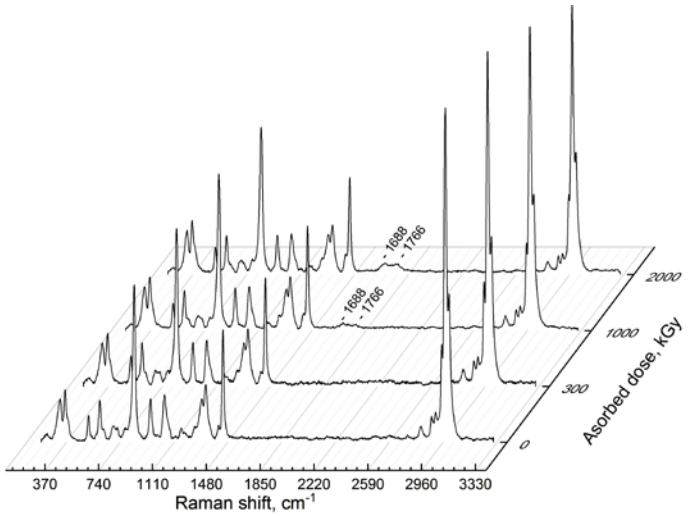

Fig.1. Dependence of the Raman spectra of ETFE on the absorbed dose

After irradiation of ETFE samples with gamma radiation, a significant change in the intensity of the Raman spectra present in the original ETFE sample was observed. In addition, with an increase in absorbed doses, new Raman spectra appear at 1688 and 1766 cm^{-1}, which, as in [1], were classified as stretching vibrations of C=C and C=O, respectively.

Analyzes of Raman spectra showed that C=O and C=C bonds were formed in irradiated ETFE samples, and their intensity increased with increasing irradiation dose. Moreover, the intensity of the spectra of the 1046 cm^{-1}, 1450 cm^{-1}, 2953 cm^{-1}, 2977 cm^{-1} and 3004 cm^{-1} modes decreases with increasing irradiation dose, which may indicate the cleavage of C-C and C-H bonds.

1. *Zhang Ya., et all.* // Iranian Polymer Journal. 2021. Vol.30. pp.393–399.

X-RAY ANALYSIS OF THE COMPOUND $CaTiO_3$

Normuradov M.T., Davlatov M.A., Davranov Kh.T., Dovranov K.
Karshi State University, Karshi, Uzbekistan

In this work, we study the structural properties of $CaTiO_3$ through the absorption properties of X-rays physicochemical properties.Figure 1 shows the spectral relationships of the $CaTiO_3$ compound obtained by the powder diffractometer method. In addition, the Miller indices are given, as well as the distance between planes d_{hkl} for these samples. We used the Rietveld method to refine the structure from X-ray powder data [1]. The principle of the method is to use independent intensity measurements at each point of the diffraction pattern, to describe the line profile using analytical functions, instead of using the integral reflection intensity. Feature parameters, including structural, device, and other characteristics, are refined using a nonlinear least-squares method. Using this refinement method, we determined the distance between the planes d_{hkl} and the Miller index (hkl). As mentioned above, powder X-ray diffraction allows for quantitative elemental analysis. The degree of crystallinity and amorphism was evaluated for the samples measured by X-ray diffraction analysis using Search and Match software [2]. For calcium titanate, the amorphous phase is 71.35% and the crystalline phase is 28.65%, respectively. In addition, the phase composition (Weight %)

and elemental composition of the $CaTiO_3$ sample was determined using the "Profex" program. The phase composition of the sample prepared for magnetron spraying corresponds to 90.7% perovskite ($CaTiO_3$), 3.8% titanium, 5.5% calcium. Our elemental analysis of the samples using Search and Match software shows that the samples have the following composition (in weight percent): 35.7% Ti, 32.2% Ca, and 32.0% O.

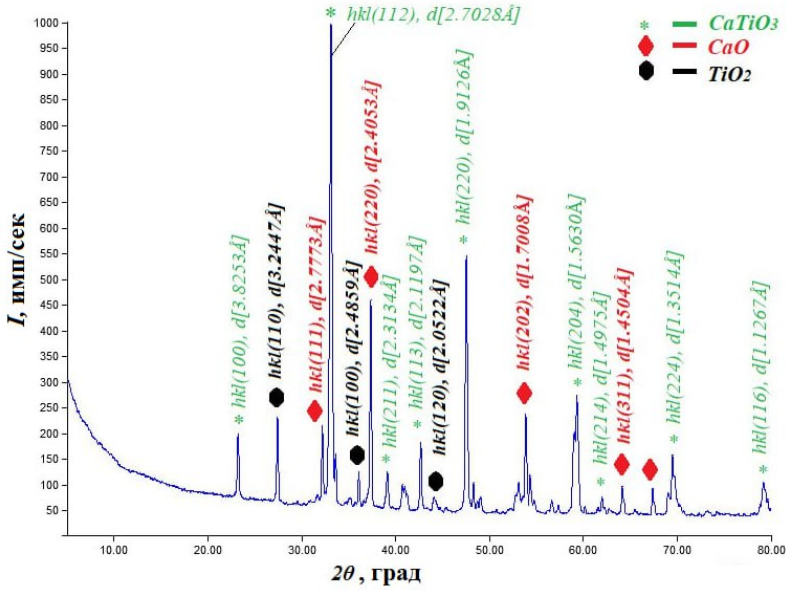

1. M.Yu. Tashmetov, F.K. Khallokov, N.B. Ismatov, I.I. Yuldashova, I. Nuritdinov, S.Kh. Umarov. Study of the influence of electronic radiation on the surface, structure and Raman spectrum of a $T_l iInS_2$single crystal. *Phys. B* 613,412879 (2021).
2. Normuradov M.T., Khozhiev Sh.T., Dovranov K.T., Davranov Kh.T., Davlatov M.A., Khollokov F.K. Development of a technology for the production of nano-sized heterostructured films by ion-plasma deposition. Structure of materials. *Ukr. J. Phys*. 2023. Vol. 68, No.3. DOI:10.15407/ujpe68.3.210.

EFFECT OF Bi- Sb(Se-Te) BASED CHALCOGENS

Gaynazarova Q.I.
Fergana State University, Fergana, Uzbekistan

Bi-Se-Sb-Te solid alloy-based elements are considered as one of the promising thermoelectric materials working in the temperature range of 200-600 K to solve current environmental and energy problems. Currently, alloys based on Bi-Sb-(Se,Te) are becoming one of the most promising thermoelectric materials for solving environmental and energy problems.

In order to increase the thermoelectric efficiency of thermoelectric materials obtained under inert gas pressure, it is necessary to correctly select the composition and operating parameters of materials based on Bi_2Te_3 and Bi_2Se_3. In order to purposefully change the parameters of the base material, we added chalcogens in excess of stoichiometry to the powder. Depending on the change of the amount of chalcogen, taking the base with optimal values of thermoelectric coefficient α =200 ÷ 240 μV/K and specific electrical conductivity σ= 60 ÷ 200 $Ohm^{-1}\cdot cm^{-1}$, their thermoelectric properties were checked. Tellurium, selenium and sulfur were used as chalcogens added to the mixture in excess of stoichiometry.

Since thermoelectric materials work at high temperatures, it was determined that the average integral value of the material's efficiency index is Z =1.59·10^{-3} grad^{-1} in the temperature range of 20÷300^{0}C from the temperature dependence of the thermoelectric parameter of the material.
The table below shows the electrophysical parameters of solid alloys with high thermoelectric properties in the Bi-Sb-Te-(Se) system.

№	chalcogens in excess of stoichiometry	$\alpha, \frac{\mu V}{K}$	$\sigma, Om^{-1}sm^{-1}$	$\alpha^2\ \sigma, \frac{\mu V}{sm \cdot {}^{\circ}C^2}$
1	Te	198	590	0.24 *mol.%*
2	Se	200	600	0.12 *mol.%*
3	S	194	580	0.08 *mol.%*

Since the alloy is not mixed in the melting process when making alloys under inert gas pressure, it is necessary to check the homogeneity of the distribution of thermoelectric properties along the length of the casting. The resulting cast has a cylindrical shape, its length is 9 cm and its diameter is 3.2 cm.

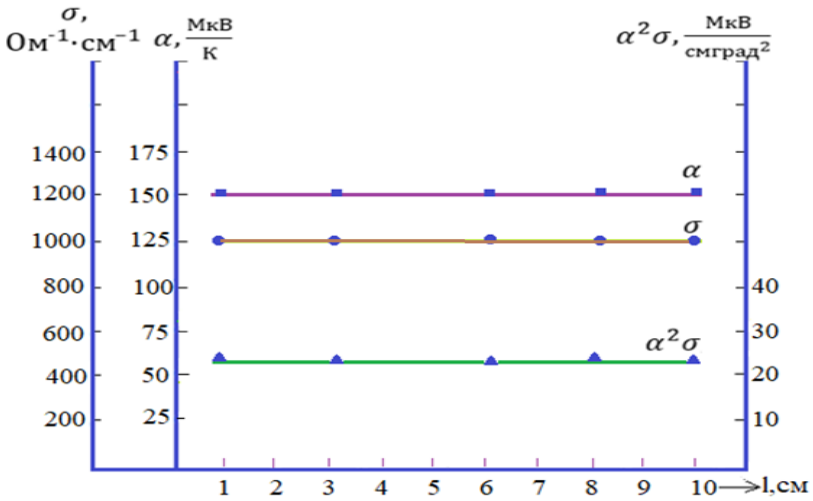

Fig.2. Variation of thermoelectric parameters along the length of Bi_2Te_3 and Bi_2Se_3 alloys

The casting is divided into 10 equal parts along its length, and the results of measuring their thermoelectric properties are shown in Fig. 2. According to the results of the research, the casting is almost homogeneous along its length according to its thermoelectric properties.

1. Azimov T.M., Gaynazarova K.I., Onarkulov M.K., Yuldashev A.A. Thermoelectric and Galvanomagnetic Properties of the Alloy Bi_2Te_3 + 0.04 Weight % Ni in the Temperature Range 77 ÷ 300 K / American Journal of Modern Physics. 2021. p. 124-128.
2. Onarkulov K.E., Usmanov Ya., Gaynazarova K.I., Azimov T.M. Semiconductor sensor for detecting volume changes at low temperatures. // European Journal of Molecular & Clinical Medicine. – 2020. No. 7. – Pp. 2353 - 2358.

DEVELOPMENT OF EFFICIENT PHOTOCELLS BASED ON SILICON MONOCRYSTALS USING ION-PLASMA INFLUENCE

Normurodov M.T., Kodirov A.R., Normurodov D.A., Zabiullokh Dansh Yar
Karshi State University, Karshi, Uzbekistan

The main problem facing modern photoenergy is the increase in the coefficient of performance (efficiency) [1]. However, although multi-stage photocells have high efficiency, the technology for their production is quite complex and requires expensive equipment. Therefore, such photocells have high prices and their use in terrestrial conditions is particularly difficult.

In this work of controlling the fundamental parameters of silicon, it should be noted that the formation of clusters of silicon atoms in a lattice of semiconductors is of great scientific and practical interest. This is mainly due to the possibility of using these materials as a new class of semiconductors with nanostructures with the discovery of rare interesting physical phenomena in them, such as the formation of nanoclusters of different natures.

Currently, the widespread use of polycrystalline silicon, and the most important research on the full use of solar energy on Earth, have made the issues of making the technology of this material cheaper and improving its electrophysical properties even more urgent. For this purpose, research on the production of polycrystalline silicon based on a new technology has been started and continues. Advances in semiconductor electronics are linked to advances in semiconductor materials technology [2]. Dramatically improving the quality of both traditional and new semiconductor materials will lead to the creation of new discrete semiconductor devices and large, ultra-large, ultra-fast integrated circuits. As a result, with a sufficient increase in the level of miniaturization of microelectronic devices, it leads to the creation of new optoelectronic and ultra-high-frequency devices. Large-scale complex problems in electronic engineering demand the creation of new semiconductor materials.

It should be noted that the formation of binary clusters in semiconductors opens up scientific directions in the field of materials science, allowing the creation of fundamentally new classes of highly sensitive photodetectors in a wide range of the spectrum. An optocoupler photoelectric converter (solar cell) is a semiconductor diode with a large surface area. Silicon and gallium arsenide largely satisfy the conditions of ideal semiconductor materials. If we compare these materials from the point of view of their suitability for the manufacture of a solar photocell with one p-n junction, then the maximum possible efficient photoelectric conversions turn out to be almost the same, and close to the absolute maximum for one junction photocell. Of course, the undoubted advantages of silicon are its high abundance in nature, non-toxicity and relative cheapness.

1. Zorop J. H., Wong A.H., Green M.A. High – efficiency PERL and PERT Selicon cells on FZ and MLZ substrates, Sol, energy. Mat. Sol cells 2001, 65, p 429-435
2. Alfyorov J. I., Andreev V. M., Rumyansev V. D. Tendensii i perspektivi razvitiya solnechnoy fotoenergetiki FTI, 2004. S 937-947

FORMATION OF CHROME DISILICIDE FILMS USING A MAGNETRON SPUTTERING DEVICE

Bekpo'latov I.R., Kholukulova S.Y., Dovranov K.T., Khaqberdiyev E.A.
Karshi State University, Karshi, Uzbekistan

Polycrystalline $CrSi_2$ films were first formed by bombarding a $CrSi_2$ target with Ar^+ ions under high vacuum conditions using a magnetron sputtering device [1]. Initially, 30-second magnetron sputtering on the Si(111) surface at room temperature resulted in the formation of incompletely coated amorphous structures. As a result of magnetron sputtering for 60 seconds at a temperature of 350 K, an amorphous film with a thickness of ~40 nm was formed. A polycrystalline film of chromium disilicide was created by the ion-plasma method for 120 seconds with a thickness of ~80 nm, heating at 750 K for 1 hour (Table 1). The film thickness was controlled using a quartz sensor of a Gold-10 magnetron device on an SP-307 monitor (growth rate 1.2-9 Å/sec).

Table 1. Formation of $CrSi_2$ nanofilms formed using a magnetron sputtering device

Spray time and speed	Vacuum and spray temperature	Phase	Formative stage
30 sec, 6.7 Å/sec	$3.8 \cdot 10^{-6}$ Torr, T=300 K	Amorphous film, not completely covered	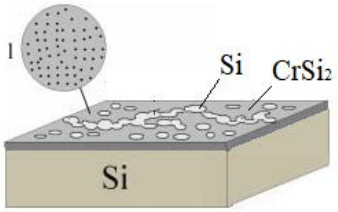
60 sec, 6.7 Å/sec	$3.8 \cdot 10^{-6}$ Torr, T=350 K	Amorphous film	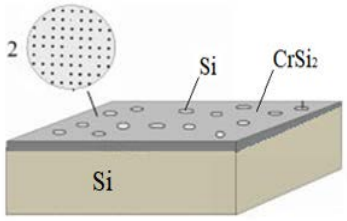
120 sec, 6.7 Å/sec	$3.8 \cdot 10^{-6}$ Torr, T=750 K	Polycrystalline film	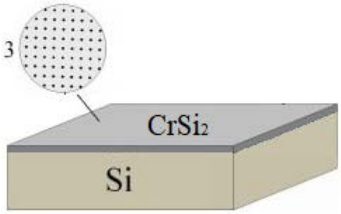

An analysis of the formation process of amorphous and polycrystalline $CrSi_2$ films formed using a magnetron sputtering device was carried out. Analysis of the thermoelectric properties and optical parameters of these thin films showed that they have high sensitivity in the visible and IR light ranges and can be used in nanoelectronic devices operating in these ranges.

1. K.T. Dovranov, M.T. Normuradov, Kh.T. Davranov, I.R. Bekpulatov. Formation of Mn_4Si_7/Si(111), $CrSi_2$/Si(111), and $CoSi_2$/Si(111) thin films and evaluation of their optically direct and indirect band gaps. Ukr. J. Phys. ISSN 2071-0186. 2024. Vol. 69, No. 1.

ELECTRICAL, MAGNETIC AND GALVONOMAGNETIC PROPERTIES OF $Fe_{85-x}Cr_xB_{15}$ $(x = 8 \div 15)$ AMORPHOUS ALLOYS

Kuvandikov O.[1], Subkhankulov I.[1], Hamraev N.S.[1], Razhabov R.M.[1], Khomitov Sh.A.[1], Turgunov O.Z.[2]

[1]Institute Engineering Physics of Samarkand State University, Samarkand, Uzbekistan
[2]Physical–Technical Institute, Uzbekistan Academy of Sciences, Tashkent, Uzbekistan

In this work the changes in the electrophysical, galvanomagnetic and magnetic properties of $Fe_{70}Cr_{15}B_{15}$; $Fe_{73}Cr_{12}B_{15}$; $Fe_{75}Cr_{10}B_{15}$; $Fe_{77}Cr_8B_{15}$ amorphous alloys under the influence of temperature, changes in these properties in the phase transition region, and the relationship between their electrophysical, galvanomagnetic and magnetic properties were studied. In the temperature range from room temperature to 800 K, the specific electrical resistance ρ in the amorphous state is greater than in their crystalline state, and the resistance temperature coefficient (RTC) in the amorphous state is smaller than in the crystalline state.

The experimental results of the temperature dependence of the Hall coefficient R_H and magnetization I_S show that in the amorphous state, the absolute values of the positive Hall coefficient and magnetization from room temperature to the phase transition temperature are greater than in the crystalline state, and their temperature coefficient is smaller than in the crystalline state. In all studied samples, the relative electrical resistance ρ in the amorphous state increases with increasing temperature and sharply decreases when the temperature reaches a certain value. The corresponding temperature is called the crystallization temperature. The experimental results of the temperature dependence of the Hall coefficient $R_H(T)$of the samples show that in the temperature range of 300-400 K, the value of the Hall coefficient jumps and decreases. This change can be explained by the transition of samples from ferromagnetic state to paramagnetic state [1]. At temperatures after the crystallization temperature T_K, the magnetizationI_s increases and tends to zero at certain temperature. This temperature corresponds to the Curie temperatureT_c of the crystalline state.

The absolute value$Fe-Cr-B$ of magnetism decreases with the increase of Cr-chromium concentration in the studied samples. This is due to the antiferromagnetic property of the element Cr. As the chromium concentration increases, the Curie temperature T_c of the samples decreases and initial temperature of crystallization T_K increases. The analysis of magnetic parameters shows that the value of magnetization decreases both in the amorphous and crystalline state with an increase in chromium concentration. When the samples are in the crystalline state, the relative electrical resistance ρ(T) decreases with the decrease in temperature. In the crystalline phase of all samples RTC is greater than in the amorphous state. The study of the Hall effect depending on the temperature allows to determine the type and concentration of current carriers in the sample. Based on the obtained experimental results, the relationship between the anomalous Hall coefficientR_H and the relative electrical resistance ρ and magnetism was studied and it was shown that the Kondorsky-Vedyaev theory for ferromagnetic crystal samples is also fulfilled for the amorphous state. It is known that in asymmetric scattering in crystals with polarized d-electron structure, the connection between $R_s$and ρ is determined by the following relation [2]:$R_s = a\rho + b\rho^2$,whereρ is the total resistance. It was shown that there is a linear relationship between the dependence$\frac{R_s}{\rho}$ of ρ on the investigated amorphous alloys.

1. Kuvandikov O.K., Subxankulov I., Imamnazarov D.H., Khomitov Sh.A. The nature of exchange interaction in amorphous alloys based on metals of the iron group with metalloids // Metallofizika i noveyshie texnologii. Ukraina. Kiev, 2022, vol. 44, No. 7, pp. 823–829. DOI: https://doi.org/10.15407/mfint.44.07.0823
2. Vyedyaev A.V., Granovskiy A.B. Teoriya anomal'nogo effekta Xolla amorfnix ferromagnetikov. – FMM,, 1984, т. 58, вып.6, с. 1084-1092.

PASSIVATION OF DEFECTS IN PEROVSKITE-BASED SOLAR CELLS USING L-4-FLUOROPHENYLALANINE

Tajibaev I.I., Zakhidov E.A., Nematov Sh.K., Kuvondikov V.O., Boynazarov I.R.
Institute of Ion-Plasma and Laser Technologies, Uzbekistan Academy of Sciences, Tashkent, Uzbekistan

In recent years, organic–inorganic halide perovskite materials(e.g., $CH_3NH_3PbI_3$, $MAPbI_3$, MA¼ CH_3NH_3) have attracted widespread attention in the scientific community due to the featuresof long carrier diffusion length, adjustable bandgap, a high absorption coefficient, and easy preparation [1,2] . After continuous exploration by researchers, the power conversion efficiency (PCE) of normal (n–i–p) PSCs exceeded 25%, and the inverted PSCs also reached 23.0% efficiency, which is comparable with traditional semiconductors and is expected to become a leader in the photovoltaic field [3–7]. Although PSCs are developing rapidly, their stability is still far from commercial standards [8,9]. Therefore, solving the inherent instability of perovskite materials is top priority, including thermal decomposition, ion migration, and crystal phase transformation of perovskite materials under extreme conditions.

The harmful defects accumulated at surfaces and grain boundaries (GBs) limit the performance and stability of perovskite solar cells (PSCs), which results from the poor crystallization and ion migration. Here, a multifunctional molecular additive L-4-fluorophenylalanine (FPA) is explored for highly efficient and stable inverted PSCs. The multifunction is realized through comprehensive defect passivation, surface hydrophobicity, and crystallization control with the multitude groups, such as the amino and carbonyl groups for passivation of the unsaturated lead defects at GBs, and the benzene ring for electron-deficient iodine defects, and the fluorine group for the improvement of crystallization and the inhibition of ions migration. The resulting inverted device shows a champion power conversion efficiency of 21.28% with negligible hysteresis. The opened FPA-modified devices maintain nearly 90% of the initial performance after high-temperature (85 °C) thermal accelerated aging for 500 h and 85% after aging for 4000 h under ambient conditions, and about 90% of the original efficiency after being maximum powerpoint tracked for 1000 h under continuous illumination. This study provides a multipronged strategy to the future design of PSCs with higher efficiency and enhanced stability.

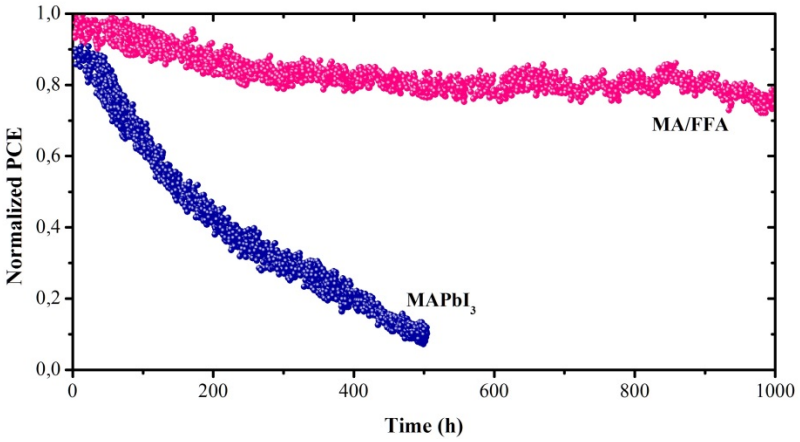

Fig.1. The MPP tracking of the encapsulated device under 1 sun continuous illumination without a UV filter at 45 °C.

PHYSICS - 2024

THE THIRD INTERNATIONAL FORUM

Samarkand, 23-25 April, 2024

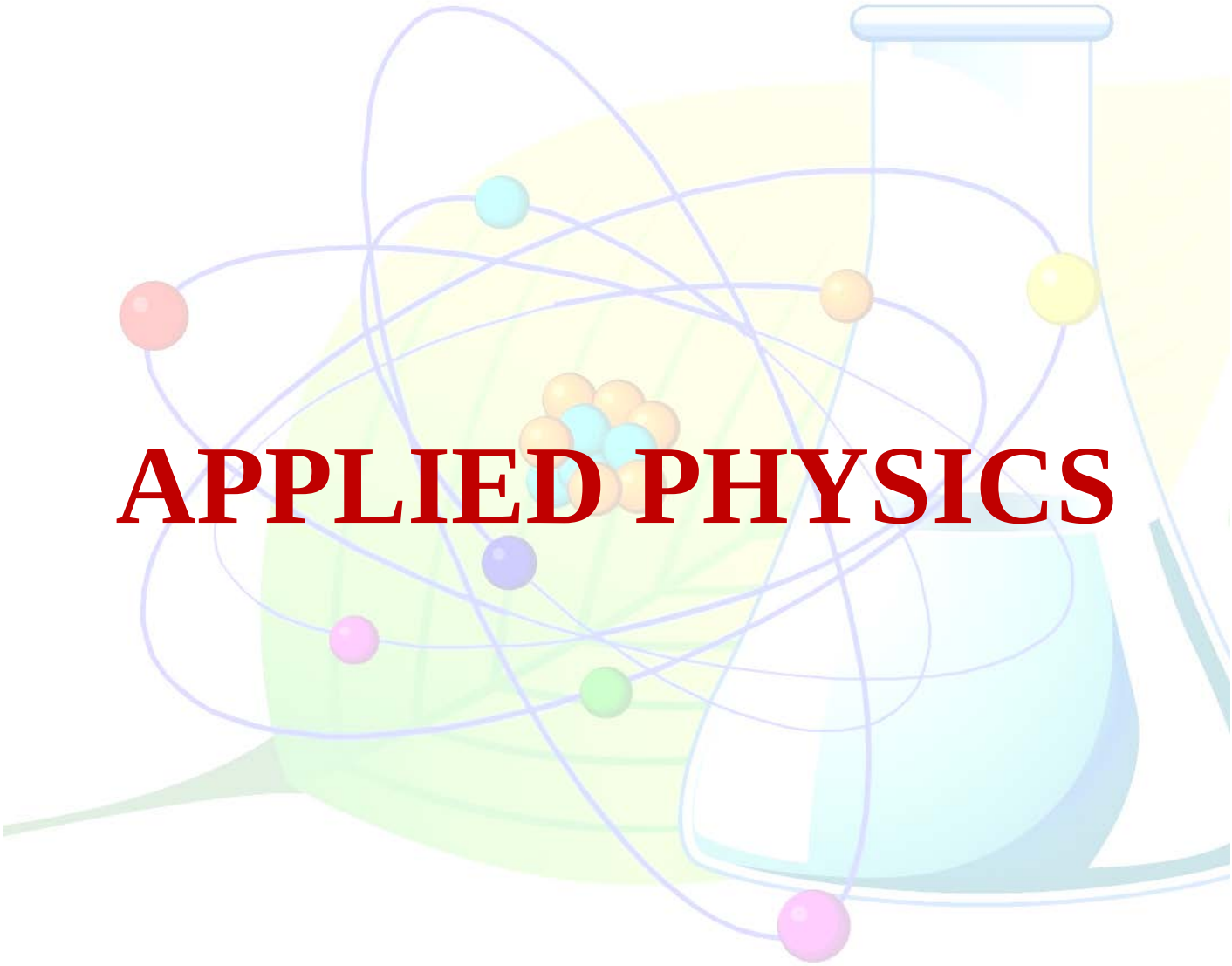

APPLIED PHYSICS

PROSPECTS OF USING NUCLEAR ENERGY IN LOW-CARBON PETROCHEMICAL PROCESSES

Mustafayev I.[1,2], Guliyeva N.[1], Chichek F.[1]
[1]*Institute of Radiation Problems, Ministry of Science and Education, Baku, Azerbaijan*
[2]*Azerbaijan University of Architecture and Construction, Baku, Azerbaijan*

In traditional petrochemical and oil refining technologies, organic fuels are burned as an energy source for chemical processes at high temperatures. Oxygen from the atmosphere is used, instead Greenhouse gas -CO_2 is released. However, these fuels, whose resources are limited, are used for burning. International agreements like the UNFCCC, the Paris Agreement, and initiatives such as the Green Deal and the World Economic Forum Davos-2019 have committed to reducing CO_2 and other greenhouse gases by promoting alternative energy sources and low-carbon technologies to mitigate climate change. Renewable energy sources and nuclear energy are suggested as alternatives.

The report discusses the experimental and computational results of applying low-carbon radiation-thermal processes in energy-intensive areas of chemical technology by applying combined options of nuclear energy, such as heat-radiation, heat-electricity. The study focused on the kinetic regularities of the radiation-thermal decomposition of pentadecane, used as a model, and the kinetics of olefins and gas generation in the range of absorbed dose up to 20 kGy, a dose rate in the range of 2.5-300 kGy/hour, and temperatures ranging from 200-500^{0}C. It was demonstrated that under optimal conditions, the radiation-thermal effect results in an olefins yield of 70%, and hydrocarbon gas yield of 3-4%. In this case, the radiation-chemical yield of the products reached 50.6 molec/100 eV for gases and 34.5 molec/100 eV for olefin liquids. The obtained results were tested on F_1=160-400C, F_2=230-310C oil fractions. The yield of olefins in F_1 fraction was 55%, and in F_2 fraction - 48%. Of particular interest is the production of high-molecular α-olefins, as their yield in these processes reaches 32%.

Currently, it is not difficult to obtain temperatures of 500-600^{0}C in nuclear reactors. The intensity of ionizing rays received in the gamma contours can faciliate these processes. Additionally, these processes can be realized in electronic accelerators capable of utilizing solar and nuclear energy.

The ratio of radiation and thermal components in radiation-thermal (Wrt) processes was calculated. It was demonstrated that the Wrt/Wt ratio depends on temperature and dose rate. The temperature dependence of the optimal dose rate was also calculated and compared with the experimental results.

Approximate technical and economic indicators of the conducted processes were calculated. These calculations included the value of radiation and heat energy, as well as the value of raw materials, the value of special initial resources, the value of the final product. Three parameters were calculated: efficiency of energy conversion, productivity and economic efficiency. A conventional comparative analysis has shown that, with appropriate energy sources and technological parameters, it is profitable to obtain relatively expensive olefins, including α– olefins, using these methods.

NEUTRON ACTIVATION ANALYSIS OF SHORT-LIVED RADIONUCLIDES AT RRC WWR-K

Bedelbekova K.A., Lennik S.G., Sokolenko E.K.
Institute of Nuclear Physics, Almaty, Kazakhstan

The Institute of Nuclear Physics has developed a set of nuclear-physical analysis methods, among which instrumental neutron activation analysis (INAA) occupies a significant place. Historically, the development of INAA began at the INP in the 1960s with the commissioning of the main irradiation facility, the WWR-K nuclear reactor. On a dedicated channel with a neutron flux density of 10^{13} particle/s/cm^2, a two-channel pneumatic system, one of whose channels was coated with cadmium, was mounted for research on short-lived radionuclides (SLR). Application of the INAA method (including SLR) allowed to solve a number of practical problems for industrial and production enterprises, as well as scientific organizations of Kazakhstan and the former USSR. After the Chernobyl accident, there was a general tendency to reduce the number of operating research reactors, which reached its climax with the collapse of the USSR: at the INP the WWR-K reactor was shut down and the two-channel pneumatic mail was dismantled.

At present, a significant amount of work has been done at the INP RK to reconstruct and convert the WWR-K reactor to low-enriched fuel (without significantly changing the neutron flux and spectrum). A new automated pneumatic transport system (PTS) has been installed for conducting INAA on SLR in a dry horizontal channel with a neutron flux density of 10^{12} particles/s/cm^2. The process of PTS control is carried out with the use of special software, which allows selecting irradiation modes, irradiation time in the channel of the reactor zone of the RRC WWR-K, possible "cooling down" time before the beginning of recording and directly recording of γ-radiation spectra. It is possible to record γ spectra of induced activity serially at certain time intervals. The method of INAA by SLR allows the determination of a number of elements: Na, K, Al, Cl, Ca, V, Mn, Mg, Cu, Co, Ba, Eu, Dy, In, Sr and others, among which most of them do not have long-lived isotopes and are determined by INAA method exclusively by SLR. This list significantly expands the list of elements to be determined and improves the sensitivity of determination of some of them. The application of the INAA method (including SLR) allowed solving a number of scientific and practical problems for industry and production enterprises.

According to ISO/IEC 17025:2017 «General requirements for the competence of testing and calibration laboratories» accredited laboratories should use the MT certified and included in the register of state measurement instruments (SMI) of the Republic of Kazakhstan. Currently, both in the SMI of the Republic of Kazakhstan and in the post-Soviet space there is no such MT for INAA on SLR. It was necessary to develop and certify such a methodology. On the basis of this, experimental works on irradiation of parallel suspensions are carried out to determine the ranges and assess metrological characteristics (in-laboratory precision, correctness and accuracy indicators). The tentative date of introduction into SMI RK is 2027. This methodology will allow to expand the list of determined elements for solving different applied and research tasks in the field of geology, ecology, and other areas.

ILU RF ELECTRON ACCELERATORS FOR E-BEAM AND X-RAY APPLICATIONS

Bryazgin A.A.
Budker Institute of Nuclear Physics, Novosibirsk, Russia

ILU type industrial accelerators are RF pulse accelerators with energy range from 0.8 to 10 MeV. First of these accelerators where designed 1970’s. But market development requires continuous modernization of accelerators. Great prospects for the use of accelerators in industry are provided by a new market - food irradiation. The report describes accelerator upgrades associated with food irradiation and sterilization. For this, accelerators must operate with energies from 5 MeV to 10 MeV in the electronic mode and in the mode of bremsstrahlung gamma radiation. Two branches of ILU accelerators are described. One is based on an ILU-10 single-cavity accelerator and a vertical beam. The second is based on the ILU-14 multi-cavity accelerator, which has a horizontal beam, see Fig. 1. Both families are modular and upgradeable.

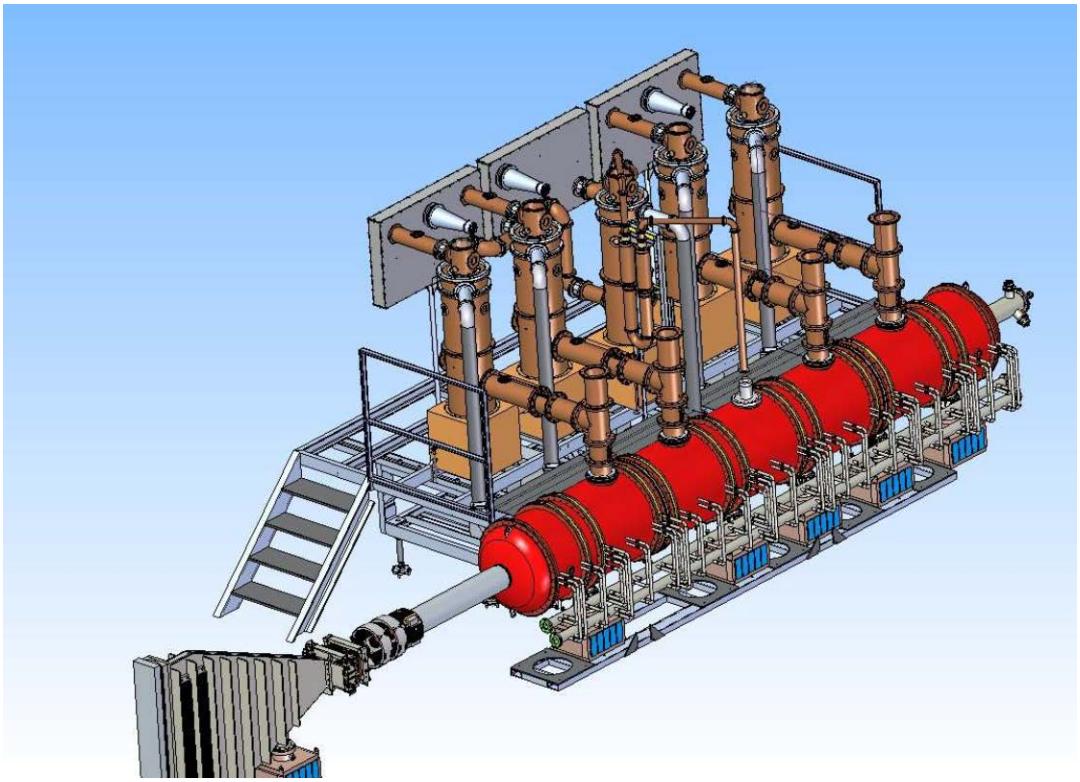

Fig. 1. Accelerator ILU-14

NUCLEAR PHYSICAL METHOD FOR EARTHQUAKE PREDICTION

Yuldashev B.S.[1], Maxsudov A.U.[2], Muminov R.A.[2], Rumyanseva E.V.[2]
[1] Uzbekistan Academy of Sciences, Tashkent, Uzbekistan
[2]Physico-Technical Institute, Uzbekistan Academy of Sciences, Tashkent, Uzbekistan

Earthquake forecasting is a pressing problem in the world, attempts have been made for many years by many countries without success to solve this problem. There is no sufficiently reliable methodology for predicting earthquakes of any time level (medium-term, short-term or operational). It is necessary to develop scientific foundations for the development of a forecasting method, which has great social and scientific significance. In order to determine earthquakes and for its prediction, various precursors contributing to various geophysical parameters are recorded. In the area of the epicenter, the process of an impending earthquake involves vast spaces and territories where earthquake precursors are recorded using various geophysical parameters.

We have developed a nuclear-physical method for early earthquake detection, based on recording the time variation in the intensity of the flow of charged particles in the earth's crust. An electronic device operating on the basis of the nuclear physics method contains special detectors used in nuclear physics to register particle flows - earthquake precursors with an active (measuring) part measuring 1 m^2. It includes two layers of scintillation counters, lined with absorbers and with a monitoring, measuring, recording of registered data and a transmitting radio-electronic system in the PC memory and is located in Tashkent in the basement, which allows reducing the contribution of particles from cosmic rays from the atmosphere by 2,5 times. Tests were carried out over a period of 1,5 years, the results obtained showed that within 2-3 days the signals relative to the background increase several orders of magnitude, and as the time of the earthquake approaches, they increase even more. The greater the amplitude of the signal, the stronger the strength of the earthquake.

But this was not enough for the forecast, the location of the epicenter of the upcoming earthquake remained unknown. To determine the location of the epicenter of the 2016 earthquake, direction detectors were invented.

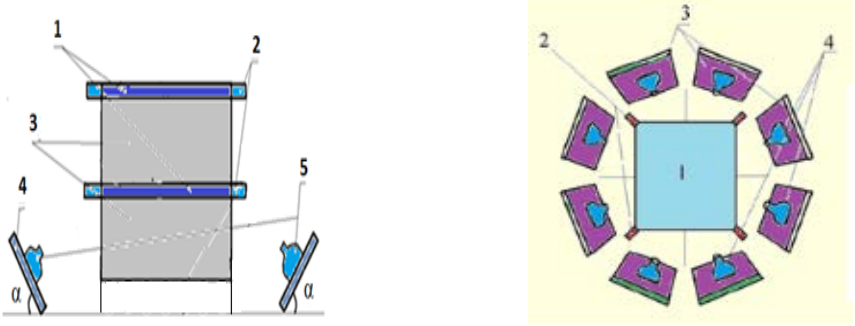

Fig.1. An upgraded electronic device (on the left is a side view and on the right is a top view) for recording the fluxes of neutrons and charged particles. 1 - predictive detectors, 2 - photomultipliers. 3 - particle energy absorber, 4 - direction detectors, 5 - photomultipliers

Obtained data from predictive signals and signals indicating the direction of the earthquake epicenter.

Assistance in creating such a device is offered to countries that wish to have forecasting instruments in seismically active regions and conduct joint research on the advance detection of strong earthquakes.

THE INFLUENCE OF THE FUEL TYPE AND ENRICHMENT DISTRIBUTION ON THE ADSR PERFORMANCE

Paraipan M.[1,2], Belov O.V.[1], Javadova V.M.[1], Kostov L.K.[1], Tran T.N.[1,3], Tyutyunnikov S.I.[1]
[1]Joint Institute for Nuclear Research, Dubna, Russia
[2]Institute of Space Science, Magurele, Ilfov, Romania,
[3]Institute of Physics, Vietnam Academy of Science and Technology, Hanoi, Vietnam

Initially, the concept of an accelerator driven subcritical reactor (ADSR) was elaborated as means to solve the problem of nuclear waste. The accent was put on the possibility to transmute the actinides from the spent nuclear fuel. In our previous works [1,2] it was shown that ADSR can represent an efficient source of energy, able to ensure a safer exploitation and a deeper burning of the actinides in comparison with a fast reactor (FR). The use of a beryllium converter gives the possibility to obtain with a beam of ^{7}Li with energy 0.25-0.3 AGeV the same net electrical power as the one realized with 1-1.5 GeV proton.

The non-uniformity of the power distribution in ADSR is more pronounced than in FR, especially in the case of a beryllium converter. A flatter distribution necessitates a gradual enrichment. The influence of the fuel type and enrichment distribution on the performance of ADSR is analyzed in the present work. The power and temperature evolution during various transients was studied searching the conditions which maximize the energy production and ensure a safe exploitation avoiding the melting of the fuel or clad. The limiting factor of the maximum power that can be achieved in ADSR is the temperature evolution in the hottest channel during an unprotected beam overpower transient. It depends on the fuel type and on the peak factor (PF) of the power distribution. The study was realized in cores with LBE and Be converters with the same geometry and number of the fuel rods, irradiated with proton and ^{7}Li beams. Metallic, oxide and nitride fuels with various enrichment distributions were taken into account. A value of 0.987 for k_{eff} was realized in each case.

The energy released and the reactivity coefficients were obtained through simulation with the toolkit Geant4. The temperature distribution, the reactivity coefficients and the power evolution were calculated with a program realized in the frame of the toolkit ROOT. The use of nitride fuel is preferable in ADSR because allows to accommodate high power densities. Electrical power of 350 MW can be achieved in nitride core and power distribution with PF ~ 4.5, and 800 MW for PF ~ 2.

1. Paraipan M., Javadova V. M., Tyutyunnikov S. I., Aspects of target optimization for ADS with light ion beams at energies below 0.5 AGeV, Progr. Nucl. En. 120 (2020) 103221
2. Paraipan M., Javadova V. M., Tyutyunnikov S. I., Influence of the particle beam and accelerator type on ADS efficiency, Nucl. Sci. Eng., DOI: 10.1080/00295639.2023.2175582

CREATION OF A CRYPTOSYSTEM THAT SATISFIES SHANNON’S PERFECT SECRECY CONDITION BASED ON THE LIEB-LINIGER MODEL

Rasulova M.Yu.
Institute of Nuclear Physics, Uzbekistan Academy of Sciences, Tashkent, Uzbekistan

One of the most pressing problems of our time is the creation of a cryptosystem that satisfies Shannon’s conditions of perfect secrecy [1], [2]. This problem was posed by Shannon back in 1948 and remains relevant to this day. Advanced Encryption Standard [3], which is the basis of the Western system, and other standards could not solve this problem because they are probabilistic and this does not allow them to determine their keys for each cell of information. Such an opportunity can be created if it is possible to solve the equation of functions N variables, where N is the number of information cells. There are several exact solvable such equations in the world and one of the possible applications of the problem of a perfect secret cryptosystem is the Lieb-Liniger model [4] of statistical mechanics.

To solve the Shannon problem, the paper considers the Lieb-Liniger model. Using the Lieb-Liniger model and using the eight-cell information, information transfer based on the three-pass protocol [5] is shown. Also, this method of information transfer is translated into matrix language. In the paper the Lieb-Liniger-based information transfer method is proven to create a perfect secrecy cryptosystem.

As is known, in well-known cryptosystems, several cells are used to express each letter of the alphabet, and such letters have different ciphertext probabilities. This can be easily used to break the encoded information. The definition of a complete system of own keys for each cell based on the Lieb-Liniger model, due to the equal probability of letters in each cell, does not allow information hacking. Therefore, this model allows you to create a cryptosystem that satisfies the conditions of perfect secrecy of information.

1. C.E.Shannon, A mathematical theory of communication, Bell System Technical Journal, 27(3), 379-423 (1948).
2. C.E.Shannon, A mathematical theory of communication, Bell System Technical Journal, 27(4), 623-656 (1948).
3. J.Daemen, V.Rijmen, The Design of Rijndael AES-The Advanced Encryption Standard, Springer, (2002).
4. E.H.Lieb and W.Liniger, Exact analysis of an interacting Bose gas. I: the general solution and the ground state, Phys. Rev., 130, 1605-1616 (1963).
5. A.Shamir, R.L.Rivest, L.M.Adleman, Mental Poker, In: Editor D. A.Klarner, The Mathematical Gardner, Wadsworth. 37-43, (1981).

COMPUTER MONITORING OF BEAM DYNAMICS IN SYNCHROTRONS

Zhabitsky V.M.
Joint Institute for Nuclear Research, Dubna, Russia

Now computers are essential in many situations implementing monitor and controlled functions of different physical processes. Many problems related with analog technologies can be avoided by using a computer. It is also possible to make much more complicated computations, such as iterations and solution of equation systems, using a computer. All nonlinear, and also many linear operations, using the analog technique can be sources of errors, which are overcome much more accurately by using a computer. The mentioned computer technologies are widely applied to monitor the dynamics of the beam in synchrotrons where the accelerating particle beam travels around a fixed closed-loop path. These charged particle accelerators are modern facilities to study the structure of matter in elementary particle physics and nuclear physics. The beam stability required for physical investigations is granted significantly by computer technologies.

Two examples are presented in the report: (1) tomographic reconstruction of the longitudinal phase space distribution of ions in bunches in the JINR booster synchrotron as a part of the NICA complex (JINR, Dubna, Russia), (2) damping of coherent transverse bunch oscillations in the Large Hadron Collider (CERN, Geneva, Switzerland). The results demonstrated in these examples have confirmed the efficiency of computer technologies to monitor the beam dynamics in synchrotrons, as well as to develop mathematical models of the charged particle motion.

STRUCTURAL INVESTIGATIONS OF FERROFLUIDS WITH ANISOMETRIC NANOPARTICLES

Balasoiu M.
[1]*Joint Institute of Nuclear Research, Dubna, Russia*
[2]*West University of Timisoara, Timisoara, Romania*
[3]*National Institute for R&D in Physics and Nuclear Engineering, Bucharest – Magurele, Romania*

Anisometric nanoparticles are nonspherical structures (e.g., prisms, rods, lamellas, etc.) with shape-dependent chemical and physical properties that can be used in important applications ranging from catalysis to sensing and optics.

In the frame of a project for the development of new fluid magneto-optical systems with an increased magneto-optical response in comparison to the already known effects, new ferrofluids with anisometric magnetic nanoparticles were prepared [1].

Various experimental X-ray and small-angle neutron scattering approaches have been successfully used over the years for the microstructural characterization of different types of ferrofluids.

In the present work, results of small-angle of neutrons and X-rays investigations of the structural properties of two ferrofluids with anisometric nanoparticles are reported [2, 3].

1. S. Lysenko, A. Lebedev, S. Astaf'eva, D. Yakusheva, M. Balasoiu et al., Physica Scripta **95**, 044007 (2020)
2. M. Balasoiu, S. Astaf'eva, S. Lysenko, D. Yakusheva, E. Kornilitsina et al., J. Surf. Invest.: X-Ray, Synchrotron Neutron Tech. **17**(3), 730-737 (2023).
3. M. Balasoiu, S. Lysenko, S. Astaf'eva, D. Yakusheva, E. Kornilitsina et al., J. Surf. Invest.: X-Ray, Synchrotron Neutron Tech. 2024 (to be published)

TRACE ANALYSIS OF URANIUM BY LASER SPECTROSCOPY AND ICP-MS

Izosimov I.N.[1], Saidullaev B.D.[2], Strashnov I.[3], Vasidov A.[2]
[1]*Joint Institute for Nuclear Research, Dubna, Russia*
[2] *Institute of Nuclear Physics, Uzbekistan Academy of Sciences, Tashkent, Uzbekistan*
[3]*The University of Manchester, School of Natural Sciences, United Kingdom*

State of the art laser spectroscopy (Resonance Ionisation Mass Spectrometry, Time Resolved Laser Inuced Fluorescence, Time Resolved Laser Induced Chemiluminecence,) and Inductively Coupled Plasma Mass Spectrometry (ICP-MS) can be very efficient for elemental and isotope composition analysis of various samples, as well as for the determination of the molecular and valence forms of uranium (speciation analysis) [1-5].

A series of RIMS measurements of reference materials with various isotope compositions ranging from depleted and natural to enriched uranium have been previously reported by our collaboration [1,2]. Simple sample preparation process not involving any chemical separation, pre-concentration or need for chemical reactions is employed. Highly selective and efficient uranium photoionisation schemes were applied. For samples of depleted uranium the 235U/238U < 0.003 ratio was determined with <7% precision (2σ errors) for the total uranium concentrations not exceeding ~80 fg per sample [1]. The details of multi-step excitation of species and time-resolved detection of resulting luminescence (TRLIF) and chemiluminescence (TRLIC) have been evaluated and applied for analysis of biological samples. Typical concentration of uranium [4] in blood plasma for different regions is ranging 0.05ng·ml-1 – 0.5ng·ml-1, and in urine is 0.2ng·ml-1-5ng·ml-1. Without mineralization, the limit of uranyl detection (LOD) by TRLIF in blood plasma has been determined 0.1ng·ml-1. After mineralization, a lower LOD ranging 0.008ng·ml-1 - 0.01ng·ml-1 has been evaluated. The limit of uranyl detection in urine in our TRLIF experiments was up to 0.005ng·ml-1. This LOD is sufficient to allow for studies the dinamics proccesses and behaviour of the of uranium in biologicas objects [3,4]. However, actinides in various valence states do not all exhibit luminescence properties. The use of chemiluminescence methods (TRLIC) for detection of actinides in solutions allows the sensitivity to reach the limit of detection (LOD) from 10-6 M to 10-13 M depending on chemical form of actinide in a solution [2-5]. TRLIC methods were applied for detection of the molecular and valence forms of uranium.

In a separate experiments, ICP-MS methods has been used for analyses [6] of the elemental and isotope composition (64 elements) of bones of dinosaurs, South mammoths, prehistoric bear and archanthropus as well as the samples of surrounding soils; everything collected in different parts of Uzbekistan. A high concentration of uranium we detected in the bones of dinosaurs (122mg/kg), South mammoth (220mg/kg), prehistoric bear (24mg/kg) and archanthropus (1.5mg/kg) compared to surrounding soils (3.7-7.8 mg/kg) and standard bones (<0.01mg/kg) was established. The standart ratio 235U/238U = 0.007 was detected for all samples, but the 234U/238U ratio differ from secular equilibrium value.

Results of the element and isotope composition analysis, and results of molecular and valence forms determination obtained by different methods are discussed.

1. I. Strashnov, et al., J. Anal. Atom. Spectroscopy, 34,1630(2019).
2. I. Strashnov, et al., J. of Radioanalytical and Nuclear Chemistry, 322, 1437(2019).
3. I.N. Izosimov, Procedia Chemistry, 21, 473(2016).
4. I.N. Izosimov, Environmental Radiochemical Analysis VI, pp. 115-130, Royal Society of Chemistry Publishing, 2019. DOI: 10.1039/9781788017732-00115
5. I.N. Izosimov, J. of Radioanalytical and Nuclear Chemistry, 304, 207(2015).
6. I.N. Izosimov, et al., Czech Chemical Society Symposium Series, 20, 116(2022).

DEFECT FORMATION IN SILICON DOPED WITH IMPURITIES OF TRANSITION ELEMENTS

Utamuradova Sh.B., Fayzullaev K.M.
Institute of Semiconductor Physics and Microelectronics at the National University of Uzbekistan, Tashkent, Uzbekistan

It is known that the introduction of so-called non-traditional impurities – impurities of transition or refractory elements that create a number of deep levels in the band gap of silicon and have a noticeable effect on the electrical parameters of silicon [1] – plays a significant role in the formation of the defective structure of silicon.

In this regard, the purpose of this work was to study the increase in resistance to external influences of silicon doped with transition elements.

Figure 1 shows the experimental Raman spectra of single-crystal Si and Cr-doped Si, taken under the same conditions on the CARS Raman Spectrometer. The Raman spectrum presented in Figure 1a contains an intense peak characteristic of silicon at 522 cm^{-1} with a full width at half maximum of 14 cm^{-1}. As can be seen from Figure 1b, further doping of n-Si single crystals with chromium leads to a significant change in their Raman spectra. The resulting spectrum contains peaks at 308, 398, 521 and 795 cm^{-1}. The vibration at 521 cm^{-1} can be attributed to silicon. When comparing the Raman spectra of n-Si and n-Si<Cr> samples, it is clear that doping with chromium leads to a significant decrease in the intensity of the fundamental vibration at 522 cm^{-1}.

.

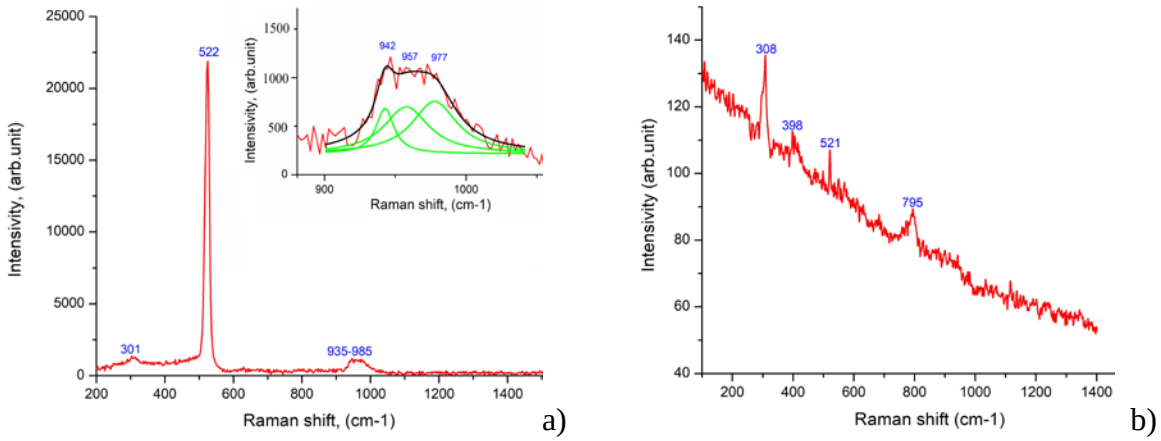

a – control sample (n-Si), b – silicon doped with chromium (n-Si<Cr>)

Fig. 1. Raman spectra of monocrystalline silicon

The results of capacitance measurements showed that the diffusion introduction of chromium atoms leads to the formation of three deep levels in the upper half of the forbidden zone, with a fixed value of ionization energy E_C - 0.20 eV, E_C - 0.41 eV and E_C - 0.51 eV, with only the last two levels associated with chromium atoms.

1. S. Z. Zainabidinov, Kh. S. Daliev, K. P. Abdurakhmanov, Sh. B. Utamuradova, I. Kh. Khomidjonov, and I. A. Mirzamurodov. The influence of the impurities with deep levels on the iron behavior in silicon. *Modern Physics Letters B*, vol. 11, no. 20, pp. 909–912, 1997
2. Sh. B. Utamuradova, Kh. S. Daliev, Sh. Kh. Daliev, and K. M. Fayzullaev. The influence of chromium and iron atoms on the processes of defect formation in silicon. *Applied Physics*, no. 6, pp. 90–95, 2019.

ELECTROCHEMICAL SYNTHESIS OF CARBON NANOSTRUCTURES FOR BIOMEDICAL AND ENVIRONMENTAL APPLICATIONS

Khaydarov R.R. [1], **Gapurova O.U.**[1], **Praveen Thaggikuppe Krishnamurthy**[2]
[1]*Institute of Nuclear Physics, Uzbekistan Academy of Sciences, Tashkent, Uzbekistan*
[2]*Department of Pharmacology, JSS College of Pharmacy, Tamil Nadu, India*

In 2021-2023, the Uzbek-Indian joint project №UZB-Ind-2021-77 “CD133 mAbs surface modified carbon nanotubes loaded with Survivin siRNA and Paclitaxel for the treatment of non-small cell lung cancer” was executed in the Institute of Nuclear Physics of the Academy of Sciences of the Republic of Uzbekistan. Within the project we have synthesisied a functionalized carbon nanotube-based drug delivery system loaded with chemotherapeutic agent Paclitaxel, and surface modified with CD133 monoclonal antibody and Survivin protein (see Fig. 1) to achieve improved bioavailability and site precisely deliver drug cargoes to the target tissue.

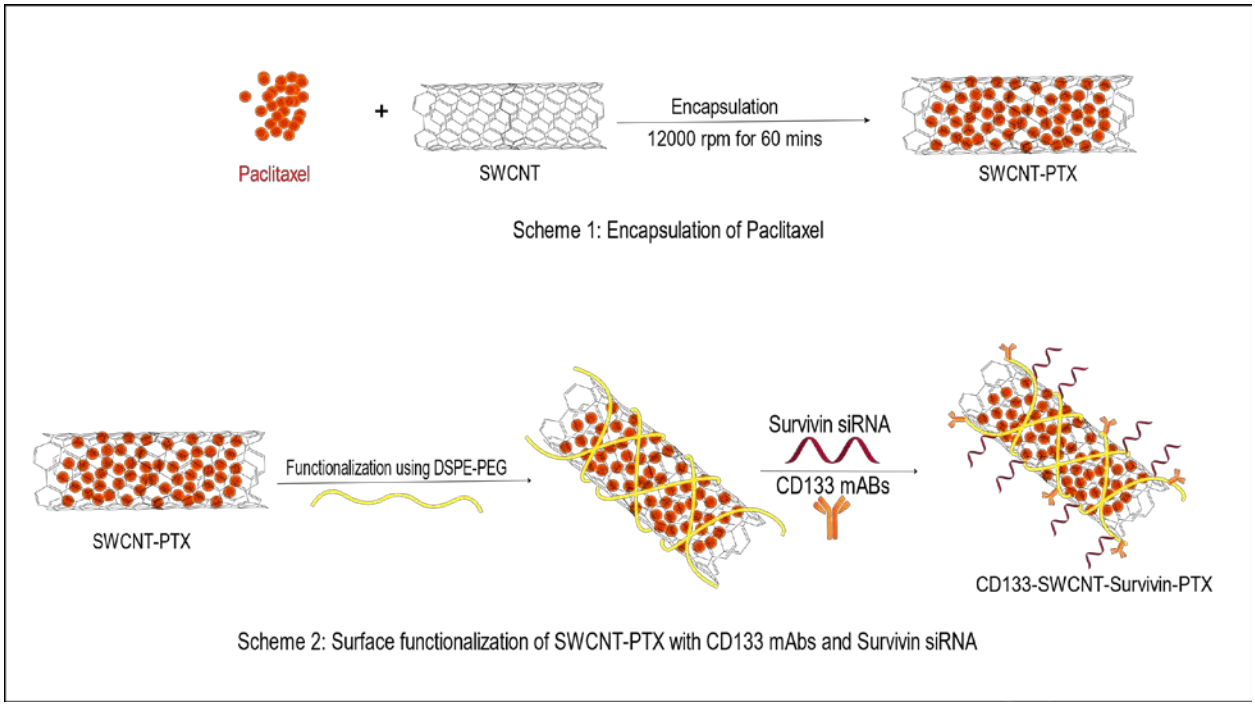

Fig. 1. Synthesis of CD133-SWCNT-Survivin-PTX

We have also developed a method of obtaining nanocarbon-conjugated polymer nanocomposites (NCPC) using nanocarbon colloids (NCC) and polyethylenimine (PEI) for water purification from metal ions. Size of NCC, process of NCPC synthesis, its chemical characteristics, ratio of NCC and PEI in NCPC, speed of coagulation of NCPC, mechanism of interaction of metal ions with NCPC, ability of removing metal ions from water by NCPC against pH have been studied. NCPC has a bonding capacity of 4.0–5.7 mmol/g at pH 6 for most of the divalent metal ions. Percent of sorption of Zn^{2+}, Cd^{2+}, Cu^{2+}, Hg^{2+}, Ni^{2+}, Cr^{6+} ions is higher than 99%. Lifetime of NCPC before coagulation in the treated water is 1 s–1000 min and depends on the ratio of polymeric molecules and carbon nanoparticle concentrations.

INVESTIGATIONS ON GREEN HYDROGEN GENERATION BASED ON SOLAR THERMOCHEMICAL CYCLE

Akhatov J.S.
Physical-technical Institute, Uzbekistan Academy of Sciences, Tashkent, Uzbekistan

At present, solar hydrogen production technology becoming more attractive and mainly includes: photocatalysis, photoelectrocatalysis, PV coupling electrolysis and thermochemical cycle. PV coupling electrolysis is the most mature technology, but it has the problems of high irreversible potential. In photocatalytic and photoelectrocatalytic methods, semiconductor materials have certain selectivity to solar spectrum, resulting in low efficiency of solar energy hydrogen production. The solar thermochemical cycle (STC) technology, which can utilize the full spectrum of solar energy, is considered as one of the most likely methods to realize large-scale and low-cost hydrogen production from solar energy. Due to the strong inertia of H_2O, direct pyrolysis requires ultra-high temperature, which is difficult to achieve in industry. The Gibbs function of the reaction and the reaction temperature can be reduced by the method of STC. Using metal oxide as intermediate medium, solar energy can produce hydrogen by redox reaction. Reactant material research has developed from volatile to non-volatile metal oxides, around 400 species classified. The research of reactant materials is still in the stage of trial. The world's leading research institutions such as DLR, PSI and ETH, PROMES, etc., are engaged in research.

The goal of our investigations in cooperation with Institute of Electrical Engineering (IEE, CAS, China) is to find solutions of the key scientific mechanism and technical problems of STC conversion of H_2O to hydrogen production from three levels: materials (materials with high efficiency and high thermochemical stability and their synthesis methods), reactors (design and creation of prototype of solar reactor with high efficiency, with different scale and continuous operation) and systems (design and performance evaluation method of heat, electricity, cold and fuel polygeneration system based on STC hydrogen production).

The design of the first prototype of a solar thermochemical reactor (STR), with redox processes based on CeO_2 occurs in inner volume, under the influence of a concentrated flow of solar radiation, has been developed. A calculation model has been developed to determine its thermal characteristics using “Comsol Multiphysics”, “Modelica” and “Solid works flow simulation”. The test bench has been created for conducting experimental studies to determine the thermal characteristics of STR prototype. A design and a pilot of the second prototype of a 10 kW STR has been created, jointly with partners from the IEE, CAS, and China. Experimental studies are being carried out to study the processes occurring in the reactor, as well as to determine the thermal characteristics of this reactor when conducting experiments using a solar concentrator at the Test Base of the Physical-technical Institute.

1. Tianzeng Ma, Mingkai Fu, Jian Cong, Xia Zhang, Qiangqiang Zhang, Jasurjon S. Akhatov, Zheshao Chang, Xin Li // Experimental study of a high-temperature porous-medium filled solar thermochemical reactor for CO production // Journal of Energy Storage 74 (2023) 109399.
2. Jian Cong, Tianzeng Ma, Zheshao Chang, Qiangqiang Zhang, Jasurjon S. Akhatov, Mingkai Fu, Xin Li // Neural network and experimental thermodynamics study of YCrO3-δ for efficient solar thermochemical hydrogen production // Renewable Energy 213 (2023) 1–10.
3. Tianzeng Ma, Jian Cong, Zheshao Chang, Qiangqiang Zhang, Jasurjon S. Akhatov, Mingkai Fu, Xin Li // Heat transfer and solar absorption analysis of multiscale CeO2 reduction for rapid H2 production prediction // International Journal of Hydrogen Energy, 47 (2022), pp. 21681-21689.

THE INAA AND ICP-MS AND TRACK ANALYSIS OF THE PREHISTORIC AND ANCIENT BONES OF UZBEKISTAN

Vasidov A.[1], Yuldashev B.S.[1], Strashnov I.[2], Izosimov I.N.[3], Saidullaev B.D.[1]
[1] Institute of Nuclear Physics, Uzbekistan Academy of Sciences, Tashkent, Uzbekistan
[2]The University of Manchester, School of Natural Sciences, United Kingdom
[3]Joint Institute for Nuclear Research, Dubna, Russia

Among the methods of radiogenic determination of the age of archaeological materials, radiometric methods of dating bone finds play an important role. These include $^{14}C/^{14}N$, $^{40}K/^{40}Ar$, $^{89}Rb/^{89}Sr$, $^{90}Sr/^{90}Y$, $^{238}U/^{207}Pb$ and $^{232}Th/^{206}Pb$ methods, which are based on the constant rate of radioactive decay of natural radioisotopes in the studied materials. As shown and follow from the results of instrumental neutron activation and ion-plasma inductive mass spectrometric analyses, radiogenic dating methods for archaeological bones are not absolutely correct and reliable, due to the increase in the content of radiometric elements in skeletons depending on the environment.

A new highly sensitive technique is proposed to estimate the age of ancient bones by the specific activity of ^{226}Ra, which is determined by the registration of ^{222}Rn α-particles using a CR-39 track detector in an isolated chamber. Comparison of specific activity of ^{226}Ra in the bones of archanthropus, southern mammoths, and dinosaurs between standard bones showed that there is a direct correlation between age and specific activity of ^{226}Ra in these bones. The work also presented the specific activity of ^{226}Ra in soils taken from the sites of detection of the studied skeletons.

METROLOGICAL EQUIPMENT FOR CALIBRATION LABORATORY

Beresneva Y.A., Guzov V.D., Kozhemyakin V.A., Lazarenko S.V.
Scientific Production Unitary Enterprise «ATOMTEX», Minsk, Belarus

Calibration of dosimetric radiation monitoring instruments: dosimeters, dosimeter-radiometers, dosimeter-spectrometers, dose rate meters, detection units, multichannel systems with detection units designed to determine the air kerma rate, ambient and directional dose equivalent rates of X-ray and gamma radiation is performed in calibration laboratories.

In order to recognise the calibration results and the calibration certificates provided at the international level, the laboratories undergo a conformity assessment procedure with a national accreditation body. National accreditation bodies that have been peer reviewed as competent sign agreements with international accreditation organisations (European Accreditation Organisation (EA), International Laboratory Accreditation Organisation (ILAC), International Accreditation Forum (IAF)) to demonstrate their competence. National accreditation bodies then assess and accredit the conformity assessment bodies to the relevant standards.

When calibration laboratories are accredited, they are assessed against the requirements of ISO/IEC 17025-2019 General Requirements for the Competence of Testing and Calibration Laboratories. The report provides information on the provision of calibration laboratory, carrying out calibration of environmental dosimeters, with calibration facilities (working standards, auxiliary equipment), discusses the following issues.

AT1117M RADIATION MONITOR WITH BDKN-06 DETECTION UNIT AND A SET OF SPHERICAL MODERATORS TO RECONSTRUCT THE ENERGY DISTRIBUTION OF NEUTRON FLUX DENSITY

Komar D.I.[1], Kozhemyakin V.A.[1], Gurinovich V.I.[1], Vasilyev A.V.[2], Ekidin A.A.[2], Pyshkina M.D.[2]

[1]Scientific Production Unitary Enterprise «ATOMTEX», Minsk, Belarus
[2]Institute of industrial ecology UB RAS, Yekaterinburg, Russia

For the most correct assessment of dose loads on personnel from neutron radiation it is necessary to have information on the energy distribution of neutron flux density at a particular workplace. Based on the reconstructed energy distribution it is possible to correct the readings of the individual dosimeter assigned to the personnel at a given workplace.

The neutron radiation detection unit BDKN-06 is a ^{3}He counter placed in a polyethylene sphere-shaped moderator. The design of BDKN-06 allows sequential measurement of pulse count rate with sphere-moderators with diameters from 3 to 12 inches. Methodological support with application of special mathematical algorithm allows to obtain energy distribution of neutron radiation flux density on the basis of measured pulse count rates with each sphere.

The dosimeter-radiometer AT1117M with the detection unit BDKN-06 and a set of moderator spheres is designed to measure the characteristics of neutron radiation in order to recover the energy distribution of neutron radiation flux density.

The neutron radiation detection unit BDKN-06 and information processing unit PU4 are placed on a tripod. The design of BDKN-06 makes it possible to measure sequentially the count rate of neutron radiation pulses by a proportional counter based on ^{3}He in moderator spheres of different diameters. The diameter of the spheres is from 3 to 12 inches.

Measurements are carried out according to the specially developed measurement technique MT AAAA.7031.004-2020 "Reconstruction of energy distribution of neutron radiation flux density. Determination of average neutron radiation flux density".

The result of neutron radiation flux density energy distribution reconstruction obtained in accordance with the technique is used to calculate such quantities as: integral neutron flux density, average neutron radiation energy by spectrum, average neutron radiation energy by dose, dose equivalent per unit flux density, dose equivalent, effective dose.

The mathematical algorithm is implemented in application software with user-friendly interface as an appendix to the measurement methodology.

NEUTRON IMAGING IN STUDYING METEORITES, ROCKS, AND ARCHAEOLOGICAL OBJECTS: COLLABORATION BETWEEN JINR AND INP AS RUz

Abdurakhimov B.A.[1,2], Tashmetov M.Yu.[2], Kichanov S.E.[1], Yuldashev B.S.[2], Kozlenko D.P.[1], Zel I.Yu.[1], Saprykina I.A.[1]

[1]Joint Institute for Nuclear Research, Dubna, Russia

[2]Institute of Nuclear Physics, Uzbekistan Academy of Sciences, Tashkent, Uzbekistan

Today, neutron imaging is actively used as a non-destructive testing method in various fields of research, from studying the inner structure of industrial, biological, geological, and engineering objects to cultural heritage objects. Therefore, neutron radiography and tomography methods have been realized in almost all neutron centers in the world. Since 2015, the NRT station at IBR-2 (FLNP JINR, Dubna) has been operated regularly for neutron tomography experiments [1]. In 2020, a neutron imaging facility [2] was commissioned on the 5th horizontal channel of the stationary reactor WWR-SM (INP AS RUz, Tashkent), developed jointly with FLNP JINR. This report presents the main technical parameters of the neutron imaging facility and the results of studying fragments of the Chelyabinsk and Kunya-Urgench meteorites, lamprophyre dikes, and archaeological objects (Qarakhanid dirham, wall fragments of the Uzundara fortress) with the neutron tomography method. In particular, tomography of meteorite fragments helped to reveal the 3D distribution of metal components corresponding to the troilite and kamacite phases. Segmented particles of kamacite in the Kunya-Urgench meteorite volume were found to have a weak axial shape texture, which could have been formed as a result of collision. Lamprophyre dikes were studied to reveal the possible connection between the inclusions in the dike body and the magma flow. With neutron tomography, it was possible to obtain the 3D distributions of such inclusions, to analyze their size, shape, and orientation, and to confirm the connection between the spatial orientation of the inclusions and the direction of magma movement. Within the framework of cooperation with archaeologists, neutron tomography was used as a non-destructive method, along with other techniques. The first cooperation works were performed on Qarakhanid copper-silver dirham and on clay mortar fragments from the walls of the ancient Uzundara fortress.

1. D.P. Kozlenko, S.E. Kichanov, E.V. Lukin et al. Neutron Radiography Facility at IBR-2 High Flux Pulsed Reactor: First Results. *Physics Procedia*. Vol. 69, pp. 87-91, 2015. (DOI: 10.1016/j.phpro.2015.07.012).
2. B.A. Abdurakhimov, M.Yu. Tashmetov, B.S. Yuldashev et al. New neutron imaging facility at the WWR-SM reactor: Design and first results. *Nuc. Inst. and Meth. in Phy. Res. Sec. A.* Vol. 989, p. 164959, 2021. (DOI: 10.1016/j.nima.2020.164959).

EXPLORING MACHINE LEARNING PERFORMANCE METRICS FOR PREDICTING HOURLY GLOBAL IRRADIANCE IN SAMARQAND

Boudjella A.[1,2], Boudjella M.Y.[2], Galety M.[3]
[1]*Samarkand International University, Samarkand, Uzbekistan*
[2]*Bircham International University Miami, USA*
[3]*University of Sciences and Technology USTO, Oran, Algerie*

We investigate the hourly Global Irradiance for assessing energy received in Samarqand using the k- Nearest Neighbor (KNN) method for classification. In this study Unsupervised transformations of the dataset are employed in learning algorithms. Two distinct data representation, two classes are generated separately from the original dataset based on captured energy load magnitudes (**Watts per square meter (W/m²)**). The unsupervised transformations of the dataset yield 0 and 1 classes, class 0 in the range of (0,500), and class1 in the range of (>500, 1032.92).To evaluate the performance, various test and training sizes are employed, comparing measurement outcomes and predicting class label descriptions for two dataset representations as the parameter for the random state (RS) ranges from 1 to 2**5**. Results obtained from the simulation indicate that accuracy is influenced by factors such as test size, the ***RS*** parameter, Keeping *k* constant **5.** Utilizing a K-nearest neighbors (KNN) classifier, the study evaluates its performance across various metrics including Test Size (TS), random state (RS), K Classifier. Global Performance Measure (GPM), Training Accuracy (TrACC), Test Accuracy (TsACC), Precision Score, Recall, F1_Score, and Specificity are presented . Analysis of the results showcases an impressive level of global performance larger than 96%, accuracy, with performance metrics averaging between 99.69% and 99.95%. The study underscores the robustness of the predictive model, demonstrating its potential for accurately forecasting hourly Global Irradiance in Samarqand, as evidenced by the high test accuracy, F1 score, precision score, and specificity achieved.

Keywords: Machine learning, hourly Global Irradiance prediction, Samarqand, K-nearest neighbors classifier, performance metrics, test accuracy, F1 score, precision score, specificity

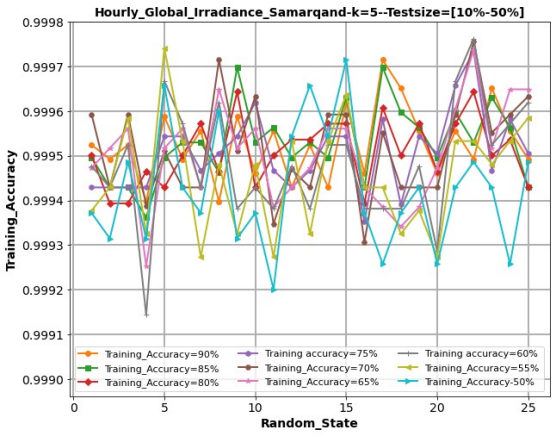

Fig. 1. Training_Accuracy vs RS.Test_Size=[10-50%]

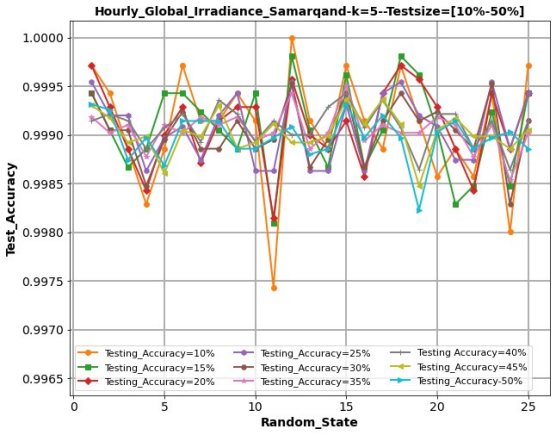

Fig.2. Test_Accuracy vs RS.Test_Size=[10-50%]

EVALUATION OF THE EFFECT OF MARITIME AEROSOLS AND RURAL AEROSOLS ON THE DIRECT NORMAL IRRADIANCE USING GEANT4

Boudjella A.
Samarkand International University, Samarkand, Uzbekistan
Bircham International University Miami, USA

This study employs the Geant4 toolkit to assess both the atmospheric transmittance and the spectral direct normal irradiance within the spectral range of 300-850nm. Simulations are conducted under an optical air mass of 1.5, considering two distinct atmospheric scenarios: one with maritime aerosols and another with rural aerosols. The transparency of the atmosphere to the Sun's radiation varies with incident wavelength and the type of aerosols present. Rural aerosols demonstrate higher atmospheric transmittance compared to maritime aerosols for wavelengths greater than 522nm, whereas the opposite trend is observed for wavelengths less than 522nm. Validation of the Geant4 simulations is performed by comparing results against those obtained from DISORT under both atmospheric conditions. . Overall, the comparison shows generally good agreement between Geant4 and DISORT. The ratio of Geant4 to DISORT transmittance was found to be less than 1.06 in both cases.

Keywords: Geant4, DISORT, rural aerosols, maritime aerosols, direct normal irradiane

PRODUCTION OF RADIOPREPARATIONS OF ALPHA-EMITTING RADIONUCLIDES

Baimukhanova A.E.[1,2], Kurakina E.S.[1], Karaivanov D.V.[1,3], Dadakhanov J.A.[1], Filosofov D.V.[1]
[1]Joint Institute for Nuclear Research, Dubna, Russia
[2]Institute of Nuclear Physics, Almaty, Kazakhstan
[3]Institute for Nuclear Research and Nuclear Energy, Bulgarian Academy of Sciences, Sofia, Bulgaria

Alpha-emitting radionuclides are used in nuclear medicine. There are some candidates suitable for efficient targeted radionuclide therapy. However, the number of these radionuclides is limited, as well as their quantity produced routinely. The reason is that the most alpha-emitters are far from the beta stability line.

In this work, the problems of production of alpha-emitting radionuclides are discussed. The possibility of producing medical radionuclides via proton irradiation of radioactive targets is considered. The optimal parameters of target irradiation and the yields of radionuclides in the reactions ^{150}Gd+p, ^{231}Pa+p and ^{226}Ra+p are evaluated. Radiochemical aspects of radionuclide isolation from macroamount of target material are considered as well.

DETECTOR SYSTEMS FOR GAMMA SPECTROSCOPY AND BIOPHOTONICS

Dunin N.[1,2], Demikhov E.[1], Fimushkin V.V.[2]
[1]*P.N.Lebedev Physical Institute of the Russian Academy of Sciences, Moscow, Russia*
[2]*Joint Institute for Nuclear Research, Dubna, Russia*

Prototypes of the single-channel and 4-channel detectors, which are discussed below, have been developed at the Laboratory of High Energy Physics in Dubna in collaboration with Lebedev Physical Institute of Russian Academy of Science. The single-channel prototype detectors with a single photomultiplier and a CsI scintillator are very much needed to measure the absolute polarization value for SPD experiment at the NICA Collider in the Joint Institute for Nuclear Research. Pretty soon the accelerated complex will be commissioned and these detectors will be especially needed for Spin Physics experiments. The single-channel detectors have been equipped with CsI scintillators. Our group has manufactured the single-channel prototypes and calibrated them using Cs137 and Co60 sources at the Laboratory of High Energy in Dubna. The operating voltage of the photomultiplier tube has been also calibrated. Besides, these detector systems can be used not only for gamma-spectroscopy, but also for biophotonics applications. We have designed a 4-channel detector to measure the ultra-weak optical radiation and improve the Signal-Noise ratio for this purpose. Ultra-weak optical radiation is characterized by low intensity and a temporal structure of narrow flashes of light. To separate the single-photoelectron useful signal (a pulse with a width of about 2-3 ns) from the single-photoelectron dark current, each channel is equipped with a discriminator circuits. The presence of a built-in selection circuit based on differential discriminators makes it possible to separate single-photoelectron pulses from the pulses with a large amplitude. The four-channel detector system has been designed for applied science as biophotonics to register the ultra-weak optical emission generated by microorganisms in active and resting phases.

The detector system is characterized by low power consumption (less than 4 Watt), wide aperture, and 4000 MHz bandwidth. To count pulses from the detector system, the data acquisition board based on the Milandr 1986BE92QI microcontroller was designed with embedded software. The following features implemented for the data acquisition board include the cyclic data transmission via the UART interface, a built-in battery, the DS18B20 digital sensor, the exFAT file system for data recording, and a removable memory card for autonomous operation without a PC. Research for the financial support within the framework of scientific project No. 19-29-10007.

MATHEMATICAL MODELING OF RADIATION-INDUCED EFFECTS IN HUMAN AND MAMMALIAN CELLS

Dushanov E.B.[1,2], Batmunkh M.[1], Lhagvaa B.[1], Togtokhtur T.[1], Vasileva M.A.[1], Glebov A.A.[1], Kolesnikova E.A.[1], Aksenova S.V.[1], Sadykova O.G.[1,2], Parkhomenko A.Yu.[1], Batova A.S.[1], Bugay A.N.[1,2]

[1]*Joint Institute for Nuclear Research, Dubna, Russia*

[2]*Dubna State University, Dubna, Russia*

One of the priorities in modern radiobiology of ionizing radiation is increasing the effectiveness of therapy for hard-to-reach tumors with secondary particles and assessing radiation safety during interplanetary manned flights. Due to the complexity of these problems, the development of methods of mathematical and computer modeling is required.

One of the priorities in modern radiobiology of ionizing radiation is assessing radiation safety during interplanetary manned flights. Due to the complexity of these problems, the development of methods of mathematical and computer modeling is required.

The goal of this study is to create a hierarchy of models that allow us to systematize experimental data and study the ways in which radiation-induced pathologies develop at different levels of organization (from molecules to cell populations) and over time (acute and long-term effects).

To solve the assigned task, a wide range of computational methods from different fields of knowledge is used (Monte Carlo modeling of the transport of charged particles through matter, molecular dynamics, polymer biophysics, models of information processing and transmission in neural networks of the brain), which are ordered into a hierarchy according to temporal and spatial the scale of ongoing processes.

In the course of solving the problem of the effect of cosmic rays on the central nervous system (CNS) during interplanetary manned flights, the influence of charged particles on the functioning of neural networks of critical parts of the brain (primarily the hippocampus) was assessed [1]. The effect of a spectrum of particles with different energies and fluences on the yield of DNA damage was examined for the first time. As a result of the development of further pathologies in the central nervous system after irradiation, the properties of mutant and oxidized forms of synaptic receptors that ensure interneuron interaction, the dynamics of neurogenesis and gliogenesis, and inflammatory reactions were studied. The data obtained were included in the modeling of the functional properties of the neural networks of the brain, which made it possible to assess the likelihood of malfunctions and predict possible observed changes in electroencephalography and functional magnetic resonance imaging signals [2].

The results obtained indicate to necessity of further development of modern computational methods to successfully solve theoretical problems in radiobiology.

1. *M.Batmunkh, L. Bayarchimeg, A.N. Bugay*, Monte Carlo Simulation Study of Primary Damage and Survival of Hippocampal Neurons following Proton and Heavy-ion Irradiation // [submitted to journal "Radiation"].

2. *Aksenova S.V., Batova A.S., Bugay A.N., Dushanov E.B.* Effect of Oxidative Stress on the Functioning of Hippocampus Glutamate Receptors // Russian Journal of Biological Physics and Chemistry, v. 8, No 2, 2024, 151-158.

RADIOCARBON DATING OF ARCHAEOLOGICAL AND NATURAL SAMPLES WITH BINP AMS AND MICADAS-28 AT AMS GOLDEN VALLEY, NOVOSIBIRSK, RUSSIA

Petrozhitskiy A.V.[1,2,3], Parkhomchuk V.V.[1], Konstantinov E.S.[1], Shakiriva T.M.[1], Parkhomchuk E.V.[2,3,4], Kutnyakova L.A.[3]

[1]Budker Institute of Nuclear Physics, Novosibirsk, Russia
[2]Novosibirsk State University, Novosibirsk, Russia
[3]Institute of Archaeology and Ethnography, Novosibirsk, Russia
[4]Boreskov Institute of Catalysis, Novosibirsk, Russia

Routine ^{14}C analysis of user samples is performed with two accelerator mass spectrometers at AMS Golden Valley: BINP AMS facility, developed by Budker Institute of Nuclear Physics, Russia and MICADAS-28 facility, developed by IonPlus AG, Switzerland. The laboratory has international index GV and provides ^{14}C analyses of various samples: collagen, cellulose, humic acids, carbonates from sediments etc. The main focus of the laboratory is to determine the age of archaeological artifacts. In 2022 BINP AMS and MICADAS-28 successfully passed the Glasgow International Radiocarbon Inter-comparison (GIRI) and at the present moment are the only accelerator mass spectrometers in Russia. Detailed description and characteristics of BINP AMS facility will be presented compared with that one's of MICADAS -28. Samples of various types dated by our laboratory will be presented as examples of our work.

POLARIZATION FACILITIES AT JINR ACCELERATOR COMPLEX

Fimushkin V.V.[1], Dunin V.B.[1], Dunin N.V.[1], Ivshin K.A.[1], Kulikov M.V.[1], Kuzyakin R.A.[1], Kutuzova L.V.[1], Shumkov A.M.[1], Solovev A.N.[1], Belov A.S.[2]

[1]Joint Institute for Nuclear Research, Dubna, Russia
[2]Institute for Nuclear Research, Moscow, Russia

Polarization facilities are developed at the JINR accelerator complex in the framework of the polarization research program under the NICA project. Those are: the polarized deuteron and proton source SPI, SPI low energy polarimeter and a linac output polarimeter.

The project assumes the design and construction of a universal high-intensity source of polarized deuterons (protons) using a charge-exchange plasma ionizer. The output $\uparrow D^+$ ($\uparrow H^+$) current of the source is expected to be at a level of 10 mA. The polarization will be up to 90% of the maximal vector (±1) for $\uparrow D^+$ ($\uparrow H^+$) and tensor (+1, -2) for $\uparrow D^+$ polarization.

The report describes the JINR polarized ion source operating by means of the atomic beam method. The latest results of the SPI testing are presented. Polarized and unpolarized deuteron beams as well as the polarized proton beam were produced to accelerate in the NUCLOTRON. The conceptual design of a new universal low energy polarimeter at NUCLOTRON is also presented. It is proposed to install a new polarimeter behind the linear accelerator. The 3He target of this setup allows one to carry out measuring both the vector polarization of protons and vector and tensor polarization of deuterons. It is assumed that the new design of the polarimeter will make it possible to measure vector and tensor polarization of deuterons at the same time. Fabrication of the modern polarimeter is in progress now.

The status of the above facilities and the results achieved are presented.

KINETICS OF RADIATION-HETEROGENEOUS PROCESSES OF WATER INTHE PRESENCE OF n-ZrO_2 AND n-TiO_2 NANOPARTICLES

Imanova G., Agayev T.
Institute of Radiation Problems, Ministry of Science and Education, Baku, Azerbaijan

The constituent parts of systems where radiation-catalytic processes occur usually differ in terms of mass and electron density, structural characteristics, electro-physical and chemical properties. The X-ray diffraction data were processed using the Full-prof program. Full-profile processing of ZrO_2 X-ray diffraction data showed that the initial sample has a monoclinic structure (space group P 21/c). Full profile processing of TiO_2 X-ray diffraction data showed that the sample has a tetragonal structure (space group P42/mnm), (figure 1).

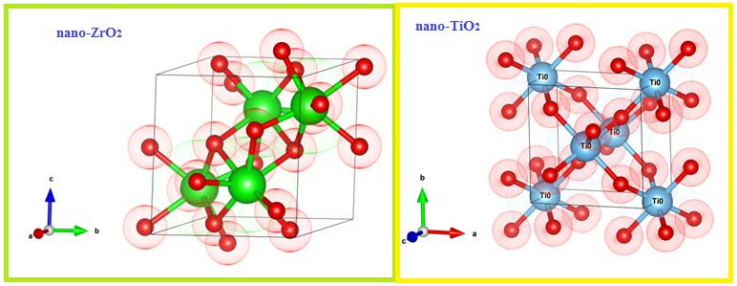

Fig.1. Crystal structures of n-ZrO_2 and n-TiO_2

The radiolysis process of water on the surface of n-ZrO_2 and n-TiO_2 nanoparticles at T=300 K was carried out by 2 methods. Hydrogen generation by water splitting is reported in nano-ZrO_2+$H_2O_{abs.}$, nano-ZrO_2+$H_2O_{liq.}$ and nano-TiO_2+$H_2O_{abs.}$, nano-TiO_2+$H_2O_{liq.}$ systems using gamma radiation and 300K temperature. The kinetics of accumulation of molecular hydrogen at a gamma radiolysis of pure water and n-ZrO_2+H_2O and n-TiO_2+H_2O systems is investigated. It is established that the radiation-chemical yield for n-ZrO_2+H_2O and n-TiO_2+H_2O systems is more ($G(H_2)$=2.14 ÷ 0.16 molecule/100 eV), than at radiolysis of a pure water ($G(H_2)$=0.45 mol./100eV). Besides, the kinetics of accumulation of molecular hydrogen radiation-thermal processes in contact of ZrO_2 and TiO_2 with water is studied. Formation of the surface active centers and secondary electrons from n-ZrO_2 and n-TiO_2, causes increase in rates of saturation of molecular molecules/g·s hydrogen at radiation-thermal processes in n-ZrO_2+H_2O and n-TiO_2+H_2O systems. Values of radiation-chemical yields are determined by value of rates of the radiation component of radiation-thermal processes of water decomposition. The received values of rates and radiation-chemical yields of molecular hydrogen are given in Table1.

Table 1. The value of the rate of the process and the radiation-chemical yield of molecular hydrogen during radiation-heterogeneous radiolysis of water in two states

Irradiated systems and process temperature, K	Particle size *d*, nm	$W(H_2)$, molecules, $g^{-1}\cdot s^{-1}$	$G(H_2)$, molecules/100eV
ZrO_2 + H_2Oads., T=300	20-30	$4.44 \cdot 10^{13}$	2.14
ZrO_2 + H_2Oliq., T=300		$2.78 \cdot 10^{14}$	13.5
TiO_2 + H_2Oads., T=300		$1.38 \cdot 10^{13}$	0.16
TiO_2 + H_2Oliq., T=300		$4{,}2 \cdot 10^{13}$	0.48

METHODOLOGICAL EXPERIMENTS ON THE STUDY OF THE GAS RELEASE FROM IRRADIATED SAMPLES OF LITHIUM CERAMICS BY THERMAL DESORPTION SPECTROSCOPY

Aitkulov M.T., Nurgozhayev B.M., Askerbekov S.K., Akhanov A.A., Shaimerdenov A.A.
Institute of Nuclear Physics, Almaty, Kazakhstan

Different types of lithium ceramics are considered as a source of tritium in the fuel cycle of a future fusion reactor. During operation, they will be exposed to various factors, which may lead to changes in their microstructure, mechanical properties, and tritium formation and release processes. Such changes may eventually lead to the destruction of the lithium ceramics, which in turn will affect the safe operation of the fusion reactor. In this regard, extensive research is being conducted to investigate the durability of the mechanical properties of lithium ceramics under high temperature conditions, while creating different annealing environments. One of the methods where it is possible to investigate the kinetics of tritium release from lithium ceramic samples under high temperature conditions (up to 1000 °C) is thermal desorption spectroscopy (TDS).

In this paper, a newly developed TDS setup is described and its characteristics, which were determined experimentally, are given. It is shown that the vacuum condition in the system will be no more than 10^{-5} torr. The temperature range of investigation in the setup is from room temperature to 900 °C. The results of methodical experiments are given, the purpose of which was to determine the optimal parameters of the setup, including the sensitivity of registration of tritium molecules.

This research has been funded by the Ministry of Science and Higher Education of the Republic of Kazakhstan (# BR21881930).

ECOLOGICAL MONITORING AND MORBIDITY RATE IN SOME REGIONS OF UZBEKISTAN

Akhmedov Ya.A., Danilova E.A., Kurbanov B.I., Osinskaya N.S.
Institute of Nuclear Physics, Uzbekistan Academy of Sciences, Tashkent, Uzbekistan

Recently the regions with intense industrial and agricultural development have been subject to significant multiple-factor anthropogenic impact which leads to environmental problems as well as to decreasing functional reserves of human body.

Such situation requires carrying out ecological monitoring – the integrated environmental survey, study of environmental changes due to natural and anthropogenic factors, evaluation and prediction, developing of actions for identifying, preventing and eliminating of damaging factors.

Therefore, carrying out of medical and ecological monitoring will allow developing of the most effective regional managerial and preventive programmes of ecological and public health survey. The analysis of the environmental state and it's dynamics through territory are the most important tasks of the bio-ecological monitoring and require to collect and analyze ecological data, such as soil, drinking (tap) water and habitants' hair. Method of neutron activation analysis has been used for element analysis.

The collected samples of soil, drinking water and habitants' hair have been analyzed for element content. The results allow us to evaluate the ecological situation in Tashkent city, Tashkent region and Surkhandaryo region, to identify territories with high content of elements, to make regions' cartograms and to identify high-risk groups of population regarding some diseases.

FERROCYANIDE SORBENTS FOR SELECTIVE REMOVAL OF Cs-137 RADIONUCLIDE

Egamediev S.Kh., Khujaev S., Nurbaeva D.A.
Institute of Nuclear Physics, Uzbekistan Academy of Science, Tashkent, Uzbekistan

The selective removal of ^{137}Cs radionuclide from liquid radioactive wastes has great importance in recent years. Hexacyanoferrates or ferrocyanides (FCNs) of transition metals (II) (Cu, Co, Fe, Ni) are very effective inorganic adsorbents for removal of ^{137}Cs radionuclide. These compounds have low solubility, high radiation and chemical stability in wide range of pH, high capacity and selectivity for Cs ions in the presence of alkaline and alkaline earth metal ions. However, FCNs are usually synthesized as fine or ultrafine grains, which are not suitable for practical applications due to their low mechanical stability and tendency to become colloidal in aqueous solution. To overcome the drawbacks the preparation of composite adsorbent has been carried out by precipitation or implantation of FCNs on different solid supports as bentonite, silicagel, zeolites, zirconium hydroxide, polyacrylonitrile and others.

The present talk deals with the procedure for the preparation of ferrocyanide sorbents based on nickel or copper ferrocyanide and macroporous KSKG silicagel and study its uptake properties for Cs-137 radionuclide from various water solutions.

The radioactive tracer technique was used for determination of the distribution coefficients (K_D) and to monitor the process of preparation of sorbents. The ^{134}Cs radionuclide was produced by irradiation of cesium nitrate salt $CsNO_3$ of pure analysis grade in WWR-SM nuclear reactor at thermal neutron flux of 5×10^{13} n/cm^2 ×s for 10 hrs.

The experimental samples of sorbents based on the nickel ferrocyanide were prepared using the macroporous silicagel of KSKG with particle size of 0.1-0.25 mm, 0.25-1 mm, 1-3 mm, 3-5 mm accordingly. It was found that the distribution coefficient of ^{134}Cs radionuclide is increased with decreasing of particle size of the original silicagel. So, the distribution coefficient of ^{134}Cs radionuclide is $(1.2\text{-}1.5)\times10^4$ when used the silicagel with particle size of 0.25-1 mm and 0.1- 0.25 mm. The adsorption degree of ^{134}Cs radionuclide achieves of more 99.6% for 24 hours from real water of liquid radioactive waste (LRW). The distribution coefficient of ^{134}Cs radionuclide is 2280 when used the silicagel with particle size of 1-3 mm. The adsorption degree of ^{134}Cs radionuclide is 99 % for 24 hours from real water of LRW.

The experimental samples of sorbent based on the copper ferrocyanide were prepared using the macroporous silicagel of KSKG with particle size of 0.1-0.25 mm, 0.25-1 mm, 1-3 mm, 3-5 mm accordingly. It was found that the distribution coefficient of ^{134}Cs radionuclide is increased with decreasing of particle size of the original silicagel. So, the distribution coefficient of ^{134}Cs radionuclide is $(1.3\text{-}1.6)\times10^4$ when used the silicagel with particle size of 0.25-1 mm and 0.1- 0.25 mm. The adsorption degree of ^{134}Cs radionuclide achieves of more 99.6% for 24 hours from real water of LRW. The distribution coefficient of ^{134}Cs radionuclide is 10^4 when used the silicagel with particle size of 1-3 mm. The adsorption degree of ^{134}Cs radionuclide is 99,9 % for 24 hours from real water of LRW.

The desorption of the ^{134}Cs radionuclide from phases of the ferrocyanide sorbent was studied by using acidic and alkaline solutions. It was found that quantitative retention of ^{134}Cs radionuclide is observed when washing by 0.5-3 mol/l HCl solutions for all samples of ferrocyanide sorbents. The desorption degree of the ^{134}Cs radionuclide is 0.1-0.3%. The desorption degree of the ^{134}Cs radionuclide is 8-35% in case when washing of ferrocyanide sorbents by using 1 mol/l NaOH solution.

THE STUDY OF THE ELEMENTAL COMPOSITION OF IRRIGATED SOILS IN THE SOUTHERN ARAL SEA REGION

Zhumamuratov A.[1], Zhumamuratov M.A.[2], Sdykov I.M.[3]
[1]Nukus State Pedagogical Institute, Nukus, Uzbekistan
[2]Nukus Innovation Institute, Nukus, Uzbekistan
[3]International Innovation Center of the Aral Sea region, Nukus, Uzbekistan

The Aral ecological disaster, which occurred in a relatively short period of time and is expressed in soil salinization, degradation of vegetation, progression of various diseases among the population and other negative processes, requires the accumulation of information about the state of individual components of the natural environment. The most dangerous type of man-made impact on the natural environment is environmental pollution by chemical elements that are involved in biological, biogeochemical, and hydrogeochemical processes.

Due to the fact that the agrogeochemistry of soils in cotton-growing areas of the Aral Sea region has been little studied, the distribution and accumulation of chemical elements in the arable layer of soils occupied by cotton is mosaic and is determined by the nature of the element content in the soil [1].

In the distribution of some elements, there is a predominant accumulation in the upper horizons of soils, in accordance with their characteristic physico-chemical properties. Thus, in the case of chromium, iron, manganese, and cobalt, the course of the curves for strongly, medium, and moderately saline soils is the same, and the maximum content of elements is found in the upper horizon, where these elements are part of the soil organic matter. The content of iron, manganese and gold in the upper horizons of soils is less than in the lower horizons and suggests that for these elements we are dealing with an alluvial process. In the latter case, the process of element dispersion is observed, which is associated with severe soil salinization.

1. Zhumamuratov A. Zh., Khatamov Sh., Ibragimov B., Tillaev T. Comparative elemental composition of modern and hidden soils of the Aral Sea region. – M.: Geochemistry. RNA, 2001. No. 3. – pp. 342-348.

FEATURES OF RAMAN SPECTRA IN POWDERS OF AROMATIC COMPOUNDS PLACED IN PHOTON TRAPS

Rakhmatullaev I.A.[1], Bunkin N.F.[2], Botirov Kh.Z.[3]
[1]Branch of National Research Nuclear University MEPhI in Tashkent, Tashkent, Uzbekistan
[2]Bauman Moscow State Technical University, Moscow, Russia
[3]Karshi State University, Karshi, Uzbekistan

Currently, despite the great successes of modern laser Raman scattering (RS) spectroscopy, there are difficulties associated with optimizing the laser light source, as well as methods for increasing the efficiency of converting exciting radiation into a Raman signal.

In this work, the task was to develop methods for recording the RS spectra of aromatic compounds, based on the use of new types of effective resonator cuvettes – photon traps (Fig. 1), which make it possible to increase the intensity of RS in relation to the intensity of exciting

radiation. The RS spectra of micropowders $C_{24}H_{16}O_2$ (POPOP) and $C_{15}H_{11}NO$ (PPO) were studied at room temperature. RS spectra were recorded using a technique described in detail in [1,2]. RS were excited by the green line of a copper vapor laser (λ=510.6 nm).

The spectrum of each compound clearly shows characteristic peaks: 1128 and 1597 cm^{-1} for POPOP and 1128 and 1588 cm^{-1} for PPO. The band in the region of 1580-1620 cm^{-1} is associated with C=C stretching vibrations of aromatic rings. The observed peak at 1128 cm-1 in both samples is associated with C-N stretching vibrations [3]. The high efficiency of converting exciting radiation into a RS signal is explained by the large value of the total path that a photon of exciting radiation travels in an ultradisperse medium located in a photon trap. This also makes it possible to observe Raman lines located near the exciting laser radiation line.

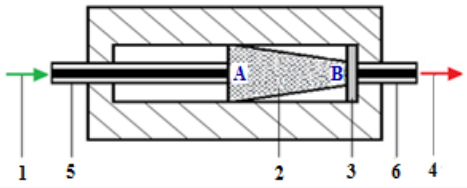

Fig. 1. Design of a photon trap with a cone resonator: 1 – exciting radiation; 2 – powder; 3- absorption filter; 4 – Raman scattering; 5 – input light guide; 6 – output light guide

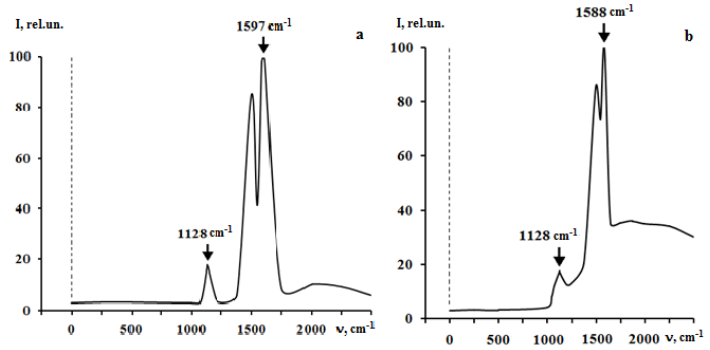

Fig. 2. Raman spectra of aromatic compounds excited by a copper vapor laser (λ_{exc}=510.6 nm): a – POPOP, b – PPO

The developed highly sensitive method for recording Raman spectra based on the developed photon traps opens up wide opportunities for recording weak signals of secondary radiation from many practically important inorganic and organic substances.

1. Gorelik V.S., Rakhmatullaev I.A. Tech. Physics. 50, No.1 (2005) 61—64
2. Davronov M.Kh., Makarov N.V., Rakhmatullaev I.A. Usp.xim.i.xim.texn. 36, No. 10 (2022) 60—63
3. Kuptsov A.Kh., Zhizhin G.N. Fourier-Raman and Fourier-IR spectra of polymers. – M: Tekhnosphere, 2013. — 696 p.

INVESTIGATION OF SENSITIVITY OF ANAPLASTIC ASTROCYTOMA TISSUE TO NEUTRON CAPTURE THERAPY IN CONDITIONS IN VITRO

Kim A.A.[1], Kulabdullaev G.A.[1], Juraeva G.T.[1], Yuldashev Dj.O.[2], Kadyrbekov N.R.[3], Beknazarov H.J.[3], Kadyrbekov R.T.[3]

[1]Institute of Nuclear Physics, Uzbekistan Academy of Sciences, Tashkent, Uzbekistan
[2]Bukhara State Medical Institute, Bukhara, Uzbekistan
[3]Republican Special Scientific and Practical Medical Center of Neurosurgery, Tashkent, Uzbekistan

Binary technologies of radiation therapy, neutron capture and photon capture therapy, are modern developing methods that can potentially significantly improve the effectiveness of radiation therapy in general. Previously, we developed a method for evaluation of radiosensitivity of anaplastic astrocytoma tissues to gamma radiation [1]. The ain of this study was to determine the

effectiveness of this method for neutron capture therapy. We carried out study on the individual assessment of radiosensitivity of human anaplastic astrocytoma tissues in conditions in vitro when irradiated with epithermal neutrons and secondary particles arising from the gadolinium-neutron capture reaction. Two groups of patients with anaplastic astrocytoma were studied – in the first group of 6 patients, samples were irradiated with doses of 5.10 and 15 Gray. In the second group of 5 patients, the samples were irradiated with doses of 20 and 40 Gy. For the experiments, living tissue sections of anaplastic astrocytoma of the human brain were used. The irradiation was carried out on specialized beam of epithermal neutrons. A standard Magnevist preparation with known gadolinium content was used as a source of gadolinium. The irradiation time of the samples was determined using simulation in the MCNP program. [2]

The study included 11 patients (7 men and 4 women) aged 23 to 66 years with a clinical diagnosis of anaplastic astrocytoma. The diagnosis was confirmed clinically and histologically. The procedure for sampling and irradiation of samples was described in detail by us in [3]. The samples were analyzed in the histological laboratory of the RSCPMCN of the Ministry of Health of the Republic of Uzbekistan using standard histological methods. Tissue samples were fixed in 10% formalin. The recorded samples were poured into paraffin wax, and sections were prepared. The prepared sections were dewaxed and stained with hematoxylin-eosin. The histological photographs obtained were processed using a stereometric grid with a step size of 5 mm. The relative area of necrotic areas was determined as a percentage using the stereometric method using the ScopeImage 9.0(X3) software.

In the first group of 6 patients, high sensitivity was observed in 3 (50%), in 2 patients (33.3%) resistance to all three doses of 5, 10 and 15 Gray was observed, and in one patient (16.7%) resistance to radiation doses of 5 and 10 Gray was observed. In the second group of five patients, all five patients showed good sensitivity to radiation doses of 20 and 40 Gray. The data obtained showed that living biopsy sections of human anaplastic astrocytoma can be used as in vitro model to study therapeutic pathomorphosis under irradiation with epithermal neutrons and secondary particles arising from the gadolinium-neutron capture reaction. One of the advantages of using living tumor slices in vitro is that the issue of gadolinium concentration in the tumor is completely solved. This model allows you to create any constant concentrations of gadolinium in the irradiated target.

1.A.A. Kim, G.A. Kulabdullaev et al. Patent of the Republic of Uzbekistan IAP 06855 (2020)
2.MCNP - A General Monte Carlo NParticle Code - Version 4C. Briestmeister J.F (2000).
3.A.A. Kim, G.A. Kulabdullaev et al. Herald of Tashkent Med. Academy,7,114-119 (2022)

DEPENDENCE OF THE ABSORBED DOSE IN HBT ON THE COMPOSITION OF THE TUMOR

Kulabdullaev G.A.[1], Abdullaeva G.A.[1], Kim A.A.[1], Yuldashev Dj.O.[2]
[1]Institute of Nuclear Physics, Uzbekistan Academy of Sciences, Tashkent, Uzbekistan
[2]Bukhara State Medical Institute, Bukhara, Uzbekistan

Changes in the composition of human brain tumors (HBT) can lead to changes in the structure and density of tumors. The study of the composition of malignant tumors is covered in many publications in the literature. The composition of HBT has been the subject of very little research. Before treatment, the parameters of mineral metabolism in blood plasma and tumor tissue were analyzed in 12 patients with malignant and 7 patients with benign HBT, as previously mentioned in

[1). Controls included brain tissue samples from 7 people who died due to injury and blood samples from 10 people who were practically healthy. A statistically significant increase in the concentration of Ca, Na and a decrease in Mg, K, P in the tumor tissue of the brain was detected compared with the brain tissue of the control group and patients with benign tumors. In the blood plasma, the content of Fe, Zn, Li and Sr also increased by 2, 2.1, 2.7 and 4 times, and Cu and Se, on the contrary, decreased by 1.7 times and 1.8 times. Therefore, it was interesting to study the effect of changes in the elemental composition of HBT on the generated absorbed dose in human HBT. Since it is difficult and in most cases impossible to directly measure the absorbed dose in human organs and tissues, modelling the irradiation process remains the only acceptable way to estimate doses. The Monte Carlo (MC) method is the only option today to calculate dose accurately in such complex cases. Calculations were carried out for a human head phantom, which has the following characteristics: a sphere with a radius of 8 cm, a skull with a thickness of 7 mm, filled with material 9 (brain) and a spherical tumour with a radius of 1.5 cm, material 8 (tumour). This phantom is located at the outlet of the horizontal channel in the irradiation box of the WWR-SM reactor of the Institute of Nuclear Physics of the Academy of Sciences of the Republic of Uzbekistan. The elemental composition of human tissues, taken from the ICRU data bank [3,4], was used for the calculations. The table shows the results obtained for calculating the dose depending on the amount of basic elements of the human brain such as H_2, O_2, N_2 and C_2.

Table. Total values of equivalent dose rates (Gy/particle) from neutrons and photons

№	Body tissue	Particle type	Total dose rate in the HBT	Total dose rate in the human brain
1	Normal tumor tissue (NTT)	n	1,01391e-4	3,9806e-6
		ph	1,92398e-6	2,44193e-7
2	O_2 decreased, H_2 increased in NTT	n	1,63849e-4	6,56869e-6
		ph	6,80364e-7	1,08366e-7
3	C_2 decreased, N_2 increased in NTT	n	1,00511e-4	3,91330e-6
		ph	2,31883e-6	2,65035e-7
4	O_2 decreased, N_2 increased in NTT	n	8,71871e-5	3,3555e-6
		ph	2,52591e-6	2,71611e-7

It can be concluded from these results that changes in the concentration of organic elements have an impact on the total equivalent dose rate. The therapeutic dose for different types of HBT can be determined based on these results and further studies

1. Krause, M.; Dubrovska et al. Adv. Drug Deliv. Rev. 2017, 109, 63–73.
2. Briesmeister J. F. et al. MCNP -4C. New Mexico: Los Alamos Nat. Lab., 2000. 736 p.
3. ICRU46,«Photon,Electron,Proton and Neutron Interaction Data for BodyTissues,MD,1992.
4. Chadwick M., Barschall H. et al. Medical Physics, 1999, 26(6), 974-991

DETECTION OF QUARK-GLUON PLASMA CONDENSATE IN A SPIRALLY CURLED HYPERSONIC JET

Khasanov Kh.
Moscow State University, Moscow, Russia
Samarkand State University, Samarkand, Uzbekistan

A special nozzle was created to study quark-gluon plasma. When inert gas exits from this device into the flooded space, a supersonic and hypersonic double helical jet with a supercompressible swirling flow structure is formed. Figure 1 shows a plasmatron of our design [1]. Figure 2 shows a Schlieren photograph demonstrating the supercompressible structure of a hypersonic jet flowing from a plasmatron in the form of a self-focusing double helix [2].

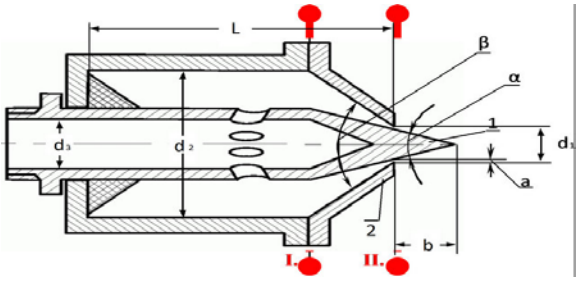

Fig. 1. Design of the plasmatron with central cone

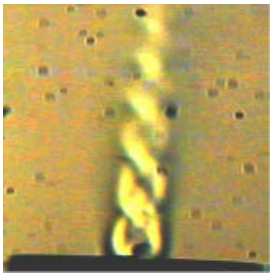

Fig. 2. The shadow photography of a hypersonic jet flowing from the plasmatron

The interaction of such a structured jet with a target is accompanied by the formation of a condensate of quark-gluon plasma on the target, which forms nucleons. Under conditions of maintaining the chemical purity of the experiment, we received that these nucleons lead to nucleosynthesis through several reaction channels.

1. Kholmurad Khasanov. Super-Compressibility Phenomenon. *Journal of Modern Physics, Vol.4 No.2(2013), Article ID:27830,8 pages DOI:10.4236/jmp.2013.42028*
2. Kholmurad Khasanov. Visualization of super-compressibility if supersonic spiral-twisted jets. *Physics Letters A*, 376 (2012), p. 748-752.

ZINC CONTENTS IN FRUITS AND VEGETABLES OF TASHKENT

Kuldjanov B., Osinskaya N.
Institute of Nuclear Physics, Uzbekistan Academy of Sciences, Tashkent, Uzbekistan

Zinc is an essential element, an antioxidant, promotes the growth of the body, supports the immune system, strengthens hair, skin, bones and nails; participates in the synthesis of the hormone insulin and in the production of testosterone; has an wound-healing and ulcer-healing effect; participates in the processes of taste perception and olfaction; is necessary for the functioning of the central nervous system, including for the processes of memorization. Some studies on the effects of zinc to the human body are given in /1, 2/.

Traditionally it is considered that the main sources of zinc are food products of animal origin. However, due to the widespread use of proper nutrition and consumption of plant products in recent decades, we have attempted to determine the zinc contents in fruit and vegetable products. Product samples were collected in the markets of Tashkent, washed in distilled water, dried to a constant weight, crushed, packed and sent for irradiation at the reactor of the Institute of Nuclear Physics of the Academy of Sciences of the Republic of Uzbekistan. The zinc contents was measured using neutron activation analysis. The obtained results are partially presented in Fig.1.

Fig.1 Zinc contents in the measured food stuff

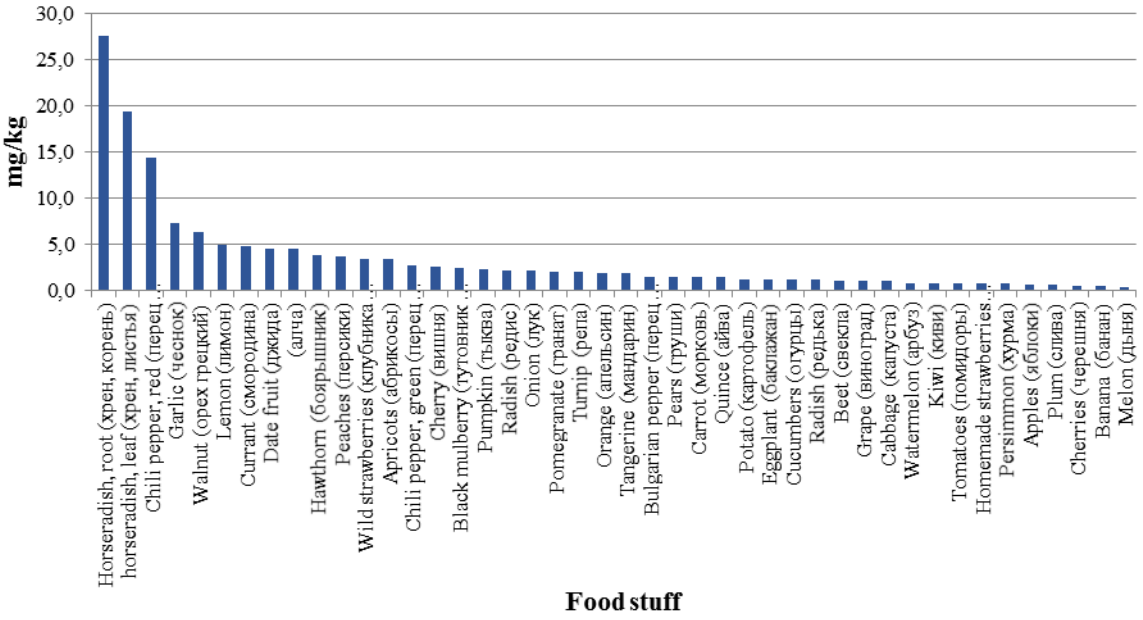

The results are discussed versus to adequate and maximum permissible levels of zinc intake.

1. Chasapis, C.T., Ntoupa, PS.A., Spiliopoulou, C.A. *et al.* Recent aspects of the effects of zinc on human health. *Arch Toxicol* **94**, 1443–1460 (2020). https://doi.org/10.1007/s00204-020-02702-9
2. Cho, YE., Choi, SH., Kwun, IS. (2023). The Micronutrient Zinc in Human Health and Disease. In: Ghosh, S., Kumari Panda, A., Jung, C., Singh Bisht, S. (eds) Emerging Solutions in Sustainable Food and Nutrition Security. Springer, Cham. https://doi.org/10.1007/978-3-031-40908-0_11

ANINNOVATIVE APPROACH TO THE TECHNOLOGY OF OBTAINING X-RADIONUCLIDES AND PRODUCING GRANULES FOR NUCLEAR MEDICINE

Markelova E.A., VasidovA., Khujaev S.
Institute of Nuclear Physics, Uzbekistan Academy of Sciences, Tashkent, Uzbekistan

Radionuclides with X-ray emission such as 125I(T1/2=60 d; Eγ=28 keV), 103Pd (T1/2=17 d; Eγ=21 keV) and 131Cs (T1/2=9.8 d, Eγ=31 keV) are successfully used all over the world.

These types of radionuclideshave short half-lives and low X-ray energies. The nuclear medicine specialists from the American company IsoRayMedical (www.isoray.com) prefer 131Cs over 125I and 103Pd due to its shorter half-life and higher x-ray energy. In the classical approach, the radionuclide is fixed in titanium capsules for implantation into the tumor.The production of X-ray sources in titanium or glass capsules radionuclides 131Cs in our conditions is limited due to some financial difficulties and the absence ofnecessaryhigh - tech equipment.

The goal of the work was to develop a technology for producing 131Cs and create spherical biopolymer X-emitters based on 131Cs radionuclide and chitosan sorbent.

The 131Cs is a daughter radionuclide of the 131Ba parent radionuclide, which is produced through the 130Ba(n,γ)131Ba reaction, after irradiation for 140 hours of 3 gr of the BaO at the nuclear reactor WWR-SM of INP of ASRUz. A radiochemical scheme and optimal conditions for the separation of 131Cs from a highly active barium solution have been developed.

The scheme uses microwave radiation and cyclic release of the target nuclide with radiochemical purity that meets medical requirements.

Chitosan and its derivatives are widely used in the nuclear medicine and the pharmaceutical industry due to the properties of biodegradability, biocompatibility, accelerating wound healing, lowering blood cholesterol and inhibiting tumor cells. The efficiency of sorption of the 131Cs ions by chitosan granules does not exceed 36%. To increase the efficiency of sorption, chitosan is modified with the addition of potassium ferrocyanide and transition metal chlorides. The chitosan used is synthesized from silkworm cocoons and provided by the Scientific Center for Chemistry and Physics of Polymers of National University of Uzbekistan. X-ray biopolymer granules were obtained based on 131CsCl and chitosan sorbent with modifying additives. To create X-ray granules, a granulation method has been developed using a two-layer precipitation bath.The angular distribution of dose activity of the granules was measured in the air, water and the biological tissue by using universal dosimeter FH-40LG Eberline. The results of measurements showed that the angular distribution γ-rays from granules were distributed identically in all directions. The received granules had been crosslinking with glutar-aldehyde solution to form hardness and hermetic spheres. The diameters and radioactivity of the granules can be regulated within 0.5±0.05 – 1.0±0.1 mm and (0.74–2.22)·108Bq/granule, respectively.

APPLICATION OF THE INAA METHOD IN AGRICULTURE, ECOLOGY AND MEDICINE

Kurbanov B.I.[1], Danilova E.A.[1], Khushvaktov N.Kh.[1], Osinskaya N.S.[1], Akhmedov Ya.A.[1], Kholov D.M.[2]

[1]Institute of Nuclear Physics, Uzbekistan Academy of Sciences, Tashkent, Uzbekistan
[2]Navoi State Mining and Technological University, Navoi, Uzbekistan

Elemental composition is a fundamental parameter of a substance, on which all its properties and structure depend, as well as the nature of physical, chemical, biological, technological and other processes. The modern level of science and technology makes it possible to determine both negligible and large quantities of elements in natural, environmental, biological and man-made objects.

This paper presents the results of a study on the use of the instrumental neutron activation analysis (INAA) method for monitoring the macro- and microelement composition of the soil in cotton-growing areas, identifying elements deficient for growing cotton, environmental monitoring to identify heavy and toxic elements around technogenic objects and establishing microelement the status of the human body based on hair analysis and the connection between the health of the population and the ecological situation of the territory.

The INAA method of the elemental composition of complex samples using research nuclear reactors and modern gamma spectrometers based on semiconductor detectors made of ultra-pure germanium makes it possible to determine the concentration of more than 40 elements in samples of soil, plants, water, food and substrates (hair) of a person with high sensitivity. In the laboratory of “Ecology and Biotechnology” of the Institute of Nuclear Physics of the Academy of Sciences of the Republic of Uzbekistan, an improved method has been developed for determining the content of macro- and microelements in natural, man-made and biological objects, which allows expanding the range of determined elements, lowering detection limits and increasing productivity.

These studies were carried out on the equipment base consisting of a research nuclear reactor of the WWR-SM type at the Institute of Nuclear Physics of the Academy of Sciences of the Republic of Uzbekistan with a thermal power of 10 MW. The samples under study, together with the standards, are packaged in a polyethylene container and irradiated in a vertical channel of the reactor with a neutron flux density of 5 x 1013 neutron/cm2 sec. The gamma spectrometric system consists of a high-purity germanium PPD with a resolution of 1.8 keV for the 60Co gamma line (1332 keV), and a registration efficiency of 20%. The use of a gamma spectrometer with such a detector made it possible to separate elements with similar energies, such as zinc and scandium, whose energies are 1115.5 and 1120.5 keV, respectively, magnesium and manganese - energies 843.8 and 846.7 keV, and determine their contents from pure peaks without taking into account the contribution of each other to friend. This has increased the sensitivity and accuracy of the determination of the above elements, which is very important when determining scandium and zinc in soils and magnesium and manganese in biological samples.

The patterns of distribution of macro- and microelements in the body were experimentally established by analyzing the hair of patients with long-term cirrhosis of the liver and parkinsonism syndrome, which showed a significantly increased content of manganese in the hair, which simultaneously correlated with the content of the gland. A statistically significant effect of manganese on the development of the disease has been established.

NUCLEAR PHYSICAL METHODS FOR MONITORING HEAVY AND TOXIC ELEMENTS ON IRRIGATED AREAS TREATED WITH PHOSPHORUS FERTILIZERS

Kurbanov B.I.[1], Akhmedov Ya.A.[1], Danilova E.A.[1], Jurakulov A.R.[2]
[1]Institute of Nuclear Physics, Uzbekistan Academy of Sciences, Tashkent, Uzbekistan
[2]Navoi State Mining and Technological University, Navoi, Uzbekistan

Phosphorus fertilizers in terms of production volume in the Republic of Uzbekistan occupy second place among produced fertilizers for agriculture. A large branch of the chemical industry has been created in the republic, which meets the needs of agriculture for phosphorus-containing fertilizers, the raw material base of which is mainly Kyzylkum phosphorites. Issues related to the transfer of toxic and radioactive chemical elements in areas with intensive use of phosphorus fertilizers into soils and plants, and their possible negative impact on the environment and public health have not been sufficiently studied.

As it is known, phosphate ore deposits around the world are characterized by high concentrations of radionuclides, and fertilizers produced on their basis are considered potential soil pollutants with heavy metals. Based on the results of leading scientists and specialists in this field, it is recommended to monitor the level of environmental safety of phosphate raw materials and fertilizers for agriculture made from it. Control is required for the content of the following chemical elements: fluorine (F), manganese (Mn), nickel (Ni), copper (Cu), zinc (Zn), arsenic (As), strontium (Sr), vanadium (V), chromium (Cr), lead (Pb), mercury (Hg), cobalt (Co), cadmium (Cd), uranium (U), thorium (Th) and yttrium (Y). However, in studies of the material composition of Kyzylkum phosphorites, there is no information about the availability of methods or instruments used to control the concentration of these elements in finished fertilizer products, which led to these studies.

This paper presents the results of a study assessing the content of the above elements in the soil of irrigated areas, to which phosphorus fertilizers were regularly applied, mainly from Kyzylkum phosphorites, using nuclear physical analysis methods.

Two territories were selected as a field for monitoring in the Kibray district of the Tashkent region, where phosphorus fertilizers have been applied for decades. The territories of the foothills of the Tien Shan, where phosphorus fertilizers have never been used, were chosen as a background area.

The table shows the results of INAA for the content of chemical elements in soil samples from agricultural land and the background area.

Table. Results of analysis of soil samples from agricultural land, ppm.

Elements	**As**	**Mn**	**Ba**	**Br**	**U**	**Ce**	**Th**	**Co**	**Cr**	**Cs**	**Cu**	**Eu**	**Mg**
Terr..№1	8.1	650	570	2.5	3.5	58	13	10	60	5.0	9.8	1.0	13000
Terr.№2	9.2	750	650	2.6	2.9	69	15	10	64	5.9	11,0	1.1	11000
Backgr. area	6.1	741	780	2.2	2.2	40	8.2	5.2	21	3.1	0.21	0.6	10900
Elements	**Zn**	**Mo**	**Sr**	**Hf**	**Ni**	**Rb**	**Sb**	**Sc**	**Sm**	**La**	**Ta**	**Tb**	**K**
Terr.№1	73.0	1.5	362	5.4	135	92	1.3	10	4.6	36.0	1.0	0.58	17000
Terr.№2	84.0	1.7	274	5.7	152	120	1.8	11	5.1	42.0	1.0	0.63	19000
Backgr.area	53.2	2.1	305	2.2	110	68	0.8	5.6	3.2	31.2	0.7	0.3	19000

THE EFFECT OF RADIATION AND MAGNETIC PULSE TREATMENT ON THE WEAR RESISTANCE OF HARD ALLOY TOOLS

Malikov Sh.R.,[1], Yuldashev M.B.,[1], Ashrapov U.T.[1], Amanov O.O.[1], Sadikov I.I [1], Karakhodjaev A[1].

[1]Institute of Nuclear Physics, Uzbekistan Academy of Sciences, Tashkent, Uzbekistan

Different hard alloy tools (HAT) with high wear resistance are widely used for drilling operations in the mining industry. The efficiency of drilling wells or boreholes, especially in hard rocks, is largely determined by the operational performance of the HAT. In this paper, the combined effect of gamma ray irradiation and magnetic pulse treatment on the wear resistance of the HAT is studied in order to determine the optimal regime of volumetric hardening to improve the mechanical and operational characteristics of the HAT. During the experiments, the optimal modes of irradiation and magnetic pulse processing were revealed.

In order to carry out the irradiation of samples with gamma radiation, a pool-type “Gamma-installation” of the Institute of Nuclear Physics of the Academy of Sciences of the Republic of Uzbekistan was used with sources of ^{60}Co (average energy of gamma rays 1.25 MeV) with a dose rate of 130 R/s at an exposure dose of $3{,}2\cdot10^4$ до $5.0\cdot10^8$ R.

The method of magnetic-pulse processing (MPT) of CT is the most effective method of bulk hardening. The possibility of using MPT for carbide tools is due to the presence of cobalt in the composition of the tool - a ferromagnetic material with high magnetic permeability.

For the implementation of magnetic-pulse processing (MPT), a magnetic-pulse installation was created (Figure 1) with a magnetic inductor **2** consisting of two pairs of electromagnetic coils and a magnetic circuit **1** on which electromagnetic coils are mounted. This design allows processing drill bits with a pulsed magnetic field and drill bits as a whole, which is a necessary condition for increasing the wear resistance of finished HAT.

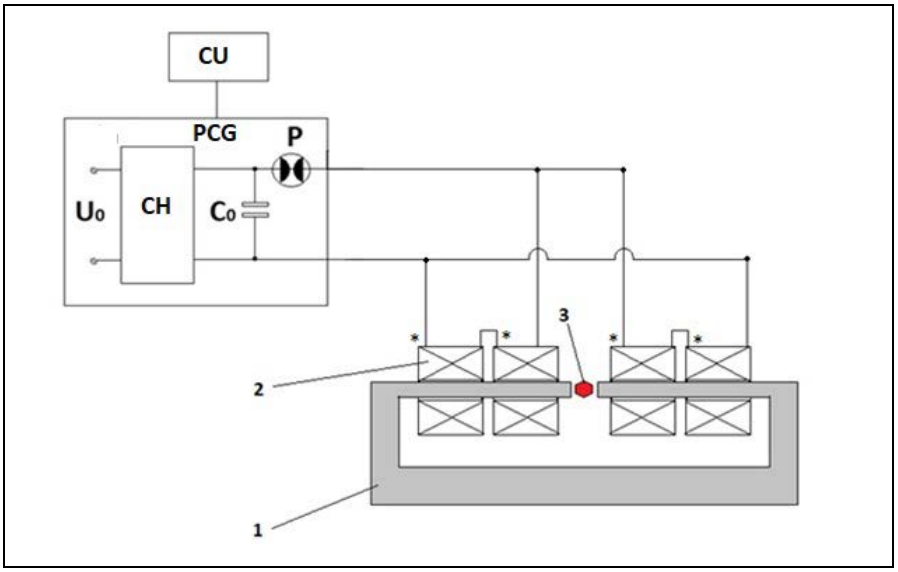

Fig.1. Block diagram of the magnetic-pulse installation: 1-magnetic core; 2 - solenoid inductors; 3 - drill bit; CU - control unit; PCG - pulse current generator; CH - charger; P - switching device; C_0 - capacitor bank; U_0 - network voltage

GAMMA SPECTROMETRIC ANALYSIS IN THE STUDY OF ARCHAEOMETALLURGICAL OBJECTS

Alibekov A.S., Sharonov I.A.
Samarkand State University, Samarkand, Uzbekistan

The result of using gamma spectrometry in the study of objects of archaeometallurgy are presented (samples taken from the remains of metallurgical furnaces discovered on the territory of the ancient monument "Eski Khovos" in the Syrdarya region of Uzbekistan in excavations numbered 3, 11 and 15/8). Two samples of slag (2/11 and 1/15-8) and three samples of clay furnace walls (3/3, 4/3 and 5/11) were examined. An analysis of these samples was conducted to determine the specific effective activity A_{Eff} (SEA) of natural dose-forming radionuclides (NDRs) ^{226}Ra (A(Ra)), ^{232}Th (A(Th)) and ^{40}K (A(K)), performed on a scintillation gamma spectrometer. The specific effective activity A_{eff} was calculated through the measured specific activities ^{226}Ra (A(Ra)), ^{232}Th (A(Th)) and ^{40}K (A(K)) using the formula $A_{Eff} = A(Ra) + 1.30 \cdot A(Th) + 0.09 \cdot A(K)$ [1].

The values of specific activity of NDRs in the samples, as well as their contributions (C) to the specific effective activity A_{Eff} are shown in Table 1. Under the contributions to A_{Eff}, we understand the values of specific activities of ^{226}Ra, ^{232}Th, ^{40}K, multiplied by the coefficients 1.0, 1.3, and 0.09, respectively.

Table 1. Values of specific activities of ^{226}Ra, ^{232}Th, and ^{40}K (in Bq/kg) and their contributions (C, in %) to the specific effective activity A_{Eff} of the studied samples

Sample	A(Ra)±ΔA	A(Th)±ΔA	A(K)±ΔA	A_{Eff}±ΔA	C(Ra)	C(Th)	C(K)
1/15-8	38.4±8.8	18.3±3.8	<40.5	65.8±10.1	58.3	36.2	5.5
2/11	37.7±5.9	27.7±2.4	260.4±27.0	97.2±7.1	38.8	37.1	24.1
3/3	26.9±8.8	40.6±5.3	1061.0±100.0	175.1±14.4	15.4	30.1	54.5
4/3	33.1±12.0	39.6±3.4	1114.2±45.0	184.8±13.4	17.9	27.8	54.3
5/11	27.8±6.6	35.2±4.2	1022.6±94.0	165.6±12.0	16.8	27.6	55.6

It is evident that the SEA of NDRs in slags is significantly lower than the SEA of NDRs in the clay material of furnace walls. The SEA of slags 1/15-8 and 2/11 slightly differ from each other, but there is a significant difference in the contributions of radium and potassium, distinguishing slag 1/15-8 from slag 2/11 - 58.3% and 38.8% by radium and 5.5% and 24.1% by potassium, respectively. Note that the neutron activation analysis of these same slag samples [2] showed a significant difference in their elemental composition - the iron content in samples 1/15-8 and 2/11 was 347000 ppm and 123000 ppm, respectively. The results of our studies allow us to say that the slags obtained during the blacksmithing processing of different iron semi-finished products, obtained at the ore melting stage, were examined.

It can be concluded that the specific activities of dose-forming radionuclides ^{226}Ra, ^{232}Th, ^{40}K in archaeometallurgical objects, along with the elemental composition of objects, can serve as an additional indicator in the identification of archaeometallurgical artifacts.

1. Methodology for measuring the specific activity of radionuclides radium-226, thorium-232, potassium-40, cesium-137, strontium-90 in samples of products from industrial enterprises, agricultural enterprises and environmental objects. MVV № 805/05. Analytical complex "RADEK". Saint Petersburg, 2005.
2. A.Alibekov et al. (2023). Neutron activation analysis of archaeometallurgical ancient artifacts found in Uzbekistan // Journal of Radioanalytical and Nuclear Chemistry, 332:1883–1891.

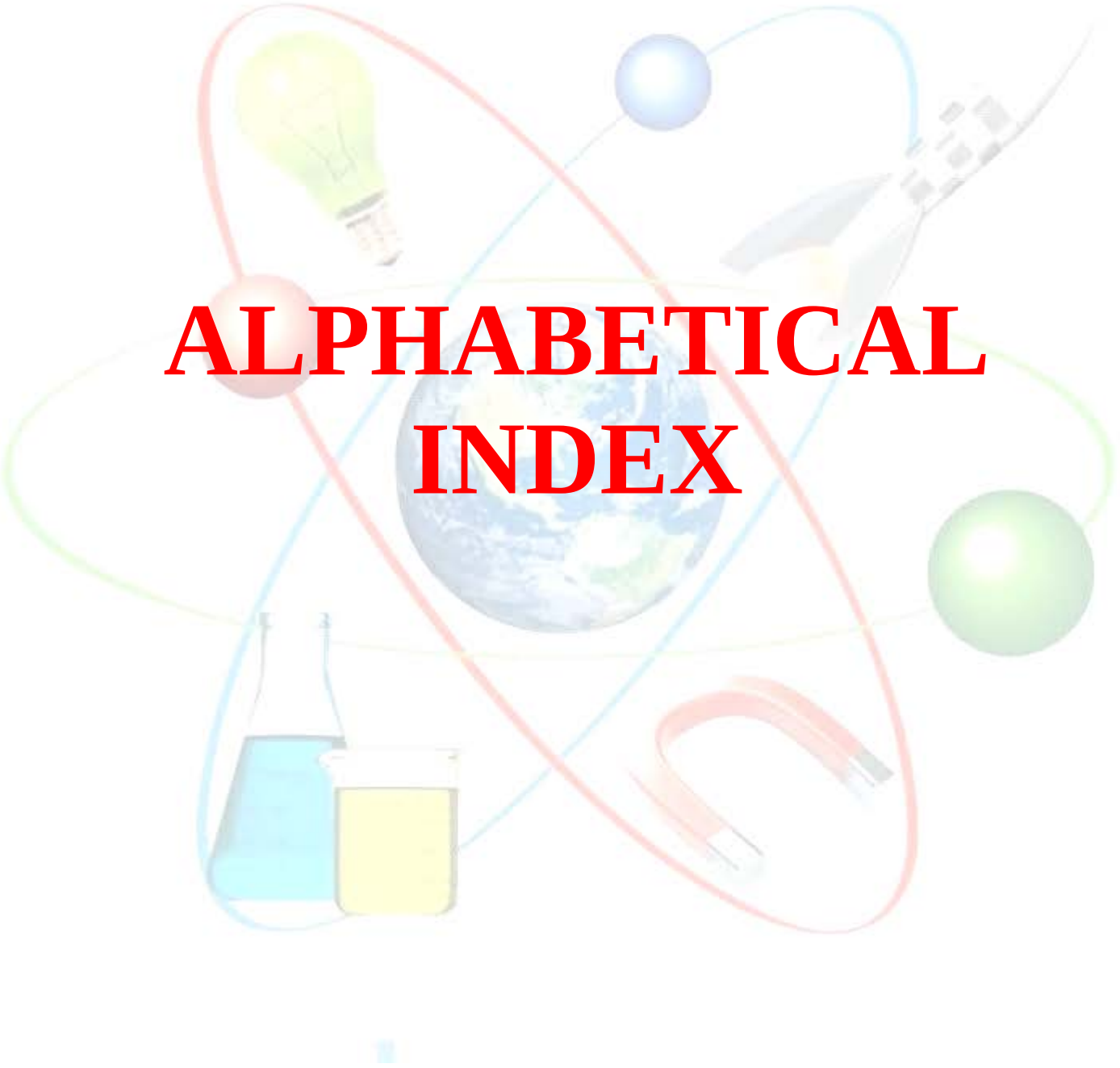

ALPHABETICAL INDEX

A

B – C

D – E

F-G

H-I-J

K

L

M

N – O

P – R

S

T – U

V– W- X- Y– Z

CONTACTS OF CONFERENCE PARTICIPANTS

NAME	*ORGANIZATION, COUNTRY*	*E-MAIL ADDRESS*
Abdujabbarov Ahmadjon	Ulugh Beg Astronomical Institute, Tashkent **UZBEKISTAN**	ahmadjon@astrin.uz
Abdullaev Fatkhulla	Physical-Technical Institute, Uzbekistan Academy of Sciences, Tashkent **UZBEKISTAN**	fatkhulla@yahoo.com
Abdurakhimov Bekhzodjon	Joint Institute for Nuclear Research, Dubna, **RUSSIA**	bekhzod@jinr.ru
Achilov Alimardon	Research Institute of Semiconductor Physics and Microelectronics at the National University, Tashkent **UZBEKISTAN**	alimardon.uzb@mail.ru
Agayev Teymur	Institute of Radiation Problems, Baku **AZERBAIJAN**	agayevteymur@rambler.ru
Ahmedov Bobomurat	Ulugh Beg Astronomical Institute, Tashkent **UZBEKISTAN**	ahmedov@astrin.uz
Aitkulov Magzhan	Institute of Nuclear Physics, Almaty **KAZAKHSTAN**	n.bahtiar73@gmail.com
Akhatov Jasurjon	Physical-Technical Institute, Uzbekistan Academy of Sciences, Tashkent **UZBEKISTAN**	jahatov@uzsci.net
Akhmedov Yakub	Institute of Nuclear Physics, Tashkent **UZBEKISTAN**	yakub8788@gmail.com
Akhmedzhanov Farkhad	Institute of Ion-Plasma and Laser Technologies, Tashkent **UZBEKISTAN**	akhmedzhanov.f@gmail.com
Alibekov Akbar	Samarkand State University, Samarkand **UZBEKISTAN**	akbaralibekov@gmail.com
Allaev Bakhtiyor	Institute of Ion-Plasma and Laser Technologies, Tashkent **UZBEKISTAN**	ba.allaev@gmail.com
Amonov Akhtam	Institute of Engineering Physics of Samarkand State University, Samarkand **UZBEKISTAN**	akhtamul@gmail.com
Asfandiyarov Ildar	Astronomical Institute, Academy of Sciences, Tashkent **UZBEKISTAN**	ildar@astrin.uz
Baimukhanova Ayagoz	Joint Institute for Nuclear Research, Dubna **RUSSIA**	ayagoz@jinr.ru
Baizakov Bakhtiyor	Physical-Technical Institute, Uzbekistan Academy of Sciences, Tashkent **UZBEKISTAN**	baizakov@uzsci.net
Bakhramov Sadulla	Academy of Sciences of the Republic of Uzbekistan, Tashkent **UZBEKISTAN**	bahramov@mail.ru
Balasoiu Maria	Joint Institute for Nuclear Research, Dubna **RUSSIA**	masha.balasoiu@gmail.com
Bedelbekova Kamshat	Institute of Nuclear Physics, Almaty **KAZAKHSTAN**	k.bedelbekova@inp.kz kamshat1980@mail.ru

NAME	*ORGANIZATION, COUNTRY*	*E-MAIL ADDRESS*
Bekmirzaev Rakhmatulla	Jizzak State Pedagogical University, Jizzak **UZBEKISTAN**	bekmirzaev@mail.ru
Belushkin Alexander	Joint Institute for Nuclear Research, Dubna **RUSSIA**	belushk@nf.jinr.ru
Beresneva Yuliya	Scientific Production Unitary Enterprise «ATOMTEX», Minsk **BELARUS**	yulia.beresneva@inbox.ru
Boudjella Aissa	Samarkand International University, Samarkand **UZBEKISTAN**	aissa.boudjella@siut.uz
Bryazgin Aleksandr	Budker Institute of Nuclear Physics, Novosibirsk **RUSSIA**	A.A.Bryazgin@inp.nsk.su
Bunkin Nikolay	Bauman Moscow State Technical University, Moscow **RUSSIA**	nbunkin@mail.ru
Churkin Igor	Budker Institute of Nuclear Physics, Novosibirsk **RUSSIA**	I.N.Churkin@inp.nsk.su
Davranov Khujamkul	Karshi State University, Karshi **UZBEKISTAN**	xujamkuldt@mail.ru
Demidov Yurii	Petersburg Nuclear Physics Institute, NRC “Kurchatov Institute”, Gatchina **RUSSIA**	Iurii.demidov@gmail.com
Doroshkevich Aleksandr	Joint Institute for Nuclear Research, Dubna **RUSSIA**	doroh@jinr.ru
Dunin Nikita	Joint Institute for Nuclear Research, Dubna **RUSSIA**	nikitadunin@jinr.ru
Dushanov Ermuhammad	Joint Institute for Nuclear Research, Dubna **RUSSIA**	dushanov@jinr.ru
Egamediev Serik	Institute of Nuclear Physics, Tashkent **UZBEKISTAN**	egamedievs@mail.ru
Egamov Sarvar	Institute of Nuclear Physics, Tashkent **UZBEKISTAN**	egamov.s@inp.uz
Elmekawy Ahmed	Joint Institute for Nuclear Research, Dubna **RUSSIA**	ahmedalmekawy@ymail.com
Ergashev Salohiddin	Samarkand State University, Samarkand **UZBEKISTAN**	ergashevsalohiddin111@gmail.com
Eshkabilov Napas	Samarkand State University, Samarkand **UZBEKISTAN**	e-napas@samdu.uz ,
Eshonkulov Gofur	National University of Uzbekistan, Tashkent **UZBEKISTAN**	info@nuu.uz
Fimushkin Victor	Joint Institute for Nuclear Research, Dubna **RUSSIA**	fimushkin@jinr.ru
Gaynazarova Kizlarxon	Fergana state University, Fergana **UZBEKISTAN**	k.gaynazarova3011@gmail.com
Gevorgyan Sergey	Joint Institute for Nuclear Research, Dubna **RUSSIA**	gevs@jinr.ru
Gordeev Ivan	Joint Institute for Nuclear Research, Dubna **RUSSIA**	gordeev@jinr.ru

NAME	*ORGANIZATION, COUNTRY*	*E-MAIL ADDRESS*
Gorshkova Yulia	Joint Institute for Nuclear Research, Dubna **RUSSIA**	Yulia.Gorshkova@jinr.ru
Gulamova Dilbar	Institute of Materials Science, Parkent **UZBEKISTAN**	ddgulamova@ mail.ru
Hajiyeva Seljan	Institute of Radiation Problems, Baku **AZERBAIJAN**	selcan.mamedkhanova@mail.ru
Ibadov Rustam	Institute of Engineering Physics of Samarkand State University, Samarkand **UZBEKISTAN**	ibrustam@mail.ru
Ibragimova Elvira	Institute of Nuclear Physics, Tashkent **UZBEKISTAN**	ibragimova@inp.uz
Imanova Gunel	Institute of Radiation Problems, Baku **AZERBAIJAN**	gunel_imanova55@mail.ru
Inoyatov Anvar	Joint Institute for Nuclear Research, Dubna, **RUSSIA**	inoyatov@jinr.ru
Irgaziev Bakhadir	National University of Uzbekistan, Tashkent **UZBEKISTAN**	irgaziev@mail.ru
Isakhanov Zinaobidin	Institute of Ion-Plasma and Laser Technologies, Tashkent **UZBEKISTAN**	za.isakhanov@gmail.com
Isayeva Elmira	Institute of Physics, Baku **AZERBAIJAN**	el_max63@yahoo.com
Ismaylov Bayram	Tashkent State Technical University, Tashkent **UZBEKISTAN**	ismaylovb81@gmail.com
Itkis Mikhail	Joint Institute for Nuclear Research, Dubna **RUSSIA**	itkis@jinr.ru
Izosimov Igor	Joint Institute for Nuclear Research, Dubna **RUSSIA**	izosimov@jinr.ru
Javadova Vafa	Joint Institute for Nuclear Research, Dubna **RUSSIA**	javadova@jinr.ru
Jumaev Mustaqim	Bukhara Engineering Technological Institute, Bukhara **UZBEKISTAN**	mrjumaev2011@mail.ru
Kadirov Asilbek	Karshi state University, Karshi **UZBEKISTAN**	asilbek_fiz-mat@mail.ru
Kapishin Mikhail	Joint Institute for Nuclear Research, Dubna **RUSSIA**	kapishin@jinr.ru
Kaxorova Aziza	Samarkand State University, Samarkand **UZBEKISTAN**	azizakakhorova@gmail.com
Khalilov Umedjon	Institute of Ion-Plasma and Laser Technologies, Tashkent **UZBEKISTAN**	umedjon.khalilov@uantwerpen.be
Khallokov Farhod	Bukhara State Medical Institute, Bukhara **UZBEKISTAN**	f_k_xalloqov@rambler.ru
Khamrakulov Farkhodjon	Samarkand State University, Samarkand **UZBEKISTAN**	x-farxodjon@mail.ru
Khasanov Kholmurad	Institute of Engineering Physics of Samarkand State University, Samarkand **UZBEKISTAN**	kholkh@bk.ru

NAME	*ORGANIZATION, COUNTRY*	*E-MAIL ADDRESS*
Khaydarov Renat	Institute of Nuclear Physics, Tashkent **UZBEKISTAN**	renat@inp.uz
Kholikulova Saodat	Karshi state University, Karshi **UZBEKISTAN**	
Khomich Vladislav	Institute for Electrophysics and Electric Power of Russian Academy of Sciences, St.Peterburg **RUSSIA**	khomich@ras.ru
Khomich Yurii	Institute for Electrophysics and Electric Power of Russian Academy of Sciences, St.Peterburg **RUSSIA**	ykhomich@yandex.ru
Khudaykulov Bekzod	Samarkand State University, Samarkand **UZBEKISTAN**	xudaykulovbekzod@samdu.uz
Khusanov Elzod	Institute of Nuclear Physics, Tashkent **UZBEKISTAN**	xusanovelzod.99@gmail.com
Khushvaktov Jurabek	Joint Institute for Nuclear Research, Dubna **RUSSIA**	khushvaktov@jinr.ru
Kirgizov Sobit	Institute of Engineering Physics of Samarkand State University, Samarkand **UZBEKISTAN**	qirgizovsobit94@gmail.com
Knyazheva Galina	Joint Institute for Nuclear Research, Dubna **RUSSIA**	knyazheva@jinr.ru
Komar Damian	Scientific Production Unitary Enterprise «ATOMTEX», Minsk **BELARUS**	damiankomar@yandex.ru
Kondratyev Vladimir	Joint Institute for Nuclear Research, Dubna **RUSSIA**	vkondrat1401@mail.ru
Korjavov Mustafa	Karshi Institute of Engineering and Economical, Karshi **UZBEKISTAN**	korjavovmustafa@gmail.com
Kuldjanov Bakhrom	Institute of Nuclear Physics, Tashkent **UZBEKISTAN**	kuldjanov@inp.uz
Kulikov Sergey	Joint Institute for Nuclear Research, Dubna **RUSSIA**	ksa@nf.jinr.ru
Kurbanov Baxtiyar	Institute of Nuclear Physics, Tashkent **UZBEKISTAN**	bkurbanov@ inp.uz; kurbanov_1960@bk.ru
Kuvandikov Oblokul	Samarkand State University, Samarkand **UZBEKISTAN**	quvandikov@rambler.ru
Kuznetsova Alena	Joint Institute for Nuclear Research, Dubna **RUSSIA**	aakuznetsova@jinr.ru
Lakaev Saidakhmat	Samarkand State University, Samarkand **UZBEKISTAN**	slakaev@mail.ru
Lanyov Alexander	Joint Institute for Nuclear Research, Dubna **RUSSIA**	Alexander.Lanyov@cern.ch
Lukin Evgenii	Joint Institute for Nuclear Research, Dubna **RUSSIA**	lukin@jinr.ru
Lukyanov Sergey	Joint Institute for Nuclear Research, Dubna **RUSSIA**	lukyan@jinr.ru

NAME	*ORGANIZATION, COUNTRY*	*E-MAIL ADDRESS*
Madatov Rahim	Institute of Radiation Problems, Baku **AZERBAIJAN**	msrahim@rambler.ru
Malikov Shavkat	Institute of Nuclear Physics, Tashkent **UZBEKISTAN**	malikov@inp.uz
Mammadova Gulshan	Nakhchivan State University, Nakhchivan **AZERBAIJAN**	gulsenmemmedova@ndu.edu.az
Markelova Elena	Institute of Nuclear Physics, Tashkent **UZBEKISTAN**	hopel1983@mail.ru
Mavlyanov Abdulaziz	Research Institute of Semiconductor Physics and Microelectronics at the National University, Tashkent **UZBEKISTAN**	samusu@rambler.ru
Melikova Sevinj	Institute of Radiation Problems, Baku **AZERBAIJAN**	sevinc.m@rambler.ru
Merkin Mikhail	Institute of Nuclear Physics, Moscow State University, Moscow **RUSSIA**	merkinm@silab.sinp.msu.ru
Mezentseva Zhanna	Joint Institute for Nuclear Research, Dubna **RUSSIA**	mzv@nf.jinr.ru
Muminov Ramizulla	Physical-Technical Institute, Tashkent **UZBEKISTAN**	detector@uzsci.net
Mustafayev Islam Israfil	Institute of Radiation Problems, Baku **AZERBAIJAN**	imustafayev@mail.ru
Muzafarova Sultanpasha	Research Institute of Semiconductor Physics and Microelectronics at the National University, Tashkent **UZBEKISTAN**	samusu@rambler.ru
Nasirov Avazbek	Joint Institute for Nuclear Research, Dubna **RUSSIA**	nasirov@jinr.ru
Nazmitdinov Rashid	Joint Institute for Nuclear Research, Dubna **RUSSIA**	rashid@theor.jinr.ru
Norbutaev Shuhrat	Institute of Nuclear Physics, Tashkent **UZBEKISTAN**	shuhratnorb4448@gmail.com
Nurgozhayev Bakhtiyar	Institute of Nuclear Physics, Almaty **KAZAKHSTAN**	magzhan.aitkulov@gmail.com
Nuritdinov Salaxutdin	National University of Uzbekistan, Tashkent **UZBEKISTAN**	nur200848@mail.ru
Olimov Kosim	Physical-Technical Institute, Academy of Sciences, Tashkent **UZBEKISTAN**	olimov@uzsci.net
Paraipan Mihaela	Joint Institute for Nuclear Research, Dubna **RUSSIA**	mihaela_paraipan@yahoo.com
Parmanova Mekhrinisa	Astronomical Institute, Academy of Sciences, Tashkent **UZBEKISTAN**	parmanovamehriniso@gmail.com
Petrozhitskiy Alexey	Budker Institute of Nuclear Physics, Novosibirsk **RUSSIA**	petrozhav@gmail.com
Polvonov Satimboy	National University of Uzbekistan, Tashkent **UZBEKISTAN**	palvanov1960@gmail.com

NAME	*ORGANIZATION, COUNTRY*	*E-MAIL ADDRESS*
Ponomarev Dmitrii	Joint Institute for Nuclear Research, Dubna **RUSSIA**	ponom@jinr.ru
Rafikov Avaz	Institute of Nuclear Physics, Tashkent **UZBEKISTAN**	makhmudov@inp.uz
Rakhimov Abdulla	Institute of Nuclear Physics, Tashkent **UZBEKISTAN**	rakhimovabd@yandex.ru
Rakhimov Bobomurod	Institute of Nuclear Physics, Tashkent **UZBEKISTAN**	murod9520@gmail.com
Rakhmatullaev Ilyos	Branch of National Research Nuclear University MEPhI in Tashkent **UZBEKISTAN**	IARakhmatullaev@mephi.ru
Rakitin Vladimir	Federal Research Center of Problems of Chemical Physics and Medicinal Chemistry, Chernogolovka **RUSSIA**	domi-tyan@yandex.ru
Ramazanov Asror	National University of Uzbekistan, Tashkent **UZBEKISTAN**	info@nuu.uz
Rasulova Fazilat	Institute of Nuclear Physics, Tashkent **UZBEKISTAN**	rasulova.inp@mail.ru
Rasulova Mukhayo	Institute of Nuclear Physics, Tashkent **UZBEKISTAN**	rasulova@live.com
Rzayeva Sitara	Institute of Physics, National Academy of Sciences, Baku **AZERBAIJAN**	eaisaeva@mail.ru
Sabirov Basar	Joint Institute for Nuclear Research, Dubna, **RUSSIA**	sabirov@jinr.ru
Sabirov Leonard	Institute of Engineering Physics of Samarkand State University, Samarkand **UZBEKISTAN**	leonard.sabirov@gmail.com
Saha Bijan	Joint Institute for Nuclear Research, Dubna **RUSSIA**	bijan@jinr.ru
Salakhitdinova Maysara	Samarkand State University, Samarkand **UZBEKISTAN**	smaysara@yandex.ru
Shahova Vera	Petersburg Nuclear Physics Institute of NRC «Kurchatov Institute», Gatchina **RUSSIA**	shakhova_vm@pnpi.nrcki.ru
Sharonov Iosif	Samarkand State University, Samarkand **UZBEKISTAN**	jsharonov@gmail.com
Sultanov Mamadali	Samarkand State University of Architecture and Construction, Samarkand **UZBEKISTAN**	Sultanovmamadali60@gmail.ru
Tashpulatov Sa’dulla	Institute of Nuclear Physics, Tashkent **UZBEKISTAN**	toshpul@mail.ru
Teymurov Eyvaz	Nuclear Research Department, Innovation and Digital Development Agency, Baku **AZERBAIJAN**	ey.teymurov@gmail.com
Titov Anatoliy	Petersburg Nuclear Physics Institute of NRC «Kurchatov Institute», Gatchina **RUSSIA**	titov_av@pnpi.nrcki.ru

NAME	*ORGANIZATION, COUNTRY*	*E-MAIL ADDRESS*
Tojiboev Ilkhomjon	Institute of Ion-Plasma and Laser Technologies, Tashkent **UZBEKISTAN**	Ilhom.tojiboyev@gmail.com
Tojiboev Olimjon	Institute of Nuclear Physics, Tashkent **UZBEKISTAN**	olimjon@inp.uz
Tojiboyev Davronbek	Institute of Nuclear Physics, Tashkent **UZBEKISTAN**	tojiboyev_davron89@mail.ru
Tojinazarov Furkat	Center for Advanced Technologies, Tashkent **UZBEKISTAN**	furqattojinazarov@gmail.com
Tsoy Eduard	Physical-Technical Institute, Academy of Sciences, Tashkent **UZBEKISTAN**	e.n.tsoy@gmail.com
Turaev Sobir	National University of Uzbekistan, Tashkent **UZBEKISTAN**	sobr8488@mail.ru
Tursunkulov Oybek	Center for Advanced Technologies, Tashkent **UZBEKISTAN**	oybtmuz@gmail.com
Tursunov Ergash	Institute of Nuclear Physics, Tashkent **UZBEKISTAN**	tursune@inp.uz
Tuymuradov Abror	National University of Uzbekistan, Tashkent **UZBEKISTAN**	abrorphy@gmail.com
Tuymurodov Dilmurod	National University of Uzbekistan, Tashkent **UZBEKISTAN**	dituymurodov@gmail.com
Urusova Elena	Institute of Nuclear Physics, Tashkent **UZBEKISTAN**	urusova01ev@gmail.com
Usarov Uktam	Samarkand State University of Architecture and Construction, Samarkand **UZBEKISTAN**	usarov-u@mail.ru
Usmanov Pazlitdin	Namangan Institute of Engineering and Technology, Namangan **UZBEKISTAN**	usmanov1956.56@mail.ru
Utamuradova Sharifa	Institute of Semiconductor Physics and Microelectronics at the National University of Uzbekistan, Tashkent **UZBEKISTAN**	sh-utamuradova@yandex.ru
Vasidov Abdisamat	Institute of Nuclear Physics, Tashkent **UZBEKISTAN**	samad@inp.uz
Verdiyeva Nurana Alishir	Ganja State University, Ganja **AZERBAIJAN**	verdiyeva.nurane@bk.ru
Voinov Alexey	Joint Institute for Nuclear Research, Dubna **RUSSIA**	voinov@jinr.ru
Voytishin Nikolay	Joint Institute for Nuclear Research, Dubna **RUSSIA**	nvoytish@jinr.ru
Yovqochev Pahlavon	National University of Uzbekistan, Tashkent **UZBEKISTAN**	yovqochevp@gmail.com
Yuldashev Djasur	Bukhara State Medical Institute, Bukhara **UZBEKISTAN**	yusupov.elmurod@mail.ru
Yuldashev Sukhrob	Samarkand State University, Samarkand **UZBEKISTAN**	Sultanovmamadali60@gmail.ru

NAME	*ORGANIZATION, COUNTRY*	*E-MAIL ADDRESS*
Yusupov Elmurod	Namangan Institute of Engineering and Technology, Namangan **UZBEKISTAN**	yusupov.elmurod@mail.ru
Zaitsev Andrei	Joint Institute for Nuclear Research, Dubna **RUSSIA**	zaicev@jinr.ru
Zakhidov Anvar	University of Texas at Dallas, Richardson, **UNITED STATES OF AMERICA**	zakhidov@utdallas.edu
Zaynabidinov Sirajidin	Andijan State University, Andijan **UZBEKISTAN**	prof_sirojiddin@mail.ru
Zhabitsky Vyacheslav	Joint Institute for Nuclear Research, Dubna **RUSSIA**	V.Zhabitsky@jinr.ru
Zikrillaev Nurullo	Tashkent State Technical University, Tashkent **UZBEKISTAN**	feruzaxonurakova@mail.com
Zinatulina Daniya	Joint Institute for Nuclear Research, Dubna **RUSSIA**	zinatulina@jinr.ru

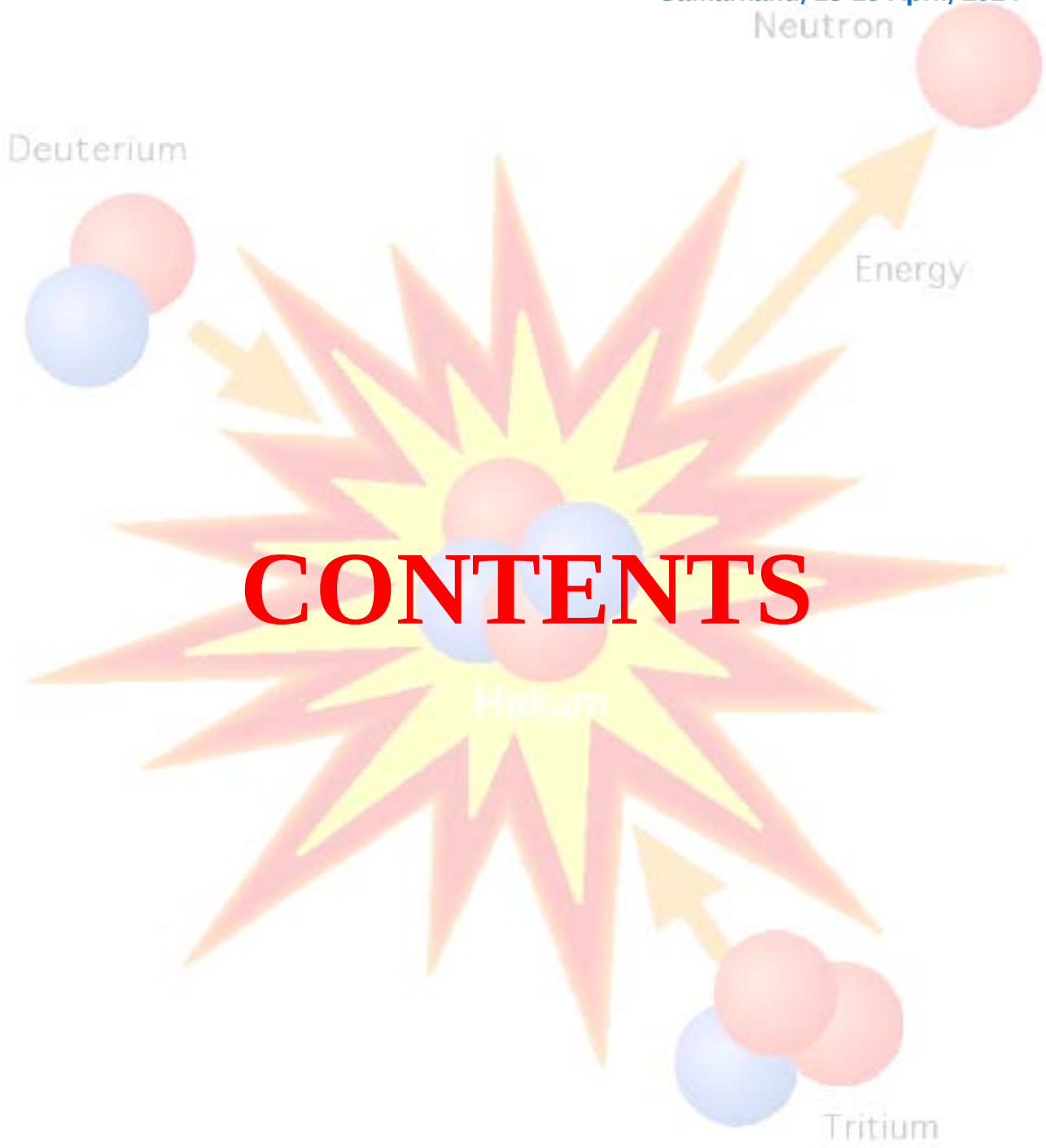

CONTENTS

C O N T E N T S

1. STRUCTURE OF MATTER AND THE UNIVERSE

2. PHYSICS OF CONDENSED MATTER

3. APPLIED PHYSICS

THE THIRD INTERNATIONAL FORUM

PHYSICS – 2024

April 23-25, 2024, Samarkand, Uzbekistan

BOOK OF ABSTRACTS

Institute of Nuclear Physics, Academy of Sciences of Uzbekistan, 2024, 174 pages.

UCHINCHI XALQARO FORUM

FIZIKA – 2024

Aprel 23-25, 2024, Samarkand, Õzbekiston

MA'RUZALAR TEZISLARI TO'PLAMI

O'zbekiston Respublikasi Fanlar Akademiyasi Yadro Fizikasi Instituti, 2024, 174 bet.

The content of all abstracts is published in the author's edition

Содержание всех тезисов публикуется в авторской редакции

Barcha tezislarning mazmuni muallif nashrida chop etiladi

Mailing address: Institute of Nuclear Physics, Ulugbek
Tashkent, UZ-100214, Republic of Uzbekistan,
Telephone: (998-71) 289-31-41, (998-71) 289-35-57
E-mail: fazilovaz@mail.ru; vleila@mail.ru

https://conference.samdu.uz/ru/index.php

Samarkand State University

WELCOME TO SAMARKAND!